UNIVERSITY OF SOUTHAMPTON

FACULTY OF MEDICINE

Clinical and Experimental Sciences

Recombinant Expression of Functional Trimeric Fragments of Human SP-A and SP-D

by

Alastair Samuel Watson

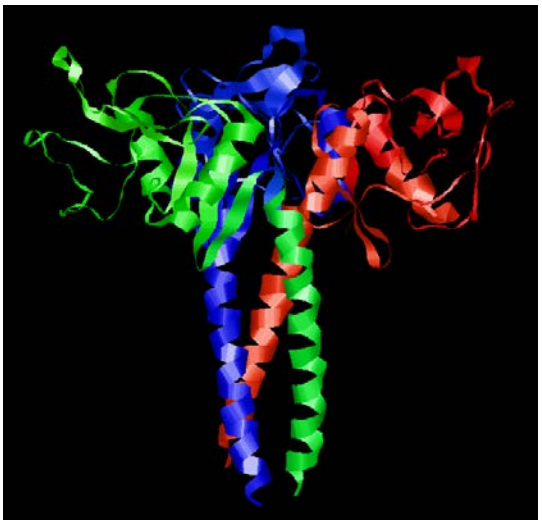

Thesis for the degree of Doctor of Philosophy

March 2016

UNIVERSITY OF SOUTHAMPTON

ABSTRACT

FACULTY OF MEDICINE

Clinical and Experimental Sciences

Doctor of Philosophy

RECOMBINANT EXPRESSION OF FUNCTIONAL TRIMERIC FRAGMENTS OF HUMAN SP-A AND SP-D

by Alastair Samuel Watson

The lung collectins, surfactant proteins A and D (SP-A and SP-D) are important innate immune molecules, localised predominantly in the pulmonary surfactant of the lung. SP-A and SP-D bind to carbohydrates on the surface of pathogens and enhance their neutralisation, agglutination and clearance. Moreover, they are important modulators of the inflammatory immune response. Lung collectins form trimers comprised of an N-terminal domain, collagen-like domain, a neck region and a C-terminal carbohydrate recognition domain (CRD). A trimeric recombinant fragment of human SP-D (rfhSP-D) comprised of only the neck, CRD and a short collagen-like stalk, which lacks the N-terminal domain important for the collectin oligomeric structure, has previously been produced. This has provided insights into the importance of the N-terminus and oligomeric structure for functions of SP-D and its mode of calcium-dependent ligand binding. Here I report the first successful expression and purification of an equivalent functional trimeric fragment of human SP-A (rfhSP-A).

Through use of a novel expression tag (NT), a functional trimeric rfhSP-A molecule was successfully expressed in *E. coli* and purified. rfhSP-A was shown to bind to various natural SP-A ligands in a calcium-dependent manner, including mannan, BBG2Na (containing respiratory syncytial virus (RSV) G protein core region), recombinant HIV gp120 IIIB protein and LPS from *K. pneumoniae*, albeit at low levels. rfhSP-A was found

to neutralise RSV and reduce infection of bronchial epithelial cells, as assessed by both RT-qPCR and flow cytometry, by up to a mean (± standard deviation) of 96.4 (± 1.9) % ($p < 0.0001$) to similar levels as the uninfected control. This fragment was significantly more effective ($p < 0.0001$) at neutralising RSV than native human (nh)SP-A which reduced infection levels by up to 38.5 (± 28.4) % ($p < 0.05$). This increased efficacy of rfhSP-A in neutralising RSV could be due to the absence of the SP-A N-terminal domain which may provide a route of entry for RSV to infect host cells; putative host cell receptors now need to be identified. Although nhSP-A and rfhSP-A were shown to bind BBG2NA, the mechanism through which SP-A neutralises RSV needs to be elucidated with purified recombinant proteins from various RSV strains.

Use of the NT tag with two point mutations (NT^{dm}) allowed the successful production of a functional trimeric rfhSP-D molecule without the requirement for refolding. Importantly, this novel expression method allowed a substantial increase in yields of rfhSP-D produced with a yield equivalent to 31.3 mg/litre of bacteria upon scale up as compared with 3.3 mg/litre obtained through the traditional refolding method; optimisation may further increase yields. rfhSP-D produced using the novel solubility tag prevented infection of RSV by up to 32.2 (± 25.6) % ($p < 0.05$), to a similar level as rfhSP-D produced using the traditional refolding method (37.8 (± 21.7) % ($p < 0.05$)). nhSP-D also reduced infection levels similarly by up to 47.2 (± 25.6) % ($p < 0.001$), suggesting that the N-terminal region and oligomeric structure of SP-D may not provide a route of entry for the virus, unlike for SP-A. nhSP-D bound various known ligands including RSV proteins, recombinant HIV gp120 proteins, inactivated HIV particles, house dust mite extracts, pollen extracts and *H. influenza*, *K. pneumoniae* and *E. coli* LPS.

rfhSP-A may allow the crystal and solution structures of the human SP-A neck and CRD domains to be resolved. Moreover, it could allow the importance of the SP-A N-terminus in its interactions with an array of different pathogens to be investigated. This study has demonstrated the use of NT^{dm} as a novel solubility tag for heterologous protein expression and has potentially increased the commercial viability of rfhSP-D. rfhSP-A and rfhSP-D may have therapeutic potential, particularly as adjunct treatments to current lipid surfactant therapies, which currently lack SP-A and SP-D. rfhSP-A and rfhSP-D could replace the deficient SP-A and SP-D in the neonatal lung and may prevent the emphysematous phenotype associated with neonatal chronic lung disease.

Publication List

Papers

- Heath C, Del Mar Cendra M, **Watson A**, Auger J, Pandey A, Tighe P, Christodoulides M. 2015. Co-Transcriptomes of Initial Interactions *In Vitro* between Streptococcus Pneumoniae and Human Pleural Mesothelial Cells. *Plos One*: 10 (11): p. e0142773.
- Fakih D, Pilecki B, Schlosser A, Jepsen C, Thomsen L, Ormhøj M, **Watson A**, Madsen J, Clark H, Barfod K, Hansen S, Marcussen N, Jounblat R, Chamat S, Holmskov U, Sorensen G. 2015. Protective effects of surfactant protein D treatment in 1,3-β-glucan-modulated allergic inflammation. *Am J Physiol Lung Cell Mol Physiol*: 309(11):L1333-43.

Immunology News

- **Watson A**. 2015. Translational Immunology. 17th International Congress of Mucosal Immunology. *Immunology news, British Society for Immunology*, September 2015 p. 40.
- **Watson A**, Whitwell H. 2013. Translational Immunology. BSI Wessex immunology group meeting. *Immunology news, British Society for Immunology*, May 2013 p. 16-17.

Patents

- Clark H, **Watson A**, Johansson J, Kronqvist N, Rising A, Madsen J. Novel Expression of functional fragments of Surfactant Proteins A and D. *Filed December 2015 (New Great Britain Patent Application No. GB1522610.3).*

Conferences

- American Thoracic Society, USA (13-18th May 2016). Poster presentation: 'First successful expression of a trimeric human fragment of SP-A and demonstration

of its increased efficacy in neutralisation of RSV compared with native human SP-A' Authors: **Watson A**, Spalluto C.M, Kronqvist N, Staples K.J, Johansson J, Wilkinson T.M.A, Madsen J, Clark H.

- 17th International Congress of Mucosal Immunology. Berlin, Germany (14th-18th July, 2015). Poster presentation: Investigating the Interaction of SP-A and SP-D with Respiratory Syncytial Virus in Human Bronchial Epithelial Cells. Authors: **Watson A**, Spalluto C.M, Whitwell H, Staples K.J, Wilkinson T.M.A, Madsen J, Clark H.
- Neonatal meeting (23-24th June 2015). Oral Presentation: 'Investigating the interaction of SP-A and SP-D with RSV for the Development of Surfactant Therapeutics'. Author **Watson A.**
- Faculty Conference. University of Southampton, UK (17th June 2015). Poster presentation: 'Investigating the Importance of the SP-A Oligomeric Structure in RSV Neutralisation'. Authors: **Watson A,** Spalluto C.M, Kronqvist N, Johansson J, Staples K.J, Wilkinson T.M.A, Madsen J, Clark H.
- Annual Oxford Developmental Biology Symposium (9th December, 2014) Poster presentation: 'Investigating the Structure/Function Relationship of Lung Collectins'. Authors: **Watson A**, Kronqvist N, Spalluto C. M, Griffiths M, Staples K.J, Wilkinson T.M.A, Johansson J, Madsen J and Clark H.
- British Society for Immunology Congress 2014. Brighton, UK (1-4th December, 2014). Poster presentation: 'Evaluating the Importance of a Common Surfactant Protein D Polymorphism in Influenza Virus Infection'. Authors: **Watson A**, Madsen J, Clark H.
- South African Immunology Society Infectious Diseases in Africa symposium. Cape Town, South Africa (21-26th October, 2014). Oral presentation and poster: 'Investigating the Importance of the Structure of Lung Collectins in their Interaction with HIV'. Authors: **Watson A**, Kronqvist N, Griffiths M, Staples K. J, Wilkinson T.M.A, Madsen J, Clark H.
- Faculty Conference. University of Southampton, UK (19th June 2014). Oral presentation: 'Investigating the Structure/Function Relationship of Lung Collectins'. Author: **Watson A**.

Contents

List of tables

List of figures

DECLARATION OF AUTHORSHIP

I, Alastair Samuel Watson

declare that the thesis entitled:

“RECOMBINANT EXPRESSION OF FUNCTIONAL TRIMERIC FRAGMENTS OF HUMAN SP-A AND SP-D”

and the work presented in the thesis are both my own, and have been generated by me as the result of my own original research. I confirm that:

- this work was done wholly or mainly while in candidature for a research degree at this University;
- where any part of this thesis has previously been submitted for a degree or any other qualification at this University or any other institution, this has been clearly stated;
- where I have consulted the published work of others, this is always clearly attributed;
- where I have quoted from the work of others, the source is always given. With the exception of such quotations, this thesis is entirely my own work;
- I have acknowledged all main sources of help;
- where the thesis is based on work done by myself jointly with others, I have made clear exactly what was done by others and what I have contributed myself;
- none of this work has been published before submission.

Signed: ……..

Date:…….

Acknowledgements

I would firstly like to thank the Medical Research Council for funding my PhD project. I am extremely grateful to my supervisors Professor Howard Clark and Dr Jens Madsen for their continual support and guidance during my project. I would like to thank the Child Health team, in particular, Dr Zofi McKenzie, Dr Harry Whitwell, Dr Rosie Mackay and Paul Townsend. Thanks to all the fellow PhD students who have helped me along the way and have made my time so enjoyable, particularly Dr Mel Jannaway who I started alongside and Dr Jess the RealRaj Rajaram who has always been there to talk.

Thank you to Prof Janne Johansson for his collaboration during my project and for hosting me at Karolinska Institutet (Sweden) and the rest of his research group for welcoming me and helping me throughout my stay. I would particularly like to thank Dr Nina Kronqvist for her help and guidance during my stay at Karolinska Institutet and her important contribution to this project.

I have benefited from many collaborations. I would like to thank Dr Tom Wilkinson and Dr Karl Staples and their team for their collaboration with the RSV neutralisation work, particularly Dr C Mirella Spalluto for her continual help and support and for making this collaboration possible. Thanks to the Dr Tao Dong research group for collaboration with the HIV work. In particular, to Dr Shoukouh Makvandi-Nejad and Dr Lili Wang for training me in handling HIV. I would like to thank Ian Mockridge and Ruth French for their collaboration and help with the SPR analysis. Thanks to Dr Paul Skipp and Dr Henrik Molina for collaboration and guidance with mass spectrometry work, Dr Mark Griffiths for supplying the BAL and Dr Jane Warner for provision of human lung tissue. I would also like to thank Prof Trevor Greenough, Dr Annette Shrive, Dr Barney Graham, Dr Jason McLellan and Dr Ultan Power for collaboration and provision of reagents.

I would like to thank Johanna Midelet who has supported me during the writing of the thesis and kept my spirits up, particularly through provision of Crêpes! Many thanks to Dr Andy Hutton for his help and support along the way, who alongside my work has succeeded in solving the co-culture equation! Finally I would like to thank my Mum for proof reading my thesis, in addition to my whole family and good friend Emma Trott for their continual support.

Definitions and Abbreviations

A	Adenine
Aa	Amino acid
AFM	Atomic force microscopy
AT2	Aldrithiol-2
ATII	Alveolar type II cell
BAL	Bronchoalveolar lavage
BBG2Na	RSV attachment glycoprotein G core region (aa130–230) fused to BB (a 28-kDa protein corresponding to the albumin-binding region of streptococcal G protein)
BCA	Bicinchoninic acid
BIA	Biomolecular interaction analysis
BS3	Bis(sulfosuccinimidyl)suberate)
BSA	Bovine serum albumin
CD	Cluster of differentiation
Collectin	Collagen containing (group III) lectins
COPD	Chronic obstructive pulmonary disease
CRD	Carbohydrate recognition domain
kDa	kilo Daltons
DAB	3,3′-Diaminobenzidine
DC	Dendritic Cell
Dd	double distilled (e.g. ddH_2O)
DPPC	Dipalmitoylphosphatidylcholine

DTT	Dithiothreitol
E	*Haemophilus Influenzae* Eagan strain
E4A	*Haemophilus Influenzae* Eagan strain mutant 4A which has a truncated LPS structure and exposed core oligosaccharides
EDC	Ethyl-3-(3-dimethylaminopropyl) carbodiimide hydrochloride
EDTA	Ethylenediaminetetraacetic acid
EGTA	Ethylene glycol tetraacetic acid
ELISA	Enzyme-linked immunosorbent assay
EU	Endotoxin unit
F protein	RSV fusion protein
G protein	RSV attachment protein
gp	Glycoprotein
hSP-A	human SP-A, not distinguishing between SP-A1 and SP-A2
HIV	Human immunodeficiency virus
HPRT1	Hypoxanthine Phosphoribosyltransferase 1
HRP	Horse radish peroxidase
HRV	Human rhinovirus
IAA	Iodoacetamide
IAV	Influenza A virus
ICAM1	Intercellular Adhesion Molecule 1
IFN	Interferon, signalling molecule
IL	Interleukin
IMDDCs	Immature monocyte-derived dendritic cells

IPTG	Isopropyl β-D-1-thiogalactopyranoside
LAL	Limulus Amoebocyte Lysate
LPS	Lipopolysaccharide, bacterial cell wall component
LB	Lysogeny broth
ManNAc	N-Acetyl-D-mannosamine
MaSP	Major ampullate spidroins of spider silk
MBL	Mannan-binding lectin
MBP	Maltose-binding protein
Min	Minute(s)
MOI	Multiplicity of infection
mU	Milli units (used for measurement of enzyme and optical density)
MWCO	Molecular weight cut off
N187S	An Asn187Ser mutation, in SP-A this removes the glycosylation site within the CRD. This was originally included in rfrSP-A due to expression in eukaryotic systems to prevent aberrant glycostylation but also included in some constructs in this study.
NHS	N-hydroxysuccinimide
nhSP-A	Native human surfactant protein A
nhSP-D	Native human surfactant protein D
NT	N-terminal domain of spider silk protein, currently being investigated for use as a solubility tag for of heterologous protein expression
NT-rfhSP-A(1)	Fusion protein of NT with recombinant fragment of human surfactant protein A1. Due to only rfhSP-A1 being used it is referred to as simply NT-rfhSP-A in Chapters 5, 6 and 7

NT-rfhSP-D	Fusion protein of NT with recombinant fragment of human surfactant protein D
NT^{dm}	NT domain with double mutant with the two point mutations: Asp40Lys and Lys65Asp
$NT_{(opt)}$	NT with optimised codons for E. coli expression. Referred to briefly to distinguish between wild type NT codon usage and optimised codons. Due to the increased levels of expression, $NT_{(opt)}$ was taken forward for future use and referred to simply as NT in Chapters 5, 6 and 7
NT^{dm}-rfhSP-A(1)	Fusion protein of NT^{dm} and rfhSP-A using rfhSP-A1. Due to only rfhSP-A1 being used it is referred to simply as NT^{dm}-rfhSP-A in Chapters 5, 6 and 7
NT^{dm}-rfhSP-D	Fusion protein of NT^{dm} and rfhSP-D
NVCL	Non-viral cell lysate, lysate of cells used to amplify virus
OD	Optical density
OGP	Octyl β-D-glucopyranoside
PAGE	PolyAcrylamide Gel Electrophoresis
PAP	Pulmonary alveolar proteinosis
PC	Phosphatidylcholine
PCR	Polymerase chain reaction
PGB1	56-residue B1 domain of bacterial membrane protein G
PVDF	Polyvinylidene difluoride
rfhSP-A	Recombinant fragment of human surfactant protein A. Importantly, due to rfhSP-A1 only being taken forward for purification and subsequent characterisation, in Chapters 5, 6 and 7, rfhSP-A1 is referred to simply as rfhSP-A (both as fusion proteins with NT and NT^{dm} and after purification)

rfhSP-A1	Recombinant fragment of human surfactant protein A composed of only surfactant protein 1.
rfhSP-A2	Recombinant fragment of human surfactant protein A composed of only surfactant protein 2
rfhSP-D	Recombinant fragment of human surfactant protein D
rfrSP-A	Recombinant fragment of rat surfactant protein A
RDS	Respiratory distress syndrome
RPM	Revolutions per minute
RSV	Respiratory syncytial virus
RU	Response units, giving an indication of levels of analytes binding during surface plasmon resonance analysis
SD	Standard deviation
SDS	Sodium dodecyl sulphate
Sec	Second(s)
Sendai F	Sendai virus expression RSV F protein
Sendai G	Sendai virus expressing BBG2Na
SFTPA1	Homo sapiens surfactant protein transcript variant 1
SFTPA2	Homo sapiens surfactant protein transcript variant 2
SIRP	Signal-regulatory protein
SP-A	Surfactant Protein A
$SP\text{-}A^{-/-}$	Surfactant protein A deficient genotype
SP-B	Surfactant protein B
SP-C	Surfactant protein C
SP-D	Surfactant protein D

SP-D$^{-/-}$	Surfactant protein D deficient genotype
SPR	Surface plasmon resonance
TAE	Tris-acetate-EDTA
TBS	Tris buffered saline (20 mM Tris, 150 mM NaCl, pH 7.4)
TBSC	TBS with 10 mM $CaCl_2$
TBSE	TBS with 50 mM EDTA
TBW	Tris buffered water (5 mM Tris, pH 7.4)
TEM	Transmission electron microscopy
Th	T helper cell, characterised by the cytokine profile produced by the T cell (e.g. either Th1 or Th2 cytokines)
TLR	Toll-like receptor
V/v	Volume/volume
W/v	Weight/volume
W/w	Weight/weight
X-gal	5-bromo-4-chloro-3-indolyl-β-d-galactopyranoside

Chapter 1: Introduction

1.1 The Immune System of the Lung

The average person inhales 10,000 litres of air each day. The lungs have an approximate surface area of 60 m^2 and are, therefore, continually exposed to an array of different pathogens, oxidants, pollutants and allergens which contaminate this air. These need to be efficiently cleared without damaging the delicate alveoli and impacting on gaseous exchange, this is the role of the lung mucosal immune system (1). The immune system is comprised of both innate and adaptive components. The adaptive immune system is comprised of highly specific cells which target antigens through the production of antibodies (as is the case for B cells) or elicit cell mediated immunity (as is the case for T cells). Together the adaptive immune system adapts and learns to recognise specific antigens on pathogens to provide effective lasting immunity upon exposure to an antigen. However, upon encounter of an antigen for the first time, an effective adaptive immune response can take time to be elicited.

Comparative to the highly specific adaptive immune system, the innate immune system is a primordial system which has broad specificity and is immediately responsive. The innate immune system is the first line of defence against pathogens and is comprised of anatomical physical barriers such as the mucociliary escalator, cellular components which phagocytose micro-organisms such as macrophages and soluble components such as antimicrobial peptides and innate immune proteins. The innate immune system of the lung provides an immediate barrier to infectious agents and calls upon the adaptive immune system only upon failure of the innate immune system to clear the pathogen. This minimises inflammation and aberrant adaptive responses and is essential for the lung to function effectively in gaseous exchange. This project focuses on surfactant proteins A and D which are essential innate immune proteins found in pulmonary surfactant. These have important roles in both preventing infection and modulating the immune system.

1.2 General Scope of the Project

Pulmonary surfactant is an essential component of the lung and forms a mobile-liquid phase which covers the alveolar epithelium to reduce surface tension and enable breathing (2, 3). Surfactant is a complex mixture of lipids (approximately 90 %) and proteins (approximately 10 %). Surfactant protein A and D (SP-A and SP-D) are known for their

roles both as innate immune molecules and as modulators of the immune system. However, they are not present in current pulmonary lipid surfactant therapeutics for treating premature neonates with surfactant deficiency (4-6). Up to 63 % of babies born < 26 weeks go on to develop major adverse outcomes including chronic lung disease at 36 weeks, neuromorbidity and retinopathy (7). The development of recombinant versions of SP-A and SP-D may show therapeutic potential as adjunct treatments to the currently available lipid surfactants. This could allow the replacement of SP-A and SP-D (deficient in the neonatal lung) and help prevent the emphysematous inflammatory phenotype associated with neonatal chronic lung disease. Furthermore, the development of recombinant versions of SP-A and SP-D will allow the delineation of their structure/function relationship, particularly the role of the N-terminal region and oligomeric structure in both maintaining lung homeostasis and interacting with pathogens to prevent infection, for example respiratory viruses.

1.3 Discovery of Pulmonary Surfactant

The presence of pulmonary surfactant in the lung was first proposed by von Neergaard in 1929 (8). von Neergaard demonstrated the importance of interfacial forces by comparing the recoil pressure of lungs filled with air to those filled with aqueous solution. However, it was not until 1955 that Pattle identified pulmonary surfactant (2, 9). Pattle described surfactant as a film of microbubbles which reduced surface tension in the lung. In 1961 Pattle and Thomas discovered pulmonary surfactant to be a mixture of both lipids and proteins (2, 9).

1.4 Synthesis and Assembly of Pulmonary Surfactant

Pulmonary surfactant is synthesised, predominately, in alveolar type II (ATII) cells within the endoplasmic reticulum (10, 11). After cellular trafficking, surfactant is stored intracellularly in organelles called lamellar bodies (12). Surfactant is then secreted into the alveolar space to form an intermediate lattice structure termed tubular myelin. Tubular myelin spreads along the air-liquid interface and acts to stabilise the collapsing pressures exerted on the epithelial side of the air-blood barrier (13). Pulmonary surfactant is continuously being reabsorbed by ATII cells and alveolar macrophages but in ATII cells it is stored and recycled (12, 13). It is because of this that treatment with exogenous surfactant has been proposed to stimulate cellular maturation and activate the endogenous surfactant recycling machinery (14, 15).

1.5 Surfactant Lipids

The lipid component of pulmonary surfactant is comprised of approximately 80 % phospholipids, predominantly phosphatidylcholine (PC) in the form of dipalmitoylphosphatidylcholine (DPPC). DPPC forms a film at the air-liquid interface and is the primary surface-tension reducing agent in surfactant (16, 17). DPPC has the capacity for high density packing at physiological temperatures which allows the expulsion of water molecules and reduction in surface tension. Pulmonary surfactant also contains neutral lipids which constitute 5-10 % of the lipid component. The major species of neutral lipids is cholesterol which is thought to be important in surfactant membrane structure and ordering of phospholipids (17, 18).

1.6 Surfactant Proteins

Four surfactant proteins have been described, SP-A, surfactant protein B (SP-B), surfactant protein C (SP-C) and SP-D. These proteins constitute 5.3 %, 0.7 %, 0.4 % and 0.6 % of the mass of pulmonary surfactant, respectively (10, 19). SP-B ((14 kDaltons (kDa)) and SP-C (6 kDa) are small hydrophobic proteins. These protein have vital roles in packaging of surfactant into lamellar bodies and transfer of phospholipids to the air liquid interface (20, 21); reviewed in (17).

In this project, I investigate the interaction of SP-A and SP-D with various known ligands, in particular respiratory syncytial virus (RSV). SP-A was first identified by King and Clements in 1972 (22). However, it was not until 1988 that, during primary culture of rat ATII cells, Persson et al. identified and characterised SP-D (originally referred to as CP4) (23). SP-A and SP-D are large hydrophilic proteins, 35 kDa and 43 kDa, respectively. These proteins have important functions as innate immune molecules and in prevention of aberrant inflammation, reviewed in (4-6).

1.7 SP-A and SP-D Structure

The human SP-A and SP-D genes are located on the long arm of chromosome 10 at the 10q22-23 locus. There are two SP-A genes, *SFTPA1* and *SFTPA2* which code for the 248 amino acid SP-A1 and SP-A2 proteins, respectively. Comparatively, there is one *SFTPD* gene which encodes for the 375 amino acid protein SP-D. SP-A and SP-D form heterotrimeric and homotrimeric basic functional units, respectively. Importantly, the SP-A1:SP-A2 composition of the SP-A heterotrimer has not been quantifiably identified using an appropriate technique, such as mass spectrometry. The trimeric subunits form higher-order oligomers through interactions with their N-terminal domains as discussed in Section 1.7.4.

SP-A and SP-D are **col**lagen containing (group III) **lectins**, referred to as **collectins**. Collectins are a family of Ca^{2+}-dependent (C-type) carbohydrate-binding soluble pattern-recognition receptors, which fulfil important roles in innate immune defence (24, 25). They are characterised by the presence of four domains, an N-terminal region, a collagenous region, an α-helical coiled-coil region (‘neck’) and a C-terminal lectin domain (also known as a carbohydrate recognition domain (CRD)) (Figure 1-1) (26). Other collectins include mannan-binding lectin (MBL), conglutinin, bovine collectin-43 kDa, collectin-46 kDa, collectin liver 1, collectin placenta 1 and collectin kidney 1 (or collectin 11) (22, 27, 28).

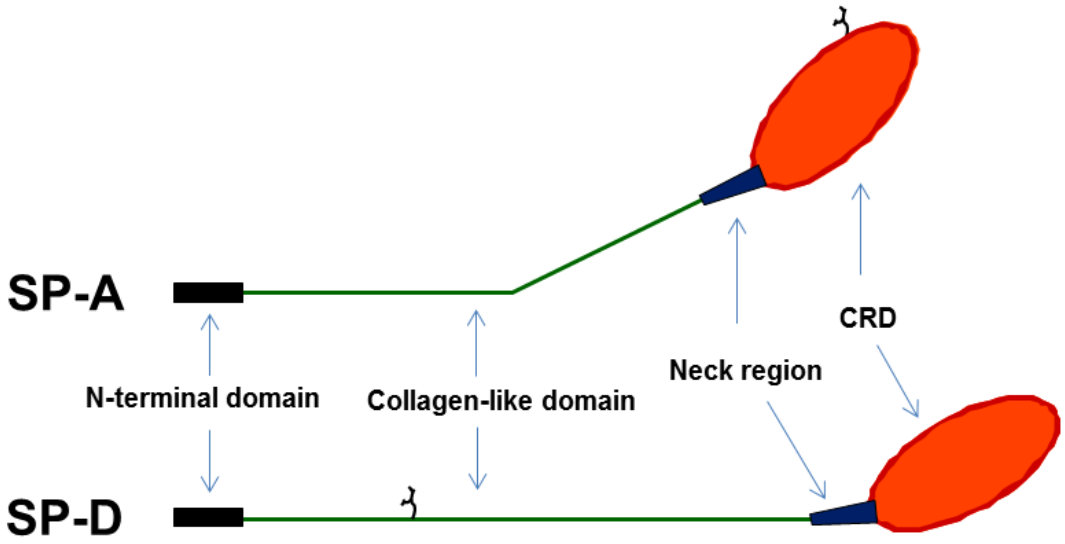

Figure 1-1: Schematic of SP-A and SP-D domains. *The four domains of SP-A and SP-D can be seen: N-terminal domain (black), collagen-like domain (green), neck region (blue) and CRD (red). Also indicated are the Asn187 and Asn70 glycosylation sites for SP-A and SP-D, respectively (Ψ).The collagen-like domain is shorter for SP-A than SP-D and contains a bend. Monomeric proteins are shown in the figure; SP-A and SP-D form functional trimeric units. Figure is not to scale.*

1.7.1 Carbohydrate Recognition Domain

Collectins characteristically interact with ligands in a calcium-dependent manner through their globular CRD. The collectin CRD contains four cysteine residues which form two disulphide bridges to allow independent assembly of their structure. The CRD is composed of two anti-parallel β sheets. One β sheet is located at the N-terminal part of the domain and consists of four strands and is flanked by two helices. The second β sheet is five-stranded and forms the carbohydrate binding site alongside a structural loop structure which is distal from the trimer centre (Figure 1-2). Interestingly, SP-A contains a 5-10 kDa glycosylation at Asn187 which has been shown to be important for interaction with influenza A virus (IAV); this glycosylation site is absent in SP-D (29, 30) (Figure 1-1).

A recombinant fragment of human SP-D (rfhSP-D) containing the SP-D CRD has been crystallised both in the native conformation and bound with a simple carbohydrate ligand; the composition and functions of rfhSP-D are further discussed in Sections 1.11 and

1.13.1 (31). These X-ray crystallography structures have provided an insight into the structure of the SP-D CRD and neck. A recombinant fragment of rat SP-A (rfrSP-A) has been produced and the crystal structure determined (32). However, an equivalent functional trimeric recombinant fragment of human SP-A (rfhSP-A) has not to date been successfully produced.

An important difference between the CRD of rfhSP-D (120 amino acids) and rfrSP-A (118 amino acids) is the planar surface of the trimeric unit for ligand recognition. Compared with the Y-shaped rfhSP-D planar surface, the surface of rfrSP-A is more widely spaced, with the CRD more closely packed to the neck and in a T-shape (Figure 1-2). The crystal structure of rfhSP-D contains more extensive stabilising interactions across the neck-CRD interface than rfrSP-A (4). In addition, rfhSP-D contains a funnel formed by the three CRDs in the centre of the trimeric rfhSP-D. Here, the three Glu232 residues in the trimer, in cooperation with three water molecules, coordinate a Ca^{2+} ion into the bottom of this funnel at calcium concentrations above 2 mM (31). This acts as a molecular switch to reduce the neutralizing effect of the Glu232 residues exerted on the Lys246 residues to alter the charge distribution on the CRD interface allowing ligand binding. This funnel is absent in rfrSP-A (32) (Figure 1-2).

Three further calcium binding sites per CRD of the rfhSP-D trimer have also been identified; the primary calcium binding site is the site of interaction with terminal monosaccharaides. However, although an equivalent primary calcium binding site has been identified for rfrSP-A, equivalent secondary and tertiary calcium binding sites have not (Figure 1-2) (32).

rfrSP-A

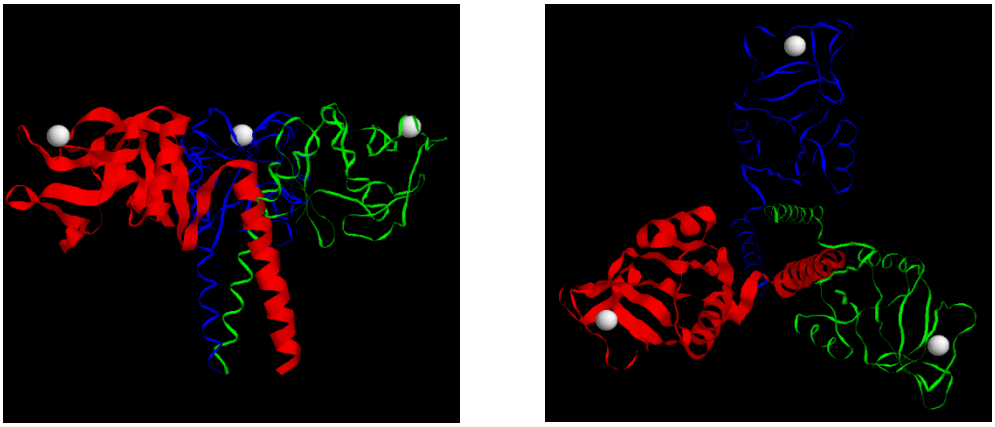

rfhSP-D

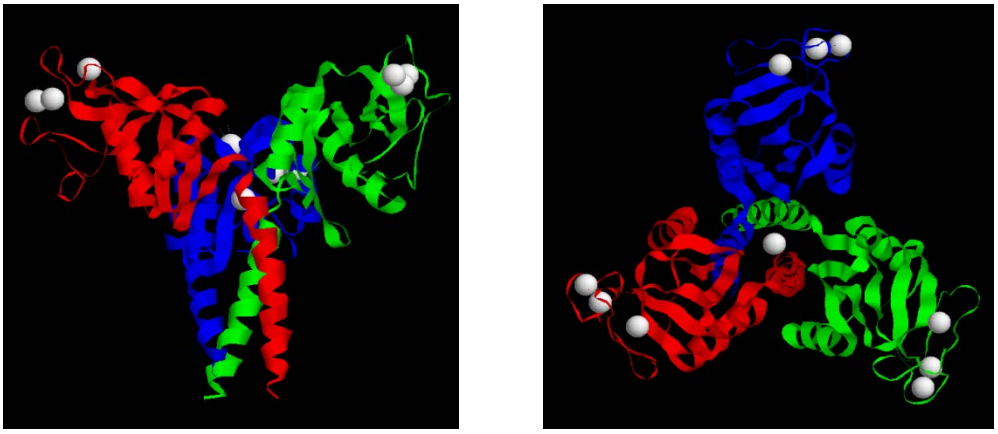

Figure 1-2: Crystal structures of rfhSP-D and rfrSP-A. *Ribbon diagrams of rfrSP-A and rfhSP-D crystal structures are shown (31, 32). Each monomeric unit is coloured separately. Calcium ions are coloured in white. Each monomer within rfhSP-A contains one calcium binding site compared to the three calcium binding sites of monomer of rfhSP-D. An additional calcium binding site is also present within the central funnel of the rfhSP-D trimer; this is absent in rfrSP-A. Differences in planar surfaces can be seen between the Y-shaped surface of rfhSP-D and the T-shaped surface of rfrSP-A. Ribbon chains for each monomer of rfrSP-A are of different thicknesses due to the information within the available PDB file. Figure was created using Raswin (version 2.7.5.2). Crystallography data was obtained from the NCBI (structure) database as PDB files (PDB ID 1R13 and PDB 1PWB for rfrSP-A and rfhSP-D, respectively) (31-33)*

1.7.2 Neck Region

The SP-A and SP-D neck regions are composed of 29 amino acid (aa) residues and 33 aa residues, respectively. The neck connects the globular CRD with the collagen-like domain and consists of 8 alpha-helical turns which are formed upon arrangement of the polypeptide chains in parallel. Each polypeptide chain contains a characteristic ‘a-b-c-d-

e-f-g' heptad repeat pattern whereby amino acid residues 'a' and 'd' are generally hydrophobic. These hydrophobic residues form the interface of the alpha-helical coil and interact to stabilise the neck.

The SP-A and SP-D necks act as initiation points for trimerisation and nucleate the formation of the collagen-like triple helix towards the N-terminus in a zipper-like fashion (34, 35). The importance of the SP-D neck region in trimerisation has been illustrated by its ability to drive trimerisation and stabilisation of thioredoxin, a non-collagenous heterologous protein (36). The collectin neck is also thought to be important for the relative orientation of the CRDs and thus the ability to recognise and bind antigen (37) in addition to binding to phospholipids (38).

1.7.3 Collagen-like Domain

The collectin collagen-like domain is composed of Gly Xaa Yaa repeats whereby 'Xaa' and 'Yaa' can be any amino acid, but most frequently proline. The SP-A collagen-like domain consists of 24 Gly Xaa Yaa repeats compared with the 59 repeats of SP-D. Each of the chains in the collectin trimer forms a polyproline II-like left-handed helix which are intertwined to form an approximately 4 nm diameter right-handed super helix (39). This structure is stabilised by interchain hydrogen bonds which form between the C-terminus of amino acids at position 'X' and the N-terminus of the glycine residues which face into the centre of the helix. The collagen-like domain is rich in hydroxylated proline and lysine residues, particularly at position 'Y'. These residues have been shown to stabilise the collagen-like domain (40-43). The rfhSP-D contains a short collagen-like stalk which is thought to act as an anchor to stabilise its trimeric structure. Importantly, this collagen-like stalk has been shown to be essential for its function *in vivo* at preventing emphysema-like morphological changes in the SP-D knock out mice as a fragment lacking the stalk was not effective (44). In generation of a functional trimeric rfhSP-A molecule, in this present study, it is hypothesised that such a collagen-like stalk would also be required.

In human SP-A, the Gly Xaa Yaa repeats are interrupted after the 12^{th} repeat causing a bend in the collagen-like helix. This bend is frequently referred to as the 'hinge region' and has implications for the structure of SP-A higher-order oligomers (45). SP-D contains

a glycosylation site within the collagen-like domain at Asn70 which is absent in SP-A (39, 46).

1.7.4 N-terminal Domain and Oligomeric Structure

The N-terminal domains of SP-A and SP-D are 7 and 25 amino acid residues, respectively. These N-terminal domains interact and form disulphide bonds to allow the formation of higher-order oligomeric structures (Figure 1-3). SP-A oligomers form through 6 trimeric units which arrange in register to create octadecameric structures and are stabilised through hydrogen bonds between the N-terminal half of the collagen-like domains. A kink in the collagen-like domain results in a structure similar to MBL and the complement component C1q (47). This structure is thought to resemble a bouquet of tulips (Figure 1-3) and is integral to the formation of tubular myelin (17). The structure of bovine SP-A has been reported to be in either an open or closed formation depending on the presence of calcium ions (48). SP-D, contrastingly, forms a dodecameric cruciform structure through association of 4 functional trimeric units (49). SP-D can then further oligomerise to form ‘stellate multimers' which resemble a bicycle wheel comprised of up to 32 trimeric units (Figure 1-3).

Oligomerisation is important for many pulmonary collectin functions, particularly as it both increases the avidity of ligand binding and increases their capacity for agglutination (33, 50-55). The importance of oligomerisation was highlighted by the discovery that a common methionine/threonine polymorphism in the *SFTPD* gene at amino acid position 11 had a significant impact on the capacity for SP-D to form higher-order oligomers and to bind gram positive and gram negative bacteria in addition to IAV (54).

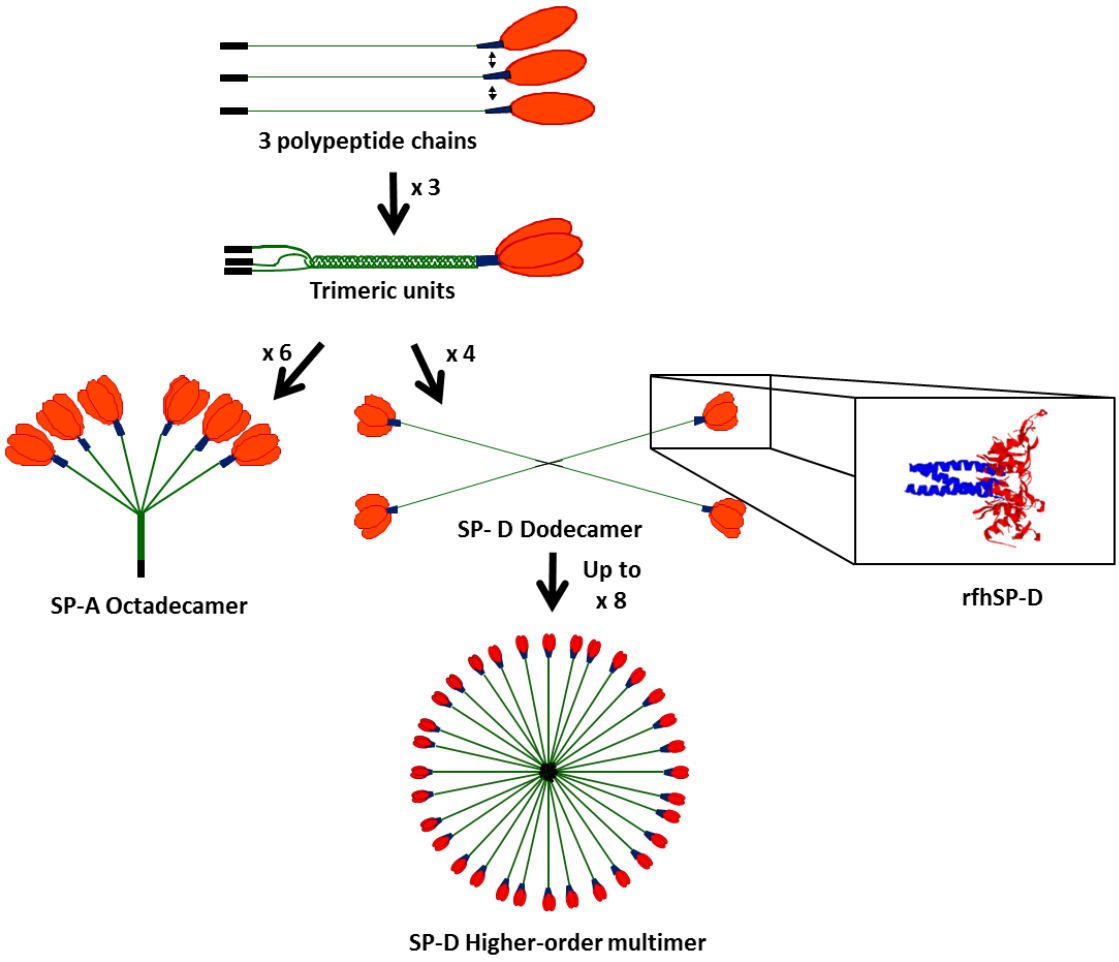

Figure 1-3: Schematic of collectin oligomerisation. *The different oligomeric states of SP-A and SP-D are shown in addition to the crystal structure of rfhSP-D (this includes the head and neck, the 8x Gly Xaa Yaa repeats of the collagen-like region which are part of rfhSP-D were not crystallised) (32). SP-A and SP-D form trimeric subunits. SP-A octadecameric are then formed by interaction of 6 of these trimers. SP-D dodecamers form through interaction of 8 trimers and can further oligomerise to form higher-order multimers composed of up to 32 trimeric subunits. Figure is not to scale.*

1.8 SP-A and SP-D Interaction with Monosaccharides

The specificity of SP-A and SP-D to different monosaccharides has been assessed using mannan coated plates and inhibiting binding to these plates by the addition of various soluble monosaccharides. Human SP-A has been shown to have the highest binding to ManNAc followed by L-fucose, maltose, glucose and mannose, respectively (56). There are mixed reports about the capacity of human SP-A to bind N-Acetylgalactosamine and N-Acetylglucosamine. Importantly, human SP-A is composed of two different gene

products, SP-A1 and SP-A2. Differences between binding preferences of these two genes have been shown with SP-A2 reported to bind to N-Acetylgalactosamine and N-Acetylglucosamine with a higher affinity than SP-A1 (57). Human SP-D has also been reported to have highest affinity to ManNAc followed by maltose, glucose, mannose, myo-inositol, galactose and N-acetyl-glucosamine respectively (58). Notably, species-specific differences in human and rat SP-D have been illustrated, with rat SP-D having a higher preference for binding to myo-inositol, maltose and glucose than ManNAc (58).

1.9 SP-A and SP-D Interactions with Lipids

SP-A predominantly recognises ordered patterns of lipids and is important for the formation of tubular myelin, a highly ordered surfactant structure (17, 59). Indeed, it has long been accepted that SP-A specifically binds to DPPC; this interaction has been shown to be through both the neck and the CRD of SP-A (60, 61). SP-A has also been shown to bind several glycolipids and glycosphingolipids (62, 63). Although SP-D binds to phosphatidylinositol and glucosylceramide in a calcium-dependent manner, it does not strongly interact with other phospholipid components (63, 64). Importantly, the strong interaction of SP-A but not SP-D with phospholipids allows their separation in bronchoalveolar lavage (BAL) samples by a simple centrifugation step (65). This has allowed the purification of SP-A and SP-D and subsequent investigation of structure and function. A list of lipid ligands with which SP-A and SP-D interact with is given in Table 1-1.

Collectin	Lipid	Reference(s)
SP-A	DPPC	(66)
	Lipid A (LPS)	(67)
	Glycolipids (galactosylceramide, lactosylceramide)	(62, 68)
	Phosphatidylglycerol	(69)
	Phosphatidylserine	(70)
SP-D	Phosphatidylinositol	(61, 64, 71)
	Glucosylceramide	(72, 73)
	Galactosylceramide	

Table 1-1: Summary of pulmonary collectin lipid ligands. *Lipid ligands which SP-A and SP-D have been shown to bind to are listed, as are relevant references in which this interactions were shown. Figure adapted from a review by Jakel in 2013 (74).*

1.10 SP-A and SP-D Receptors

The search for collectin receptors has been on-going since discovery of the proteins. SP-A and SP-D are 'sticky' proteins and strongly interact with various lipids, carbohydrates and protein ligands. Many SP-A and SP-D soluble protein binding partners have been identified. In addition, SP-A and SP-D have been shown to interact with cell-surface receptors of various cell types including ATII cells, macrophages and neutrophils. The functional consequences of many of these interactions still, however, needs to be elucidated. Moreover, the receptors which mediate many of the functions of the lung collectins are still to be identified. A list of proteins which have been found to interact with SP-A and SP-D is given in (Table 1-2).

	Protein	Interacting collectin	Reference (s)
Receptors			
	Surfactant protein receptor-210	SP-A	(75)
	Toll like receptor (TLR)4 and MD-2	SP-A	(76)
	Complement receptor 3 (Cluster of differentiation (CD)11b CD18)	SP-A	(77)
	C1qRp	SP-A	(78, 79)
	Signal-regulatory protein (SIRP)-alpha	SP-A / SP-D	(80)
	ATII receptors	SP-A / SP-D	(81-83)
	CD14	SP-A / SP-D	(84)
	Calrecticulin-CD91 complex	SP-A / SP-D	(85-88)
Other ligands			
	Immunoglobulins	SP-A	(89)
	Decorin	SP-A	(90)
	Defensins	SP-D	(91, 92)
	gp340/DMBT1	SP-A / SP-D	(93, 94)
	Myeloperoxidase	SP-A / SP-D	(95)
	C1q	SP-A / SP-D	(96, 97)
	MFAP4	SP-A / SP-D	(98, 99)

Table 1-2: Summary of SP-A and SP-D protein ligands and receptors. *Listed are receptors and other protein ligands which SP-A and SP-D have been shown to bind to and interact with; relevant references where these interactions have been illustrated are also shown. This Figure was adapted from a review by Jakel in 2013 (74). A receptor is defined as a cell-surface protein which, upon interaction of SP-A or SP-D, transmits a signal to a cell. Proteins which do not transmit a signal are termed 'other ligands'.*

1.11 SP-A and SP-D Function

1.11.1 Interaction with Pathogens

SP-A and SP-D bind to a wide variety of pathogens including gram negative and gram positive bacteria, viruses and fungi. In 1990 van Iwaarden et al. highlighted the importance of SP-A as an opsonin which enhanced the phagocytosis of *Staphylococcus aureus* by rat macrophages (100). Kuan et al. then identified that SP-D bound to and agglutinated *Escherichia coli* (Y1088) in a calcium-dependent manner (101). Since these early experiments, both SP-A and SP-D have been shown to opsonise and agglutinate an array of different pathogens; a summary of pathogens which SP-A and SP-D interact with is given in Table 1-3 and Table 1-4, respectively. Importantly, the binding of lung collectins to bacteria has been shown to occur through different mechanisms. Although lipopolysaccharide (LPS) is a ligand for both SP-A and SP-D, SP-A has been shown to interact preferentially with the Lipid A moiety of LPS on gram negative bacteria (102). Contrastingly, SP-D interacts with the core oligosaccharides (101) . Thus, both SP-A and SP-D are known to bind rough LPS more effectively than smooth LPS due to the exposed lipid A and core oligosaccharides.

The capacity for SP-A and SP-D to bind glycosylated proteins on the surface of viral capsids is becoming increasingly understood. This is particularly the case for various enveloped RNA viruses including RSV, HIV and IAV. These interactions can lead to neutralisation through prevention of their glycosylated attachment proteins from binding to the host cell. This can prevent viral entry whilst enhancing their aggregation, opsonisation and clearance by phagocytes (103). Below I discuss in further detail the interaction of SP-A and SP-D with different viruses, particularly RSV (Subsection 1.11.2), which is the main focus of this study.

Microbial target	**Reference(s)**
E. coli J5	(104)
S. aureus	(105)
Streptococcus pneumonia	(106)
Group A *Streptococcus*	(107)
Group B *Streptococcus*	(108, 109)
Haemophilus influenza Type A	(107)
Klebsiella pneumoniae	(110)
Pseudomonas aeruginosa	(111, 112)
Mycoplasma pulmonis	(113)
Mycobacterium tuberculosis	(114)
Influenza virus Type A	(115)
Herpes Simplex virus	(116)
HIV	(117)
RSV	(118)
Aspergillus fumigatus	(119)
Pneumocystis carinii	(120)
Cryptococcus neoformans	(121)

Table 1-3: Summary of pathogens which SP-A interacts with. *Listed is a summary of pathogens which SP-A interacts with. This figure was adapted from a paper by Clark et al. in 2004 (122).*

Microbial target	Reference(s)
E. coli J5	(101)
Salmonella minnesota	(101)
H. influenzae Type A	(107)
K. pneumonia	(123)
P. aeruginosa	(124)
Helicobacter pylori	(125)
M. tuberculosis	(126)
Influenza virus Type A	(127)
Respiratory Syncytial Virus	(128)
HIV	(129)
Pneumocystis carinii	(130)
Aspergillus fumigatus	(131)
Cryptococcus neoformans	(121)

Table 1-4: Summary of pathogens which SP-D interacts with. *Listed are a summary of pathogens which SP-D interacts with. This figure was adapted from a paper by Clark et al. in 2004 (122).*

1.11.2 Interaction with RSV

RSV is a highly prevalent virus which primarily infects the immunocompromised, including young children and premature neonates, and is an important cause of chronic obstructive pulmonary disease (COPD) exacerbations (132). RSV is a virus with high infectivity tropism to the superficial respiratory epithelium and causes pathology induced by the cytopathic effects of viral infection in addition to aberrant inflammatory responses in the host. There is also compelling evidence that both host innate and adaptive immune factors are also central to pathogenesis, reviewed in (133).

1.11.2.1 *Introduction to RSV Infection*

RSV is known to alter macrophage and dendritic cell (DC) biology to reduce the production of interferon (IFN)s and interleukin (IL)-12. RSV produces IFN antagonists

and increases the secretion of IL-10, IL-11 and prostaglandin E2, thus skewing the T helper cell (Th)2/Th1 balance. This decreased ability for IFN sensing of the virus, skewing of the Th2/Th1 balance and exaggerated inflammatory processes are important pathogenic features of RSV infection and lead to narrowing of the airways and clinical symptoms of bronchiolitis (134).

It is still unclear as to which host cell molecule(s) is/are the 'RSV receptor(s)' to allow entrance of the virus to the host cell. However, various molecules have been proposed, including intercellular adhesion molecule (ICAM)-1 (135), heparin (136), annexin II (137), TLR4 (138) and fractalkine receptor (CX3CR1) (139). Cell surface glycosaminoglycans, particularly heparan sulphates, have been shown to be important for infection (140). The highly glycosylated G protein (approximately 80-100 kDa) of RSV is important in targeting the ciliated cells of the airways. Comparatively, the glycosylated trimeric RSV F protein formed of two disulphide-linked subunits, F_1 (55 kDa) and F_2 (20 kDa), is important for fusion of the virus to the target cell. RSV F protein is a type I fusion protein and has a metastable structure in its pre-fusion conformation. RSV F protein undergoes substantial structural rearrangement allowing entry into the host cell to form a highly stable post-fusion structure (141).

The RSV G protein is highly glycosylated, these glycosylations shield the protein backbone from antibody neutralisation. Upon infection, a soluble G protein is also produced to act as a decoy to help elude the immune system. The RSV G protein has been shown to have important roles in antagonism of fractalkine to prevent the influx of NK cells, $CD4^+$ T cells and $CD8^+$ T cells. Moreover, it has been shown to suppress inflammatory responses to agonists of TLR2, TLR4, and TLR9, thus preventing detection of the virus (133). Contrasting to the G protein, the RSV F protein binds to TLR4 and CD14 and initiates signalling to induce inflammation.

A humanised monoclonal antibody directed against the RSV F protein (palivizumab) has been established for therapeutic purposes. However, treatment with this antibody is only recommended for children at increased risk of severe disease and is not effective in the treatment of active infection (142). Other treatments have also been ineffective, including ribavirin, which is only routinely used for treatment of immunocompromised individuals. Antibodies directed against RSV G protein are now being investigated due to their

capacity to decrease the virus-induced host inflammatory response and improve outcomes in mice (143).

1.11.2.2 *The Interaction of SP-A and SP-D with RSV*

Genetic polymorphisms for SP-A and SP-D genes have been shown to associate with susceptibility to severe RSV infection, highlighting their importance in the immune response to RSV (144). SP-$A^{-/-}$ and SP-$D^{-/-}$ mice have been generated and shown to have both a decreased capacity for RSV clearance and an increased inflammatory response within the lung (118, 145).

nhSP-D has been shown to bind to Vero cells infected with vaccinia virus expressing F or G proteins of RSV (145). nhSP-D also enhanced phagocytosis of RSV by mouse alveolar macrophages and increased oxygen radical production. A rfhSP-D has been shown to bind to the RSV G protein in a calcium-dependent manner through its CRD. This reduced viral titres both *in vitro* and in a mouse model (128). However, this rfhSP-D was produced in a different way to the well-established rfhSP-D used in this study as it was expressed as a fusion protein with maltose binding protein (MBP). SP-A has been shown to enhance the uptake of RSV by monocytes and macrophage cell lines. This was shown to reverse IL-10 production and TNF-α production suppression attributed to infection of macrophage cell lines in the absence of SP-A (146). SP-A has also been shown to bind RSV through the G protein in a calcium-dependent manner to neutralise infectivity and enhance clearance *in vivo* (118, 147). However, a contradictory study has shown SP-A to reduce RSV infection through binding to the fusion (F) protein of RSV but not the G protein (147). Moreover, it has been suggested that SP-A may facilitate RSV entry to cells in an *in vitro* HEp-2 cell infection model (148). In this present study it was hypothesised that SP-A is important for neutralisation of RSV but may also provide a route of entry for RSV, mediated via its N-terminal domain and oligomeric structure which interact with putative receptors for SP-A on the cell surface. Alternatively, enhanced RSV agglutination may result in enhanced uptake of RSV by the cell through endocytosis.

The interaction of SP-A and SP-D with RSV has until now been studied in either HEp-2 cells, monocytes, U937 macrophages or *in vivo* mouse models (128, 146). There is a substantial lack of studies looking at the interaction of SP-A and SP-D with RSV in other relevant human models of the bronchial epithelium. Through generation of a recombinant

version of SP-A lacking the N-terminal domain, this study aims to elucidate the importance of the N-terminal domain in the capacity of SP-A and SP-D to either neutralise or provide a route of entry for RSV in a relevant *in vitro* model of bronchial epithelial cells.

1.11.3 Interaction with Other Viruses

SP-A and SP-D are also important in interacting with other viruses. The interaction of SP-A and SP-D with IAV is well characterised. SP-D binds to high-mannose oligosaccharides in proximity to sialic acid binding sites of hemagglutinin and can therefore neutralise IAV by sterically inhibiting attachment of IAV to host cells (127, 149). SP-D has also been shown to bind to neuraminidase; this could potentially inhibit the release of viral progeny through restricting enzyme activity (150). Moreover, SP-D has been shown to enhance clearance of IAV by neutrophils (151). SP-A has also been shown to neutralise IAV. However, this was shown to be through a calcium-independent mechanism by interaction with its sialyated glycan on Asn187 within the CRD (152). SP-D binds and aggregate SARS virus, this was suggested to be through direct interaction with the viral spike glycoprotein (153). SP-A, however, has been shown to bind to the herpes simplex virus through its N-linked oligosaccharides and enhances uptake by rat alveolar macrophages (116). In addition to the lung alveoli, SP-A and SP-D are expressed on most other mucosal surfaces including the vaginal mucosa (154-156), this could therefore, be a relevant mechanism for the clearance of herpes simplex virus within the female reproductive tract.

SP-A and SP-D could also be important mediators of HIV infection both at the primary site of infection, the female genitourinary tract, and in the lung, a common HIV reservoir site (157, 158). Both SP-A and SP-D have been shown to bind to HIV envelope glycoprotein (gp)120 in a calcium-dependent manner. Moreover, they were shown to neutralise HIV and prevent direct infection of a T-cell-like line, PM1. Surprisingly, however, SP-A and SP-D enhanced the infection of immature monocyte-derived dendritic cells (IMDDCs) and upon culture with PM1 cells, transfer to the T cell line was subsequently increased (117, 129). This suggests that SP-A and SP-D are effective in preventing direct infection of T cells. However, HIV manages to utilise SP-A and SP-D to infect T cells through transfer from iMDDCs. The mechanism by which the collectins enhance this transfer, however, has not been elucidated. This enhanced uptake may be

through the oligomeric structure of SP-D allowing enhanced uptake of HIV by the DCs or could be through the interaction of the N-terminal domain with a receptor on the DCs. A rfhSP-D molecule (discussed in Section 1.13.1), lacking the N-terminal domain has also been shown to neutralise HIV. However, its interaction with DCs was not studied. rfhSP-D may have therapeutic potential in neutralising HIV and preventing infection of T cells whilst not enhancing uptake by DCs. In this study, the capacity of SP-A and SP-D to bind inactivated HIV particles and gp120 molecules of different strains is tested.

1.11.4 Effects on Innate Immune Cells

Alongside binding, agglutination and neutralisation of pathogens, the pulmonary collectins have been shown to interact with neutrophils, monocytes and macrophages and directly enhance phagocytosis in addition to other cellular functions (1, 122, 159). SP-A and SP-D have been shown to enhance the capacity of human neutrophils to phagocytose *E. coli*, *S. pneumoniae*, and *S. aureus* (160). Moreover, SP-D has been shown to enhance phagocytosis of mucoid *P. aeruginosa* by alveolar macrophages without causing agglutination (124). SP-A induces production of peroxynitrite by alveolar macrophages and enhances their mycoplasmacidal activity (161, 162). Moreover, SP-A has been shown to directly enhance the killing of *K. pneumoniae* (strain K21a) by macrophages, potentially through increasing the activity of the macrophage mannose receptor (110). Pulmonary collectins are also widely recognised for their chemotactic effects on alveolar macrophages and neutrophils (94, 163-165). SP-A and SP-D also stimulate directional actin polymerisation of alveolar macrophages, a process important for many functions of alveolar macrophages, including motility (94).

Interestingly, SP-A and SP-D have been shown to have opposing effects on the capacity of macrophages to phagocytose *Mycobacterium tuberculosis.* SP-D agglutinates *M. tuberculosis* but inhibits phagocytosis (126). However, *M. tuberculosis appears to* exploit SP-A, through utilising the capacity of SP-A to promote macrophage phagocytosis to gain access to macrophages where they reside intracellularly and replicate (166).

1.11.5 Direct Microbicidal Activity

Both SP-A and SP-D have been shown to have phagocyte-independent direct microbicidal activity. Wu and colleagues discovered that SP-A and SP-D are capable of

arresting gram negative bacterial growth, decreasing their viability, increasing their membrane permeability and inducing bacterial killing (167, 168). They found that rough LPS strains of bacteria were most prone to microbicidal activity by collectins. However, *ompA* deleted strains with smooth LPS were also found to have increased susceptibility to collectin microbicidal activity. Natural *Bordetella pertussis* has been found to be resistant to the microbicidal activity of pulmonary collectins. However, LPS mutant strains lacking terminal sugars were found to be susceptible. This highlights the importance of terminal trisaccharides (also known as a 'glycan shield') in protecting bacteria from collectin microbicidal activity (168).

SP-A and SP-D have also been shown to inhibit growth and viability of fungi, for example the opportunistic pathogens, *Histoplasma capsulatum* and *Candida albicans* (169, 170). Although many of the ligands for SP-A and SP-D on fungal pathogens have been identified, the mechanism behind this direct microbicidal activity still needs to be elucidated (171).

1.11.6 Immunoregulatory Functions of Collectins

SP-A and SP-D have been recognised as necessary antecedents for, upon requirement, the development of an effective adaptive immune response. Ansfield and co-workers observed in 1979 that lymphocytes residing in the lung were in a hyporesponsive state (172). An inflammation free state in the resting lung is key to preventing damage of the lung and allowing effective lung function. It is now widely understood that SP-A and SP-D have important roles in regulating the immune system and preventing aberrant inflammation; reviewed in (1). SP-A has been shown to downregulate inflammatory cytokine production by human alveolar macrophages and monocytes when induced by *C. albicans* (173). SP-A has also been shown to inhibit inflammatory cytokine production upon administration in SP-$A^{-/-}$ mice (174). Importantly, in the presence of rough LPS but not smooth LPS, SP-A has been shown to enhance the production of tumour necrosis factors. This highlights the importance of the type of pathogen for the functional outcome of collectin interactions (84, 175).

SP-$D^{-/-}$ mice have increased levels of IL-6 and IL-12 and an increased proliferation of lymphocytes and activation of T lymphocytes. Moreover, SP-$D^{-/-}$ mice have been shown to have an increased severity of infection upon challenge with *P. carinii* and develop an

emphysema-like pathology (176, 177). The inflammatory phenotype of SP-D$^{-/-}$ mice highlights the importance of SP-D in regulating induction of inflammatory cytokine production. SP-D$^{-/-}$ mice develop an emphysematous-like pathology with accumulations of foamy apoptotic and necrotic alveolar macrophages and lipidosis. Both SP-A and SP-D have been shown to bind to apoptotic macrophages through different mechanisms (178, 179). Moreover, treatment of SP-D knock out mice with rfhSP-D was shown to decrease the number of apoptotic and necrotic macrophages and RNA of inflammatory cytokines and largely correct the emphysematous phenotype found in the SP-D knock out mice (180, 181). This perhaps suggests that modulation of the inflammatory response is mediated by the collectin CRD. Due to the efficacy of rfhSP-D in pre-clinical animal models, it is tempting to hypothesise that replacement of deficient SP-D in the neonatal lung with rfhSP-D may aid in the prevention of the chronic inflammation and emphysematous phenotype found in neonatal chronic lung disease.

Both SP-A and SP-D are now widely accepted as being capable of inhibiting T cell proliferation by both an IL-2-dependent mechanism and an IL-2-independent mechanism, the latter involving attenuation of calcium signalling (177, 182-184). Thus, SP-A and SP-D have been suggested to be an important bridge between the innate and adaptive immune system (1, 185). The roles of SP-A and SP-D in the adaptive immune system have become particularly apparent due to the finding that SP-A and SP-D have been shown to influence DC function. For instance, SP-A has been shown to inhibit DC maturation (186). SP-D has also been shown to opsonise but reduce the presentation of an *E. coli* antigen by lung derived DCs (187). In addition to their effects on lymphocytes and DCs, SP-A and SP-D have been implicated in having important roles in prevention of allergen induced inflammation discussed below; reviewed in (188-190). They also have roles in chemotaxis and degranulation of eosinophils (191, 192).

An intriguing model proposed by Gardai et al. in 2003 describes a mechanism through which SP-A and SP-D act in a dual manner to maintain a hyporesponsive state in the healthy lung at rest but initiate an effective immune response upon presence of a pathogen (80). In the healthy lung, the SP-A and SP-D were shown to interact with the signal-regulatory protein (SIRP) α receptor on macrophages through their CRDs. This was shown to suppress the production of pro-inflammatory mediators. However, upon binding of the collectin to LPS and occupation of the collectin CRD, the collectin tail was shown to bind calrecticulin/CD91 present on the surface of macrophages. This enhanced the

production of pro-inflammatory mediators. The mechanisms by which the pulmonary collectins regulate the immune system are, however, likely to be more complicated than this and dependent on the presence and type of pathogen, type of immune cell, time of exposure, and state of cell activation (1). However, rfhSP-A or rfhSP-D containing the anti-inflammatory CRD and lacking the pro-inflammatory N-terminal region may have therapeutic potential in various inflammatory lung diseases. This is particularly the case for use of rfhSP-D to replace SP-D, levels of which are decreased in patients with COPD and severe asthma and premature neonates who develop neonatal chronic lung disease (193, 194).

1.11.7 Binding to Allergens

SP-A and SP-D bind a variety of allergens and have roles in both allergen scavenging to enhance their clearance whilst directly interacting with immune cells to preventing allergen-induced inflammation. SP-A and SP-D have been shown to bind *Dermatophagoides pteronyssinus* 1 and *Dermatophagoides farinae* 1 house dust mite extracts (195). Importantly, this has been shown to prevent binding of IgE from sera of mite-sensitive asthmatic children to immobilised house dust mite (196). SP-A has been shown to bind grass pollen extracts of *Populus nigra*, *Poa pratensis*, *Secale cerale* and *Ambrosia elatior* (197). Comparatively, SP-D binds *D. glomerata* and decreases pollen-induced IgE-dependent mast cell degranulation: this was not demonstrated for SP-A (198). rfhSP-D has been shown to be effective in decreasing allergic inflammation and 1,3 β-glucan mediated neutrophilic inflammation in SP-D$^{-/-}$ mice (199). Furthermore, SP-A and SP-D are known to bind *aspergillus fumigatus* through the two immunodominant glycoprotein allergens, gp55 and gp45 and protect mice against pulmonary hypersensitivity (200-202). The capacity of SP-A and SP-D to bind and enhance clearance of allergens, whilst regulating the immune system, highlights their importance in the prevention of allergy.

1.12 Exogenous Surfactant Therapeutics

A clinical correlation between pulmonary surfactant and respiratory distress syndrome (RDS) was first established in 1959 by Avery and Mead (203). It is now understood that up to approximately week 39 of gestation ATII cells, the predominant source of

pulmonary surfactant, are still developing and increasing in number (204). Premature neonates born with underdeveloped lungs are, therefore, frequently born with surfactant deficiency which, prior to availability of treatment with lipid surfactant, was often a fatal condition. In 1980 Fujiwara et al. undertook the first successful trial of surfactant replacement in neonates with infant respiratory distress syndrome (previously known as hyaline-membrane disease) (205). This success led to the widespread use of exogenous surfactant as a replacement therapy and is now widely recognised as a milestone in the improvement of preterm neonatal care (206-209). Surfactant therapy has led to increased survival after preterm birth. However, the corollary to this is the survival of neonates with oxygen-therapy induced damaged lungs. Many of these neonates develop an inflammatory emphysematous-like phenotype which results in prolonged requirement for oxygen and resultant neonatal chronic lung disease (208, 210-214). Neonates with chronic lung disease are at increased risk of subsequent infection and mortality as a consequence of viral infections which are normally trivial in individuals with healthy lungs (215).

Currently, commercial surfactants are derived from BAL or lung tissue of bovine or porcine origin (216, 217). Natural pulmonary surfactant therapeutics have, however, been criticised due to cost, limited supply, batch-batch differences and potential risk of immunogenic and infectious complications (216, 218). Moreover, the purification of surfactant through use of organic solvents removes the hydrophilic proteins such as SP-A and SP-D and the majority of the hydrophobic proteins such as SP-B and SP-C which, as discussed in Sections 1.6 and 1.11, have important biophysical and immunological functions, particularly in neonates with a still developing adaptive immune system (219). Synthetic pulmonary surfactant therapies have been developed but are still not commercially available. A new synthetic pulmonary surfactant containing SP-B and SP-C analogues has shown promise in an immature lamb lung model, shown to be non-toxic in a phase I trial and is now undergoing phase II trials (216). The further development of protein-containing synthetic surfactant therapies including recombinant SP-A and SP-D could lead to safer, more economical surfactant therapeutics which, alongside the biophysical properties of the current surfactant therapeutics, having anti-pathogenic and immunomodulatory functions. This is particularly important as infection and inflammation have been shown to lead to surfactant inactivation and an increased risk in the development of chronic lung diseases (220-223).

1.13 Recombinant Pulmonary Collectins

Various recombinant SP-A and SP-D proteins have been developed and provided a wealth of structural and functional information; reviewed in (4). In particular, a functional trimeric truncated version of SP-D, rfhSP-D, lacks the majority of the collagen domain and thus can be produced in an *E. coli* expression system. This rfhSP-D is composed of the CRD, neck and 8 x Gly Xaa Yaa triplicate repeats of the collagen-like domain. Due to rfhSP-D lacking the majority of the collagen-like domain and the N-terminal domain, rfhSP-D can not oligomerise and remains as a functional trimer. rfhSP-D has been shown to be correctly folded by both disulphide mapping and X-ray crystallography (31). Moreover, X-ray crystallography of rfhSP-D has provided the molecular detail needed for a comprehensive understanding of the collectin binding of SP-D to ligands, as discussed in Section 1.7.

1.13.1 Potential of rfhSP-D

Despite the inability of rfhSP-D to form higher-order multimers, it has been shown to maintain many functions of the native full-length molecule; reviewed in (224). Importantly, the rfhSP-D lacks the N-terminal domain which has been shown to enhance inflammatory cytokine production by macrophages (80). rfhSP-D is effective in down-regulating allergic hypersensitivity in mice sensitised to allergens of *A. fumigatus* (131). rfhSP-D has been shown to increase phagocytosis of different *H. influenzae* strains by macrophages (225). Moreover, treatment of SP-D$^{-/-}$ mice with rfhSP-D has been shown to both decrease mortality upon challenge with *A. fumigatus* and correct the emphysema-like phenotype seen in SP-D$^{-/-}$ mice (181, 226). Treatment of mice with rfhSP-D has also been shown to reduce allergen induced immune responses, lipidosis, alveolar macrophage accumulation, alveolar macrophage apoptosis, ATII cell hyperplasia and the production of proinflammatory chemokines (131, 180, 181, 227-229). Of additional interest for treatment of premature neonates is, as discussed in Subsection 1.11.2, the capacity for rfhSP-D to reduce RSV infection both *in vitro* and in an *in vivo* mouse model (128).

rfhSP-D is currently produced using an *E. coli* expression system. The protein is then purified from inclusion bodies using 8 M urea with subsequent refolding. The capacity for production of rfhSP-D in high quantities relative to full-length SP-D using an *E. coli* expression system, alongside its capacity to be lyophilised and resuspended whilst still

maintaining functionality, potentiates its therapeutic use (224). However, further work needs to investigate the potential of expressing rfhSP-D as a soluble protein. This would increase the potential for development of a viable industrial scale production process and the development of rfhSP-D into a therapeutic.

1.13.2 Generating rfhSP-A

Due to the successful production of a functional rfhSP-D trimer with an *E. coli* expression system, it would seem likely that an equivalent functional rfhSP-A trimer could also be created, though to date this has not been possible. As discussed in Section 1.7.1, a rfrSP-A construct has been established, but differences between rat and human SP-A call for generation of a rfhSP-A (4, 119). Moreover, rat SP-A has one SP-A coding gene, but human SP-A is composed of two different gene products (230). A recombinant full-length human SP-A protein has previously been produced using a eukaryotic expression system by Nycomed GmbH (previously known as Altana Pharma AG). However, problems have been encountered due to the inability to cheaply produce high quantities of this protein in addition to problems with handling and aggregation (231). A functional rfhSP-A protein expressed in a bacterial expression system would overcome these problems. Moreover, the generation of rfhSP-A would provide the platform to delineate structural and functional information about human SP-A. Attempts have been made to produce a rfhSP-A protein. However, these have lacked the collagen-like stalk thought to be important for stabilising the trimeric structure of the molecule and have not been demonstrated to be trimeric (232, 233).

In order to generate a rfhSP-A protein with a physiological SP-A1:SP-A2 ratio, it is important to first identify the natural ratio in the human lung. This is particularly the case as functional differences between SP-A1 and SP-A2 have been identified, including their binding preferences and capacities to oligomerise (57, 234, 235). SP-A2 has been shown to have an enhanced ability to induce TNF-α and IL-8 production by macrophage-like THP-1 cell line (236, 237), phosphatidylcholine secretion by type II alveolar cells and phagocytosis of *Pseudomonas aeruginosa* by rat alveolar macrophages (238). A 2:1 ratio of SP-A1 to SP-A2 in the lung has been proposed previously (239, 240). This study used a SP-A1 specific antibody and Western blotting and the ratio was shown to vary in different patient populations (241). To date, the SP-A1 to SP-A2 ratio has not been determined using a quantitative approach such as mass spectrometry.

1.13.3 Use of a Novel Solubility Tag for Producing rfhSP-A and rfhSP-D

The current way to produce rfhSP-D is through expression in *E. coli*, purification from inclusion granules using 8 M urea and subsequent refolding. However, this procedure results in a substantial loss in protein yield through misfolding and precipitation of the protein. The use of a novel solubility tag for production of rfhSP-D and rfhSP-A proteins could prevent the need for protein refolding and thus lead to a more efficient way of producing high levels of rfhSP-D and rfhSP-A cheaply, for potential therapeutic use. A novel solubility tag is currently under investigation for use in heterologous protein expression. This novel solubility tag is the N-terminal domain (NT) from spider silk protein.

1.13.3.1 *Spider Silk and the Role of the NT domain*

Spider silk is produced through the assembly of large proteins (spidroins) which assemble into one of the toughest known biomaterials. The major ampullate spidroin (MaSp) 1 is composed of 3 regions, a long repetitive region of approximately 3,500 residues, a highly conserved N-terminal domain of approximately 130 residues (NT), and a less conserved C-terminal domain of approximately 100 residues (242, 243). Despite spidroins being highly prone to aggregation, they are stored in the silk gland as soluble proteins at high concentrations of up to 50 % (w/w) (244). This soluble protein is processed into silk fibres upon transport through an elongated duct with a decreasing pH gradient (245). The NT domain has been evolutionarily conserved for at least 125 million years (243) and proposed to function as a pH-regulated relay which has dual functions in maintaining spidroin solubility in the silk gland whilst enabling fibre formation at lower pH in the spinning duct. This occurs through dimerisation and subsequent protein aggregation upon lowering of the pH (246, 247).

1.13.3.2 *The Formation of NT Dimers*

NT is folded as a five-helix bundle and forms homodimers whereby each monomer arranges in antiparallel orientation to the other when the pH is lowered below pH 6 (246, 248). A recent study has delineated the important residues in the pH-dependent dimerisation of the NT domain and proposed a model through which this dimerisation occurs (249). NT monomeric subunits have a pronounced dipolar character with clusters of acidic (Asp39, Asp40, Glu79, Glu84, Glu85, Glu119 and Asp134) and basic residues

(His6, Arg60 and Lys65) at opposite ends of the subunit. In the first step of dimerisation, there is an initial association of monomeric units which is mediated through electrostatic interactions with residues Lys65, Arg60 and the highly conserved residue Asp40, being key mediators. Upon decreasing the pH, residues Glu79 and Glu119 become protonated which allows the formation of dimeric units. These dimers are stabilised in the final step following the further protonation of Glu84. Comparative to the Glutamic acid residues, residues Asp40, Lys65 and Arg60 remain charged and contribute to stability of the dimer by the formation of inter-subunit salt-bridges.

In the above mentioned study, single mutants of NT where acidic and basic amino acids Asp40 and Lys65 were replaced by the neutrally charged amino acid N were produced. These mutants were stabilised as monomers with a lower propensity to form dimeric subunits as the pH was lowered. Moreover, upon reversal of the charge of amino acid 40 by a Asp40Lys mutation, NT domains remained as stable monomers and were unable to dimerise throughout the tested pH range of 7.5-5.0.

1.13.3.3 *NT and NT^{dm} for use as Solubility Tags*

Recently, NT has been suggested to be useful as a general solubility tag for expression of heterologous proteins. An unpublished study has shown its capacity to enable high-level expression of soluble SP-C33Leu (250), a peptide of SP-C which is currently being investigated for its use in synthetic surfactant formulations; SP-C33Leu is extremely hydrophobic and prone to aggregation in hydrophilic solutions. NT may, therefore, allow the expression of rfhSP-A as a soluble protein. In addition, it could allow the soluble production of high levels of rfhSP-D without the need for refolding and thus subsequently reduce the attributed protein loss and increase protein yields.

Due to the new understanding of the importance of Asp40 and Lys65 in NT dimer formation (discussed above), a double mutant NT molecule (NT^{dm}) has been generated at Karolinska Institutet, Sweden, where the charges of amino acids Asp40 and Lys65 have been reversed with Asp40Lys and Lys65Asp mutations incorporated through site-directed mutagenesis. It was, hypothesised that the charge reversal of these key amino acids would prevent the electrostatic interactions between the NT subunits, prevent salt bridge formation and thus prevent formation of dimers and aggregates. This is hypothesised to increase the solubility of NT and potentiate its use as a solubility tag for heterologous protein expression.

1.14 Aims

The aims of this project are:

1) To purify nhSP-A and nhSP-D, characterise their oligomeric states and determine the SP-A1:SP-A2 ratio in the human lung quantitatively using mass spectrometry.

2) To clone SP-A1 and SP-A2 and express and purify a rfhSP-A molecule, equivalent to rfhSP-D.

3) To investigate the utility of NT and NT^{dm} as novel solubility tags for allowing heterologous expression of soluble rfhSP-A and rfhSP-D and subsequent purification without the need for protein refolding.

4) To purify functional trimeric rfhSP-A.

5) To purify functional trimeric rfhSP-D after expression as a soluble protein using NT or $NT^{dm.}$

6) To characterise the capacity of rfhSP-A to bind to known natural SP-A ligands compared with nhSP-A and nhSP-D.

7) To use rfhSP-A and rfhSP-D to characterise the importance of the SP-A and SP-D N-terminal domain (and oligomeric structures) in neutralisation of a clinically relevant strain of RSV using human bronchial epithelial cells.

Chapter 2: General Methods

2.1 General Reagents

Unless otherwise stated, in all chapters, reagents were purchased from Sigma-Aldrich (UK)

2.2 Gel Filtration

Gel filtration was undertaken using either small analytical or large preparative gel filtration columns from GE Healthcare, UK. These were Superose 6 columns with either a 24 ml or 110 ml bed volume or superdex 200 columns with either a 24 ml or 80 ml bed volume. Superose 6 columns were used for nhSP-A and nhSP-D and superdex 200 columns for all recombinant proteins. Columns were equilibrated in 20 mM Tris, 150 mM NaCl, pH 7.4 (TBS), containing 5 mM EDTA (gel filtration buffer). Elution from the column was at a flow rate of 0.3 ml/min. Upon elution, fractions were taken and stored at -20 °C until use. Elution was controlled using an ÄKTA purifier UV900 monitor (GE Healthcare) with Unicorn (v4.10) software (Amersham Biosciences UK), absorbance at λ = 280 nm was recorded. The molecular weight of the eluted proteins was assessed by comparison with 200 µg of protein standards from a Molecular Weight Markers for Gel Filtration Chromatography kit. Percentages of protein within a single peak as compared to the whole was calculated using the curve integration tool on the Unicorn software.

2.3 Determining Protein Concentrations

To calculate protein concentrations, the absorbance at λ = 280 nm was used as a guide; the protein concentration was calculated using the following equation:

$$Concentration = \frac{Absorbance}{Molar\ extinction\ coefficient\ x\ Path\ length} \times Dilution\ factor$$

Where stated, protein concentrations were also confirmed using a bicinchoninic acid (BCA) assay, as previously described (251). Briefly, 4 % (weight (w)/volume (v) (w/v)) $CuSO_4$ in water was mixed with bicinchoninic acid in a 1:49 ratio to generate $CuSO_4$:BCA solution. 120 µl of $CuSO_4$:BCA solution was then added to 15 µl of protein sample in individual wells of a Greiner (UK) CELLSTAR 96 well plate. Samples were

incubated at 37 °C for 30 min and analysed at λ = 550 nm using an iMark Microplate Absorbance Reader (Bio-Rad, UK). Protein concentrations were determined by comparison to a standard curve generated with a 6 step dilution series of different bovine serum albumin (BSA) concentrations (0.1 mg/ml to 1 mg/ml). Samples were analysed in duplicates.

2.4 SDS-PAGE

Sodium dodecyl sulphate (SDS)-polyacrylamide gel (PAGE) analysis was undertaken through electrophoresis at 200 volts for approximately 60 min using NuPAGE® Bis-Tris Precast Gels (Invitrogen, UK). Protein samples were prepared according to manufacturer's instructions. 7 µl of SeeBlue Plus2 standard (Invitrogen) was analysed alongside protein samples to allow determination of molecular weight, unless otherwise stated. Gels were then stained with SimplyBlue SafeStain (Invitrogen) for 1 hour, unless otherwise stated. A silver staining kit (Bio-Rad) was also used, according to manufacturer's instructions. Alternatively gels were used for SDS-PAGE with Western blotting analysis. Electrophoresis was undertaken in reducing conditions unless otherwise stated. Non-reduced SDS-PAGE gels were also used, where stated, by preparing samples without the inclusion of reducing agent, according to manufacturer's instructions.

2.5 Western Blotting

Proteins were transferred to a Polyvinylidene difluoride (PVDF) membrane using an iBlot Dry Blotting System with an iBlot Transfer Stack (PVDF) (Invitrogen), according to manufacturer's instructions. All incubations of the membrane were undertaken at room temperature with rocking of the membrane. Primary and secondary antibodies used for Western blot analysis are given in Table 2-1. Membranes were blocked in TBS with 0.1 % Tween-20 (wash buffer) containing 5 % (w/v) skimmed milk, overnight. 10 ml of primary antibody diluted 1:1,000 in wash buffer containing 5 % (w/v) skimmed milk was then applied to the membrane and incubated for 1 hour. Membranes were then washed three times with wash buffer for 5 minutes (min). 10 ml of secondary antibody diluted 1:10,000 in wash buffer containing 5 % (w/v) skimmed milk was then applied to the

membrane and incubated for 1 hour. Membranes were then washed three times with wash buffer for 5 min.

To visualise the proteins, ECL Western Blotting Detection Reagents (reagent 1 and 2) were used (GE Healthcare). ECL Western Blotting Detection reagents 1 and 2 were mixed in a 1:1 ratio prior to use. 750 µl of this mix was then applied to a clean plastic surface, and then the membrane was placed on top of the surface, face down. This was left to incubate at room temperature for 1 min, after which excess detection reagent was blotted off using filter paper. RX NIF X-ray film (FujiFilm, UK) was then exposed to the membrane by placement on top; cling film was used to separate the film and the membrane. Exposure times were between 30 sec – 3 min (or longer for over exposed films). Development was undertaken using PD-5 Print Developer (Fotospeed, UK) until sharp bands could be seen (approximately 1 min). X-ray film was fixed using FX50 Fixer (Fotospeed). Molecular weights of bands were determined by tracing the bands corresponding to the marker. This was undertaken through the use of Glogos II Autorad Markers (Stratagene, UK).

Antibody	**SP-A**	**SP-D**
Primary	Monoclonal Mouse α-nhSP-A antibody HYB 238-04 (1 mg/ml) (kindly provided by Prof Uffe Holmskov, University of Southern Denmark (252))	Polyclonal Rabbit α-rfhSP-D antibody (1.6 mg/ml)(As previously used for Western blotting (253))
Secondary	HRP-conjugated Goat α-Mouse IgG (H+L) antibody (Life Technologies, UK) (62-6520)	HRP-conjugated Goat α-Rabbit IgG (H+L) antibody (Life Technologies, UK) (65-6120)

Table 2-1: List of antibodies used for Western blot analysis and ELISA. *Listed are primary and secondary antibodies used to detect SP-A or SP-D during Western blot analysis*

2.6 ELISA

Rabbit polyclonal α-rfhSP-D antibody (1.6 mg/ml) (Table 2-1) was diluted 1:1,000 in carbonate buffer (pH 9.6) and applied to Nunc-Immuno Maxisorp 96 well microtitre plates. These were left overnight at 4 °C. The wells were washed four times with 150 µl/well of 5 mM $CaCl_2$, 0.05 % Tween 20 in TBS (wash buffer). Unbound sites were then blocked by incubation with 150 µl/well of wash buffer for 15 min at room temperature with shaking (450 revolutions per minute (rpm)). After removal of the wash buffer, 100 µl of diluted sample were applied to the wells. The 96 well Maxisorp plates were then incubated at 4 °C overnight. After washing as above, the plates were incubated for 1 hour at room temperature with 100 µl/well of biotinylated monoclonal mouse α-human SP-D (Hyb 246-04). The samples were washed as above and the plates were incubated for 1 hour at room temperature with 100 µl/well of 1:30,000 diluted streptavidin-horse radish peroxidase (HRP) in wash buffer. Again, the samples were washed as above, after which, 100 µl/well of 3, 3', 5, 5' tetramethyl benzidine reagent mix was added; this was incubated for 15-30 min at room temperature. 50 µl/well of 0.5 M H_2SO_4 was subsequently added and the absorbance was measured at $\lambda = 450$ nm using an iMark Microplate Absorbance Reader.

2.7 Determination of Endotoxin Levels

Levels of endotoxin in protein preparations were determined using a Limulus Amebocyte Lysate (LAL) chromogenic assay (Lonza, UK) which includes LAL enzyme, LAL substrate, LAL reagent water and endotoxin standard. LAL assay was undertaken according to manufacturer's instructions. Briefly, samples were diluted in LAL reagent water and aliquoted into a 96 well plate, to which 50 µl of LAL enzyme was added; this was incubated at 37 °C for 10 min. 100 µl of LAL substrate was then added to each sample. The reaction was undertaken for 6 min at 37 °C, after which, it was stopped by addition of 100 µl of 10 % sodium dodecyl sulphate in LAL reagent water (v/v). An iMark Microplate Absorbance Reader was used to determine the absorbance of each sample at $\lambda = 405$ nm. A 4 point serial dilution of standards containing endotoxin were also analysed for comparison and calculation of absolute endotoxin levels (1 endotoxin unit/ml (EU/ml) to 0.125 EU/ml). Samples were analysed in duplicates.

Chapter 3: Purification and Characterisation of nhSP-A and nhSP-D

3.1 Introduction

In this study, rfhSP-A was characterised for its ability to bind known ligands of SP-A as compared with native human SP-A (nhSP-A). Moreover, rfhSP-A and rfhSP-D were used to characterise the importance of the SP-A and SP-D N-terminal domain and oligomeric structure in neutralisation of RSV. Thus it was first important to purify nhSP-A and nhSP-D.

The work in this chapter therefore explores different techniques for purifying nhSP-A and nhSP-D from human lung and characterises the oligomeric structures of the purified proteins. In addition, it describes attempts to use mass spectrometry to allow quantification of the SP-A1 to SP-A2 ratio in the human lung to allow later production of a rfhSP-A fragment with a physiological SP-A1:SP-A2 ratio (Aim 1 - Section 1.14).

nhSP-A and native human SP-D (nhSP-D) are routinely purified from BAL from patients with pulmonary alveolar proteinosis (PAP). PAP is a rare disease characterised by the accumulation of surfactant in the lung. Patients require routine therapeutic washing of the lung to remove excess surfactant. After separation of nhSP-A and nhSP-D in BAL by a simple centrifugation step, nhSP-D is purified using carbohydrate affinity chromatography. This exploits the calcium-dependent binding of SP-D to the carbohydrate ligand and allows specific elution of nhSP-D through addition of manganese, which competes with calcium at binding sites in the CRD. Historically, nhSP-D has been purified using maltose affinity chromatography with subsequent gel filtration (65). However nhSP-D has been reported to have a higher binding avidity to N-acetyl-mannosamine (ManNAc) than maltose (58). ManNAc affinity chromatography may, therefore allow purification of higher yields of nhSP-D as compared with maltose affinity chromatography.

Comparatively, nhSP-A is routinely purified from the surfactant lipid pellet using a method based on butanol extraction (254). However, an alternative purification method has also been described and is based on isolation of the nhSP-A from the washed BAL pellet by washing with ethylene glycol tetraacetic acid (EGTA) (255). In comparison to EDTA, rather than generally chelating divalent cations, EGTA chelates calcium preferentially. This allows purification of SP-A specifically whilst other proteins bound in a general divalent cation-dependent manner remain bound. In this chapter this method is compared with the butanol extraction method to allow subsequent identification of any

potential structural differences in nhSP-A which are dependent on the purification method. Purification through washing with EGTA allows purification of nhSP-A without extraction of lipids. This, could, therefore, be an ideal way to quantifiably identify nhSP-A-associated lipids by mass spectrometry rather than testing binding using purified SP-A which has previously been done (17).

The human SP-A locus constitutes two functional genes *SFTPA1* (SP-A1) and *SFTPA2* (SP-A2) and a pseudogene. Four SP-A1 alleles (6A, $6A^2$, $6A^3$, and $6A^4$) and six SP-A2 alleles (1A, $1A^0$, $1A^1$, $1A^2$, $1A^3$, and $1A^5$) are most frequently found in the general population. Importantly, there are only ten amino acid differences between the characterised SP-A1 and SP-A2 alleles. However, as discmn jkussed in Chapter 1, SP-A1 and SP-A2 genes have structural and functional differences and the SP-A1:SP-A2 ratio may be altered in different lung disease states reviewed in (256).

Through use of an SP-A1 specific antibody, an SP-A1:SP-A2 ratio in the human lung, has been investigated (241). However, no one has as yet identified such a ratio using a suitable quantification technique such as mass spectrometry, this chapter describes attempts to do this. Establishment of a rapid approach for quantification of such a ratio could lead to use of this ratio as a potential biomarker for different lung diseases. Moreover, to generate a rfhSP-A protein with a physiological SP-A1:SP-A2 ratio, it is important to first characterise the natural ratio in the human lung.

3.1.1 Aims

In order to study the importance of the SP-A and SP-D N-terminal domain and oligomeric structure in their interaction with RSV, this chapter set out to purify nhSP-A and nhSP-D from human lung using different techniques for later comparison in functional assays with rfhSP-A and rfhSP-D (Chapter 7) and characterise their oligomeric structures. This chapter also reports attempts to characterise the SP-A1:SP-A2 ratio in human lung using a quantitative mass spectrometry technique for potential subsequent production of a rfhSP-A molecule with a native SP-A1:SP-A2 ratio (Aim 1 - Section 1.14).

3.2 Methods

3.2.1 Preparing BAL

nhSP-A and nhSP-D were purified from alveolar lung lavage from PAP patients. BAL was collected from patients at the Royal Brompton Hospital with informed consent and necessary ethical permission (the Royal Brompton and Harefield Research Ethics Committee NRES 10/H0504/9). A Material Transfer Agreement has been signed between the Royal Brompton and Harefield NHS Foundation Trust and University of Southampton (UK) covering this usage.

BAL was thawed and supplemented with EDTA (10 mM final concentration) and Tris (20 mM final concentration). BAL was made to pH 7.4 with HCl and left to stir at room temperature for one hour with subsequent centrifugation at 10,000 x g for 45 min. The supernatant and pellet were stored separately at -20 °C until use for the purification of nhSP-D or nhSP-A, respectively.

3.2.2 Purifying nhSP-D

nhSP-D purification was based on a method previously described by Strong and colleagues (65). 3 L of nhSP-D containing BAL supernatant (prepared as in 3.2.1) was thawed and split into two batches of 1.5 L, after which, approximately 15 ml of maltose or ManNAc coupled sepharose beads were added. The BAL was then equilibrated to TBS containing 50 mM $CaCl_2$ and stirred at 4 °C overnight. The carbohydrate coupled beads with bound nhSP-D were then packed into a column and a “high salt” wash was performed with 50 ml of TBS containing 5 mM $CaCl_2$, 1 M NaCl before the column was equilibrated back into TBS containing 5 mM $CaCl_2$. The nhSP-D was then eluted from the column by flowing through TBS with 100 mM $MnCl_2$. The elutant was immediately buffer exchanged into TBS containing 5 mM EDTA by concentration using Ambicon Ultra centrifugal filters (100 kDa molecular weight cut off (MWCO) (Millipore, UK) and subsequent dilution. The column was then washed with gel filtration buffer.

Purified nhSP-D was further purified using gel filtration. Fractions containing protein at the correct elution volume were analysed by Enzyme-linked immunosorbent assay (ELISA), pooled and confirmed to be nhSP-D by Western blotting. Purified nhSP-D was

concentrated using Ambicon Ultra centrifugal filters (100 kDa MWCO). Concentrated protein was treated for endotoxin by addition of 1/5th of the protein sample volume of pre-washed Polymyxin B-Agarose beads. Endotoxin bound Polymyxin B beads were removed by centrifugation at 15,000 x g for 5 min. SP-D containing supernatant was then recovered, filtered using a 0.45 µm filter (Merck Millipore, UK) and stored at -20 °C. nhSP-D was tested for endotoxin concentrations as described in Section 2.7.

3.2.3 Purifying nhSP-A

3.2.3.1 *Butanol Extraction*

nhSP-A was purified using an adapted version of a previously established butanol extraction method (254). 1.5 ml of thawed nhSP-A-containing BAL pellet (prepared as in 3.2.1) was added, dropwise, into 75 ml of stirring 1-butanol. This was left to stir at room temperature for 3 hours and subsequently subject to centrifugation at 10,000 x g for 30 min (4 °C); after resuspension of pellets, centrifugation was repeated. The resulting pellets were dried by steady flow of nitrogen and resuspended in 5 ml of 20 mM Octyl β-D-glucopyranoside (OGP) in TBS but with only 5 mM Tris buffered water (TBW), (OGP/NaCl/TBW), pH 7.4. This was then subject to centrifugation at 114,500 x g for 30 min (4 °C), after which, the resulting pellet was resuspended in OGP/TBW and again subject to centrifugation. The pellet was then resuspended in 5 ml of TBW, made to 100 mM OGP and mixed at room temperature for 30 min.

To remove endotoxin, 0.42 ml of washed Polymyxin B-Agarose beads were added to the purified nhSP-A. This mixture was then dialysed into TBW using SnakeSkin dialysis tubing (10,000 Da MWCO) (Thermo Scientific Pierce, USA). Dialysis was undertaken at room temperature for >8 hours; this was repeated at least 4 times. To remove Polymyxin B-Agarose beads with bound endotoxin, nhSP-A was subject to centrifugation at 3,000 x g for 10 min, after which, the supernatant was subject to centrifugation at 114,500 x g for 60 min (4 °C). The nhSP-A containing supernatant was then removed, filtered using a 0.45 µm filter stored at 4 °C and stored as aliquots at -20 °C. nhSP-A was tested for endotoxin concentrations as described in Section 2.7.

3.2.3.2 *Washing with EGTA*

nhSP-A was purified from the surfactant pellet with EGTA using a method previously described (255). 1 ml of thawed nhSP-A-containing BAL pellet (prepared as in 3.2.1) was washed 5 times by suspension in 4 ml of TBS with 1 mM $CaCl_2$ and subsequent centrifugation at 100,000 x g for 20 mins. nhSP-A was subsequently eluted by washing 3 times through suspension in TBS with 2 mM EGTA and 1 mM $MgCl_2$ and subsequent centrifugation at 100,000 x g for 20 mins. The eluted nhSP-A was pooled and filtered using a 0.22 μm filter.

3.2.4 Transmission Electron Microscopy

Transmission electron microscopy (TEM) was undertaken to visualise the oligomeric structure of purified nhSP-D. 5 μl of nhSP-D (0.22 mg/ml) protein sample was placed on a formvar-carbon coated grid (Agar Scientific, UK) and left to bind for 5-10 min, after which, the sample was blotted off using a piece of filter paper. Samples were negatively stained using 5 μl of a 2 % uranyl acetate stain solution in water (volume/volume (v/v)) for 10 sec and analysed using a Technai12 Transmission Electron Microscope (FEI, Eindhoven, The Netherlands) at 75 kV.

3.2.5 Mass Spectrometry

3.2.5.1 *Overview of Approach for Detecting SP-A1 and SP-A2*

To allow the detection of the SP-A1:SP-A2 ratio in nhSP-A, distinct SP-A1 and SP-A2 peptides must be generated which are small enough for detection by mass spectrometry. Digestion of SP-A with trypsin and CNBr was employed to generate distinct SP-A1 and SP-A2 peptides. Peptides which could allow the identification of an SP-A1:SP-A2 ratio are shown in Figure 3-1.

A

M+WLCPLALNLILM+AASGAVCEVK=DVCVGSPGIPGTPGSHGLPGR=DGR=**DGLK**=G
DPGPPGPM+**GPPGEM**+PCPPGNDGLPGAPGIPGECGEK=GEPGER=GPPGLPAHLDEEL
QATLHDFR=HQILQTR=GALSLQGSIM+TVGEK=VFSSNGQSITFDAIQEACAR=AGGR=I
AVPR=NPEENEAIASFVK=K=YNTYAYVGLTEGPSPGDFR=YSDGTPVNYTNWYR=**GEP**
AGR=GK=EQCVEM+YTDGQWNDR=NCLYSR=LTICEF

B

M+WLCPLALNLILM+AASGAACEVK=DVCVGSPGIPGTPGSHGLPGR=DGR=**DGVK**=G
DPGPPGPM+GPPGETPCPPGNNGLPGAPGVPGERGEK=GEAGER=GPPGLPAHLDEELQ
ATLHDFR=HQILQTR=GALSLQGSIMTVGEK=VFSSNGQSITFDAIQEACAR=AGGR=IAV
PR=NPEENEAIASFVK=K=YNTYAYVGLTEGPSPGDFR=YSDGTPVNYTNWYR=**GEPAG**
R=GK=EQCVEM+YTDGQWNDR=NCLYSR=LTICEF

C

SP-A1	**SP-A2**
DGLK	DGVK
GPPGEM	No fragment generated
GEPAGR*****	GEPAGR*****

Figure 3-1: Schematic of fragments generated by digestion with trypsin and CNBr for subsequent mass spectrometry. *Peptides generated by digestion of SP-A1 (**A**) and SP-A2 (**B**) with trypsin and CNBr are shown using the one letter amino acid code. Indicated are the cleavage sites for trypsin (=, grey) and CNBr (+, green) Also indicated is the leader sequence which is considered to be cleaved from SP-A1 and SP-A2 in the mature proteins (blue) (257). Peptides of interest are indicated (underlined and yellow). Potential peptides to allow the quantification of relative SP-A1 and SP-A2 concentrations are summarised (**C**).To note: due to the absence of a methionine at position 66 and the generation of a peptide with a molecular weight above the detection limit, no equivalent peptide for the SP-A1 'GPPGEM' peptide would be detected for SP-A2. Upon use of the SP-A1 'GPPGEM' peptide, an SP-A1:SP-A2 ratio would be calculated by comparison against the total amount of SP-A using the peptide, 'GEPAGT' (*****).*

3.2.5.2 *Analysis by Mass Spectrometry after Digestion with CNBr and Trypsin*

100 µg of purified nhSP-A was dried using a SpeedVac Concentrator (Eppendorf, UK), reconstituted in 70 % formic acid and digested with a crystal of CNBr at 37 °C overnight. This was then dried as above, reconstituted in 200 µl of 100 mM ammonium bicarbonate

and again dried to remove acidic residues. Samples were then reduced by addition of 100 µl of 100 mM ammonium bicarbonate containing 2 µg of dithiothreitol (DTT), samples were reduced at 60 °C for 1 hour. Cysteine residues were alkylated by addition of 10 µg of iodoacetamide (IAA), alkylation was undertaken in the dark, at 21 °C for 20 min. The sample was then digested with 2 µg of trypsin (porcine, modified, sequencing grade) (Promega) at 37 °C overnight. Samples were then dried and reconstituted in 100 µl of 98 % double distilled water (ddH_2O), 2 % Acetonitrile, 0.1 % formic acid.

2 µl of prepared sample (2 µg) was separated on an LC column (Waters, Acuity UPLC PST C18 nanoAcquity column 1.7 µm x 75 µl x 150 mm). Buffer was flown through the column at 300 nl/min for 1 hour with an acetonitrile gradient increasing from 3 % to 97 %. The separated sample was then fed into the mass spectrometer (Waters, Synapt G2S) by nano-spray. The mass spectrometer was operated with collision energies oscillating between 15 kV to 40 kV. Analysis was undertaken using MS^E, with 1 sec scan times, under resolution mode. Mass spectrometry data was analysed on ProteinLynx Global Server Version 3.0 (Waters) through searching against a UniProt human database. Modification of cabominomethyl cysteine residues was taken into account as were the possible hydroxylation of lysine and proline residues, N-linked glycosylation of asparagine residues and oxidation of methionine residues.

3.2.5.3 *Collagenase and Trypsin Digestion of nhSP-A*

Partial collagenase digestion of nhSP-A was undertaken with 3 µg of protein in TBS containing 10 mM $CaCl_2$ (in a final volume of 40 µl). Digestion was undertaken with 0.03 milli units (mU), 0.10 mU or 0.30 mU of collagenase from *Clostridium histolyticum* (type I) at 37 °C for 1 hour. Inactivation of collagenase was undertaken by heating at 80 °C for 20 min. Subsequent trypsin digestion was undertaken by addition of 2 µl of 0.25 % GIBCO Trypsin-EDTA (Invitrogen) and incubation at 37 °C overnight (final reaction volume 42 µl). Digestion with trypsin alone was undertaken as above but without addition of collagenase.

3.2.5.4 *Analysis by Mass Spectrometry after Digestion with Lys-C*

To test digestion of nhSP-A with Lys-C, nhSP-A was first denatured in 100 M ammonium bicarbonate 8 M urea, pH 8.5. nhSP-A was then reduced by adding DTT to 33 mM (final concentration) and incubated for 30 min at room temperature. To alkylate cysteine

residues, IAA was added to 100 mM (final concentration) and incubated at room temperature in the dark. Subsequently, nhSP-A was diluted to 100 mM ammonium bicarbonate 4 M urea and digested with Lys-C over night with a Lys-C:nhSP-A ratio of either 1:50 or 1:20 (w/w), after which, nhSP-A was diluted to 100 mM ammonium bicarbonate, 2 M urea with subsequent addition of trypsin (or not) at a Lys-C:nhSP-A ratio of either 1:50 or 1:20 (w/w) and incubation overnight. In some of the nhSP-A digests, additional trypsin was added after 6 hours of trypsin digestion. Incubations with Lys-C and trypsin were undertaken at 37 °C. After digestion, samples were dried and subsequently analysed by SDS-PAGE or mass spectrometry

Mass spectrometry was undertaken by Henrik Molina at the Proteomic Resource Center at Rockefeller University, New York, USA as previously described (258). Briefly, mass spectrometry was undertaken using a LC-MS/MS (Ultimate 3000 nano-HPLC) mass spectrometry system coupled to a Q-Exactive Plus mass spectrometer, Thermo Scientific) as previously described (258). Peptides were separated on a C18 column (12 cm/75 µm, 3 µm beads, Nikkyo Technologies, Japan) at 200 nl/min with a gradient increasing from 5 % Buffer B/95 % buffer A to 45 % buffer B/55 % Buffer A in 82 min (buffer A: 0.1% formic acid, buffer B: 0.1 % formic acid in acetonitrile). LC-MS/MS experiments where performed as either data dependent or parallel reaction monitoring.

3.3 Results

3.3.1 Purification of nhSP-D

To use in functional assays to compare against rfhSP-A and rfhSP-D, nhSP-D was purified using both maltose and ManNAc affinity chromatography. The two different affinity columns were compared in terms of the yield and purity of the final purified nhSP-D. Gel filtration is standardly used as an additional purification step and was therefore, also investigated for its importance in generating a pure nhSP-D preparation.

3.3.1.1 *Comparison of Maltose and ManNAc Affinity Purification*

BAL from a single patient was used to allow the comparison of maltose and ManNAc affinity chromatography. To compare these different affinity purification techniques, affinity chromatography, gel filtration, ELISA, SDS-PAGE and Western blotting was undertaken (by Alastair Watson and Zofi McKenzie). nhSP-D was successfully purified using both techniques. Upon elution of nhSP-D with $MnCl_2$, a peak in absorbance at λ = 280 was seen for both maltose and ManNAc affinity chromatography techniques (Figure 3-2). To remove remaining protein from the columns, they were subsequently washed with EDTA which also resulted in a peak of absorbance at λ = 280 (Figure 3-2). The collected nhSP-D containing fractions eluted by $MnCl_2$ were pooled, and further purified by gel filtration.

To further purify nhSP-D and characterise its oligomeric state, gel filtration was subsequently undertaken. Maltose affinity purified protein eluted from a 110 ml bed volume gel filtration column, in one single peak between 42-50 ml (Figure 3-3A) with an estimated size of approximately 1,700 kDa. ManNAc affinity purified protein also eluted from the gel filtration column, predominantly, in one peak. This peak was, however, wider with an elution volume between 42-54 ml (Figure 3-3A). In addition, a small secondary peak was seen at an elution volume 62-71 ml with an estimated approximately 800 kDa size as determined by comparison with gel chromatography standards (data not shown).

Upon analysis of gel filtration fractions by ELISA, the peaks in absorbance at λ = 280 were confirmed to be nhSP-D (Figure 3-3B). ELISA analysis indicated that nhSP-D was shown to elute from the gel filtration column between 47-52 ml and 47-60 ml for the

maltose affinity and ManNAc affinity purified proteins, respectively. Interestingly, a small amount of nhSP-D was shown to be present in the secondary peak of gel filtration of nhSP-D which had been purified with ManNAc affinity chromatography.

From 1.5 L of BAL, maltose or ManNAc affinity column purification with subsequent gel filtration yielded approximately 300 µl of purified protein at 0.22 mg/ml and 0.66 mg/ml, respectively. In addition use of the ManNAc affinity column yielded lower contamination with endotoxin than use of a maltose affinity column (0.015 ng/µg of endotoxin compared with >0.05 ng/µg). ManNAc affinity chromatography, therefore, resulted in a higher protein yield and was adopted for future purifications. Despite only micrograms of purified nhSP-D being obtained, SDS-PAGE and Western blot analysis indicated that both maltose and ManNAc purification yielded pure protein preparations with minimal contamination by nhSP-A (Figure 3-4). Both reducible monomeric and non-reducible dimeric SP-D was seen upon assessment by SDS-PAGE, as is standardly seen. Although only small amounts of nhSP-D were initially purified in this comparison a later purification of nhSP-D from 4 L of BAL from a different patient using ManNAc affinity chromatography yielded 4.9 mg of pure protein with only 0.006 ng/µg of endotoxin.

A Maltose Affinity Chromatography

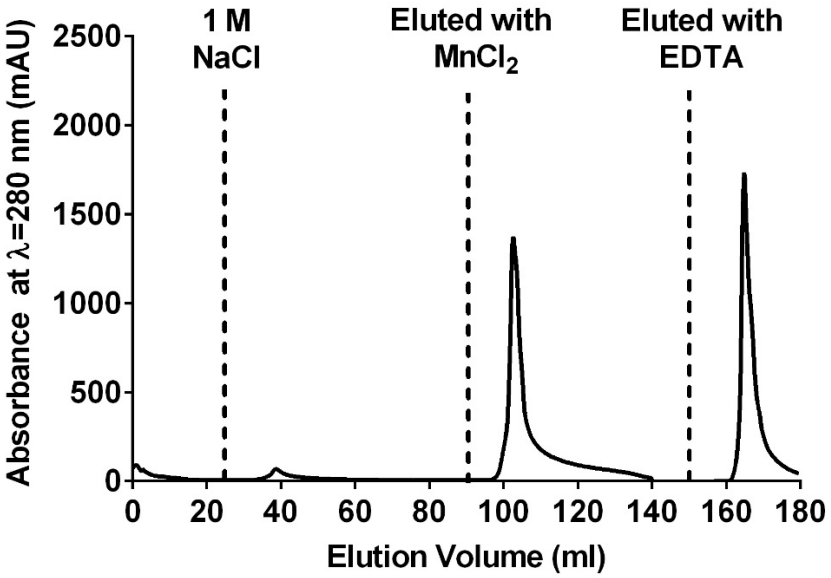

B ManNAc Affinity Chromatography

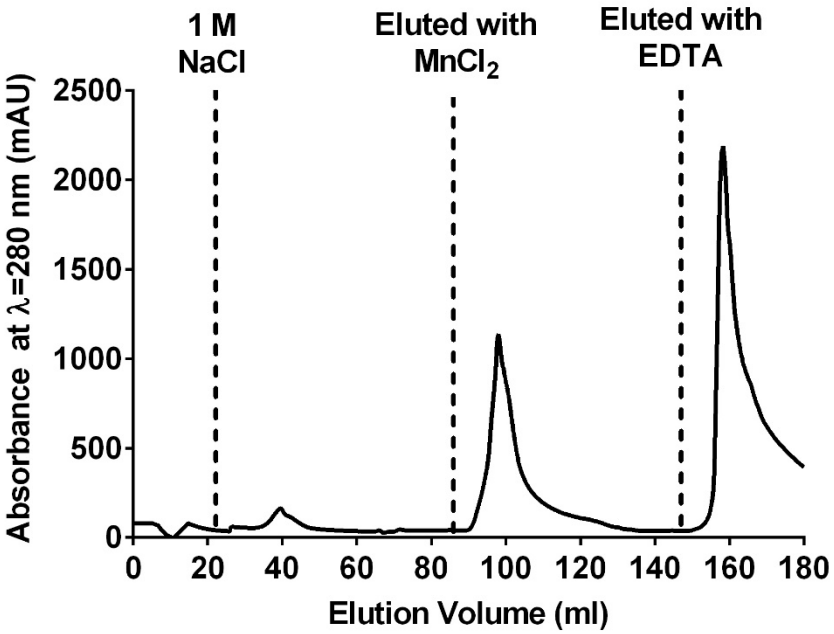

Figure 3-2: Maltose and ManNAc affinity purification of nhSP-D *Shawn are absorbance readings at λ = 280 nm upon elution of protein from either a maltose sepharose (**A**) or ManNAc sepharose (**B**) column. The column was equilibrated in gel filtration buffer and subsequently washed with a high salt wash (1 M NaCl). Buffer containing $MnCl_2$ was then added to specifically elute nhSP-D. Buffer containing EDTA was then used to elute any other proteins bound to the column. Peak absorbance readings corresponding to elution with $MnCl_2$ or EDTA containing buffer are indicated. Affinity chromatography was undertaken by Alastair Watson and Zofi McKenzie.*

A Gel Filtration

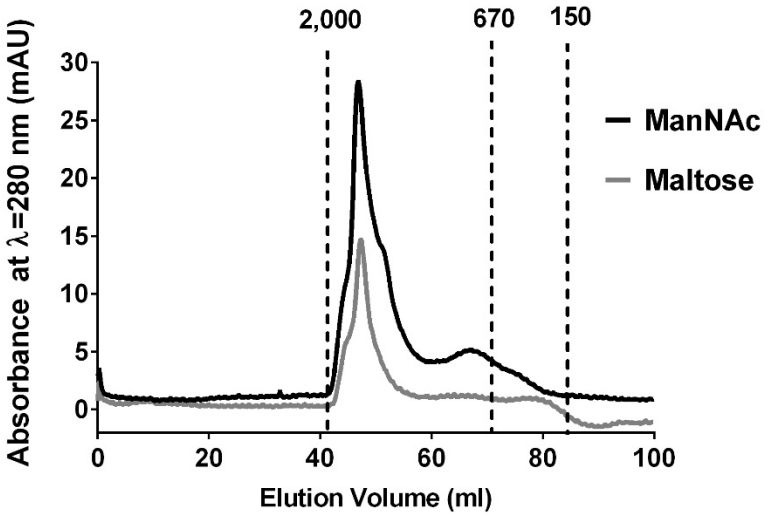

B ELISA of Gel Filtration Fractions

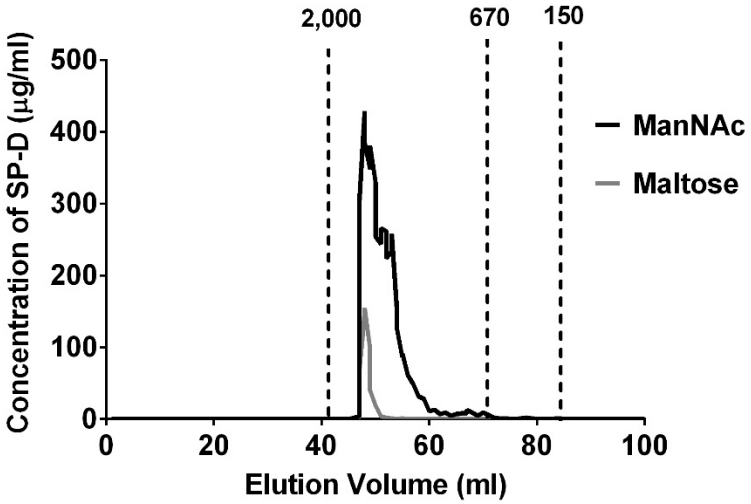

Figure 3-3: Gel filtration of nhSP-D and analysis of fractions by ELISA. *Shown are absorbance readings at λ = 280 nm upon elution from a 110 ml superpose 6 gel filtration column (**A**). Gel filtration was undertaken after affinity chromatography with either a maltose sepharose or ManNAc sepharose column. Fractions were then analysed by an SP-D ELISA (**B**). During SP-D ELISA analysis, protein concentrations were calculated by comparison with known concentrations of recombinant SP-D produced in human embryonic kidney cells, as previously described (54). Gel filtration and ELISA analysis were undertaken by Alastair Watson and Zofi McKenzie. Indicated are elution volumes of molecular weight standards blue dextran (2,000 kDa), bovine thyroglobulin (670 kDa) and alcohol dehydrogenase (150 kDa).*

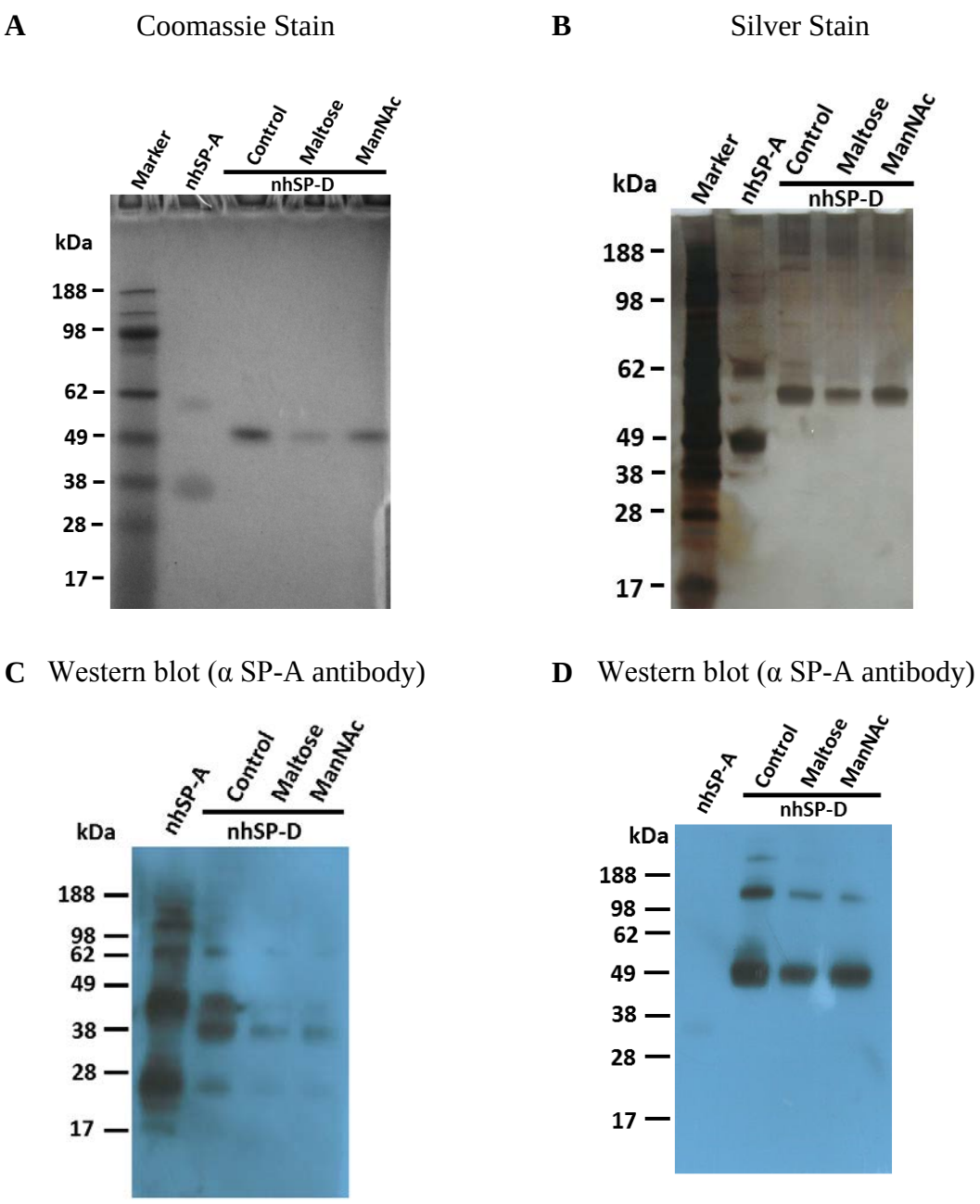

Figure 3-4: Comparison of Maltose and ManNAc affinity purification of nhSP-D by SDS-PAGE and Western blot analysis. *nhSP-D preparations purified by maltose and ManNAc affinity chromatography with subsequent gel filtration were analysed by SDS-PAGE under reducing conditions. Previously purified nhSP-A and nhSP-D were also analysed as positive controls. 1 µg of each sample, as determined by absorbance at λ = 280 nm, was loaded on to each gel. Gels were stained with either SimplyBlue SafeStain (**A**) or silver stain (7 min development) (**B**). Identical gels to **A** and **B** were also analysed by Western blot analysis using primary antibodies against nhSP-A (**C**) and rfhSP-D (**D**); Western blot exposures were for 3 min. SDS-PAGE gels and Western blots were undertaken by Alastair Watson and Zofi McKenzie.*

3.3.1.2 *Assessing the Importance of Gel Filtration*

Due to only small amounts of nhSP-D being initially purified and large quantities of protein being lost at each purification step, the importance of gel filtration for generating a pure nhSP-D preparation was assessed. Upon analysis with SDS-PAGE and Coomassie staining, nhSP-D was seen to be pure after maltose or ManNAc affinity chromatography (Figure 3-5A and data not shown). Importantly, no additional purity could be discerned after the additional gel filtration purification step. Upon analysis by Western blot analysis, bands seen on the SDS-PAGE gels were confirmed to be immunoreactive to a polyclonal rfhSP-D antibody (Figure 3-5C). In addition, Western blot analysis indicated minimal contamination of the purified nhSP-D by nhSP-A (Figure 3-5B). Western blot analysis indicated that an additional gel filtration step did not appear to reduce the small amount of nhSP-A contamination in the purified nhSP-D (Figure 3-5). Importantly, protein yield was lost through gel filtration. It was therefore decided that gel filtration would be undertaken only if the purified nhSP-D was not of sufficient purity, as determined by SDS-PAGE, Western blot analysis and analytical gel filtration.

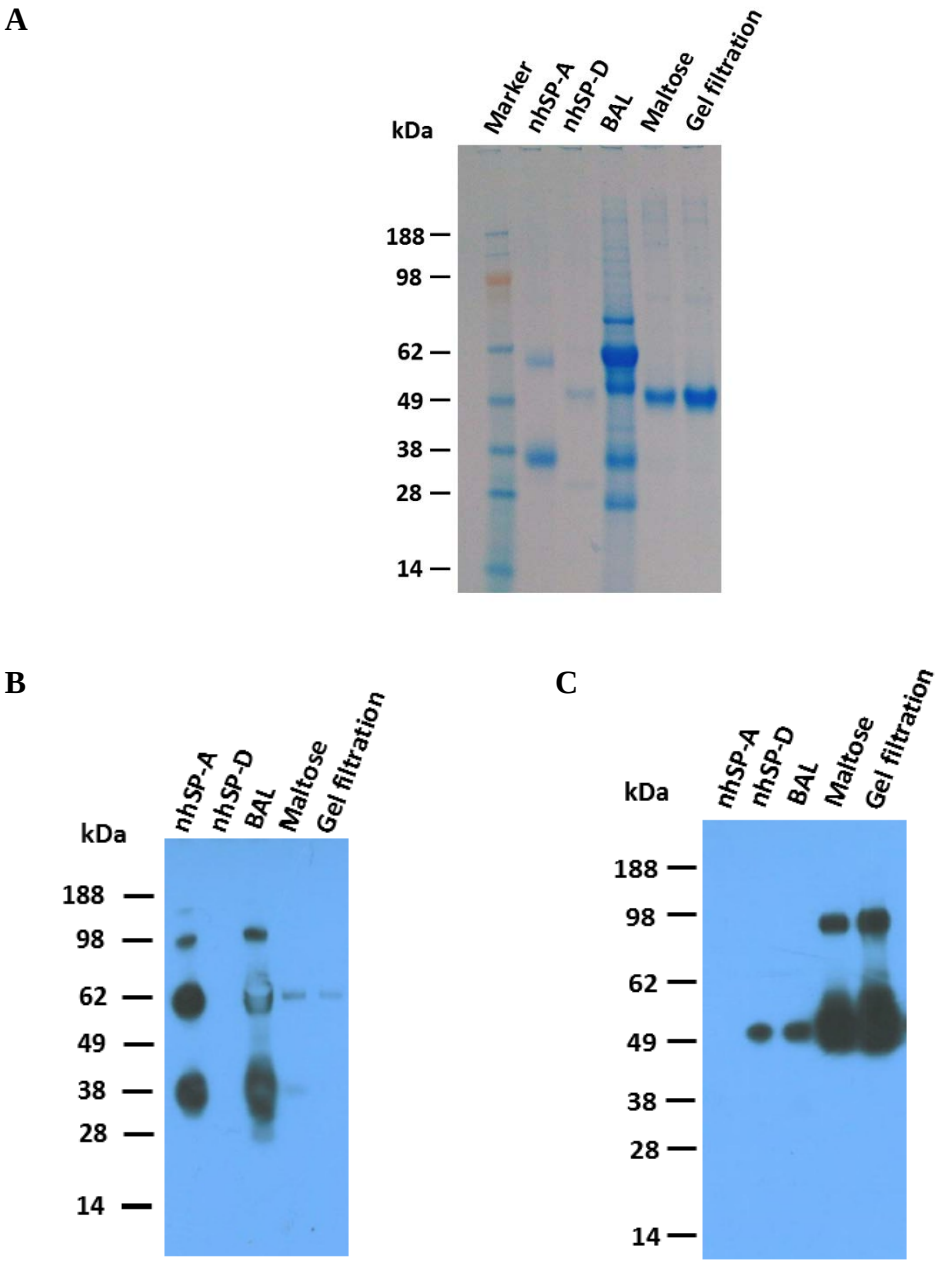

Figure 3-5: SDS-PAGE and Western blot analysis of the impact of gel filtration on nhSP-D purity.*Shown is a reduced SDS-PAGE gel comparing nhSP-D purified by only maltose affinity chromatography (Maltose) or by both maltose affinity chromatography and subsequent gel filtration (Gel filtration) (**A**). Previously purified nhSP-A and nhSP-D were analysed as positive controls. 1 µg of each protein sample, as determined by absorbance at λ = 280 nm, was analysed. 10 µl of BAL fluid was also analysed to identify the initial amount of SP-A and SP-D in the BAL. 0.5 µg of each protein and 5 µl of BAL fluid were also analysed by Western blot analysis using primary antibodies against nhSP-A (**B**) and rfhSP-D (**C**), Western blot exposures were for 30 sec.*

3.3.2 Characterisation of nhSP-D by TEM

To further investigate the structure and oligomeric states of the purified nhSP-D, TEM was implemented. TEM indicated that the nhSP-D purified by ManNAc affinity/gel filtration was a predominantly higher-order structures with some dodecamers (Figure 3-6). The nhSP-D consisted of clumps of aggregated protein. Due to the difficulty in identifying nhSP-D structures, oligomeric states could not be quantified.

A

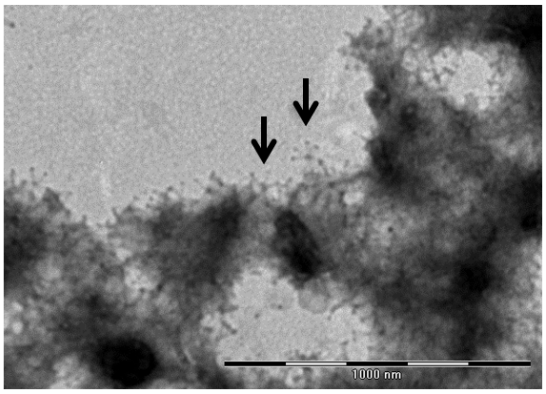

B

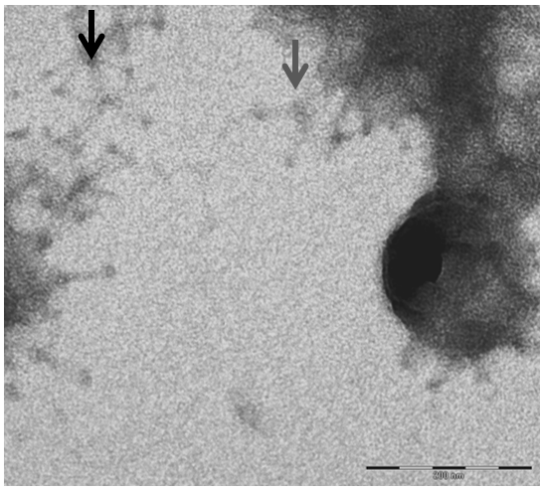

Figure 3-6: Analysis of nhSP-D by TEM. *nhSP-D purified by maltose affinity purification and subsequent gel purification was imaged by TEM using (**A** and **B**). Indicated are dodecameric (grey arrow) and higher-order multimeric (black arrows) structures. Scale bars are shown and represent 1,000 nm and 200 nm for **A** and **B**, respectively. Purification and characterisation of nhSP-D was undertaken by Alastair Watson and Zofi McKenzie.*

3.3.3 Purification of nhSP-A

3.3.3.1 *Purifying nhSP-A by Butanol Extraction*

nhSP-A was successfully purified from BAL of 16 different patients by butanol extraction. Upon analysis by SDS-PAGE, bands were seen at the expected size of approximately 36 kDa with non-reduced higher-order oligomers (Figure 3-7). Protein concentrations were analysed by both absorbance at λ = 280 nm and confirmed by BCA assay. Except for 'nhSP-A sample 6' both techniques resulted in similar calculated protein concentration. Upon averaging both techniques, concentrations of purified nhSP-A ranged from approximately 0.2 mg/ml to approximately 1.8 mg/ml with a mean (± standard deviation (SD)) of 2.8 (± 2.7) total purified nhSP-A. nhSP-A purified by butanol extraction was not endotoxin treated as undertaken for nhSP-D. However, upon measurement had low endotoxin levels (< 0.001 ng/µg). The identity and purity of nhSP-A was confirmed using mass spectrometry (data not shown).

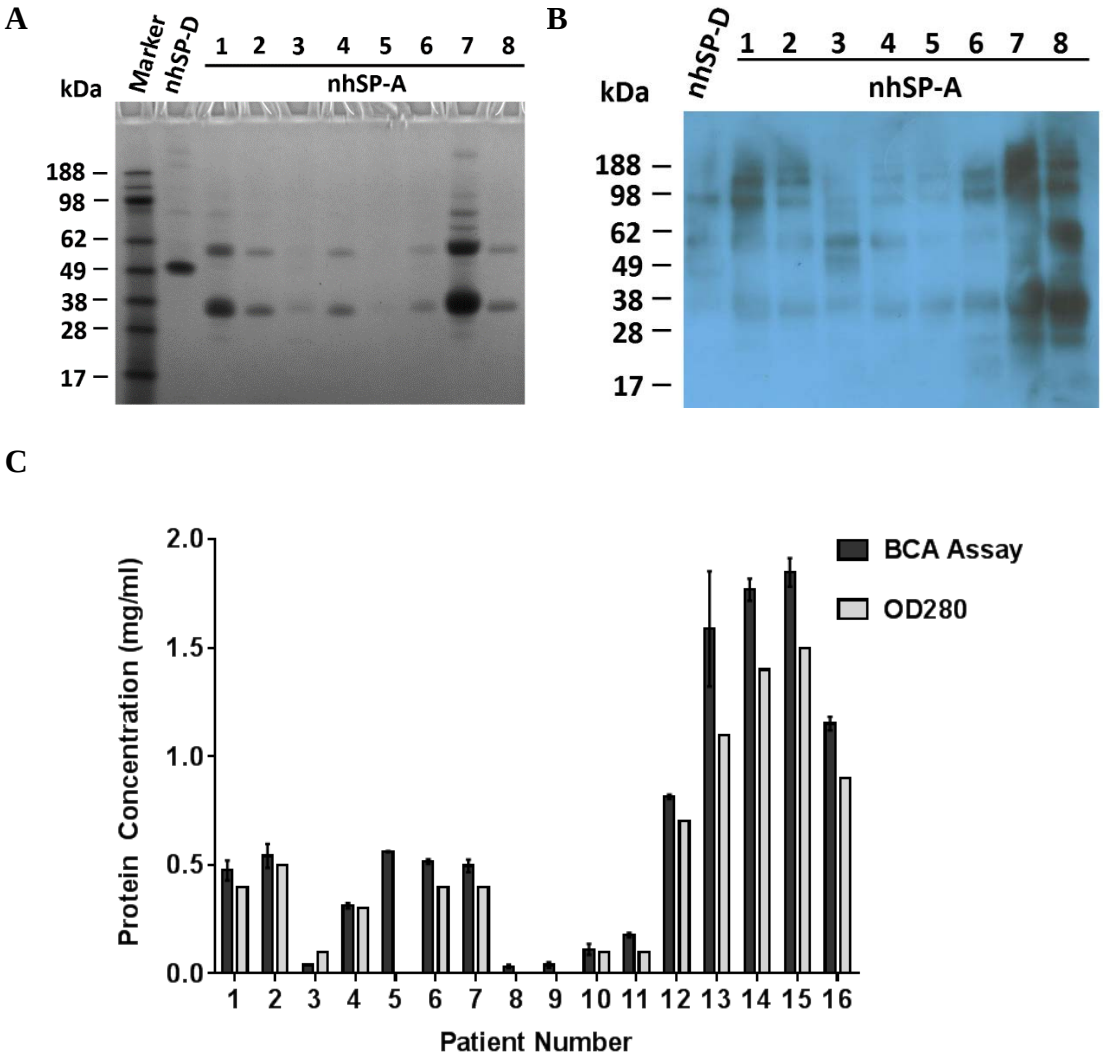

***Figure 3-7: Analysis of nhSP-A purity and concentration.**. Purified nhSP-A from 8 different patients was analysed by SDS-PAGE (**A**). Purified nhSP-D was also analysed for comparison (-C). Protein concentrations for nhSP-A purified from 16 different patients were calculated using absorbance at λ = 280 nm and confirmed with BCA assay (**B**). BCA assay was undertaken in duplicates. Mean (± SD) is shown. 5 min exposure*

3.3.3.2 *Purifying nhSP-A by Washing with EGTA*

To compare with the standardly used protocol of purifying nhSP-A by butanol extraction, the alternative method of washing the BAL with EGTA to purify nhSP-A was investigated. Purification of nhSP-A through this method without butanol extraction could allow later determination of the natural lipids in the lung which are bound by nhSP-A. The BAL pellet was washed 5 times in the presence of calcium, which was sufficient to remove the majority of the contaminants (Figure 3-8). nhSP-A was specifically

released from the pellet upon washing with EGTA, with low amounts of protein being released from the pellet in the third wash, as determined by OD at λ-280 nm. Using this method to purify nhSP-A from 1 ml of BAL from 6 different patients a mean (± SD) of 2.9 (± 1.4) mg of nhSP-A was purified. However, despite being able to purify nhSP-A using this method, after washing with EGTA, the majority of the nhSP-A still remained in the pellet. The nhSP-A purified by washing with EGTA was pooled and stored for characterisation of oligomeric state.

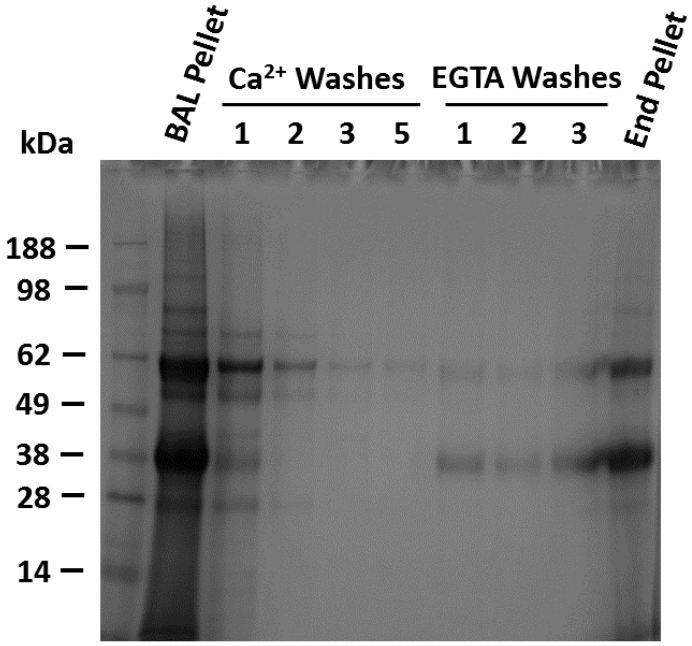

Figure 3-8: SDS-PAGE of nhSP-A purified without butanol. *Shown is SDS-PAGE analysis of samples taken from the BAL pellet prior to washing, supernatants after washing with in the presence of calcium up to five times. Also analysed was the nhSP-A purified from the pellet by washing in the presence of EGTA up to three times. The pellet was also analysed after purification of nhSP-A (end pellet). Shown is representative analysis of six different patients. Note EGTA wash 3 is contaminated by spill over from 'End Pellet' well.*

3.3.3.3 *Characterising the Oligomeric State of nhSP-A*

The oligomeric state of nhSP-A purified by each technique was analysed by gel filtration. The profile of different oligomeric states of nhSP-A purified by butanol extraction was similar between all four patients (Figure 3-9A). The majority of the protein was spread between three overlapping peaks between the 2,000 kDa and 669 kDa protein standards, with the major peak eluting just before the 669 kDa marker, likely corresponding to octadecameric nhSP-A. There was also an additional peak of protein which eluted at

approximately 22 ml, likely degraded protein. nhSP-A from all 4 patients purified using butanol extraction had a similar profile of oligomeric states.

Comparatively, a larger proportion of the nhSP-A purified by washing with EGTA appeared to have a considerably higher molecular weight than the butanol extracted nhSP-A. The major peak for nhSP-A purified by EGTA washing eluted for both patients just before the 2,000 kDa marker, which likely represents aggregated or nhSP-A of a higher order oligomer than the octadecamer (Figure 3-9B). The secondary protein peak eluted at a similar volume to the butanol extracted nhSP-A, just before the 669 kDa marker, likely representing the octadecameric nhSP-A. An additional peak was also seen at either approximately 21 ml or approximately 22 ml. The profile of the different molecular weights of nhSP-A purified by EGTA washing were similar between both patients. Importantly, there was an apparent absence of 105 kDa trimeric nhSP-A in all of the patients with nhSP-A purified by butanol extraction and EGTA washing.

A **Purified by Butanol Extraction**

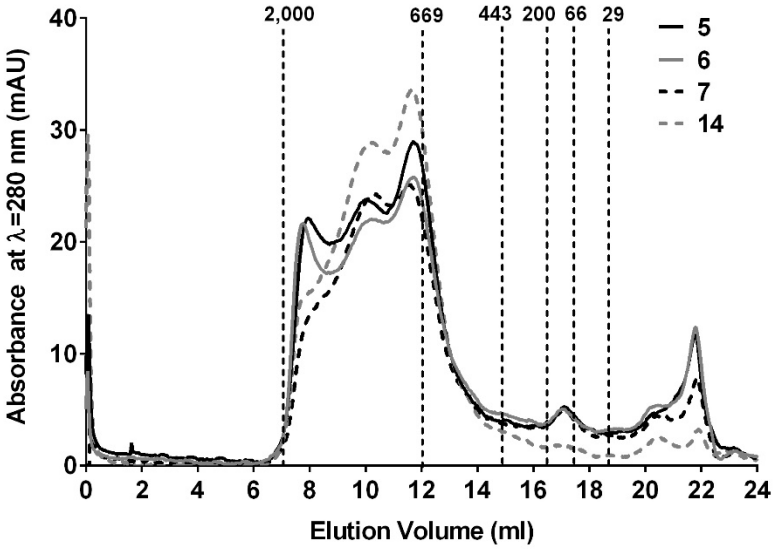

B **Purification with EGTA**

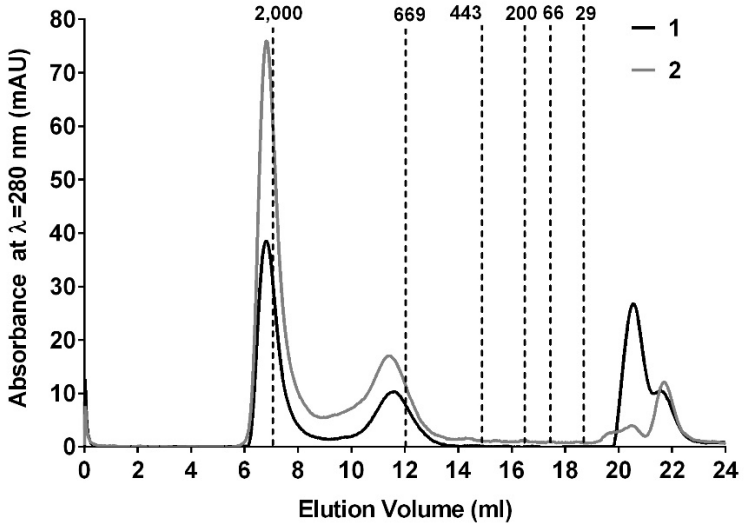

Figure 3-9: Analysis of nhSP-A oligomeric structure. *nhSP-A purified by either butanol extraction (**A**) or using the alternative method of EGTA release from the pellet (**B**) was analysed by gel filtration using a 24 ml superose 6 column. The absorbance at λ = 280 nm (mAU) was continually measured and is shown. Elution volumes of nhSP-A were compared with various protein standards including 29 kDa carbonic anhydrase (29), 66 kDa BSA (66), 200 kDa β-amylase (200), 443 kDa apoferritin (443), 669 kDa thyroglobulin and 2,000 kDa blue dextran (2,000). nhSP-A from four different patients purified by butanol extraction was analysed (patient 5, 6, 7 or 14). nhSP-A from two different patients purified by washing with EGTA was analysed (Alternative 1 and Alternative 2).*

3.3.4 Mass Spectrometry of nhSP-A – Characterising the SP-A1:SP-A2 Ratio

3.3.4.1 *Initial Mass Spectrometry*

nhSP-A purified from BAL by butanol extraction was digested with trypsin and CNBr to produce peptides small enough to be analysed by mass spectrometry. Through mass spectrometry and comparison of identified peptides with a human proteome database, the purified protein was confirmed to be nhSP-A. Importantly, nhSP-D was not identified in the nhSP-A preparation, highlighting the purity of nhSP-A isolated by butanol extraction.

Preliminary analysis of nhSP-A mass spectrometry allowed only 61.8 % of the SP-A sequence to detected (Figure 3-10). Importantly, the peptides which could potentially allow distinction between SP-A1 and SP-A2 were not identified by mass spectrometry (Figure 1-1). This was hypothesised to be due to inefficient cleavage by trypsin or the cleaved fragments not being suitably ionised for detection by mass spectrometry.

M+WLCPLALNLILM+AASGAVCEVK=DVCVGSPGIPGTPGSHGLPGR=DGR=**D**
GLK=GDPGPPGPM+**GPPGEM**+PCPPGNDGLPGAPGIPGECGEK=GEPGER=GPP
GLPAHLDEELQATLHDFR=HQILQTR=GALSLQGSIM+TVGEK=VFSSNGQSITF
DAIQEACAR=AGGR=IAVPR=NPEENEAIASFVK=K=YNTYAYVGLTEGPSPGDF
R=YSDGTPVNYTNWYR=**GEPAGR**=GK=EQCVEM+YTDGQWNDR=NCLYSR=L
TICEF

Key

Fragment identified
Fragment not identified
Leader sequence
Fragments that could distinguish between SPA1 and SPA2
+ Cyanogen bromide cleavage site
= Trypsin cleavage site

Figure 3-10: Analysis of nhSP-A by mass spectrometry. *Shown is the amino acid sequence for SP-A1 with CNBr (+) and trypsin cleavage sites (=). Fragments identified by mass spectrometry are highlighted (green) as are fragments not detected (red). SP-A1 specific peptides (DGLK and GPPGEM), in addition to a peptide (GEPAGR) which would allow quantification of total levels of SP-A are indicated (bold). Also indicated is the leader sequence which is considered to be cleaved from SP-A1 and SP-A2 in the mature proteins (blue) (257).*

3.3.4.2 *Optimising the Cleavage of SP-A through Partial Digestion with Collagenase*

To try and increase the capacity for trypsin digestion and the proportion of SP-A detectable by mass spectrometry, partial-digestion of nhSP-A with collagenase was investigated. It was thought that this would allow more efficient unwinding of the collagen-like domain and an increased access of trypsin.

After titration of a collagenase concentration at which only partial collagenase digestion occurred (data not shown), the capacity for collagenase to aid the digestion of nhSP-A by trypsin was investigated. Upon analysis by SDS-PAGE, the majority of nhSP-A was digested upon digestion with trypsin alone (Figure 3-11). However, a smear of higher order products which likely correspond to undigested and partially digested nhSP-A was also seen under non-reducing conditions (Figure 3-11A). Pre-treatment of nhSP-A with increasing collagenase concentrations and subsequent digestion with trypsin did appear to slightly reduce the smear corresponding to undigested and partially digested nhSP-A. However, the change was unable to be accurately distinguished using SDS-PAGE under non-reducing conditions. In addition, undigested or partially digested nhSP-A could not easily be seen using SDS-PAGE under reducing conditions (Figure 3-11B). No conclusions could therefore be drawn about the impact of collagenase pre-treatment on trypsin digestion of nhSP-A.

Three additional bands could be seen upon SDS-PAGE analysis under non-reducing conditions. An additional band could also be seen upon analysis by SDS-PAGE gels under reducing conditions. However, these extra bands also appear in previously analysed negative controls containing trypsin only (data not shown). Importantly, partial digestion of nhSP-A with collagenase did not enhance the coverage of nhSP-A that was detected upon analysis my mass spectrometry.

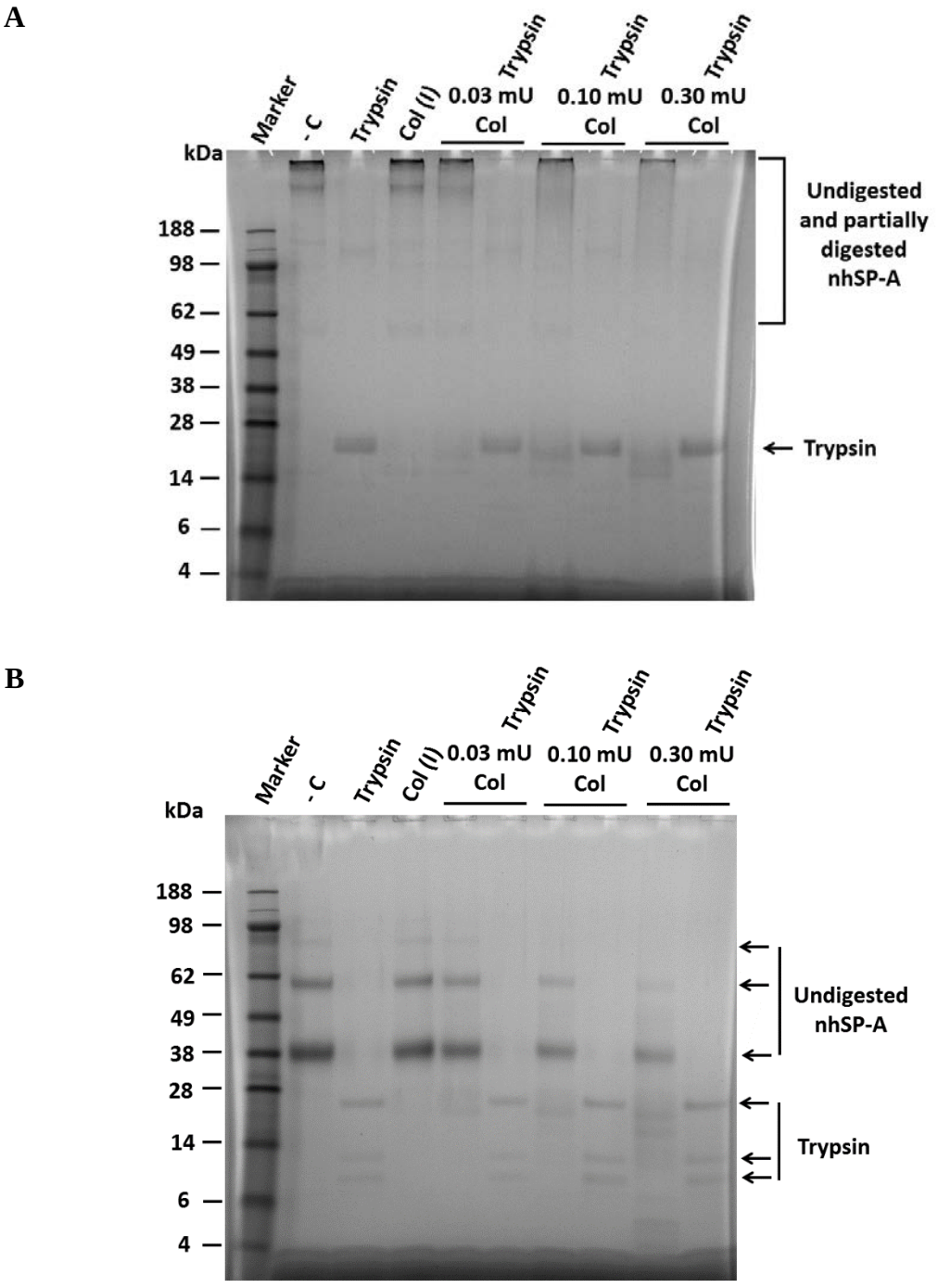

Figure 3-11: SDS-PAGE analysis of trypsin digestion efficiency after partial digestion with collagenase. *The impact of partial digestion with collagenase on trypsin digestion of nhSP-A was analysed by SDS-PAGE under non-reducing (**A**) and reducing conditions (**B**). 5 µg of nhSP-A was analysed and was either undigested (- C), digested with trypsin alone (Trypsin), partially digested with inactivated collagenase (Col (I)) or partially digested with varying concentrations of collagenase (0.03 mU Col, 0.1 mU Col or 0.3 mU Col) and subsequently left (blank) or digested with trypsin (Trypsin).*

3.3.4.3 *Optimising Cleavage of nhSP-A to Identify SP-A1 and SP-A2*

It was also hypothesised that denaturation of nhSP-A in 8 M urea and subsequent use of the protease Lys-C in 4 M urea would enable improved digestion of nhSP-A and detection by mass spectrometry. nhSP-A was denatured in 8 M urea with subsequent cleavage with Lys-C in 4 M urea with additional digestion with trypsin when diluted to 2 M urea. This digestion condition was compared to digestion with Lys-C alone or trypsin alone and analysed by SDS-PAGE, but as above improved digestion could not be detected by SDS-PAGE (Figure 3-12).

Mass spectrometry of the denatured, Lys-C and trypsin digested nhSP-A was then undertaken by Henrik Molina at the Proteomic Resource Center at Rockefeller University, New York, USA. Upon analysis by mass spectrometry, there was an improved coverage of detection than previously obtained with 90.7 % of both SP-A1 and SP-A2 being detected compared with the previous 61.8 %. Importantly, this higher detection coverage meant that peptides which distinguished between SP-A1 and SP-A2 were successfully detected (detected unique peptides are listed in Table 3-1). These unique peptides allowed the identification of the genotype of the patient who's SP-A was purified. The analysed patient had SP-A corresponding to a 6A3 genotype for SP-A1 and 1A0 genotype for SP-A2. Peptides from no other genotype were detected. SP-A1 6A3 and SP-A2 1A0 genotypes have a frequency in the general population of approximately 23% and approximately 55%, respectively (259).

Despite unique peptides between SP-A1 and SP-A2 being detected, they were relatively long, the smallest of which was 28 amino acids. Digestion of SP-A with Lys-C and trypsin after denaturation in 8 M urea was not sufficient to allow detection of the SP-A1 peptides 'DGLK' and 'GPPGEM', the SP-A2 peptide 'DVGK' or the SP-A peptide and 'GEPAGR' alone, these were only detected as part of larger peptides. In addition the peptide 'GEPAGR' which could be used for quantification of total SP-A was not detected alone but as part of a larger peptide. Due to the inability to detect these peptides alone which is essential for quantification of the ratio of SP-A1:SP-A2 in the sample, further mass spectrometry was not undertaken. Of note, proline residues within the detected peptides were partially hydroxylated; this was highly variable.

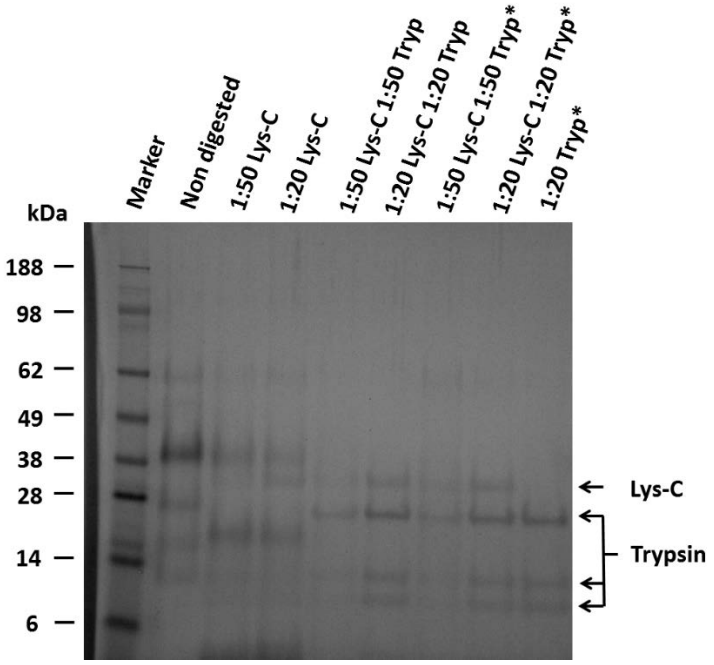

Figure 3-12: SDS-PAGE analysis of digested nhSP-A. *nhSP-A digested in various conditions were analysed by SDS-PAGE. Conditions included digestion of nhSP-A with Lys-C diluted either 1:50 or 1:20 only, with trypsin diluted 1:20 only, with both Lys-C diluted either 1:50 or 1:20 and subsequent digestion with trypsin diluted either 1:20 or 1:50. Extra trypsin diluted either 1:50 or 1:20 was added to some of the samples after 6 hours of trypsin digestion (*****). All samples were denatured in 8 M urea prior to digestion, Lys-C digestion was undertaken in 4 M urea and trypsin was undertaken in 2 M urea. Indicated are bands corresponding to the Lys-C and trypsin added into the assay. A non-digested nhSP-A was also analysed for comparison.*

SFPA1 unique peptides	**SFPA2 unique peptides**
DVCVGSPGIPGTPGSHGLPGRDGR**DG LK**	DVCVGSPGIPGTPGSHGLPGRDGR**DG VK**
GDPGPPGPM**GPPGEM**PCPPGNDGLP GAPGIPGECGEK	GDPGPPGPM**GPPGET**PCPPGNNGLP GAPGVPGER
GDPGPPGPMGPPGEMPCPPGNDGLP GAPGIPGECGEK	GDPGPPGPM**GPPGET**PCPPGNNGLP GAPGVPGERGEK
GEPGERGPPGLPAHLDEELQATLHDF R	GEAGERGPPGLPAHLDEELQATLHDF R

Table 3-1: Summary of detected peptides which distinguish SP-A1 and SP-A2. *Listed are the peptides identified by mass spectrometry which are distinct between SP-A1 and SP-A2. In grey are amino acids which are distinct between SP-A1 and SP-A2. In bold are peptides which if detected alone rather than in a longer peptide could be used to quantify the SP-A1:SP-A2 ratio. Mass spectrometry was undertaken by Henrik Molina at the Proteomic Resource Center at Rockefeller University.*

3.4 Summary of Results

The work in this chapter investigated different ways of purifying nhSP-A and nhSP-D from human lung, characterised their oligomeric structures and identified SP-A1 and SP-A2 using mass spectrometry. Attempts to quantify an SP-A1:SP-A2 ratio in nhSP-A are detailed. This chapter addressed Aim 1 - (Section 1.14):

- To purify nhSP-A and nhSP-D, characterise their oligomeric state and determine the SP-A1:SP-A2 ratio in the human lung quantitatively using mass spectrometry.

The main findings of this chapter are given below:

- Purification with ManNAc affinity chromatography allowed effective purification of nhSP-D from human BAL and gave higher protein yields than using the standardly used maltose affinity chromatography. Gel filtration did not appear to increase the purity of the nhSP-D protein preparation.
- Purified nhSP-D was in the structure of higher order oligomers with the majority of protein being of an apparent molecular weight of approximately 1,700 kDa, with a proportion also being approximately 800 kDa. Higher order oligomers of nhSP-D were successfully identified by TEM.
- nhSP-A was purified using both butanol extraction and the alternative method of washing with EGTA. Pure nhSP-A was successfully isolated from BAL of a total of 22 different patients. Similar yields were obtained with each purification technique.
- Purified nhSP-A was in the structure of higher order oligomers with apparent molecular weight of approximately 2,000 to 669 kDa. Importantly, the apparent molecular weight was increased in nhSP-A purified by washing with EGTA.
- Peptides distinguishing between SP-A1 and SP-A2 were successfully identified using mass spectrometry. However, due to the difficulty of detecting peptides, SP-A1:SPA2 ratios were not quantified.

3.5 Discussion

In order to characterise the importance of the N-terminus and oligomeric structure of SP-A and SP-D in their interaction with RSV, nhSP-A and nhSP-D were purified for later comparison in functional assays with rfhSP-A and rfhSP-D (Chapter 7). This chapter evaluates different ways of purifying nhSP-A and nhSP-D from human lung, characterising their oligomeric structures and identifying a SP-A1:SP-A2 ratio using mass spectrometry (Aim 1 - Section 1.14).

3.5.1 Purification of nhSP-D

In this chapter BAL from a single patient was used to allow the side by side comparison of both maltose and ManNAc affinity chromatography for the purification of nhSP-D. ManNAc affinity chromatography gave higher yields of final purified protein in addition to lower levels of endotoxin. This technique was therefore taken forward for future purification of nhSP-D and the purified protein used in functional assays. nhSP-D and nhSP-A have previously been reported to have higher avidities for ManNAc than maltose and thus may account for the increased yields obtained through using ManNAc affinity purification (58, 77). Indeed, ManNAc affinity chromatography has previously been reported to improve recovery of nhSP-D purified from amniotic fluid as compared with maltose affinity (260). In addition, ManNAc affinity chromatography increased recovery of lower oligomeric structures including trimeric units. In this present study, the majority of nhSP-D purified by both affinity methods was of higher order structure with an estimated size of approximately 1,700 kDa. However, a smaller secondary peak corresponding to nhSP-D of an estimated approximately 800 kDa size was also purified through use of ManNAc affinity chromatography (Figure 3-3). This secondary peak was, however, not seen when using maltose affinity chromatography, perhaps due to the lower avidity of binding which nhSP-D has for this sugar (Figure 3-3).

Due to nhSP-A also having a higher avidity of binding for ManNAc, it was thought that use of ManNAc affinity chromatography may increase levels of nhSP-A contamination. However, levels of nhSP-A contaminating the purified nhSP-D were negligible, with any bound nhSP-A remaining bound to the affinity column, thus highlighting the specificity of eluting nhSP-D with $MnCl_2$ (Figure 3-5). It was clear that patient variability was an important factor influencing yields of purified nhSP-D. This was apparent from the range

of 0.66 mg of protein purified from 1.5 L of BAL (0.44 mg/l) to 4.9 mg from 4L (1.23 mg/l). This may in part be a consequence of different lavage techniques and resultant concentrations of surfactant in the lavage. However, a large part of this likely stems from the heterogeneity of the group of diseases which comprises patients with PAP (261).

Incorporation of a gel filtration step during purification did not increase the purity of nhSP-D as determined by SDS-PAGE and Western blot analysis (Figure 3-5). Thus due to protein loss associated with this purification step, during future purifications of nhSP-D, gel filtration was first used only as an analytical tool with subsequent later use if the nhSP-D was not of high purity. nhSP-D is reported to be of a mixture of oligomeric states in the lung (39). The predominance of highly oligomeric SP-D of an apparent molecular weight of approximately 1.7 MDa with only small amounts of lower (apparent approximately 800 kDa) molecular weight protein in this present study was surprising. With a trimeric nhSP-D protein with a predicted molecular weight of 129 kDa, the approximately 1.7 MDa protein constitutes a theoretical multimer containing approximately 13 trimeric units. However, this is likely an overestimate due to the variable glycosylation at the N-terminal tail which has been reported to give a nhSP-D monomer of up to a 50 kDa size (262) comparative to the reported 43 kDa SP-D monomer (263). Indeed in this present study a reduced nhSP-D monomer upon analysis by SDS-PAGE migrated at approximately 50-52 kDa (Figure 3-5). Due to the expansive structures of the nhSP-D multimers, the true molecular weight may be lower than that determined by gel filtration as compared with the more compact structures of blue dextran and thyroglobulin. Thus, the secondary peak with an apparent approximately 800 kDa seen with the ManNAc affinity chromatography could correspond to a dodecameric structure (predicted molecular weight of 516). Surprisingly, however, previous analysis of an approximately 800 kDa peak of SP-D purified by gel filtration by atomic force microscopy (AFM) highlighted this peak to correspond predominantly to trimeric structures (approximately 150 kDa). AFM was also attempted in this present study; however, due to the machinery set up, protein structures could not be resolved (data not shown) and the oligomeric structure of SP-D could not be confirmed.

The degree of oligomerisation of purified nhSP-D may also be influenced by patient variability. This may explain the apparent highly oligomeric SP-D purified in this present study. nhSP-D has been known to be influenced by both genetic and environmental factors. A common Met/Thr11 point mutation has been shown to be important in

influencing the degree of SP-D oligomerisation where the Thr11 genotype has been shown to have a higher ratio of lower molecular weight SP-D (263). In addition, nitrosylation of SP-D has been shown to be integral in disruption of the SP-D oligomeric state through interrupting interacting cysteine residues at the N-terminus (264). Different inflammatory states within the lung may, therefore have an influence on SP-D oligomerisation. Human PAP patients have been reported to have an accumulation of higher-order SP-D with a >90 % of the accumulated SP-D appearing near the void volume when analysed by gel filtration (265). This could explain the highly oligomeric nhSP-D which was purified in this present study. The degree of nhSP-D oligomerisation is known to influence SP-D function and thus patient to patient variability should be considered an important factor in functional assays (33, 50-55). nhSP-D from a single patient was used in all functional assays in this present study.

In this study the quantification of the oligomeric states of maltose and ManNAc purified nhSP-D by TEM was attempted. However, structures could only be resolved when in complex with clumps of aggregated protein, thus quantification was not possible. The aggregated protein was likely an artefact of protein drying, fixing or staining (Figure 3-6). TEM and AFM have previously been optimised and implemented to successfully visualise nhSP-D (39, 263), respectively. Optimisation of these techniques could allow determination of differences in oligomeric structure between different patients and between the impacts of the purification technique. In addition, it could allow the visualisation of rfhSP-D and rfhSP-A.

3.5.2 Purification of nhSP-A

nhSP-A was purified from the lungs of 22 different PAP patients to attempt to quantify a SP-A:SP-A2 ratio in the human lung using mass spectrometry. nhSP-A was initially purified using the widely used butanol extraction technique (254). Protein purified using this technique from a single patient was later used in functional assays to compare with rfhSP-A. However, to assess the impact of nhSP-A purification on its oligomeric structure in addition to allowing the potential subsequent quantification of nhSP-A-associated lipids by mass spectrometry, nhSP-A was later purified through the alternative technique of washing the BAL pellet with EGTA. Both techniques gave similar yields of protein with a mean (± SD) of 2.8 (± 2.7) mg purified from 1.5 ml of BAL using butanol extraction or 2.9 (± 1.4) mg purified from 1.0 ml of BAL purified through EGTA washing.

Future lipid extraction of nhSP-A purified by EGTA washing and analysis by mass spectrometry could allow the determination of which natural lipids in the lung SP-A binds to. Interestingly, upon analysis of the remaining pellet after EGTA washing by SDS-PAGE, a large proportion of the nhSP-A remained in the pellet (Figure 3-8). This could be protein either associated with the lipid pellet in a calcium independent manner or aggregated insoluble protein. Indeed, although SP-A mediated phospholipid vesicle aggregation is widely known to be calcium-dependent, there have been reports suggesting the capacity of SP-A to interact with DPPC vesicles in a calcium-independent manner, reviewed in (266). nhSP-A purified by butanol extraction had minimal levels of endotoxin despite not being endotoxin treated. Endotoxin levels were not, however, quantified for nhSP-A purified by EGTA washing and due to the absence of butanol extraction may be considerably higher.

The oligomeric structure of nhSP-A purified by butanol extraction was similar between different patients with the majority of the nhSP-A eluting in 3 independent peaks between the 669 kDa and 2000 kDa molecular weight markers with the prominent peak of a predicted approximately 700 kDa (Figure 3-9A). This contrasted with nhSP-A purified by EGTA washing where nhSP-A from both patients eluted with a prominent gel filtration peak eluting earlier than the void volume with an apparent molecular weight of >2,000 kDa and a smaller secondary peak eluting just before the 669 kDa marker (Figure 3-9B). Although the approximately 700 kDa peaks may correspond to octadecameric SP-A with a reported molecular weight of 630 kDa (35 kDa per monomer), similarly to purified nhSP-D, a large proportion of the nhSP-A purified from PAP patients was of considerably higher molecular weight than expected. This is particularly the case for nhSP-A purified by EGTA washing.

Indeed, nhSP-A purified from PAP patients using butanol extraction has previously been reported to be of higher order oligomers than that of healthy patients with a majority of protein being of apparent >2,000 kDa (267, 268). These gel filtration profiles were similar to those obtained in this present study for the protein purified by washing with EGTA. Moreover, upon analysis by SDS-PAGE, nhSP-A from PAP patients has been reported to contain non-reducible bands at 62 kDa; these non-reducible bands were also seen in this present study (Figure 3-7) (269). This difference in SP-A structure has been suggested to have an impact on function where the higher order SP-A found in PAP patients had a higher propensity to self-aggregate and bind non-specifically and failed to form tubular

myelin structures (267). However, this contrasts with a previous report that SP-A purified from PAP patients was a mixture of oligomeric states with lower order oligomers including trimers (270).

Differences in surfactant composition and SP-A structure have been reported between patients and between the left and right lung of the same patient (269). This contrasts with this present study where a similar profile of nhSP-A oligomeric states was seen between different patients when the same purification technique was used, likely a consequence of the patient cohort used in this present study.

In this present study, the difference in nhSP-A oligomeric states dependent on the purification technique could be due to a number of factors. It could be due to a differential propensity of higher order nhSP-A to elute from the pellet in the presence of EGTA than the normal octadecamer. Alternatively, it could be due to SP-A purified by EGTA washing remaining bound to some lipids. This in itself could alter the molecular weight of the SP-A, or could lead to further non-specific binding, self-aggregation or the formation of supraquaternary structures. Supraquaternary structures of bovine SP-A have previously been described; however these were shown to form in a calcium-dependent manner (271). It is thus important to bear in mind the potential differences of SP-A purification method and patient variability when interpreting results from different studies. It is also important to consider that whilst during the purification of nhSP-D functional carbohydrate binding protein is selected for by carbohydrate affinity chromatography, this selection process is not widely undertaken upon purification of nhSP-A. nhSP-A purifications may therefore, contain a proportion of non-functional protein. This is particularly pertinent due to the protein being purified from PAP patients where the SP-A likely has a higher retention time in the alveolus and may be exposed to oxidative enzymes or proteases to a varying degree depending on the patient.

3.5.3 Quantifying the SP-A1:SP-A2 Ratio in the Human Lung

Through use of an SP-A1 specific antibody, an SP-A1:SP-A2 ratio in the human lung, has been investigated (241). However, no one has as yet identified such a ratio using a suitable quantification technique such as mass spectrometry. In order to quantify large proteins by mass spectrometry, peptides are first generated by digestion with specific enzyme(s). These peptides have different propensities to ionise and be detected by mass

spectrometry. Therefore, to accurately quantify a peptide, a known amount of an equivalent labelled peptide is required for analysis alongside. Thus in order to quantify an SP-A1:SP-A2 ratio, suitable detectable peptides which distinguish between SP-A1 and SP-A2 first needed to be identified.

Upon analysis of amino acid differences between SP-A1 and SP-A2 genotypes, the peptide '-DGVK-' was found consistently in all 6 of the most frequent SP-A2 alleles. Importantly, this peptide would theoretically be generated upon cleavage of SP-A2 with trypsin. However, although the equivalent SP-A1 peptide '-DGLK-' is present in 3 of the most common SP-A1 alleles, a point mutation where L is substituted for V is seen in the most common allele $6A^2$, present in approximately 55% of the general population (272). Thus meaning that in approximately 55 % of the population, use of these peptides would not allow differentiation between SP-A1 and SP-A2. Should this peptide be used to distinguish SP-A1 and SP-A2 specifically in patients without the $6A^2$ genotype, homozygous patients for $6A^2$ could be identified by the apparent total absence of SP-A1 and excluded from the analysis. However, patients analysed who are heterozygous for $6A^2$ would not be distinguished and a false SP-A1:SP-A2 ratio would be determined. Use of this peptide would, therefore, require patient genotyping first with subsequent exclusion of those with the $6A^2$ genotype from analysis.

The amino acid sequence recognised by the SP-A1 specific antibody previously characterised antibody (241), '-CPPGN**D**GLPGAPG**I**PGE**C**GEK-', contains 3 amino acids (bold) which are consistently different between all the common genotypes. However this sequence does not contain appropriate arginine or lysine residues to allow Lys-C or trypsin digestion of the protein for subsequent quantification. Neither does it contain methionine residues to allow cleavage by CNBr. Moreover, the presence of 5 proline residues in this sequence makes it particularly problematic due to potential differences in hydroxylation as described previously (273) and in this present study. To quantify these peptides with variable hydroxylation, labelled peptides covering all possible combinations of proline hydroxylation would be required.

The only suitable peptide which could allow specific quantification of SP-A1 is '-MGPPGEMP-' which when cleaved at the C-terminus of methionine resides with CNBr would give 'GPPGEM'. However, the equivalent SP-A2 peptide is '-MGPPGET-' and thus would not be generated by CNBr cleavage and would result in a peptide which is too

long and contains too many proline residues to allow use in quantification. The peptide 'GEPAGR', however, is constitutively present in both SP-A1 and SP-A2 (SP-A constitutive peptide), is suitable for quantification and is also generated upon digestion with CNBr. Use of both 'GPPGEM' and 'GEPAGR' peptides could therefore allow an SP-A1:total SP-A ratio to be quantified and subsequent calculation of a SP-A1:SP-A2 ratio. However, due to the presence of two proline residues in the SP-A1 specific peptide, 'GPPGEM', 4 labelled peptides with each potential hydroxylation pattern would be required for quantification, i.e. GPPGEM, G**P**PGEM, GP**P**GEM and G**PP**GEM, (hydroxylated in bold). Moreover, two labelled peptides for the peptide 'GEPAGR' would also be required, i.e. GEPAGR and GE**P**AGR, (hydroxylated in bold). This means a requirement of 6 labelled peptides to allow determination of the SP-A1:total SP-A ratio. This approach may have limitations with regards to cost but appears to be the only feasible method to quantify a SP-A1:SP-A2 ratio by mass spectrometry. To overcome this problem, enzymatic modification of SP-A to add or remove all hydroxyl groups had also been considered. However, this would introduce additional problems due to uncertainty of enzyme efficacy in completion of the reaction.

Problems were also encountered with detection of SP-A peptides upon analysis by mass spectrometry. Initial digestion of nhSP-A with trypsin resulted in a low sequence coverage (61.8 %) without SP-A1 or SP-A2 specific peptides or the SP-A constitutive peptide being detected. However, denaturation of nhSP-A in urea and subsequent digestion with Lys-C and trypsin overcame this problem with 90.7 % of the sequence of both SP-A1 and SP-A2 being detected. This is due likely to the denaturation conditions allowing unfolding of the collagen-like domain and subsequent access of the enzymes to the cleavage sites. Alternatively, it could be due to use of a different mass spectrometry protocol. Use of this denaturation approach successfully allowed the distinction of specific peptides belonging to either SP-A1 or SP-A2. These were, however, part of larger peptides >27 aa (Table 3-1). The SP-A constitutive peptide was also only detected as part of a longer peptide, likely a consequence of either inefficient enzyme cleavage or an inability of the successfully cleaved peptide to ionise.

Further optimisation of cleavage conditions and addition of a CNBr cleavage step are required to allow identification of SP-A1 specific and SP-A constitutive peptides suitable for comparison against their labelled counterparts for quantification of a SP-A1:SP-A2 ratio. Despite these problems, further work allowing identification of a SP-A1:SP-A2

ratio in the human lung could be important in associating such a ratio with different diseases of the human lung and development of a suitable biomarker.

3.5.4 Summary

In summary, during this study both nhSP-A and nhSP-D were successfully purified using different techniques for use in functional assays to compare against rfhSP-A and rfhSP-D. Differences between the purification techniques were identified and discussed and, in addition to patient variability, should be considered when interpreting and comparing literature. Looking forward, the lack of a selection process for functional nhSP-A should be considered, particularly when comparing its function against nhSP-D which is selected for through use of carbohydrate affinity chromatography. Peptides which distinguished between SP-A1 and SP-A2 were detected by mass spectrometry. However, further optimisation of protein preparation prior to mass spectrometry needs to be undertaken to allow detection of peptides suitable for quantifying an SP-A1:SP-A2 ratio. However, it is possible that an aberrant SP-A1:SP-A2 ratio may alter SP-A function and, this ratio could potentially be used as a potential biomarker for various lung diseases.

Chapter 4: Cloning and Expression of Recombinant Collectins

4.1 Introduction

A functional rfhSP-D molecule composed of the CRD, neck and a short collagen-like stalk has been produced and has given insights into the structure/function relationship of SP-D and its mode of calcium-dependent ligand binding. This protein has potential for treatment of various respiratory diseases, particularly as an adjunct treatment to lipid surfactant therapies which currently lack SP-A and SP-D for the possible prevention of neonatal chronic lung disease. The rfhSP-D collagen-like stalk is hypothesised to act as an anchor to stabilise its trimeric structure *in vivo* at 37 °C. A rfrSP-A molecule has successfully been created and crystallised (32). However, human and rat SP-A proteins are different, particularly as human SP-A is composed of two gene products and rat only of one gene product. Others have tried to create a functional trimeric rfhSP-A molecule; however these attempts have not been successful, potentially due to the absence of the collagen-like stalk, which was previously shown to be essential for the function of rfhSP-D in preventing emphysema-like morphological changes in the SP-D$^{-/-}$ mice (44).

This chapter set out to clone rfhSP-A1 and rfhSP-A2 molecules which contain a Gly Xaa Yaa collagen-like stalk and are equivalent to rfhSP-D. rfrSP-A was previously produced in insect cells, capable of adding N-linked glycosylation to proteins (32). Thus, to prevent aberrant glycosylation, a point mutation was included to change Asn187 to Ser (N187S). In this present chapter, this N187S mutation was included in additional constructs (rfhSP-A1^{N187S} and rfhSP-A2^{N187S}) to allow potential future use in mammalian expression systems, in addition to possible functional studies about the impact of this mutation.

The current methodology for production of rfhSP-D involves expression and storage in insoluble inclusion granules which require solubilising with denaturation and concomitant loss in protein yields. The use of a solubility tag for production of rfhSP-D as well as rfhSP-A proteins could prevent the need for protein refolding. In addition, it could lead to a considerable increase in protein yield.

The NT domain of MaSp 1 of spider silk is thought to be responsible for the capacity to store the silk protein in the silk gland as soluble proteins of concentrations up to 50 % (w/w) despite being very prone to aggregation (244). Moreover, NT has been speculated to be useful as a general solubility tag for expression of heterologous proteins (250). It was also hypothesised that by reversal of the charged amino acids responsible for salt bridge formation and assembly of NT into dimers and aggregates upon lowering of the

pH, the solubility of NT would be increased. This chapter therefore set out to subclone rfhSP-A and rfhSP-D as fusion genes with NT (NT-rfhSP-A1 and NT-rfhSP-D) and NT^{dm} (containing the Asp40Lys and Lys65Asp point mutations (NT^{dm}-rfhSP-A1 and NT^{dm}-rfhSP-D)). An additional protein which is currently being investigated for its use as a solubility tag for heterologous protein expression is the 56-residue B1 domain of bacterial membrane protein G (PGB1), which has previously been described (274). PGB1 has previously been used to allow high levels of protein expression (150 mg/l of bacterial culture after purification with ion exchange chromatography and gel filtration (275). In this chapter the ability of PGB1 to act as an expression partner/solubility tag as compared with NT is described for the expression and purification of rfhSP-D.

To allow purification of the rfhSP-A and rfhSP-D fusion proteins with NT and NT^{dm} upon expression, a His_6-tag was included in the subcloned constructs. This would allow efficient purification by nickel affinity chromatography. Moreover, after expression and purification, to allow testing of the functionality of rfhSP-A and rfhSP-D produced through this method, a protease cleavage tag was included. A schematic illustrating the created NT-rfhSP-D and NT-rfhSP-A1 constructs is shown in Figure 4-1.

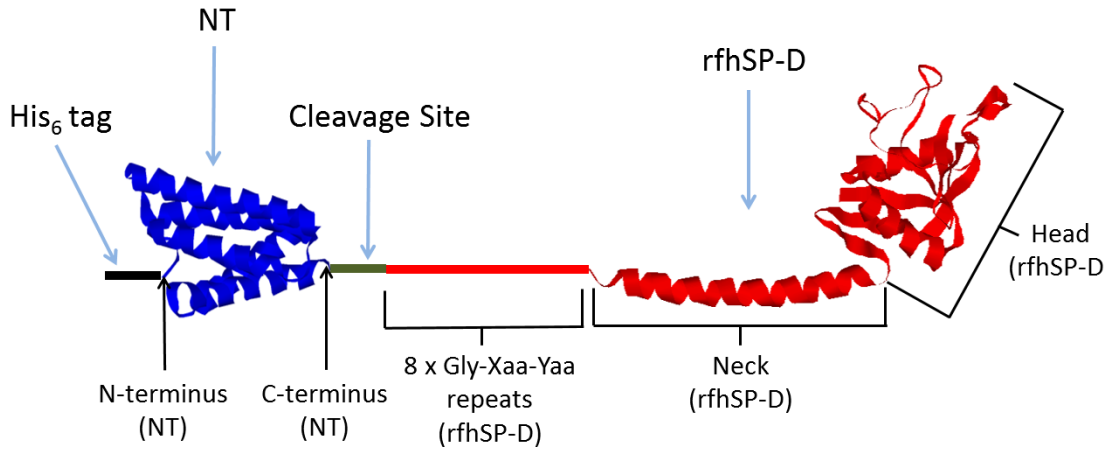

Figure 4-1: Representative schematic of Fusion NT-rfhSP-D and NT-rfhSP-A constructs. *Illustrated is a schematic representing NT-rfhSP-D and NT-rfhSP-A1, including a His_6-tag (black), NT (blue) and rfhSP-D (red). A cleavage site (green) is also indicated which was incorporated in the NT-rfhSP-A1 construct (*****); cleavage sites were either thrombin or human rhinovirus 3C protease cleavage sites. However, the cleavage site was not incorporated in the NT-rfhSP-D construct. The crystal structure for rfhSP-D was chosen for this figure as rfhSP-A has not yet been produced or crystallised. The C and N terminus of NT are labelled below the structure. Also labelled are the 8x Gly Xaa Yaa repeats, neck and head of rfhSP-D. The orientation and structure of this protein may not be accurate. This figure is not exactly to scale, however, rfhSP-D, NT and the 8 x Gly Xaa Yaa representation are approximately to scale.*

4.1.1 Aims

This chapter set out to address the initial parts of aims 2 and 3 (Section 1.14), to clone and express an rfhSP-A molecule which is equivalent to rfhSP-D. To clone rfhSP-A and rfhSP-D as fusion genes with NT and NT^{dm} and test their use as expression tags to allow high levels of heterologous protein expression. This chapter also set out to clone rfhSP-$A1^{N187S}$ and rfhSP-$A2^{N187S}$ constructs for potential future use in mammalian expression systems and investigation of the functional importance of this point mutation.

4.2 Methods

4.2.1 General DNA Techniques

4.2.1.1 *Design of Primers*

Primers were designed by analysing DNA sequences downloaded from the NCBI (Nucleotide) database and ordered from Invitrogen. Sequences and primers are listed in tables below. Primers were designed using sequences of the following mRNA transcripts obtained from the NCBI (Nucleotide) database:

- Homo sapiens surfactant protein A1 (SFTPA1), transcript variant 1, mRNA (NCBI Reference Sequence: NM_005411.4)
- Homo sapiens surfactant protein A2 (SFTPA2), mRNA (NCBI Reference Sequence: NM_001098668.2)

Primer	**Sequence**
SP-A F	CCTCATCTTGATGGCAGCCTCTGG
SP-A R	TCCCATGGCCTAAATGCCTCTCAGAA

Table 4-1: Primers used for cloning of SP-A DNA genes. *Listed are primers used to amplify both SP-A1 and SP-A2 cDNA sequences by PCR.*

Primer	Sequence
R2 (SP-A1)	**GGAGCTAGC**GGAGCCCCTGGTATCCCTGGAGAGT
R2 (SP-A2)	**GGAGCTAGC**GGAGCCCCTGGTGTCCCTGGAGAGC
F2	**GGAGGATCC**CCCATGGCCTAAATGCCTCTCAGAACTCAC
FM	GTACCAGTTGGTGTAGCTTACAGGGGTCCC
RM	GGGACCCCTGTAAGCTACACCAACTGGTAC

Table 4-2: Primers used for amplification of rhSP-A1, rfhSP-A2, rfhSP-A1^{N187S}.and rfhSP-A2^{N187S}.*Listed are the primers used for amplification of rfhSP-A1, rfhSP-A2, rfhSP-A1^{N187S}.and rfhSP-A2^{N187S}. These primers were also used to screen for E. coli containing the aforementioned genes. Indicated in bold for R2 and F2 primers are the 9 base overhangs incorporated which correspond to 3x arbitrary nucleotides and a Nhe1 or BAMH1 restriction enzyme site (underlined), respectively. FM and RM primers were used for incorporation of a 3 bp mutation in the sequence of rfhSP-A1 and rfhSP-A2 during site specific mutagenesis by overlap extension (3 bp mutation is highlighted in grey). This 3 bp mutation corresponds to an amino acid substitution of N187S.*

Primer	Sequence
NT-rfhSP-A1F	**TATATTGAATTC**ACTGGTGCCACGCGGT TCTCCGGGTATTCCGGGTGAA
NT-rfhSP-A1R	**CCGCGCAAGCTT**TCAAAATTCACAAAT CGTCAGGCGAGAGTACAGGC

Table 4-3: Primers used for amplification of rfhSP-A1 for generation of NT-rfhSP-A1 and screening bacterial colonies.*Listed are the primers used for incorporation of appropriate restriction enzyme sites to allow subcloning of rfhSP-A1 into a pET vector as a fusion gene with NT. Indicated in bold are the 12 bp overhangs incorporated which correspond to 6x arbitrary nucleotides and a EcoR1 or HindIII restriction enzyme site (underlined), respectively.*

Primer	Sequence
T7F	TAATACGACTCACTATAGGG
T7R	GCTAGTTATTGCTCAGCGG
M13F	TGTAAAACGACGGCCAGT
M13R	CAGGAAACAGCTATGACC

Table 4-4: Primers used for sequencing of DNA constructs.*Listed are the primers used to sequence different constructs containing pET vectors (T7 primers) and pCR2.1 vectors (M13 primers). NTF and NTR primers were used for sequencing of NT-rfhSP-A1 or NT-rfhSP-D constructs.*

4.2.1.2 *Agarose Gel Electrophoresis*

130 ml, 1.3 % (w/v) agarose gels were made by dissolving agarose in 40 mM tris-acetate, 1 mM EDTA, pH 8.0 (TAE buffer) through heating using a microwave. After cooling to approximately 60 °C, 13 µl of SYBR Safe (Invitrogen) was added. DNA was separated by electrophoresis at 100 volts for 50 min using TAE buffer. For determining DNA sizes,

a 1 Kb Plus DNA Ladder (Thermofisher Scientific, UK) was used, unless otherwise stated.

4.2.1.3 *PCR*

Polymerase chain reaction (PCR) was undertaken with a "proof reading" PCR enzyme using PCR reaction mix with appropriate template DNA (Table 4-5). Specific primers were used for each PCR reaction and are listed in Tables below. The PCR was undertaken with an initial incubation at 98 °C for 5 min followed by 40 PCR amplification cycles including the following steps:

- Denaturation at 98 °C for 5 sec
- Annealing for at 68 °C or 64 °C for 20 sec (PCR for initial cloning was undertaken at 68 °C. All other PCR reactions used an annealing temperature at 64 °C)
- Elongation at 72 °C for 60 sec

A final elongation step at 72 °C for 7 min was undertaken after the amplification cycles. This PCR protocol was used for cloning, subcloning, site specific mutagenesis by overlap extension and screening of *E. coli* colonies.

- Component	Volume
Template (1/20 diluted human lung cDNA / purified DNA plasmid / bacterial colony)	3.0 µl / 1.0 µl / 1 bacterial colony
10 mM dNTP Mix (Invitrogen)	1.5 µl
10x Pfx50 PCR Mix (Invitrogen)	5.0 µl
Forward primer (10 µM)	1.5 µl
Reverse primer (10 µM)	1.5 µl
Pfx50 DNA Polymerase (Invitrogen)	1.0 µl
Nuclease-free water	36.5 µl

Table 4-5: PCR reaction mix.*The volume of each component included in the PCR reaction mix is listed. This reaction mix was used for cloning, subcloning and screening of transformed E. coli. 1/20 diluted cDNA, purified DNA construct or a bacterial colony picked from an LB-agar plate was used as template for PCR, respectively.*

4.2.1.4 *Purification of DNA by Gel Extraction*

Following gel electrophoresis, amplicons of the correct size were excised from the agarose gel using a Qiagen Gel Extraction Kit (Invitrogen), according to manufacturer's instructions. The DNA was eluted in 30 µl of elution buffer.

4.2.1.5 *TA Cloning*

TA cloning was undertaken using a TA Cloning kit (with pCR2.1 Vector) (Invitrogen). 3' adenine (A) overhangs were first added to gel purified PCR amplicons using Taq DNA polymerase (Invitrogen) through incubation at 72 °C for 10 min in 3' A overhang reaction mix (Table 4-6); gel purification was undertaken as in Section 4.2.1.4. The amplicons with added 3' A overhangs were then ligated into a pCR2.1 cloning vector in a 3:1 molar fragment:vector ratio by incubation in the TA cloning ligation mix (Table 4-7) at 14 °C

overnight. Negative controls of TA cloning ligation mix without vector were also included for comparison.

To calculate the required amount of fragment for a 3:1 fragment:vector ratio the following formula was used whereby F = fragment and V = vector:

$$FAmount\ (ng)\ = \frac{Fsize\ (bp) \times VAmount(ng)}{Vsize\ (bp)}$$

Component	**Volume**
Purified hSP-A gene amplicons	5.0 µl
10 mM dNTP Mix	0.3 µl
10x PCR master Mix (Invitrogen)	0.4 µl
50 mM $MgCl_2$	0.2 µl
Taq DNA polymerase (Invitrogen)	0.2 µl (1 unit)
Nuclease-free water	43.9 µl

Table 4-6: TA cloning mix for addition of 3' adenine overhangs.*The volume of each component included in the reaction mix for addition of 3' adenine overhangs is listed in addition to the amount of Taq DNA polymerase enzyme used in units.*

Component	Volume
10x Ligation Buffer (Promega)	1.0 µl
hSP-A gene amplicons (with 3' A overhangs)	2.5 µl (9.6 ng)
T4 DNA Ligase (Promega)	1 µl (4 Weiss units)
pCR2.1 vector	2.0 µl (50 ng)
Nuclease-free water	3.5 µl

Table 4-7: TA cloning mix for ligation. *The volume of each component included in the ligation mix for ligating hSP-A into the pCR2.1 cloning vector is listed. Also stated is the mass of DNA used in the ligation and the amount of T4 DNA Ligase enzyme in units.*

4.2.1.6 *Purification of DNA Plasmids*

Single colonies were isolated from agar plates and grown in 5 ml of lysogeny broth (LB) at 37 °C overnight with shaking (225 rpm). Bacterial culture was undertaken with an appropriate antibiotic for selection (70 µg/ml kanamycin or 100 µg/ml ampicillin). Bacterial cells were harvested by centrifugation at 4,000 x g for 20 min. After resuspension, DNA was extracted using a Qiagen miniprep kit (Invitrogen), according to manufacturer's instructions. DNA was eluted in 30-40 µl of nuclease-free water.

4.2.1.7 *Sequencing of DNA Plasmids*

Purified DNA plasmids were sequenced by Source Bioscience (Oxford, UK). Constructs containing pET vectors were sequenced using T7 primers. TA cloned constructs containing the pCR2.1 vector were sequenced using M13 primers (primers are listed in Table 4-4). Results were analysed using Chromas Lite programme (version (v) 2013).

4.2.1.8 *Calculation of DNA and RNA Concentrations*

DNA and RNA concentrations were determined by analysis with a NanoDrop 1000 spectrophotometer (Thermo Scientific, USA), according to manufacturer's instructions. Concentrations were calculated using the below formulas:

$$DNA\ Concentration\ (ng/\mu l) = absorbance\ at\ \lambda = 260\ nm\ \times\ 50$$

$$RNA\ Concentration\ (ng/\mu l) = absorbance\ at\ \lambda = 260\ nm\ \times\ 40$$

4.2.2 General Bacterial Techniques

4.2.2.1 *Transformation of Competent E. coli*

DNA constructs were transformed into One Shot TOP10 chemically competent cells (Invitrogen), BL21 (DE3) competent cells (Promega, UK) or Rosetta (DE3) competent cells (kindly provided by Dr Anna Tocheva, University of Southampton). Transformation was undertaken using the heat shock method. Briefly, *E. coli* were incubated on ice with 2 µl of the TA cloning ligation mix (Table 4-7) or 0.5 µl of purified plasmid for 30 min; a positive control of *E. coli* transformed with 1 µl of pUC19 plasmid and a negative control of corresponding ligation mix without fragment were also included. *E. coli* were then subject to heat shock at 42 °C for 30 sec. 250 µl of SOC medium (room temperature) was then added to the cells. The transformed bacterial cells were incubated at 37 °C for 60 min, with shaking at 225 rpm.

4.2.2.2 *Culturing E. coli on LB Agar Plates*

20 ml LB-agar plates were made with appropriate antibiotics, 70 µg/ml kanamycin or 100 µg/ml amp. *E. coli* were spread onto pre-warmed plates and incubated at 37 °C overnight, after which, colony numbers were counted. For identification of bacteria containing pCR-2.1 vectors with an insert, blue/white screening was performed. This was done by spreading and drying 40 µl of 5-bromo-4-chloro-3-indolyl-β-d-galactopyranoside (X-gal) (40 mg/ml) on the LB-agar plate surface prior to spreading of *E. coli*.

4.2.3 Summary of Cloning and Subcloning

SP-A1 and SP-A2 cDNA sequences were TA cloned using oligo dT primed cDNA. cDNA was generated from RNA isolated from human lung tissue, kindly provided by Dr Jane Warner. Ethical permission exists for the use of human lung tissue resected with informed consent from patients undergoing thoracic surgery at Southampton General Hospital (Southampton & SW Hants LREC 08/H0502/32). Primers were used which did not distinguish between the two genes but which allowed amplification of both genes and subsequent screening to identify plasmids containing either the SP-A1 or SP-A2 cDNA sequences. Plasmids containing SP-A1 and SP-A2 cDNA sequences were identified after initial screening by sequencing (Source BioScience, UK). After TA cloning, PCR was implemented to generate rfhSP-A1 and rfhSP-A2 sequences which contained Nhe1 and BamH1 restriction enzyme cleavage sites, 5' and 3' of the genes, respectively. The rfhSP-A1 and rfhSP-A2 DNA sequences upon cloning into pET21a^{+} and pET24a^{+} vectors are given in Appendix (Figure 8-1), as are the corresponding amino acid sequences.

rfhSP-A1 and rfhSP-A2 sequences were then used for site specific mutagenesis by overlap extension to generate equivalent DNA sequences with an N187S mutation, rfhSP-A1^{N187S} and rfhSP-A2 ^{N187S}. rfhSP-A1, rfhSP-A2, rfhSP-A1^{N187S} and rfhSP-A2^{N187S} sequences were then TA cloned to allow efficient cleavage of the restriction enzymes sites and subsequently subcloned into pET expression vectors. pET 21 and 24 vectors were used for the expression of rfhSP-A1 and rfhSP-A2, which contain either an ampicillin or kanamycin gene, respectively. Alongside the expression of rfhSP-A1 and rfhSP-A2 separately, the expression of both genes simultaneously could potentially allow for the production of rfhSP-A containing both gene products.

After pilot expression experiments which did not show expression of rfhSP-A1 and rfhSP-A2 (Figure 4-12), the entire rfhSP-A1 sequence was synthesised to contain codons and GC content optimal for expression in *E. coli*. rfhSP-A1 with optimised codons was subsequently cloned into a pET expression vector and taken forward for the generation of NT-rfhSP-A1 and NT^{dm}-rfhSP-A1.

rfhSP-A1 was cloned as a fusion gene with NT through the use of PCR to incorporate appropriate EcoR1 and HindIII restriction enzyme cleavage sites, 5' and 3' of the gene, respectively. This allowed ligation of rfhSP-A1 into the pET vector as a fusion gene with NT. NT-rfhSP-D and PGB1-rfhSP-D were cloned into pET expression vectors by Kerstin

Nordling, Karolinska Institutet, Sweden. Subcloning of rfhSP-A constructs is summarised in Figure 4-2.

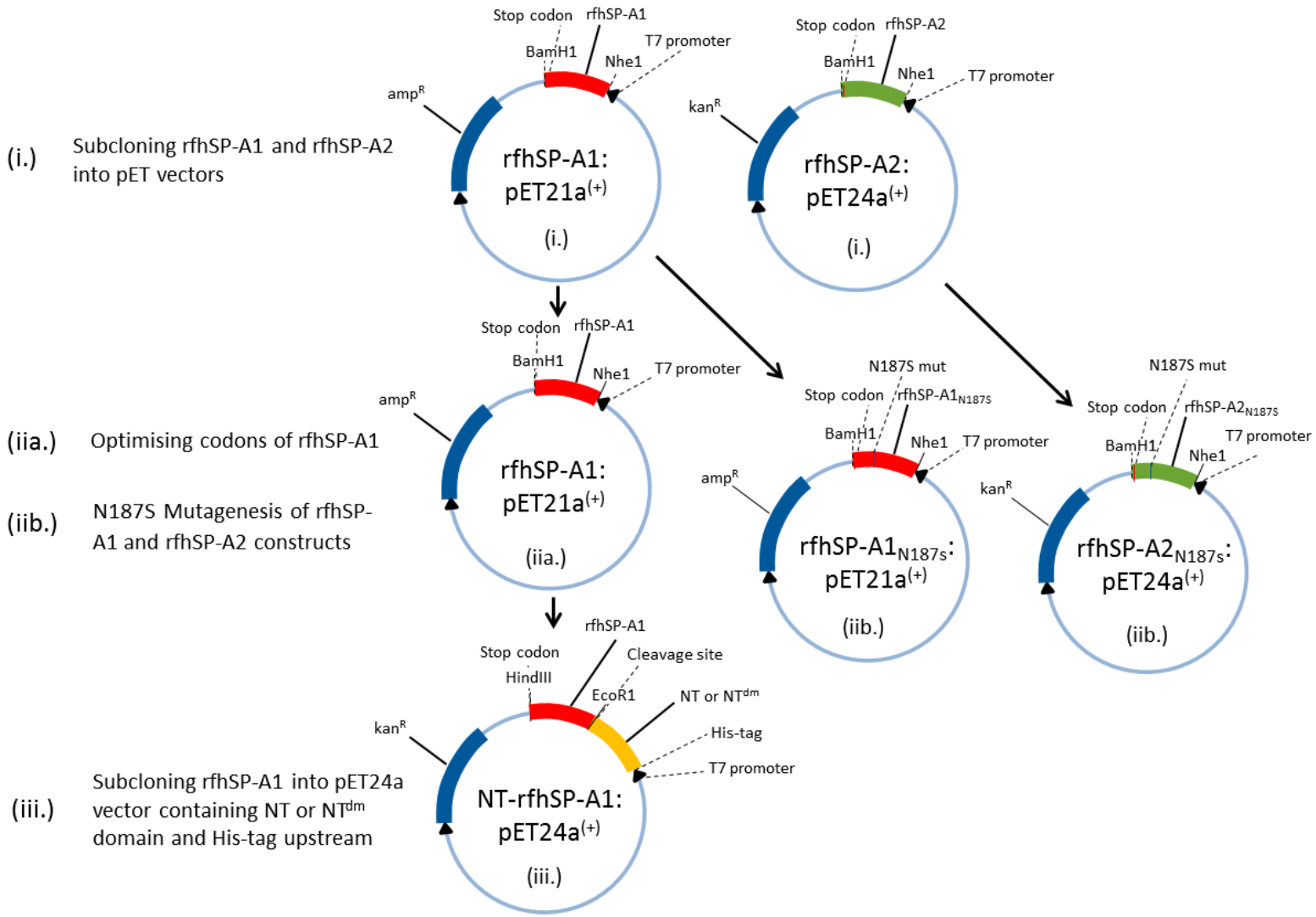
(i.)
Subcloning rfhSP-A1 and rfhSP-A2 into pET vectors
(iia.)
Optimising codons of rfhSP-A1
(iib.)
N187S Mutagenesis of rfhSP-A1 and rfhSP-A2 constructs
(iii.)
Subcloning rfhSP-A1 into pET24a vector containing NT or NTdm domain and His-tag upstream
Stop codon
rfhSP-A1
BamH1
Nhe1
T7 promoter
ampR
rfhSP-A1: pET21a(+)
(i.)
rfhSP-A2
kanR
rfhSP-A2: pET24a(+)
(i.)
rfhSP-A1: pET21a(+)
(iia.)
N187S mut
rfhSP-A1N187S
rfhSP-A1N187s: pET21a(+)
(iib.)
rfhSP-A2N187S
rfhSP-A2N187s: pET24a(+)
(iib.)
HindIII
Cleavage site
EcoR1
NT or NTdm
His-tag
NT-rfhSP-A1: pET24a(+)
(iii.)

Figure 4-2: Schematic outlining the subcloning of different rfhSP-A constructs. *Different constructs subcloned into pET21a$^+$ and pET24a$^+$ expression vectors are shown. Different genes are indicated including, rfhSP-A1 (red), rfhSP-A2 (green), NT (yellow) and ampicillin and kanamycin antibiotic resistance (blue). Also indicated are T7 promoters and restriction enzyme sites used for subcloning of the constructs (BamH1, Nhe1, HindIII and EcoR1). The different steps in the cloning of the different rfhSP-A constructs include, subcloning of rfhSP-A1 and rfhSP-A2 into pET vectors (**i.**), optimisation of rfhSP-A1 codons for expression in E. coli (**iia.**), N187S mutagenesis of rfhSP-A1 and rfhSP-A2 to remove the Asn187 glycosylation site (**iib.**) and subcloning of rfhSP-A1 (with optimised codons) into a pET24a+ vector downstream of NT or NT^{dm} (**iii.**). For simplicity, TA cloning steps are not included in the figure. However, TA cloning was implemented after amplification of genes using PCR due to problems with digestion of PCR amplicons. TA cloning steps for generation of NT-rfhSP-D and NT^{dm}-rfhSP-D are also not shown byt were cloned as in (**iii**.).*

4.2.4 Cloning of Human SP-A Genes

4.2.4.1 *RNA Extraction*

RNA was extracted from patient lung tissue taken from cancer patients with informed consent. Lung tissue was kindly provided by Dr Jane Warner. Ethical permission exists for the use of human lung tissue resected with informed consent from patients undergoing thoracic surgery at Southampton General Hospital (Southampton & SW Hants LREC 08/H0502/32). RNA was extracted using an RNeasy Minikit Qiagen (2010). Initially, 50 mg of lung tissue was homogenised for 60 second (sec)s in 1.2 ml of RLT buffer containing 143 mM β-mercaptoethanol. 700 µl of lung homogenate was then used for RNA purification, according to manufacturer's instructions. RNA was eluted with 50 µl of nuclease-free water.

4.2.4.2 *Production of cDNA*

cDNA was produced using the Superscript III reverse transcriptase kit (Invitrogen), according to manufacturer's instructions. RNA was initially denatured by incubating the denaturation reaction mix (Table 4-8) at 65 °C for 10 min followed by incubation on ice for 2 min. Denatured RNA was then used to synthesise cDNA with oligo(dT)$_{20}$ priming through incubation of the cDNA synthesis reaction mix (Table 4-9) at 50 °C for 45 min. The cDNA synthesis reaction was inactivated by incubation at 70 °C for 15 min and stored at -20 °C.

Component	Volume
Oligo(dT)$_{20}$ primer (Invitrogen)	1 µl (2.5 ng)
10 mM dNTP Mix (Invitrogen)	1 µl
RNA purified from human lung	2 µl (163.0 ng)
Nuclease-free water (Invitrogen)	9 µl

Table 4-8: RNA denaturation reaction mix components.*The volume of each component included for denaturation of RNA is listed. Also stated is the weight of lung RNA and Oligo(dT)$_{20}$ primer used.*

Component	Volume
RNA denaturation reaction mix product (Table 4-8)	13 µl
5 x First-Strand Buffer (Invitrogen)	4 µl
DL-Dithiothreitol (0.1 M)	1 µl
RNaseOUT Recombinant RNase Inhibitor (Invitrogen)	1 µl (40 units)
Superscript III RT (Invitrogen)	1 µl (200 units)

Table 4-9: cDNA synthesis reaction components. *The volume of each component included for synthesis of cDNA is listed as is the amount of each enzyme used in units.*

4.2.5 TA Cloning Human SP-A genes

hSP-A genes were amplified through PCR using primers, which did not distinguish between SP-A1 and SP-A2 (Table 4-1). PCR was undertaken using the PCR reaction mix given in (Table 4-5). PCR was undertaken as described in Section 4.2.1.3.

4.2.6 PCR and Subcloning of rfhSP-A1 and rfhSP-A2 by TA Cloning

To subclone rfhSP-A1 and rfhSP-A2 (containing the CRD, neck and 8x Gly Xaa Yaa repeats) and allow subsequent subcloning into pET21a+ or pET24a+ expression vectors, specific primers were designed containing overhangs with unique restriction sites corresponding to Nhe1 and BamH1 (primers shown in Table 4-2). Importantly, use of the NheI restriction enzyme site allowed fusion of rfhSP-A1 and rfhSP-A2 in frame with an ATG start codon upon subcloning into expression vectors. PCR was undertaken as described above (Section 4.2.1.3) using the reaction mix in (Table 4-5) to produce rfhSP-A1 and rfhSP-A2 using SP-A1:pCR2.1 and SP-A2:pCR2.1 constructs as templates, respectively. rfhSP-A1 and rfhSP-A2 amplicons with incorporated restriction sites were then TA cloned.

4.2.7 Site Specific Mutagenesis by Overlap Extension

Site specific mutagenesis by overlap extension PCR was utilised to mutate the SP-A glycosylation site at Asn187 in rfhSP-A1 and rfhSP-A2 as previously described (276). The mutation changed the DNA triplicate from AAC (Asn residue) to AGC (Ser residue) to generate rfhSP-A1^{N187S} and rfhSP-A2^{N187S} constructs.

Site specific mutagenesis by overlap extension uses 3 PCR amplification reactions and is summarised in Figure 4-3. PCR reactions 1 and 2 were undertaken first with the corresponding reaction mixes (reaction mixes in Table 4-10 and Table 4-11, respectively). SP-A1:pCR2.1 or SP-A2:a1pCR2.1 plasmids were used as a template. PCR reaction 3 was subsequently undertaken using the corresponding reaction mix (reaction mix in Table 4-12). For PCR reaction 3, PCR reaction 1 and PCR reaction 2 amplicons were used as a template. After site specific mutagenesis by overlap extension, amplicons with the incorporated N187S mutation were TA cloned.

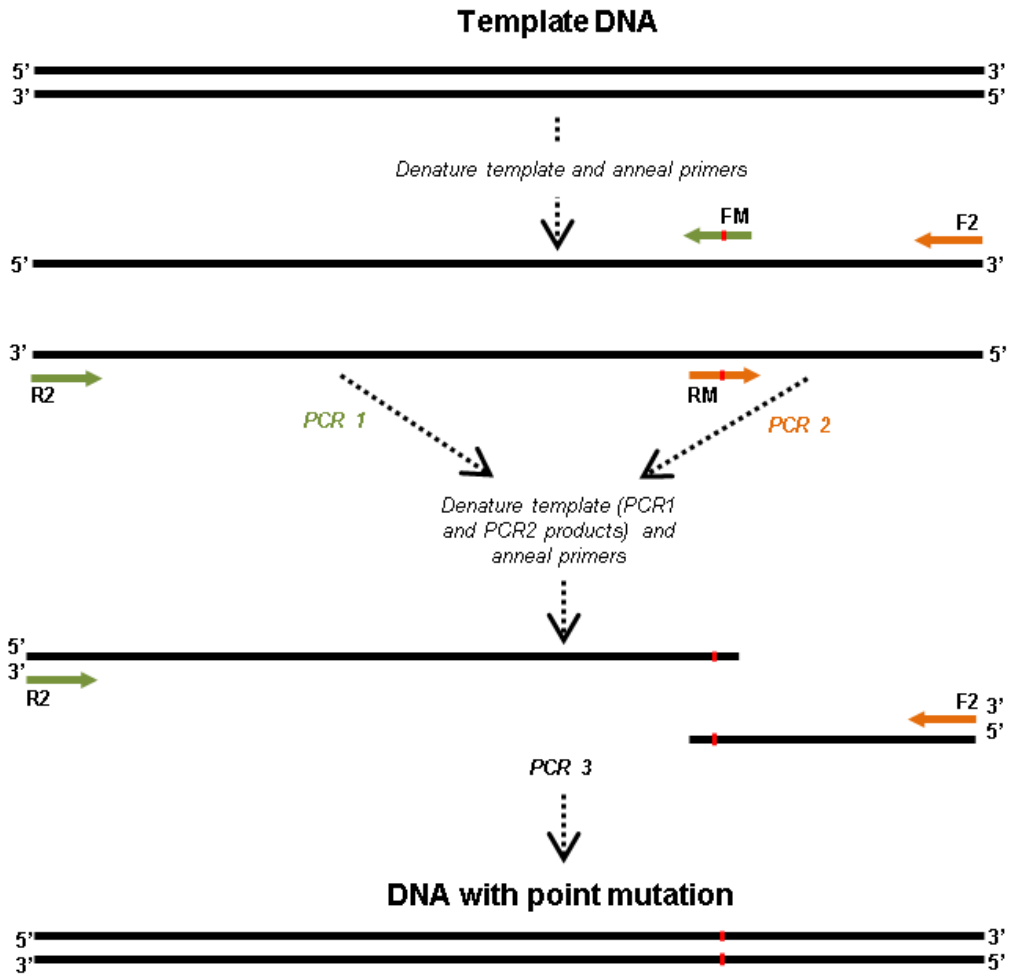

Figure 4-3: Schematic of Site specific mutagenesis by overlap extension PCR. *Displayed is a schematic illustrating the principle behind site specific mutagenesis by overlap extension. This method involves using two individual PCR reactions, PCR reaction 1 and PCR 2, to create two overlapping fragments of the target amplification region. These amplicons both have the targeted point mutation incorporated and are used as a template to produce the full-length target region with the mutation incorporation in PCR reaction 3.*

Component	**Volume**
rfhSP-A1 or rfhSP-A2 PCR amplicons (Table 4-5)	0.5 µl
10 mM dNTP Mix	0.6 µl
10 x Pfx50 PCR Mix	2.0 µl
R2 forward primer (10 µM)	0.6 µl
FM reverse primer (10 µM)	0.6 µl
Pfx50 DNA Polymerase	0.4 µl (2 units)
Nuclease-free water	15.3 µl

Table 4-10: Reaction mix for mutagenesis PCR reaction 1. *The volume of each component included in the PCR reaction mix for mutagenesis PCR reaction 1 is listed. Also stated is the amount of Pfx50 DNA polymerase enzyme used in units. Purified rfhSP-A1 and rfhSP-A2 genes, generated by PCR were used as a template.*

Component	**Volume**
rfhSP-A1 or rfhSP-A2 amplicons (Table 4-5)	0.5 µl
10 mM dNTP Mix	0.6 µl
10 x Pfx50 PCR Mix	2.0 µl
RM forward primer (10 µM)	0.6 µl
F2 reverse primer (10 µM)	0.6 µl
Pfx50 DNA Polymerase	0.4 µl (2 units)
Nuclease-free water	15.3 µl

Table 4-11: Reaction mix for mutagenesis PCR reaction 2. *The volume of each component included in the PCR reaction mix for mutagenesis PCR reaction 2 is listed. Also stated is the amount of Pfx50 DNA polymerase enzyme used in units. Purified rfhSP-A1 and rfhSP-A2 genes amplified by PCR were used as a template.*

Component	Volume
Mutagenesis PCR reaction 1 product (Table 4-10)	0.5 µl
Mutagenesis PCR reaction 2 product (Table 4-11)	0.5 µl
10 mM dNTP Mix	3.0 µl
10x Pfx50 PCR Mix	5.0 µl
R2 forward primer (10 µM)	3.0 µl
F2 reverse primer (10 µM)	3.0 µl
Pfx50 DNA Polymerase	1.5 µl (7.5 units)
Nuclease-free water	83.5 µl

Table 4-12: Reaction mix for mutagenesis PCR reaction 3. *The volume of each component included in the PCR reaction mix for Mutagenesis PCR reaction 2 is listed. Also stated is the amount of Pfx50 DNA polymerase enzyme used in units. Mutagenesis PCR reaction 1 and 2 products were used as a template for full-length amplification of rfhSP-A1^{N187S} and rfhSP-A2^{N187S}.*

4.2.8 Subcloning into Expression Vectors

TA cloned constructs were used to subclone the corresponding rfhSP-A genes into pET vectors through digestion with appropriate restriction enzymes and subsequent ligation as in Section 4.2.1.5, but using ligation mix given in Table 4-14. Unless otherwise stated, enzymes were purchased from Promega. A summary of the constructs used for subcloning into pET vectors and the corresponding pET vector constructs which were created is given in Table 4-13.

TA cloned construct	Generated construct
SP-A1:pCR2.1	SP-A1:pET21a^{+}
SP-A2:pCR2.1	SP-A2:pET24a^{+}
SP-A1^{N187S}:pCR2.1	SP-A1^{N187S}:pET21a^{+}
SP-A2^{N187S}:pCR2.1	SP-A2^{N187S}:pET24a^{+}

Table 4-13: Summary of constructs used for subcloning into expression vectors and generated constructs. *Listed are the TA cloned constructs used for subcloning into expression vectors, the corresponding subcloned constructs are also listed.*

Component	Amount
Vector	50 ng
Fragment	(A 2:1 molar ratio)
T4 DNA Ligase buffer (Promega)	1.0 µl
T4 DNA Ligase (Promega)	0.3 µl (1 unit)
Nuclease free water	To a final volume of 10 µl

Table 4-14: Ligation mix. *The amount of each component included in the ligation mix is listed. Also stated is the amount of T4 DNA Ligase used in units. Amount of fragment was added according to the wanted vector:fragment molar ratio, calculated as in Section 4.2.1.5.*

4.2.8.1 *Digestion of DNA for Subcloning into Expression Vectors*

To generate fragments for subcloning into expression vectors, 1 µg of rfhSP-A1:pCR2.1, rfhSP-A2:pCR2.1, rfhSP-A1^{N187S}:pCR2.1 and rfhSP-A2^{N187S}:pCR2.1 were separately digested using BamHI and NheI restriction enzymes at 37 °C for 2 hours with restriction digestion mix (Table 4-15). 1 µg of pET21a^{+} and pET24a^{+} vectors were also digested.

After digestion, enzymes were denatured by heating at 65 °C for 15 min. Vectors were dephosphorylated to prevent religation. Fragments and vectors were then gel purified as in Section 4.2.1.4.

Component	Amount
DNA	1 µg
10 x Multicore buffer (Promega)	2.0 µl
Restriction enzyme 1 (Promega)	0.5 (5 units)
Restriction enzyme 2 (Promega)	0.5 (5 units)
BSA (Promega)	0.3 µl
Nuclease-free water	to 20 µl total volume

Table 4-15: Restriction digestion mix. *The amount of each component included in the restriction digestion mix is listed. Also stated is the amount of restriction enzymes used in units and weight of DNA. Restriction enzymes used for subcloning of rfhSP-A1, rfhSP-A2, rfhSP-A1^{N187S} and rfhSP-A2^{N187S} were Nhe1 and BamH1. For subcloning of NT-rfhSP-A1 HindIII and EcoR1 restriction enzymes were used.*

4.2.8.2 *Dephosphorylation of Expression Vectors*

Dephosphorylation was undertaken after cooling of digestion reaction mixes by addition of 2 µl of Thermosensitive Alkaline Phosphatase and incubation at 37 °C for 30 min. The enzyme was then inhibited by heating at 65 °C for 10 min

4.2.8.3 *DNA Ligation*

Vectors and fragment were ligated in a 2:1 molar ratio. 50 ng of vector was used in ligation reactions; fragment amount was calculated using the molar ratio equation described in Section 4.2.1.5. Ligation reactions were undertaken with 50 ng of digested and dephosphorylated vector with the appropriate amount of digested fragment. The DNA

was incubated at 14 °C overnight in nuclease-free water with 1 µl of T4 DNA Ligase buffer, 0.3 µl of T4 DNA Ligase (1 Weiss unit) (final volume of 10 µl). A negative control reaction was also undertaken using digested and dephosphorylated vector without fragment ($pET21a^+ C^-$ and $pET24a^+ C^-$).

4.2.9 rfhSP-A1 Gene Optimisation

The codon usage and GC content of the rfhSP-A1 gene was optimised for expression in *E. coli* by Genscript, Inc (USA). As part of this service, the optimised gene was cloned into a $pET21a^+$ expression vector. The optimised rfhSP-A1 gene with optimised codons was used downstream for subcloning into NT-rfhSP-A1 and NT^{dm}-rfhSP-A1 constructs, see below.

4.2.10 Subcloning of NT-rfhSP-A1 and NT^{dm}-rfhSP-A1

PCR was undertaken using SP-A1:$pET21a^+$ as a template and primers containing overhangs with EcoR1 and HindIII restriction enzyme cleavage sites (primers listed in Table 4-3). After gel purification, PCR amplicons were TA cloned and subsequently subcloned into expression vectors, as described in Section 4.2.8. Bacterial colonies transformed with TA cloned rfhSP-A were screened by PCR using above mentioned primers. For subcloning of NT-rfhSP-A1, digestion was undertaken using EcoR1 and HindIII restriction enzymes. The rfhSP-A1 sequence was subcloned into an expression vector containing NT upstream (Figure 4-2.) allowing for subcloning of rfhSP-A1 into NT^{dm} expression vectors which was kindly carried out by Nina Kronqvist at Karolinska Institutet (Sweden) to contain either a thrombin or a human rhinovirus (HRV) 3C protease cleavage site.

4.2.11 Subcloning of NT-rfhSP-D, PGB1-rfhSP-D and NT^{dm}-rfhSP-D

NT-rfhSP-D, $NT_{(opt)}$-rfhSP-D (containing NT with codons optimised for expression in *E. coli*) and PGB1-rfhSP-D sequences cloned in $pET21a^+$ expression vectors, were subsequently generated and kindly provided by Kerstin Nordling, Karolinska Institutet (Sweden). Subcloning of the rfhSP-D into NT^{dm} expression vectors was kindly undertaken by Nina Kronqvist at Karolinska Institutet (Sweden). rfhSP-D was subcloned as above to include either a thrombin or a HRV 3C protease cleavage site.

4.2.12 Expression in *E. coli*

BL21 (DE3) *E. coli* were used for expression unless otherwise stated. Transformed bacteria were used to inoculate 10 ml of LB media containing appropriate antibiotic (70 µg/ml kanamycin or 100 µg/ml amp). This was incubated at 37 °C overnight, with shaking (240 rpm). 5 ml of overnight culture was used to inoculate 500 ml of antibiotic containing LB which was grown at 37 °C until absorbance at $\lambda = 600$ nm reached 0.8-1.0 (approximately 3 hours). Expression was induced by addition of Isopropyl β-D-1-thiogalactopyranoside (IPTG) to a final concentration of 0.5 mM. Bacterial expression was undertaken with shaking (240 rpm) for 4 hours at 37 °C for rfhSP-A and rfhSP-D or for 16 hours at 30 °C for NT-rfhSP-A, NT-rfhSP-D and PGB1-rfhSP-D. Expression of NT^{dm}-rfhSP-A and NT^{dm}-rfhSP-D was undertaken by Nina Kronqvist at the Karolinska Institutet with shaking (240 rpm) for 16 hours at 20 °C. These expression conditions were used except for in initial expression trials where tested conditions are stated. Bacteria were harvested by centrifugation at 4,000 x g for 20 min. After removal of supernatant, bacteria were stored at -20 °C until protein purification.

4.3 Results

4.3.1 Cloning of SP-A

RNA was purified from human lung tissue and used to create cDNA. (Figure 4-4). Primers complementary to human SP-A (hSP-A) DNA, which did not distinguish between SP-A1 and SP-A2 were used for initial cloning. Optimisation of PCR indicated that all annealing temperatures between 58 °C to 68 °C allowed the production of a 741 bp amplicon, which corresponds to the amplified SP-A cDNA sequences (Figure 4-5). The highest temperature of 68 °C was used for subsequent PCR reactions.

After gel purification, the 741 bp amplification products were ligated into a pCR2.1 TA cloning vector and used to transform competent Top10 *E. coli* cells. To identify colonies which contained a pCR2.1 plasmid with an insert, blue/white screening was implemented (Figure 4-6A). Single white *E. coli* colonies which contain a pCR2.1 vector with an insert were screened using PCR (Figure 4-6B). After plasmid purification of positive colonies, SP-A1:pCR2.1 and SP-A2:pCR2.1 constructs were identified by sequencing. SP-A1:pCR2.1 and SP-A2:pCR2.1 constructs were successfully generated and purified which corresponded to the below common genotypes:

- hSP-A1 $6A^2$
- either hSP-A2 $1A^1$ or $1A^3$ (Due to the leader sequence of the SP-A genes not being cloned, the cloned hSP-A2 sequence was equivalent to both hSP-A2 $1A^1$ and hSP-A2 $1A^3$ genotypes)

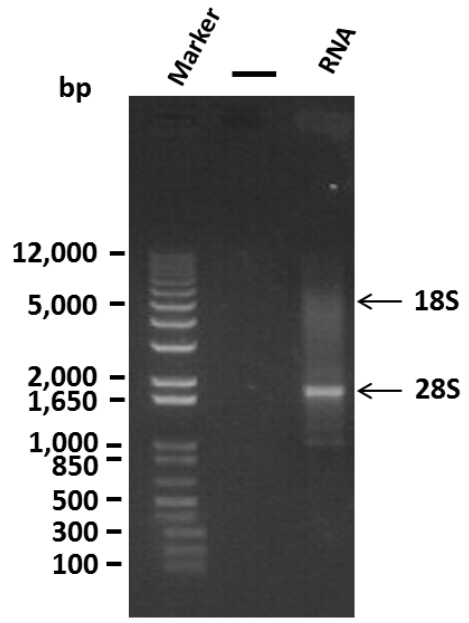

Figure 4-4: Agarose gel electrophoresis analysis of RNA purified from human lung. *RNA analysed by agarose gel electrophoresis is shown. Bands corresponding to 18S and 28S ribosomal RNA are indicated. An empty well between the marker and analysed RNA is indicated (-).*

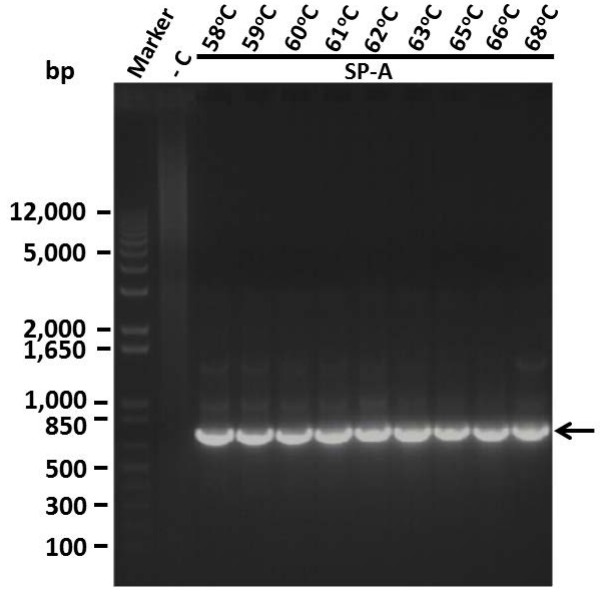

Figure 4-5: Analysis of PCR optimisation using agarose gel electrophoresis. *Shown is agarose gel electrophoresis analysis of PCR reactions undertaken with primers for amplification of SP-A cDNA sequences using cDNA generated from human lung tissue as a template. PCR reactions were undertaken at different temperatures ranging from 58 °C to 68 °C. A negative control without cDNA as a template was also analysed (-C). Indicated (arrow) are SP-A sequence amplicons of expected 741 bp size.*

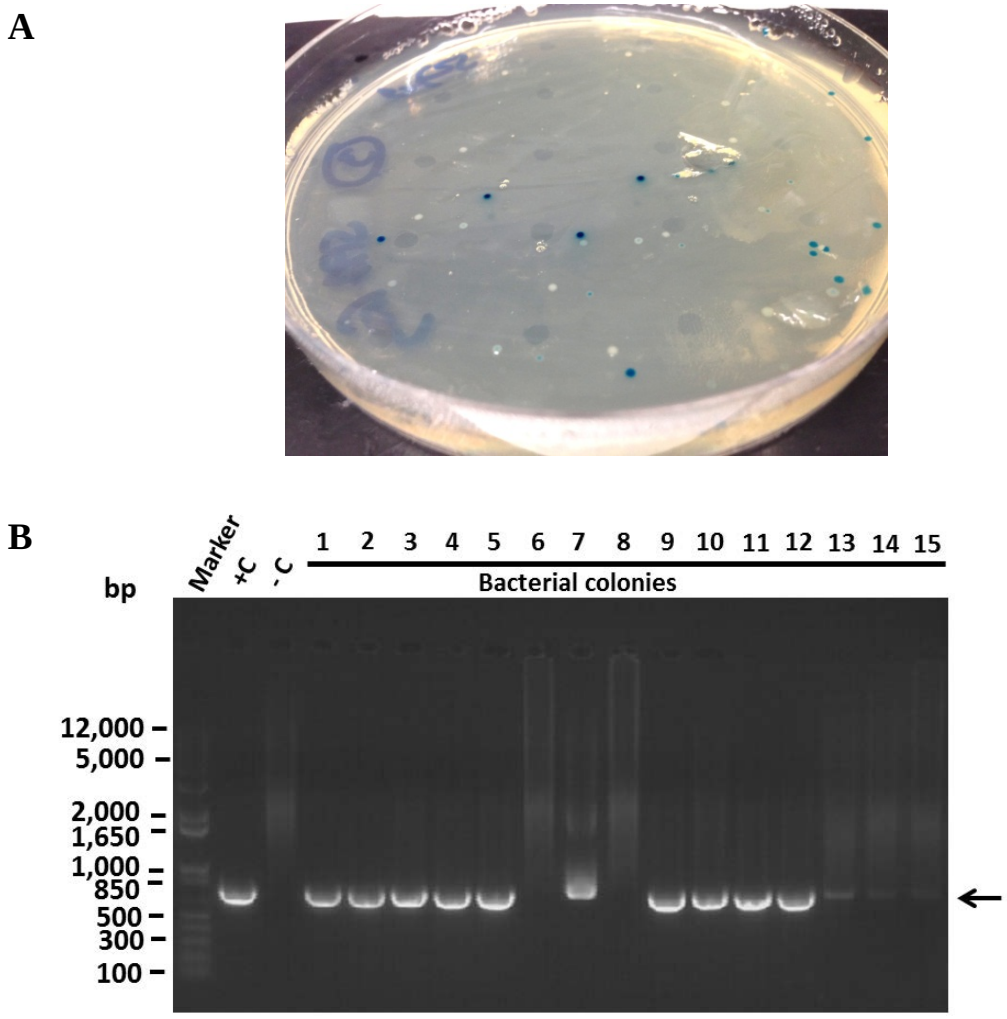

Figure 4-6: Screening of E. coli for identification of pCR2.1:hSP-A containing colonies. *Shown in* ***A*** *is a representative photograph of an LB-agar plate (containing Kanamycin and X-gal) used for blue/white screening of E. coli transformed with TA cloned pCR2.1:hSP-A.* ***B*** *shows PCR screening of individual white E. coli colonies. A positive control of hSP-A purified DNA was included as was a negative control where PCR was undertaken without template DNA. Indicated are amplicons corresponding to expected size of 741 bp.*

4.3.2 Subcloning of rfhSP-A1 and rfhSP-A2

PCR was successfully implemented to specifically amplify targeted 559 bp rfhSP-A1 and rfhSP-A2 sequences (Figure 4-7). After gel purification, these amplified sequences were TA cloned and used to transform bacteria. As in Section 4.3.2, blue/white screening and subsequent screening with PCR was implemented and allowed the identification of plasmids containing rfhSP-A1 and rfhSP-A2 (data not show). Plasmid purification and sequencing of plasmids confirmed that rfhSP-A1 and rfhSP-A2 with appropriate

restriction enzyme sites had successfully been TA-cloned to create rfhSP-A1:pCR2.1 and rfhSP-A2:pCR2.1 constructs. TA cloning was implemented as an intermediate step to subcloning into expression vectors due to problems with direct digestion of PCR products.

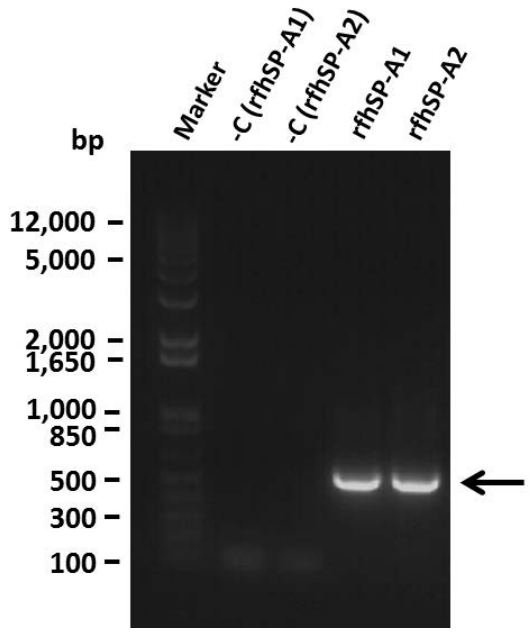

Figure 4-7: Analysis of PCR amplification of rfhSP-A1 and rfhSP-A2 by agarose gel electrophoresis. *PCR reactions for amplification of rfhSP-A1 and rfhSP-A2 sequences were analysed by agarose gel electrophoresis. Indicated (arrow) are the bands corresponding to the rfhSP-A1 and rfhSP-A2 amplicons. Negative control PCR reactions were also undertaken which lacked template DNA (-C (rfhSPA1) and –C (rfhSP-A2)).*

4.3.3 Site Specific Mutagenesis by Overlap Extension

To create constructs without an Asn187 glycosylation site, specific mutagenesis by overlap extension was implemented. PCR reactions 1 and 2 were used to generate two overlapping sequences with the N187S mutation incorporated in both the antisense and sense strand, respectively. PCR reactions 1 and 2 were undertaken successfully to generate amplicons of expected size, 420 bp and 169 bp, respectively. PCR reaction 3 was then successfully implemented to amplify the full-length rfhSP-A1 and rfhSP-A2 sequences with the incorporated N187S mutation of expected size, 559 bp (rfhSP-A1^{N187S} and rfhSP-A2^{N187S}) (Figure 4-8). These sequences were then gel purified, TA cloned and screened using both blue/white screening and PCR, as described in Section 4.3.2 (data

not shown). The plasmid purification and subsequent sequencing allowed the successful identification of rfhSP-A1^{N187S}:pCR2.1 and rfhSP-A2^{N187S}:pCR2.1 constructs.

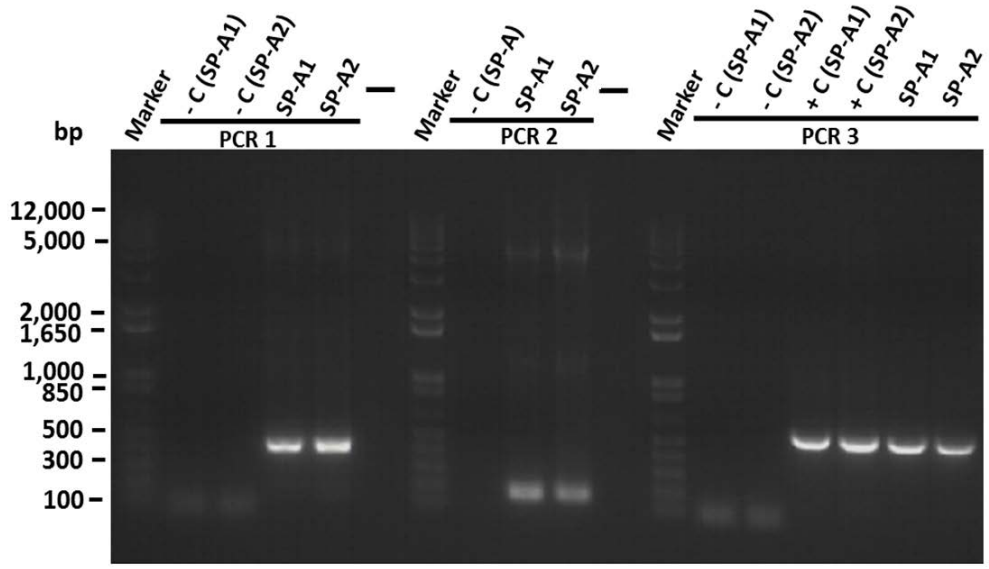

Figure 4-8: Analysis of site specific mutagenesis by overlap extension using agarose gel electrophoresis. *Analysed are amplification products after PCR reactions 1, 2 and 3 for site specific mutagenesis by overlap extension. Negative controls were also included in analysis which were generated through PCR without the use of template DNA (due to different R2 primers being used for the amplification of rfhSP-A1 and rfhSP-A2 in PCR reaction 1, 2 controls were included (-C (SP-A1) and –C (SP-A2)). For PCR reaction 3, positive controls were also included through the use of rfhSP-A1:pCR2.1 or rfhSP-A1:pCR2.1 as a template in the PCR reaction in place of amplification products from PCR reactions 1 and 2. Empty wells on the gel are indicated (-).*

4.3.4 Subcloning of rfhSP-A1 and rfhSP-A2 into Expression Vectors

rfhSP-A1:pCR2.1, rfhSP-A2:pCR2.1, rfhSP-A1^{N187S}:pCR2.1 and rfhSP-A2^{N187S}:pCR2.1 constructs were used for subcloning of corresponding rfhSP-A fragments into pET vectors. Analysis by agarose gel electrophoresis indicated that pET vectors digested with Nhe1 and BamH1 restriction enzymes were successfully linearised (Figure 4-9). This was determined by the absence of supercoiled plasmids which migrates through an agarose gel more easily than linearised DNA. Due to the fragment being cut from the pET vectors being only 33 bp in size, it could not be identified using agarose gel electrophoresis. However, upon digestion of TA cloned rfhSP-A constructs, a fragment of expected 548 bp size was cleaved from the vectors and identified. Digested vectors and fragments were

gel purified and used for ligation. After, transformation of bacteria and purification of plasmids, successfully cloned pET vector plasmids were identified by sequencing. Sequencing of the purified constructs confirmed that rfhSP-A1:pET21a^{+}, rfhSP-A2:pET24a^{+}, rfhSP-A1^{N187S}:pET21a^{+} and rfhSP-A2^{N187S}:pET24a^{+} constructs were successfully generated.

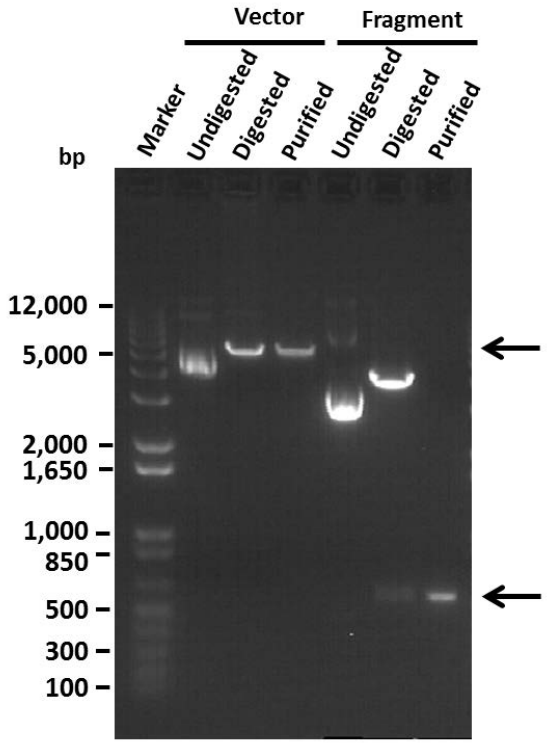

Figure 4-9: Analysis of restriction enzyme digestion reactions by agarose gel electrophoresis. *Indicated are samples analysed by agarose gel electrophoresis. Included were both the pET21a+ vector (vector) and the rfhSP-A1:pCR2.1 fragment containing vector (fragment). Samples were either left undigested, or digested with both Nhe1 and BamH1 restriction enzymes. Gel purified vector and fragment (indicated by arrows) were also analysed by agarose gel electrophoresis (Purified). Results shown are for digestion of pET21a+ vector and rfhSP-A1:pCR2.1. However, results are representative for digestion of pET24a+, rfhSP-A2:pCR2.1, rfhSP-A1^{N187S}:pCR2.1 and rfhSP-A2^{N187S}:pCR2.1.*

4.3.5 Subcloning of rfhSP-A1 for Expression with Solubility Tags

4.3.5.1 *Subcloning of NT-rfhSP-A1*

To investigate the impact of NT on the expression levels and solubility of rfhSP-A1 protein, rfhSP-A1 (with optimised codons for bacterial expression) was subcloned into a pET24a$^+$ vector containing NT. PCR was implemented to generate a rfhSP-A1 amplicon with appropriate EcoR1 and HindIII restriction enzyme sites (Figure 4-10). This amplicon was then TA cloned and used to transform *E. coli*. The *E. coli* colonies containing the generated NT-rfhSP-A1:pCR2.1 construct were screened using PCR with subsequent analysis by agarose gel electrophoresis (Figure 4-11).

For subcloning and generation of NT-rfhSP-A1, the previously generated NT-rfhSP-D:pET24a$^+$ construct, containing EcoR1 and HindIII restriction enzyme sites either side of rfhSP-D was used as the vector for ligation of the rfhSP-A1 into. The NT-rfhSP-D:pET24a$^+$ and rfhSP-A1:pCR2.1 constructs were digested with EcoR1 and HindIII to create fragments of expected size, 539 bp and 556 bp, respectively (Figure 4-10 and data not shown). Digested rfhSP-A1 fragment and NT:pET24a$^+$ vector were then ligated to successfully generate NT-rfhSP-A1:pET24a$^+$. The sequence of the NT-rfhSP-A1:pET24a$^+$ construct was confirmed by sequencing.

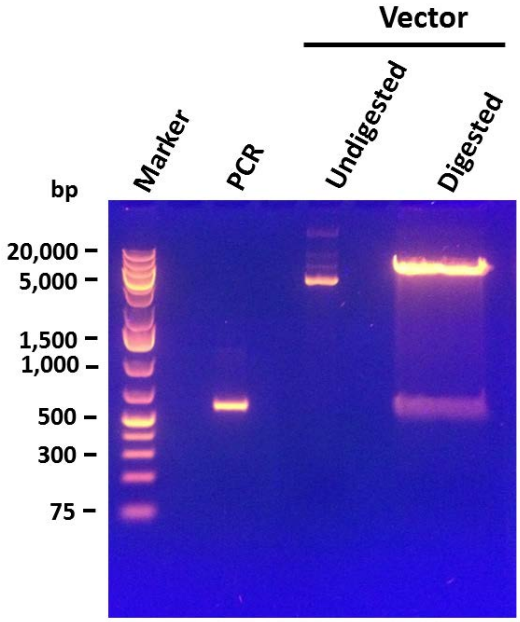

Figure 4-10: Analysis of rfhSP-A1 amplification by PCR and digestion of NT-rfhSP-D:pET24a$^+$ using agarose gel electrophoresis. *PCR amplification of rfhSP-A1 to incorporate EcoR1 and HindIII restriction enzyme sites was analysed by agarose gel electrophoresis.*

Undigested NT-rfhSP-D:pET24a$^+$ construct and NT-rfhSP-D:pET24a$^+$ digested with EcoR1 and HindIII were also (Vector/Undigested and Vector/Digested, respectively). After digestion of rfhSP-A1:pCR2.1 to create a rfhSP-A1 fragment, ligation was undertaken with NT:pET24a$^+$ without taking a picture; rfhSP-A1:pCR2.1 is, therefore, not shown in this figure. Sizes analysed by agarose gel electrophoresis of DNA were identified by comparison with GeneRuler 1 kb Plus DNA Ladder (75 to 20,000 bp) (Thermo Scientific).

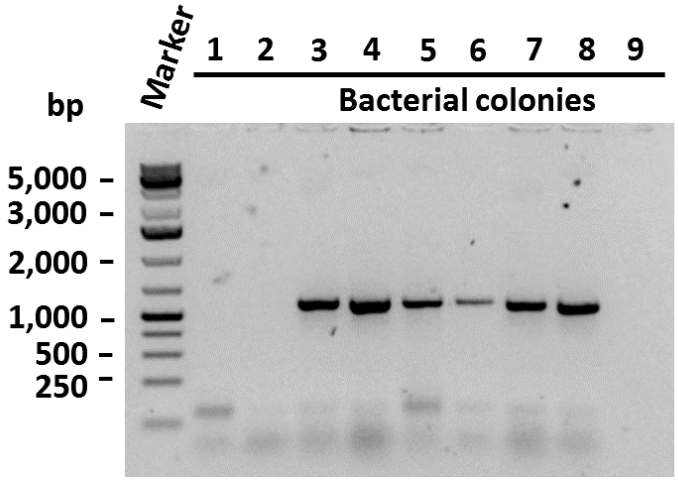

Figure 4-11: Screening TA cloned colonies for containment of rfhSP-A. *Bacterial colonies were screened by PCR with subsequent analysis by agarose gel electrophoresis to allow determination of the bacteria containing plasmids with rfhSP-A1. Sizes analysed by agarose gel electrophoresis of DNA were identified by comparison with GeneRuler 1 kb Plus DNA Ladder (75 to 20,000 bp) (Thermo Scientific).*

4.3.5.2 *Subcloning of NT^{dm}-rfhSP-A1*

NT^{dm}-rfhSP-A was subcloned as above by Nina Kronqvist to include a thrombin cleavage site or a HRV 3C protease site (Karolinska Institutet (Sweden)).

4.3.6 Subcloning of rfhSP-D for Expression with Solubility Tags

4.3.6.1 *Subcloning of NT-rfhSP-D*

NT-rfhSP-D was subcloned initially by Kerstin Nordling (Karolinska Institutet (Sweden)) without the inclusion of a protease cleavage site in addition to PGB1-rfhSP-D for comparison. NT-rfhSP-D was subsequently subcloned by Nina Kronqvist to include a thrombin or HRV 3C cleavage site (Karolinska Institutet (Sweden)).

4.3.6.2 *Subcloning of NT^{dm}-rfhSP-D*

NT^{dm}-rfhSP-D was subsequently subcloned by Nina Kronqvist to include a thrombin cleavage site or a HRV 3C protease site (Karolinska Institutet (Sweden)).

4.3.7 Expression of rfhSP-A1 and rfhSP-A2

4.3.7.1 *Expression of rfhSP-A1 and rfhSP-A2 without a Solubility Tag*

The ability to express rfhSP-A1 and rfhSP-A2 proteins using BL21 (DE3) *E. coli* was investigated. Expression of rfhSP-A1 and rfhSP-A2 was not detectable using SDS-PAGE with subsequent Coomassie staining (Figure 4-12A). Upon analysis by Western blotting, small levels of rfhSP-A1 and rfhSP-A2 expression were detected in induced bacteria (Figure 4-12B). However, expression levels were too low to warrant subsequent purification.

Due to rfhSP-A1 and rfhSP-A2 containing multiple codons rarely used by *E. coli*, the possibility of expressing these proteins in Rosetta (DE3) *E. coli* was investigated (Figure 4-12C). In addition, the ability of different bacterial colonies to express rfhSP-A1 upon optimisation of codons for expression in *E. coli* was also investigated (Figure 4-12D). Both expression of rfhSP-A1 in Rosetta (DE3) bacteria and expression of rfhSP-A1 with optimised codons with different bacterial colonies gave similarly low levels of protein expression. The amount of protein expression increased gradually with increasing lengths of expression time. However, after 5 hours of expression, the amount of protein produced by the *E. coli* was still minimal and could not be identified by SDS-PAGE with Coomassie staining but only through the use of Western blotting (Figure 4-12E). The IPTG concentration and expression temperatures also did not substantially affect protein expression levels (Figure 4-12F).

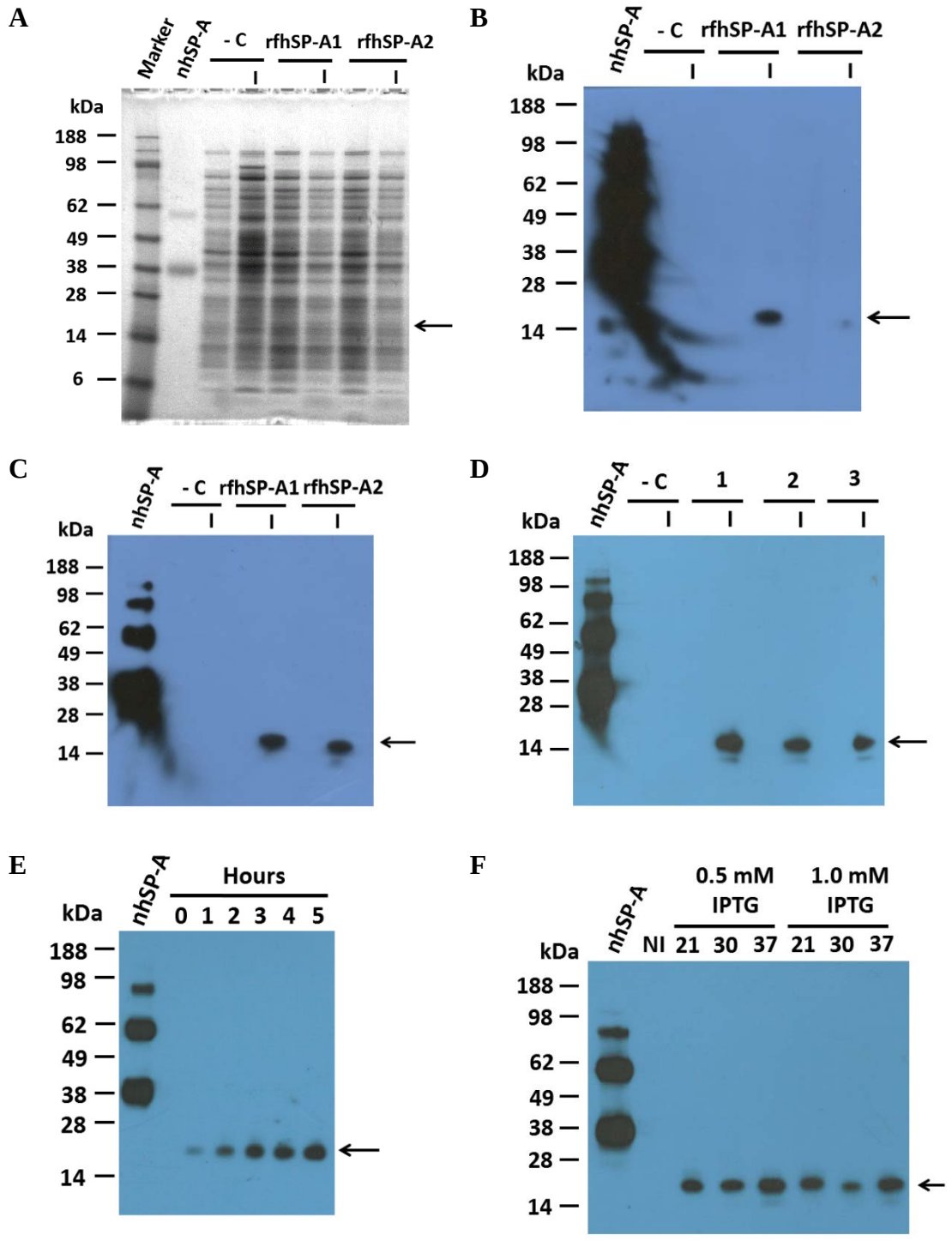

Figure 4-12: SDS-PAGE and Western blot analysis of rfhSP-A1 and rfhSP-A2 expression. *The expression of rfhSP-A1 and rfhSP-A2 was analysed using reduced SDS-PAGE with Coomassie staining (**A**) and Western blotting (**B-F**). For analysis by SDS-PAGE, 1 ml of bacterial pellet was resuspended in phosphate-buffered saline (550 µl * the OD at λ = 595 nm after protein expression). This bacterial suspension was then diluted in 4 x concentrated sample buffer and 10 x concentrated reducing agent and heated to 100 °C to lyse the bacteria. 25 µl of bacterial lysate was applied to the SDS-PAGE gel. Expression of rfhSP-A1 was compared between different colonies using Western blot analysis (colony number 1, 2 or 3) (**D**). The expression of rfhSP-A1*

*with codons optimised for bacterial expression was analysed under different conditions using Western blot analysis. Different conditions included, lengths of expression time (0, 1, 2, 3, 4 or 5 hours) (**E**) and different incubation temperatures (21 °C (overnight incubation), 30 °C (4 hour incubation) or 37 °C (4 hour incubation)) with varying IPTG concentrations (0.5 mM or 1.0 mM) (**F**). Expression was undertaken with BL21 (DE3) bacterial cells (**A** and **B**) or Rosetta (DE3) bacterial cells (**C** to **F**). **A** to **D**, bacteria which were induced (I) or not induced (blank) are indicated. **E** and **F**, bacteria which were not induced are also indicated (0 hours or NI, respectively). Western blot analysis was undertaken using a primary antibody against nhSP-A. For SDS-PAGE and Western blot analysis, 1 µg and 0.5 µg of nhSP-A was also analysed as a positive control, respectively. For Western blot analysis, exposure times were between 3-7 min. The relative expression can be compared with reference to the 0.5 µg of nhSP-A positive control analysed on each blot. Bands corresponding to rfhSP-A1 or rfhSP-A2 are indicated (arrow).*

4.3.7.2 *Expression of rfhSP-A1 using NT*

The NT domain was subsequently investigated for its capacity to be used as a general expression partner for the expression of large amounts of soluble rfhSP-A1 and rfhSP-D. In contrast to the previous attempts to express rfhSP-A where only very small amounts were expressed (Figure 4-12), NT allowed high levels of expression of NT-rfhSP-A1. This protein was retained within the bacteria and not exported to the supernatant (Figure 4-13A). Interestingly, optimisation of NT codon usage and GC content allowed higher levels of expression than native NT domain (Figure 4-13A). NT(opt)-rfhSP-A1 was, therefore, used in subsequent experimentation (referred to from here simply as NT-rfhSP-A). NT-rfhSP-A1 gave the highest levels of expression at 30 °C after 8-16 hours (Figure 4-13C). On subsequent occasions, NT-rfhSP-A1 was therefore expressed for 16 hours.

A

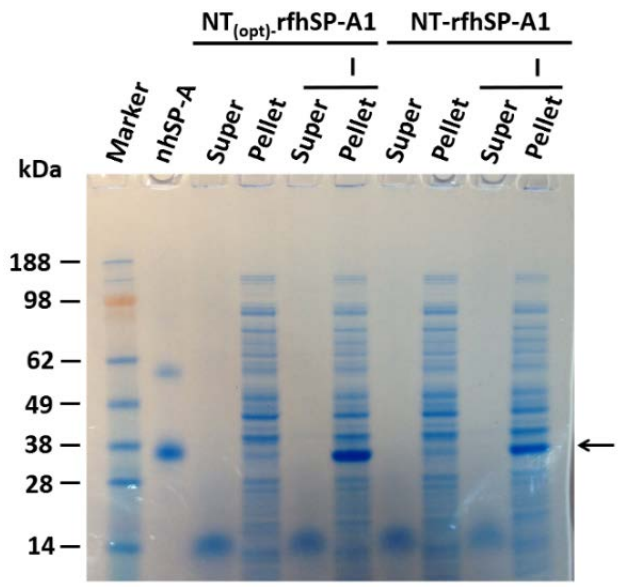
NT(opt)-rfhSP-A1
NT-rfhSP-A1
I
I
Marker
nhSP-A
Super
Pellet
Super
Pellet
Super
Pellet
Super
Pellet
kDa
188
98
62
49
38
28
14

B

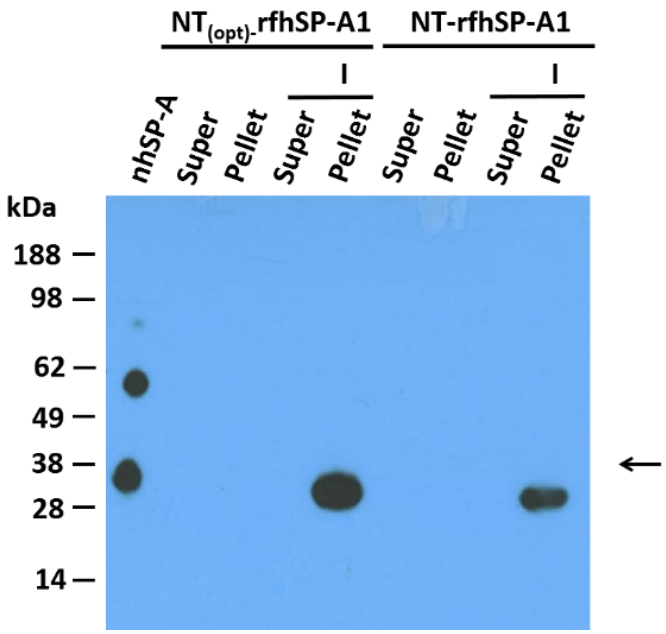
NT(opt)-rfhSP-A1
NT-rfhSP-A1
I
I
nhSP-A
Super
Pellet
Super
Pellet
Super
Pellet
Super
Pellet
kDa
188
98
62
49
38
28
14

C

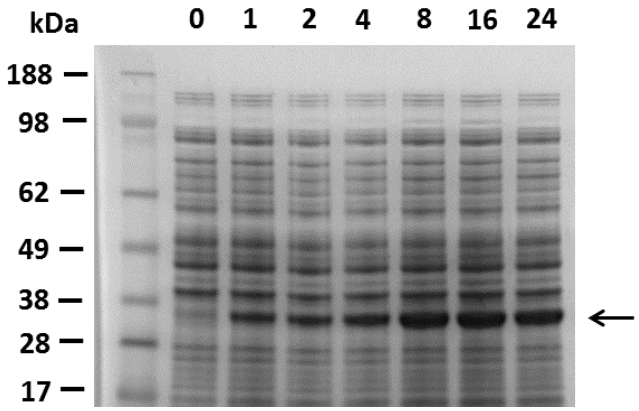
kDa
0
1
2
4
8
16
24
188
98
62
49
38
28
17

Figure 4-13: SDS-PAGE and Western blot analysis of NT-rfhSP-A1 expression. *The expression of NT-rfhSP-A1 at 30 °C was analysed using reduced SDS-PAGE (**A**) and Western blot analysis using a primary antibody against nhSP-A (**B**). For analysis by SDS-PAGE, 1 ml of bacterial pellet was resuspended in phosphate-buffered saline (550 µl * the OD at λ = 595 nm after protein expression). This bacterial suspension was then diluted in 4 x concentrated sample buffer and 10 x concentrated reducing agent and heated to 100 °C to lyse the bacteria. 25 µl of bacterial lysate was applied to the SDS-PAGE gel. Expression was compared between NT with either codons and GC content optimised for expression in E. coli NT ($NT_{(opt)}$-rfhSP-A1) or native NT (NT-rfhSP-A1). Indicated is the bacterial pellet (Pellet) or the supernatant upon removal from the bacteria containing pellet (Super). Bacteria were analysed before and after expression (I). For SDS-PAGE and Western blot analysis, 1.0 µg and 0.5 µg of nhSP-A was analysed as a positive control, respectively. Bands corresponding to NT-rfhSP-A1 are indicated (arrow). Western blot exposures were for <1 min.*

4.3.7.3 *Expression of rfhSP-A1 using NT^{dm}*

Expression of NT^{dm}-rfhSP-A1 including a thrombin cleavage site and a 3C protease cleavage site was undertaken at Karolinska Institutet (Sweden) by Nina Kronqvist (data not shown). Expression levels were similar in *E. coli* as those for NT-rfhSP-A1.

4.3.8 Expression of rfhSP-D

4.3.8.1 *Expression of rfhSP-D without a Solubility Tag*

Comparatively to rfhSP-A1, using the same expression system, rfhSP-D gave good expression levels in BL21 (DE3) bacteria and was detectable by SDS-PAGE analysis (Figure 4-14A). Western blotting analysis confirmed the expressed protein to be immunoreactive against a polyclonal α-rfhSP-D antibody (Figure 4-14B). However, the α-rfhSP-D antibody also cross-reacted with numerous *E. coli* proteins in addition to nhSP-A.

Absorbance measurements at λ = 280 nm readings were similar between rfhSP-A1 and rfhSP-D, indicating that the low amounts of rfhSP-A1 expression was unlikely to be due to toxicity of the protein to the bacterial cells (data not shown).

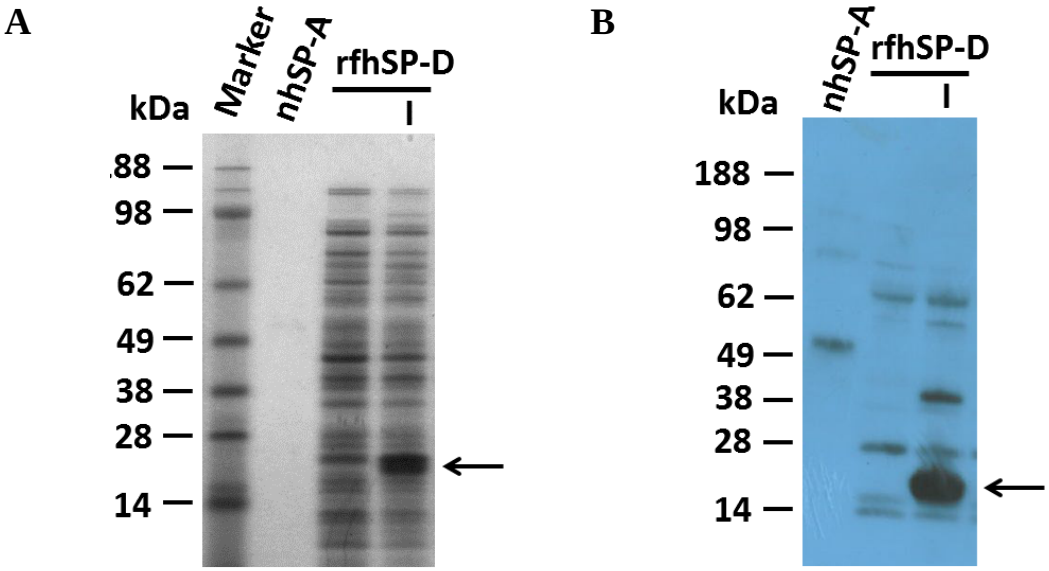

Figure 4-14: SDS-PAGE and Western blot analysis of rfhSP-D expression. *The expression of rfhSP-D was analysed using reduced SDS-PAGE (**A**) and Western blotting (**B**). For analysis by SDS-PAGE, 1 ml of bacterial pellet was resuspended in phosphate-buffered saline (550 µl * the OD at λ = 595 nm after protein expression). This bacterial suspension was then diluted in 4 x concentrated sample buffer and 10 x concentrated reducing agent and heated to 100 °C to lyse the bacteria. 25 µl of bacterial lysate was applied to the SDS-PAGE gel. Western blot analysis was undertaken using a primary antibody against rfhSP-D. Bands corresponding to rfhSP-D are indicated (arrow). 0.5 µg of nhSP-A was also analysed as a negative control. Bacteria were analysed pre-induction (blank) or after induction (**I**).*

4.3.8.2 *Expression of rfhSP-D using NT*

NT also allowed for high levels of expression of NT-rfhSP-D at both 20 °C and 37 °C. Expression was compared to that with the use of another expression tag/solubility enhancer which is currently being investigated, PGB1. PGB1-rfhSP-D gave similar expression levels as NT-rfhSP-D (Figure 4-15). Both expression tags gave considerably higher levels of expression than expressing rfhSP-D alone (compare with Figure 4-14).

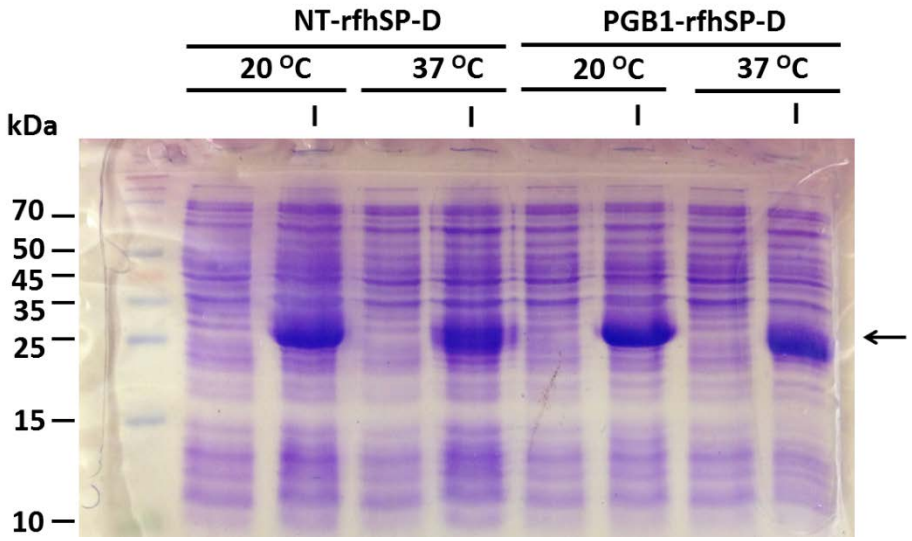

Figure 4-15: Analysis of NT-rfhSP-D and PGB1-rfhSP-D expression by SDS-PAGE.*The expression of NT-rfhSP-D and PGB1-rfhSP-D was analysed by reduced SDS-PAGE under different temperatures (20 °C (overnight incubation) or 37 °C (4 hour incubation)). Bacteria were analysed both before (blank) and after expression (I). 20 µl of bacterial suspension containing 5 µl of reducing buffer (8 M urea, 1.6 % SDS (v/v), 7 % glycerol, (v/v), 4 % β-mercaptoethanol, 0.0016 % BromphenolBlue) was applied to the SDS-PAGE gel after heating at 96 °C for 5 mins. The band corresponding to expressed protein is indicated (arrow). NT-rfhSP-D and PGB1-rfhSP-D DNA constructs were generated and kindly provided by Kerstin Nordling.*

4.3.8.3 *Expression of rfhSP-D using NT^{dm}*

Expression of NT^{dm}-rfhSP-D including a thrombin cleavage site and NT^{dm}-rfhSP-D including a 3C protease cleavage site was undertaken at Karolinska Institutet (Sweden) by Nina Kronqvist (data not shown). Expression levels were similar in *E. coli* as those for NT-rfhSP-D.

4.4 Summary of Results

Within this chapter, SP-A1 and SP-A2 were cloned and the use of NT and NT^{dm} in allowing the heterologous protein expression of rfhSP-A1 and rfhSP-D was tested, addressing the initial parts of Aims 2 and 3 (Section 1.14):

- To clone SP-A1 and SP-A2 and express and purify a rfhSP-A molecule, equivalent to rfhSP-D.
- To investigate the utility of NT and NT^{dm} as novel solubility tags for allowing heterologous expression of soluble rfhSP-A and rfhSP-D and subsequent purification without the need for protein refolding.

The subsequent parts of Aims 2 and 3 were addressed in Chapter 5. The main results reported in this chapter are:

- SP-A1 and SP-A2 were successfully cloned from human lung with subsequent subcloning of rfhSP-A1 and rfhSP-A2 into expression vectors, with and without the incorporation of a N187S point mutation.
- rfhSP-A1 and rfhSP-D were successfully subcloned as fusion constructs with either NT or NT^{dm} with incorporation of a His_6-tag and protease cleavage site.
- NT and NT^{dm} successfully allowed the expression of NT-rfhSP-A1 in *E. coli*; expression of rfhSP-A1 alone was not possible.
- NT and NT^{dm} allowed expression of NT-rfhSP-D and NT^{dm}-rfhSP-D to a considerably higher level than possible through expression of rfhSP-D alone.

4.5 Discussion

Despite attempts using currently available expression systems in bacteria, insect cells and mammalian systems by various groups including our own, it has not been possible to date to create a functional trimeric rfhSP-A molecule. This would be a useful tool for analysing the structure/function relationship of SP-A. In addition, the current method for producing rfhSP-D is laborious and results in relatively small yields of functional protein. In this chapter, SP-A1 and SP-A2 were cloned, rfhSP-A1 and rfhSP-A2 were subcloned with and without N187S point mutations. In addition, the use of NT and NT^{dm} in allowing the heterologous protein expression of rfhSP-A1 and rfhSP-D was investigated, addressing the initial parts of Aims 2 and 3 (Section 1.14).

SP-A1 and SP-A2 were successfully cloned from human lung. Upon sequencing it was confirmed that the hSP-A1 $6A^2$ and either hSP-A2 $1A^1$ or $1A^3$ alleles were cloned; since the leader sequence of SP-A was not cloned, the cloned hSP-A2 sequence corresponded to both hSP-A2 $1A^1$ and $1A^3$ and thus the specific genotype of the patient could not be identified.

Various problems were overcome during the cloning of these genes. Firstly, despite testing a range of different annealing temperatures used during PCR, primers specific for either SP-A1 or SP-A2 cross-hybridised at all tested temperatures. Thus it was decided to first clone SP-A using primers which did not distinguish between the two genes, followed by subsequent identification of either SP-A1 or SP-A2 through sequencing of all clones. Additional problems were met upon attempting to directly subclone PCR products into expression vectors. Three arbitrary nucleotides after the restriction digestion sites were included in the primers to facilitate subcloning. Despite this, the issue of subcloning PCR products proved to be a problem. Cleaning up the PCR product to remove contaminating salts or increasing enzyme digestion time did not resolve this problem. However, inclusion of an additional TA cloning step with subsequent digestion allowed efficient cleavage of the DNA to generate single-stranded overhangs. Notably the problem of directly cloning PCR products was also encountered upon subcloning of rfhSP-A1 and rfhSP-D into a vector containing NT, despite 6 extra arbitrary bases being included after the restriction enzyme site in the primer. Again, TA cloning was employed as an intermediate step to successfully overcome this issue. rfhSP-$A1^{N187S}$ and rfhSP-$A1^{N187S}$ mutants were successfully subcloned as previously undertaken for rfrSP-A (32). This

could subsequently allow the impact of this point mutation on SP-A structure or function to be determined.

rfhSP-A1, rfhSP-A2, rfhSP-A1^{N187S} or rfhSP-A2^{N187S} were only expressed in *E. coli* at extremely low levels. Levels of expression were below the detection limit of SDS-PAGE with subsequent Coomassie staining and only detectable upon over-exposure of the X-ray film during Western blotting (Figure 4-12). This was surprising as with the same expression system and methodology, rfhSP-D could successfully be expressed (Figure 4-14). In accordance with the widely reported common reasons for problems with heterologous protein expression in *E. coli* (reviewed in (277)), extensive expression trials were undertaken. These included alteration of: i.) IPTG concentrations; ii.) expression times; iii.) expression temperatures and iv.) antibiotic concentrations. However, varying these conditions had only a marginal impact on expression yields. Upon analysis of the DNA sequence, the rfhSP-A1 and rfhSP-A2 sequences had a number of codons rarely used by *E. coli*; this was therefore thought to be the problem preventing the expression. However, expression of rfhSP-A1 was also not possible upon use of BL21 derived Rosetta (DE3) bacteria which contain a plasmid encoding tRNAs for rarely used codons. Moreover, optimisation of rfhSP-A1 codons for expression in *E. coli* also did not increase levels of protein expression, highlighting that low expression levels were not caused by codon usage.

One possible reason for the inability to express rfhSP-A1 or rfhSP-A2 in *E. coli* could be due to toxicity mediated by the rfhSP-A proteins themselves. Indeed, nhSP-A has been widely reported to bind to LPS and mediate increased membrane permeability and bacterial lysis. However, similar phenomena have also been shown for rfhSP-D, which can be expressed at high levels (167, 168). Upon induction of protein expression and measurement of optical densities, bacterial growth did not appear to be slower than for bacteria expressing rfhSP-D. However, initial toxicity can also result in negative plasmid selection and plasmid instability preventing the protein from being expressed (278). An alternative reason for the inability of *E. coli* to express rfhSP-A1 and rfhSP-A2 could be due to the bacteria having difficultly translating the amino acid sequence of the initial N-terminus of the protein. This could lead to ribosomal stalling and detachment of the ribosome from the RNA preventing translation. Indeed, the presence of numerous prolines at the site of protein synthesis has previously been reported to have a negative effect on the elongation of protein translation in *E. coli* (279). Thus, the presence of the

collagen-like stalk present at the N-terminus of rfhSP-A1 and rfhSP-A2, which contains multiple proline residues, may prevent *E. coli* from expressing these proteins.

No one has successfully expressed an equivalent rfhSP-A molecule containing the 8 x Gly Xaa Yaa collagen-like stalk (which is thought to be important in stabilising the trimer). Expression levels, therefore, can not be compared. A recombinant fragment of rat SP-A has previously been expressed in insect cells (32). However rat and human SP-A sequences are considerably different and this protein lacked the 8 x Gly Xaa Yaa contained within the construct used in this study. A rfhSP-A molecule has previously been successfully expressed without the 8 x Gly Xaa Yaa as a fusion protein with MBP in *E. coli* (280). However, only approximately 13 mg of misfolded rfhSP-A was obtained and the majority of this protein was lost during refolding and subsequent chemical cross-linking which was required for trimerisation; importantly, chemical cross-linking was shown to have limited efficiency. A rfhSP-A has previously been reported to be expressed at low levels without a fusion protein. However, similar problems were encountered to those described above (233). It was hypothesised in this present study that the inclusion of the 8 x Gly Xaa Yaa collagen-stalk encoded by the constructs may overcome the issues of failing to express and purifying a functional trimeric rfhSP-A molecule.

rfhSP-A1 was taken forward in this present study for the expression as a fusion protein with either NT or NT^{dm}. Use of both of these expression partners overcame the problems discussed above and allowed high levels of heterologous expression in *E. coli* (Figure 4-13 and date not shown, respectively). As later discussed in Chapter 6, NT-rfhSP-A1 is primarily monomeric and only trimerises upon removal of NT. Perhaps this inability of rfhSP-A to trimerise when fused with NT prevents the rfhSP-A molecule from functioning and causing toxicity to the *E. coli*, thus allowing efficient expression. Alternatively, the ability of this fusion protein to be expressed could be mediated through an amino acid sequence difference at the translational start point allowing efficient initiation and elongation of translation.

In addition to allowing expression of rfSP-A1, use of NT as an expression partner increased the expression of rfhSP-D considerably (compare Figure 4-15 with Figure 4-14). Unlike rfhSP-A1, codon usage of the rfhSP-D sequence was not optimised for *E. coli* expression. The codon usage of NT could, therefore, be more suited for expression

in *E. coli* and allow efficient initiation and elongation of translation allowing rfhSP-D to be efficiently translated downstream.

Spiders naturally express vast amounts of silk which contain a large, repetitive and very GC-rich region which can constitute up to 60 % of the spiridon.(281). Alongside having unusually large pools of alanyl- and glycyl-tRNA (282), the ability to translate large amounts of spider silk may be coded for within the amino acid sequence of NT, to allow fast and efficient initiation and elongation of translation. This may also lead to efficient translation in heterologous *E. coli* systems, as seen in this present study. Upon comparison of NT and NT^{dm}, levels of expression for both rfhSP-A1 and rfhSP-D were similar. Use of PGB1 as an expression partner also allowed the expression of both rfhSP-A1 and rfhSP-D. However, expression levels were considerably lower than those using NT or NT^{dm} as an expression partner after recloning to include a HRV 3C protease cleavage site, particularly for rfhSP-A (data not shown). Thus NT and NT^{dm} were taken forward for evaluation of their utility as solubility tags to enable high levels of soluble expression of rfhSP-A1. Importantly, only rfhSP-A1 was taken forward for purification and structural and functional characterisation (and not rfhSP-A2). Therefore, throughout Chapters 5, 6 and 7 rfhSP-A1 is referred to simply as rfhSP-A (also for NT-rfhSP-A1 and NT^{dm}-rfhSP-A1 which are referred to simply as NT-rfhSP-A and NT^{dm}-rfhSP-A, respectively).

4.5.1 Summary

In summary SP-A1 and SP-A2 were successfully cloned from human lung mRNA. rfhSP-A1 and rfhSP-A2 were subcloned into expression vectors but could not be expressed in *E. coli* without the use of an expression partner. NT and NT^{dm} successfully overcame these issues and allowed high levels of expression of both rfhSP-A1 and rfhSP-D as fusion proteins. This is the first time a rfhSP-A molecule has successfully been expressed with the 8 x Gly Xaa Yaa thought to be important in stabilising the trimer. These experiments also demonstrated for the first time that NT and NT^{dm} may have a more general utility as expression partners for heterologous proteins in *E. coli*.

Chapter 5: Purification of Recombinant Collectins

5.1 Introduction

The formation of insoluble aggregates is a common problem faced upon expression of proteins in heterologous systems. It was hypothesised that the NT domain and NT^{dm} would have utility as general solubility tags to allow high levels of soluble expression in heterologous systems. rfhSP-A and rfhSP-D were expressed at high levels as fusion proteins with NT and NT^{dm} in Chapter 4, highlighting their use as expression partners. This chapter set out to characterise whether these proteins were expressed as soluble or insoluble proteins.

To allow further purification, nickel affinity chromatography was implemented, using the His_6-tag which was cloned N-terminally of NT and NT^{dm} (Figure 4-1). Subsequently, it enzymatic removal of the NT and NT^{dm} tags through use of the cleavage site between the NT or NT^{dm} domain and rfhSP-A or rfhSP-D could be undertaken. Importantly, due to the His_6-tag being N-terminal of the NT domain, subsequent purification by nickel affinity chromatography would allow removal of NT and NT^{dm} and subsequent purification of rfhSP-A and rfhSP-D. Moreover, upon cloning to include a HRV 3C proteases cleavage site, due to the presence of a His_6-tag on this enzyme, HRV 3C enzyme would also be efficiently removed alongside NT^{dm}.

The amino acid sequences for: NT-rfhSP-A; rfhSP-A after cleavage from NT-rfhSP-A; NT^{dm}-rfhSP-A; rfhSP-A after cleavage from NT^{dm}-rfhSP-A; NT^{dm}-rfhSP-D and rfhSP-D after cleavage from NT^{dm}-rfhSP-D and rfhSP-D produced through the traditional refolding method are given in Appendix (Figure 8-2). To note, due to the protein cleavage site used in the NT^{dm} constructs, the 7^{th} Xaa of the 8 x Gly Xaa Yaa collagen-like stalk is missing after purification of rfhSP-A and rfhSP-D. rfhSP-D is also missing the start codon methionine present in the rfhSP-D produced using the traditional refolding method.

5.1.1 Aims

The overarching aim of experiments reported in this chapter was to purify rfhSP-A after expression as fusion proteins with NT or NT^{dm}. A further aim was to assess the utility of NT and NT^{dm} as expression partners/solubility tags in a heterologous expression system to allow the soluble expression of rfhSP-D and its subsequent purification without the need for refolding, Aims 2 and 3 (Section 1.14).

5.2 Methods

5.2.1 Bacterial Cell Lysis

Bacterial cell pellets from 500 ml bacterial cultures were thawed and resuspended in 40 ml of 20 mM Tris, 1.5 mM $MgCl_2$, pH 8. Bacterial cells were lysed at 4 °C for 1 hour by addition of lysozyme to a concentration of 0.7 mg/ml and DNase (100 Kunitz units) (Qiagen, UK). Lysed bacteria were subject to centrifugation at 27,000 x g at 4 °C for > 30 min. After removal of the supernatant, the lysate pellet was stored at -20 °C until use for purification. NT^{dm}-rfhSP-A and NT^{dm}-rfhSP-D were lysed as above, however, with resuspension of 250 ml of bacterial cell pellets in 30 ml of 20 mM Tris, 1.5 mM $MgCl_2$, pH 8. In addition, after lysis, bacterial lysates were subject to sonication directly, as described in Section 5.2.7.

5.2.2 Purification of NT-rfhSP-A and NT-rfhSP-D using 2 M Urea

Bacterial lysate pellets were resuspended in 40 ml of 20 mM Tris, 2 M urea, pH 8. The cell lysate solution was then subject to up to 6 x 5 min cycles of sonication (5 sec on, 5 sec off), on ice, at maximum amplitude using a Soniprep 150 sonicator (MSE LTD, UK). Soluble and insoluble fractions were separated by centrifugation at 27,000 x g at 4 °C for > 30 min. Soluble protein was then purified immediately by nickel affinity chromatography.

5.2.3 Washing Insoluble Bacterial Lysate

To initially determine whether NT-rfhSP-A was expressed as a soluble protein or stored in bacterial inclusion bodies, whole bacterial lysate was washed in TBS containing 1 % Triton-X100 at varying pH values ranging from 5-10.

To wash inclusion bodies containing NT-rfhSP-A or rfhSP-D, insoluble bacterial lysate was homogenised in TBS containing 1 % Triton-X100 (40 ml per 500 ml bacterial culture). Inclusion bodies were then isolated by centrifugation at 5,000 x g for 25 min. This was repeated a total of three times with the final wash being in TBS without Triton X-100.

5.2.4 Purification with 8 M Urea and Refolding

Inclusion bodies were resuspended in 40 ml of TBS with 5 mM $CaCl_2$ and 5 % glycerol (v/v), pH 7.4 (solubilisation buffer) with 8 M urea, and left to solubilise at 4 °C for 1 hour with mixing. The solubilised bacterial lysate was then subject to centrifugation at 27,000 x g at 4 °C for > 30 min. The supernatant was then dialysed using 2 L of solubilisation buffer with 4 M urea in a bucket using SnakeSkin dialysis tubing (10,000 Da MWCO) at room temperature over a period of > 2 hours. This dialysis was repeated with solubilisation buffer containing 2 M urea and, subsequently, 1 M urea. The dialysis was then repeated a further 2 times with TBS containing 5 mM $CaCl_2$, pH 7.4 and subsequently 2 more times with TBS without $CaCl_2$, pH 7.4. The bacterial lysate solution was then subject to centrifugation at 27,000 x g at 4 °C for > 30 min. The soluble protein containing supernatant was then removed, filtered (0.45 µm) and further purified by nickel affinity chromatography.

5.2.5 Nickel Affinity Chromatography

NT-rfhSP-A and NT-rfhSP-D purified from the soluble fraction by sonication with 2 M urea were applied to 2 x 1 ml Nickel Columns (Clontech, Basingstoke, UK) which were subsequently washed 4 times with 5 ml of 20 mM Tris, pH 8 containing decreasing concentrations of urea: 2 M, 1.5 M, 1 M and 0.5 M. Contrastingly, NT-rfhSP-A and NT-rfhSP-D purified after refolding from inclusion bodies were dialysed into 20 mM Tris with 0.5 M NaCl and 20 mM imidazole and subsequently applied to the nickel affinity column. Nickel affinity columns were washed with > 20 ml of 20 mM Tris, 20 mM Imidazole, pH 8 or until a baseline of absorbance at λ = 280 nm was reached. Bound protein was eluted with 20 mM Tris, pH 8.0 initially containing 100 mM imidazole and subsequently 200 mM and 300 mM, respectively. Purified protein was dialysed overnight at 4 °C into 20 mM Tris, pH 8. Purified protein was subject to centrifugation at 4,000 x g, filtered (using a 0.45 µm filter), after which, the NT or NT^{dm} tag was removed as described below.

Initial purifications used TBS for application to and washing of the nickel columns. However, after optimisation to allow enhanced protein purity, 20 mM Tris containing 0.5 M NaCl and 20 mM Imidazole was used.

5.2.6 Removal of NT by Cleavage

To optimise cleavage of NT-rfhSP-A, a three-fold dilution series of thrombin protease (GE Healthcare) was created (3.3 to 90.0 Units/mg of protein). Cleavage was undertaken in a final volume of 150 µl in 20 mM Tris pH 8 at either 4 °C or 22 °C for 6 hours. Cleavage of NT-rfhSP-A was analysed by SDS-PAGE. After optimisation, cleavage and removal of NT was scaled up where a concentration of 10 units/mg for 6-8 hours was chosen.

5.2.7 Purification of NT^{dm} Fusion Proteins and Subsequently rfhSP-A and rfhSP-D

The initial purification on a nickel column of expressed NT^{dm}-rfhSP-A and NT^{dm}-rfhSP-D was carried out by Nina Kronqvist at the Karolinska Institutet (Sweden). Bacterial suspensions were lysed as above and subsequently subject to sonication in 20 mM Tris, pH 8 with/without 2 M for NT^{dm}-rfhSP-A and NT^{dm}-rfhSP-D, respectively. Sonication was undertaken at 80 % amplitude for a total time of 2 mins with pulses of 1 sec on and 1 sec off (1 min effective time). After sonication, lysed bacteria were subject to centrifugation at 27,000 x g at 4 °C for > 30 min, after which, NT^{dm}-rfhSP-A and NT^{dm}-rfhSP-D were purified by nickel affinity chromatography, as above. NT^{dm}-rfhSP-A and NT^{dm}-rfhSP-D were cleaved using thrombin as above or using HRV 3C protease containing a His_6-tag, made in house at Karolinska Institutet (Sweden).

5.2.8 Purification of rfhSP-A

To remove NT and NT^{dm} after cleavage, cleaved fusion proteins were applied to 2 x 1 ml nickel columns which had been equilibrated in 20 mM Tris, pH 8.0. rfhSP-A and rfhSP-D which had flown through the column were stored in -80 °C until further purified by either affinity chromatography or gel filtration. NT and NT^{dm} were eluted from the nickel column using Tris with 300 mM imidazole, pH 8 and disposed of.

5.3 Results

5.3.1 Purification of rfhSP-A

5.3.1.1 *Purification of NT-rfhSP-A from Soluble Fraction*

Despite allowing high levels of expression, NT-rfhSP-A was expressed predominantly as an insoluble protein. rfhSP-A was resuspended in 2 M urea and subject to sonication to try and disrupt potential interactions with insoluble material. However, only a small proportion of NT-rfhSP-A was soluble; the majority of NT-rfhSP-A remained in the insoluble fraction (Figure 5-1). Upon application of the soluble NT-rfhSP-A to a nickel column, a proportion of protein bound to the column, as seen by the decrease of NT-rfhSP-A in the flow through. However, a large proportion of the protein did not bind and remained in the flow through (Figure 5-1). Upon elution of NT-rfhSP-A from the nickel column, only 1 mg of dilute (0.1 mg/ml) protein was purified from a 500 ml bacterial culture. Upon removal of NT, this would corresponded to approximately 0.25 mg of rfhSP-A per litre of bacterial culture. NT-rfhSP-A was successfully confirmed to contain immunoreactive rfhSP-A by Western blotting using a polyclonal antibody (Figure 5-1B).

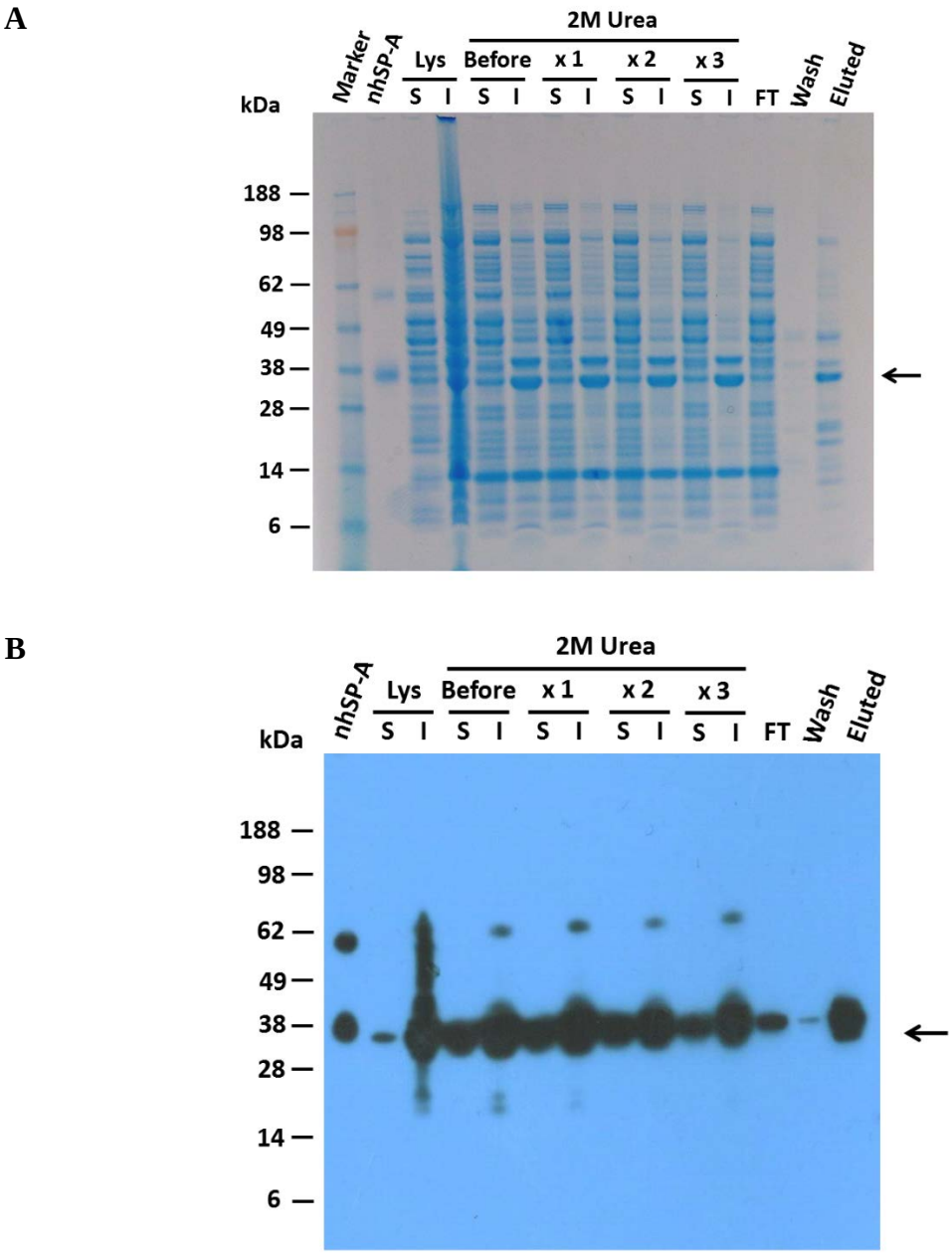

Figure 5-1: SDS-PAGE and Western blot analysis of NT-rfhSP-A purification using 2 M urea. *Each step of NT-rfhSP-A purification was analysed by reduced SDS-PAGE (**A**) and Western blotting using a primary antibody raised against nhSP-A (**B**). Analysed samples included soluble (S) and insoluble (I) protein fractions after lysis of bacteria (Lys), resuspension of bacterial lysate pellet in 2 M urea (Before) and resuspension of bacterial lysate pellet in 2 M urea and subsequent sonication between 1 and 3 times (x 1, x 2 or x 3). After sonication 3 times, soluble protein was applied to a nickel column. Also analysed are samples taken from nickel affinity chromatography, including the flow through of the column (FT), wash step with 15 mM imidazole (wash) and protein eluted from the column specifically with 300 mM imidazole (eluted). 0.5 µg of purified nhSP-A was also analysed as a positive control (nhSP-A).*

To determine whether NT-rfhSP-A was indeed expressed as an insoluble protein contained within the inclusion bodies or whether it was expressed as a soluble protein which associated with the insoluble bacterial cell lysate, the insoluble material was washed in different conditions to try and separate inclusion bodies from associated proteins. Washing whole insoluble bacterial cell lysate up to 3 times in 1 % Triton X-100 did not increase the solubility of NT-rfhSP-A (Figure 5-2 A). Furthermore, washing with 1 % Triton X-100 at different pH values did not affect the solubility of NT-rfhSP-A (Figure 5-2 B). Noticeably, after washing the inclusion bodies twice in 1 % Triton X-100 at pH 7.4, inclusion bodies were obtained containing predominantly NT-rfhSPA1 with comparatively less of the bacterial protein contaminants than pre-washing. Washing of inclusion bodies with 1 % Triton X-100 was therefore employed for downstream purification of rfhSP-A from inclusion bodies.

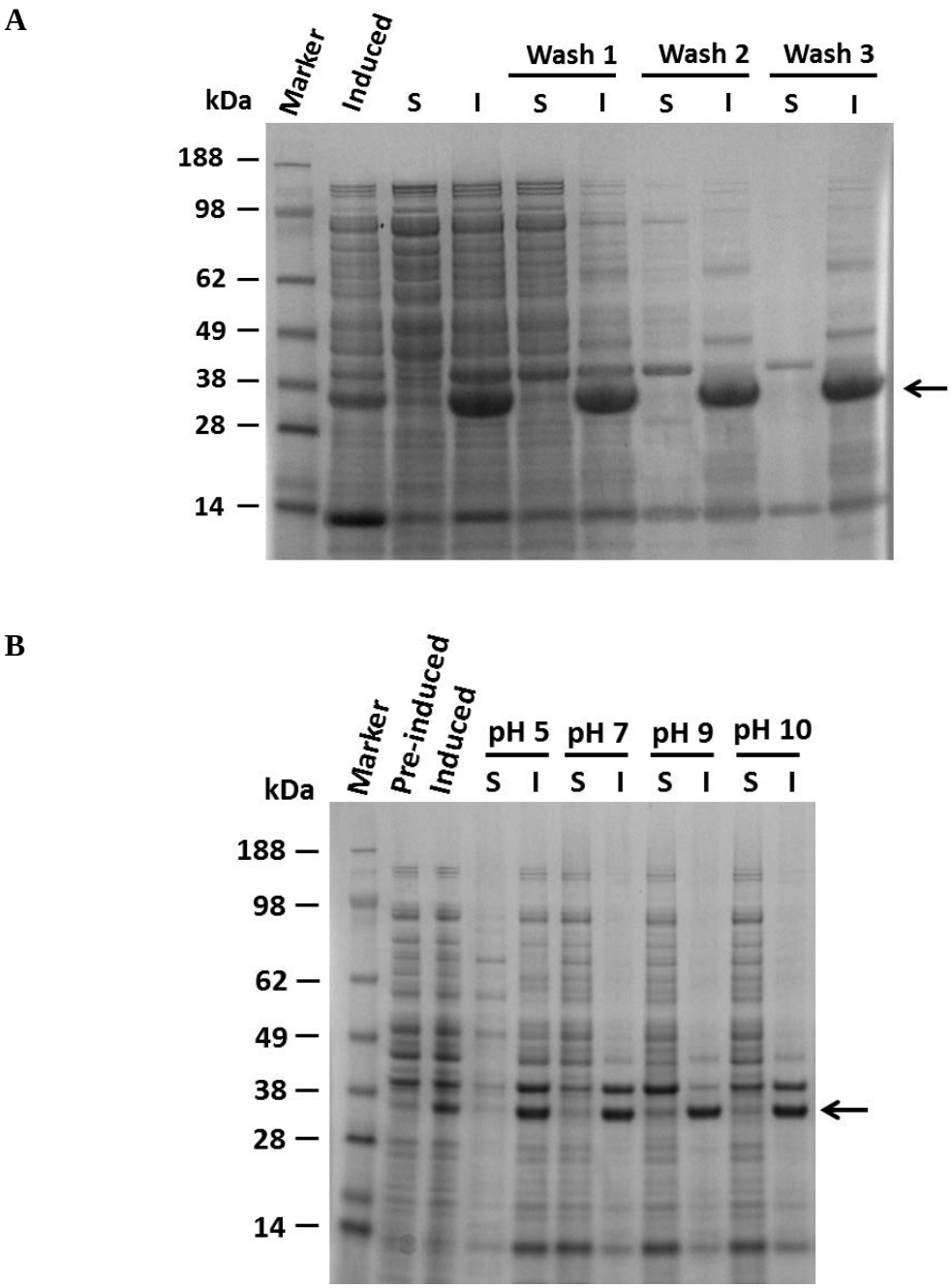

Figure 5-2: Washing of bacterial cell lysate in different conditions. *The soluble (**S**) fraction of bacterial cell lysate in addition to the insoluble cell lysate after washing in TBS containing 1 % triton-X100 at pH 7.4 up to three times (**I**) were analysed by SDS-PAGE (**A**). Insoluble fraction of bacterial cell lysate was also analysed after washing in TBS containing 1 % triton-X100 with varying pH values (5, 7, 9, 10) (**B**). SDS-PAGE was analysed with subsequent Coomassie staining, indicated are the bands corresponding to NT-rfhSP-A (arrow).*

5.3.1.2 *Purification of NT-rfhSP-A from Insoluble Fraction*

NT-rfhSP-A was successfully solubilised from inclusion bodies using 8 M urea (Figure 5-3A). NT-rfhSP-A was subsequently refolded by diluting the urea through dialysis as traditionally done for rfhSP-D. During the refold, 77 (± 7.4) % of the protein precipitated as indicated by the cloudy appearance of the protein solution (Table 5-1). However, a proportion of the NT-rfhSP-A remained soluble (Figure 5-3B) and was available for further purification with nickel affinity chromatography. The majority of NT-rfhSP-A bound to the nickel column with very little in the flow through. (Figure 5-4). Moreover, only a small amount of NT-rfhSP-A was lost during washing of the column. NT-rfhSP-A was successfully purified with only small amount of contaminating proteins (Figure 5-4A). The eluted NT-rfhSP-A protein was confirmed to be immunoreactive to a monoclonal α-SP-A antibody by Western blot analysis (Figure 5-4B).

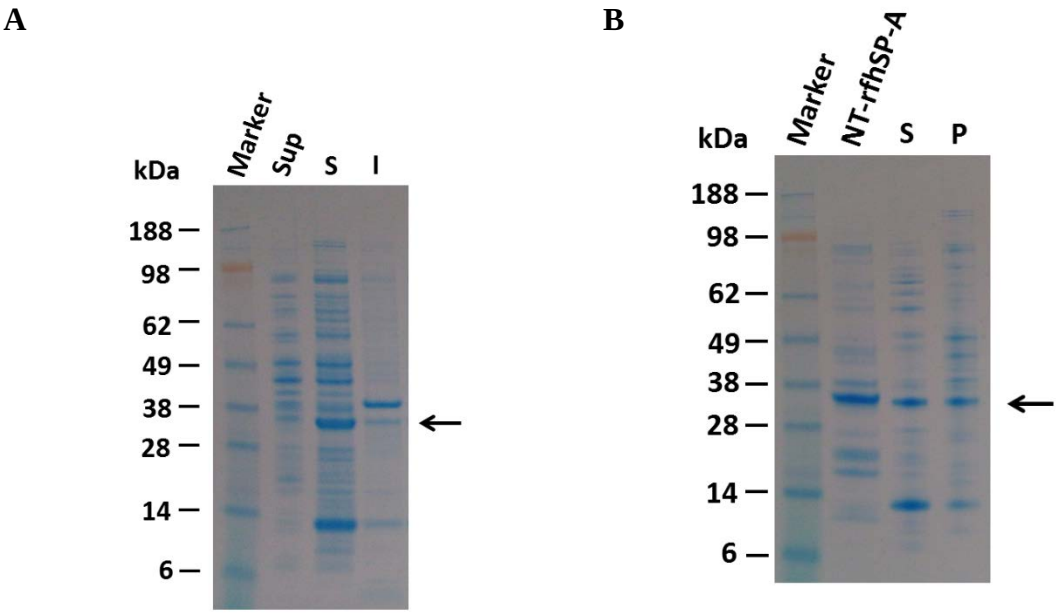

Figure 5-3: SDS-PAGE analysis of NT-rfhSP-A solubilised using 8 M urea. *NT-rfhSP-A solubilised using 8 M urea with subsequent refolding was analysed using reduced SDS-PAGE. In **A**, after lysis of bacteria and subsequent centrifugation, the supernatant (sup) and pellet were separated. The bacterial lysate pellet was then solubilised using 8 M urea and soluble (S) and insoluble (I) proteins separated. During refolding of solubilised protein, a fraction of proteins precipitated. Analysed soluble (S) and precipitated protein samples (P) are indicated in **B**. 1 µg of NT-rfhSP-A previously purified by 2 M urea and subsequent nickel affinity chromatography was also analysed as a positive control (NT-rfhSP-A).*

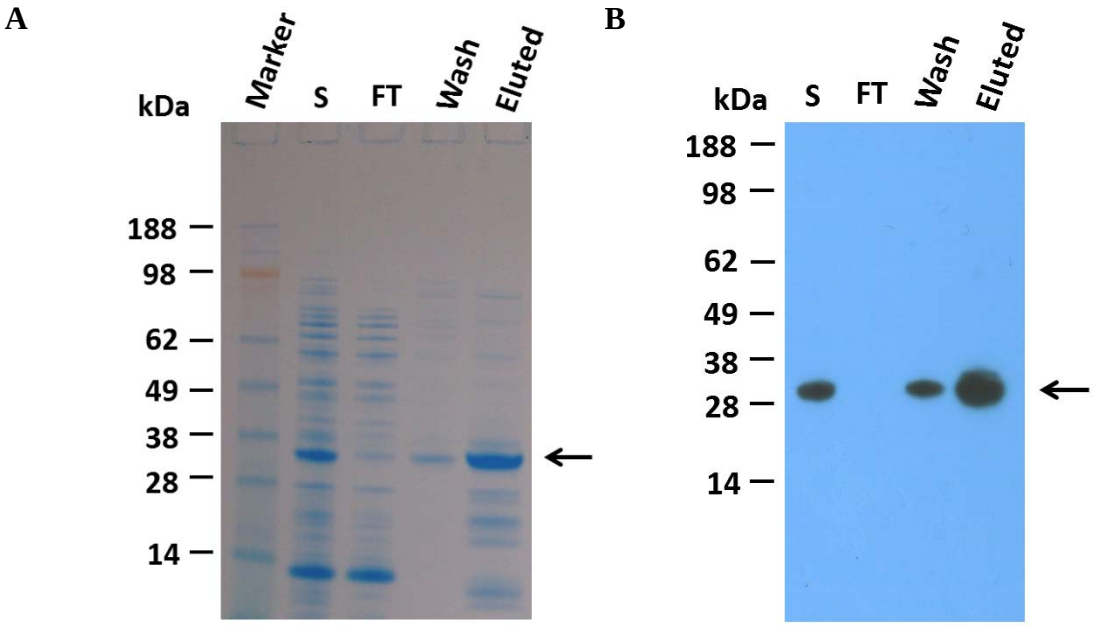

Figure 5-4: SDS-PAGE and Western blot analysis of NT-rfhSP-A purified by Nickel affinity chromatography. *Samples taken during nickel affinity chromatography were analysed by SDS-PAGE (**A**) and Western blotting using a primary antibody raised against nhSP-A (**B**). Analysed samples included soluble protein prior to application to the nickel column (S), flow through from the column (FT), protein eluted during washing of the column with 15 mM imidazole (Wash) and protein specifically eluted from the column with 300 mM imidazole (Eluted). Indicated arrows are protein bands corresponding to rfhSP-A.*

5.3.1.3 *Purification of rfhSP-A from NT-rfhSP-A*

After purification of NT-rfhSP-A, the NT tag was removed through use of the thrombin cleavage site. An overnight cleavage of NT-rfhSP-A resulted in non-specific cleavage of rfhSP-A (data not shown). Optimal cleavage conditions were therefore identified using a shorter 6 hour incubation at different temperatures with different thrombin concentrations. With a 6 hour incubation time, thrombin cleaved NT-rfhSP-A specifically without any non-specific cleavage. Cleavage was more effective at 22 °C than 4 °C with the majority of the protein being cleaved using a thrombin concentration of 10 units/mg of protein (Figure 5-5). Due to the cost of the enzyme, this concentration was employed for future cleavage and removal of NT. The identity of NT-rfhSP-A and rfhSP-A was confirmed to be immunoreactive to a monoclonal α-SP-A antibody through Western blotting (Figure 5-5B).

To remove the cleaved NT tag, the protein solution was passed through additional nickel affinity columns to which the NT tag bound and the rfhSP-A flowed through. This

allowed the purification of rfhSP-A to a high level of purity (Figure 5-6). The identity and purity of rfhSP-A was confirmed by Western blot analysis (Figure 5-6B) and mass spectrometry (data not shown). Upon development of the rfhSP-A purification procedure, the stringency was increased during nickel affinity chromatography to include use of 20 mM imidazole and 500 mM NaCl in the buffer during application of the protein and washing of the column. This allowed much higher purity of NT-rfhSP-A and rfhSP-A to be purified (compare Figure 5-6 with Figure 5-4).

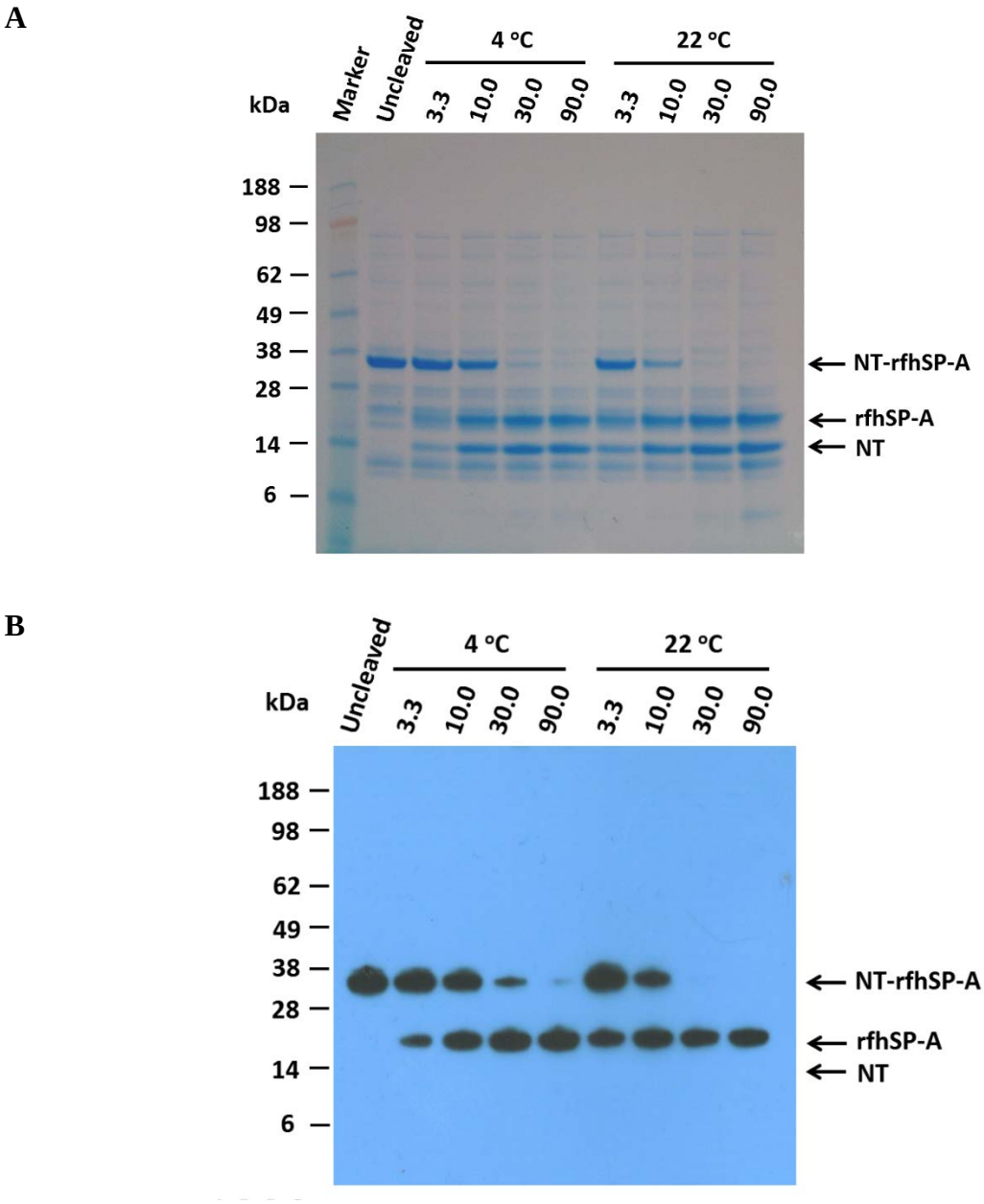

Figure 5-5: Analysis of NT-rfhSP-A thrombin cleavage trials by SDS-PAGE and Western blot analysis. *Cleavage trials of NT-rfhSP-A using thrombin were analysed by SDS-PAGE (**A**) and Western blotting using a primary antibody raised against nhSP-A (**B**). Analysed samples included uncleaved NT-rfhSP-A (uncleaved) and a threefold dilution series of thrombin concentrations (3.7, 11.1, 33.3 or 99.9 units of protease per mg of protein). Cleavage was undertaken at either 4 °C or 22 °C. Indicated (arrows) are protein bands corresponding to uncleaved NT-rfhSP-A and rfhSP-A once cleaved from the construct.*

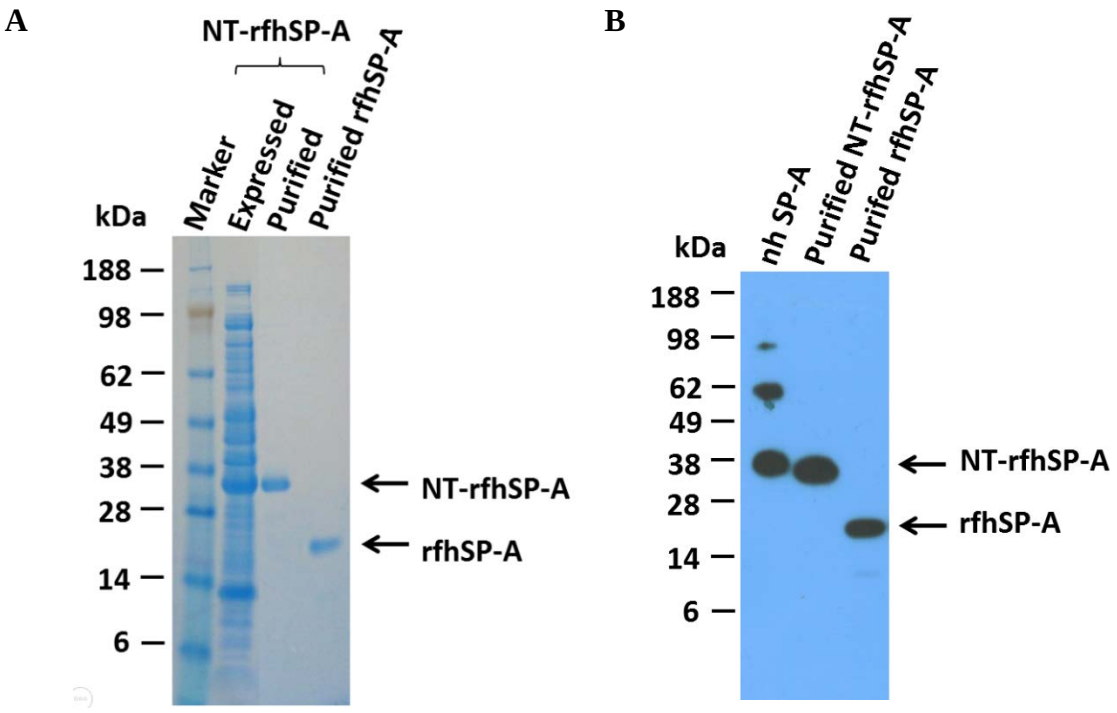

Figure 5-6: Removal of NT and purification of rfhSP-A. *Samples of expressed and purified NT-rfhSP-A and purified rfhSP-A after cleavage were analysed by SDS-PAGE with subsequent Coomassie staining (**A**) or Western blotting using an antibody against nhSP-A (**B**). Purification was undertaken with the increased stringency using 20mM imidazole and 500 mM NaCl upon loading protein and washing the nickel affinity column. Indicated are bands corresponding to NT-rfhSP-A and rfhSP-A.*

5.3.1.3.1 rfhSP-A Yields

Purification of rfhSP-A by refolding NT-rfhSP-A was undertaken a total of 24 times. After optimisation, pure rfhSP-A was successfully obtained with a mean yield (± SD) of 12.7 (± 4.4) mg/litre of bacterial culture post purification by nickel column; alteration of the refold protocol affected the yield of NT-rfhSP-A only minimally and is discussed in Chapter 6 (Table 6-2). Protein loss was encountered during precipitation of rfhSP-A during refolding. Increasing the purity with the further purification steps resulted in the total concentration of protein being approximately halved, namely during nickel affinity purification of NT-rfhSP-A and cleavage of the NT domain and subsequent rfhSP-A purification. Average yields of rfhSP-A at each stage of purification are summarised in Table 5-1.

Stage	Average Protein yield (mg) (Mean (±SD)
Total Solubilised Protein	234.0 (± 63)
Refolded protein	53.6 (± 23.6)
NT-rfhSP-A	24.0 (± 5.6)
rfhSP-A	12.7 (± 4.4)

Table 5-1: Yield of purified protein at each purification step. *Shown are the mean values (*± SD*, n = 24) for yields of protein obtained after each sequential purification step including yield after solubilisation using 8 M urea, yield after refolding NT-rfhSP-A and yield after removal of NT tag and purification of rfhSP-A.*

5.3.1.4 *Purification of rfhSP-A as a Soluble Protein using NT^{dm}*

To overcome the issues associated with purifying rfhSP-A as an insoluble protein, expression and purification of rfhSP-A was trialled with NT^{dm}. NT^{dm}-rfhSP-A was expressed, purified and cleaved at Karolinska Institutet (Sweden) by Nina Kronqvist. Western blot analysis and further purification (including carbohydrate affinity purification and gel filtration) of rfhSP-A was undertaken at University of Southampton by Alastair Watson.

Use of NT^{dm} gave similar expression levels to use of the NT. However, the majority of NT^{dm}-rfhSP-A was expressed as a soluble protein which was purified using nickel affinity chromatography without the need for solubilisation and refolding. NT^{dm} was effectively removed by cleavage with HRV 3C protease with subsequent purification of rfhSP-A (Figure 5-4). Expression and purification of rfhSP-A using NT^{dm} yielded a mean (± SD) of 23.3 (± 5.4) mg/litre of bacteria (n = 4), which is higher than the average 12.7 (± 4.4) mg/litre obtained using NT through refolding. rfhSP-A was confirmed to be immunoreactive to a monoclonal α-SP-A antibody by Western blotting (Figure 5-4 B).

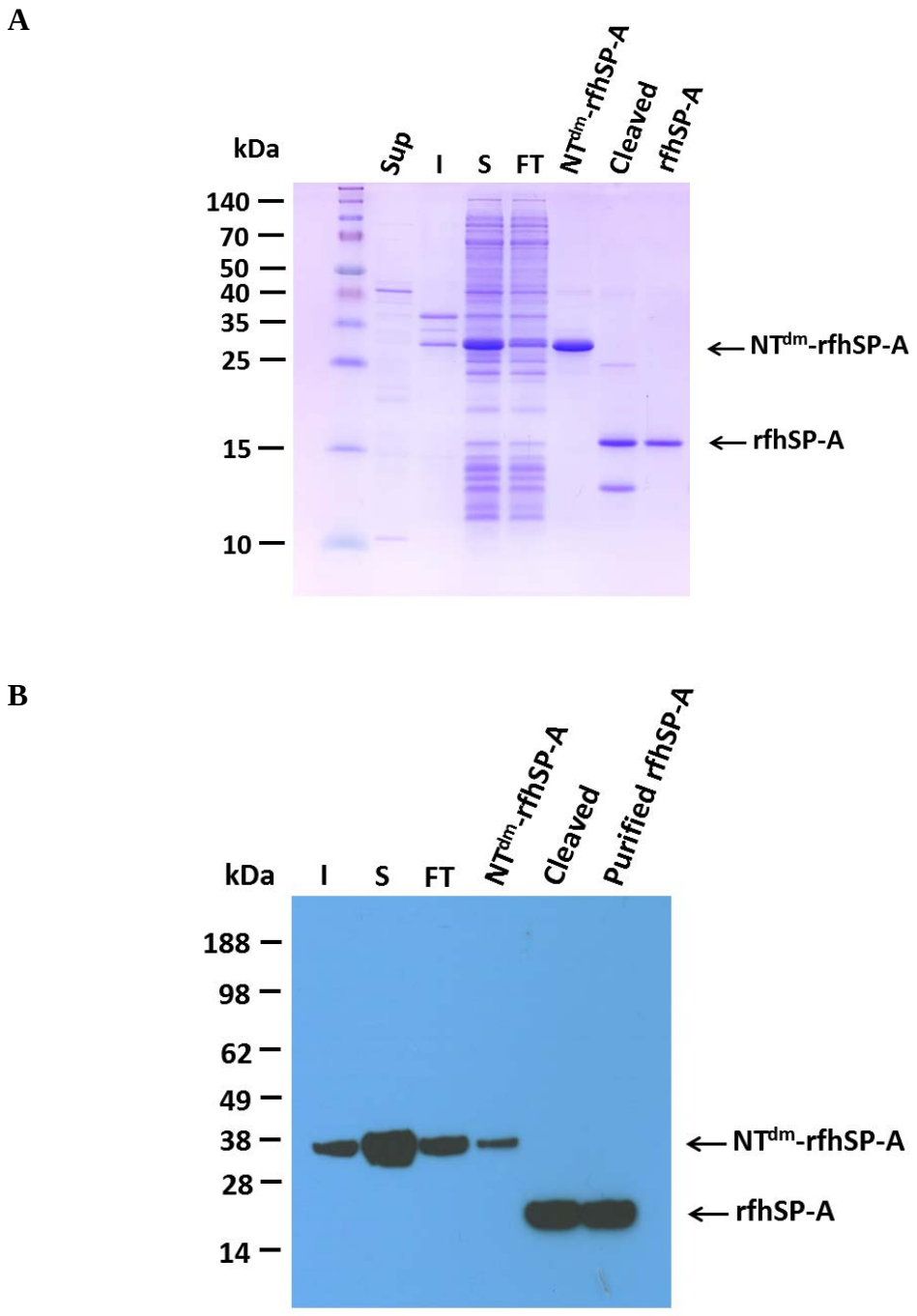

Figure 5-7: Purification of rfhSP-A as a soluble protein using NT^{dm}-rfhSP-A. *Samples at each step of purification of rfhSP-A as a soluble protein from NT^{dm}-rfhSP-A were analysed by SDS-PAGE and analysed by Coomassie staining (**A**) or Western blotting using an α-nhSP-A antibody (**B**). Samples analysed included: supernatant after bacterial harvest (Sup), insoluble fraction after cell lysis and sonication (I), soluble fraction after cell lysis and sonication (S), flow through of nickel column (FT), purified NT^{dm}-rfhSP-A (NT^{dm}-rfhSP-A), cleaved NT^{dm}-rfhSP-A, (Cleaved), purified rfhSP-A (rfhSP-A). Purification and cleavage of NT^{dm}-rfhSP-A and SDS-PAGE with Coomassie staining were undertaken at Karolinska Institutet (Sweden) by Nina Kronqvist. Western blot analysis was undertaken at University of Southampton by Alastair Watson. Spectra BR and SeeBlue Plus2 pre-stained markers were used for analysis of Coomassie stained gel (**A**) and Western blotting (**B**) respectively.*

5.3.2 Purification of rfhSP-D

5.3.2.1 *Purification of rfhSP-D without a Solubility Tag*

Although rfhSP-A was not successfully expressed without expression as a fusion protein, rfhSP-D was successfully expressed and purified using the traditional refolding method. This was undertaken by Alastair Watson and Henry Hole at University of Southampton. rfhSP-D was solubilised using 8 M urea and refolded. After washing of inclusion bodies, soluble contaminants were successfully removed. Analysis of samples indicated that washing of the inclusion bodies 4 times was necessary with contaminating soluble protein still being present after the 4th wash (Figure 5-8). rfhSP-D was successfully solubilised using 8 M urea to give 110 mg of soluble protein from 1 litre of bacteria. The rfhSP-D was then refolded by dialysis using the traditional method. After refolding, 16.5 mg of protein was isolated, the majority of which was rfhSP-D but with a considerable level of contaminating proteins (Figure 5-8); during the refold process, 85 % of the solubilised protein precipitated. Successfully refolded protein was stored for further purification of functional rfhSP-D with carbohydrate affinity chromatography (see Section 6.3.4.1).

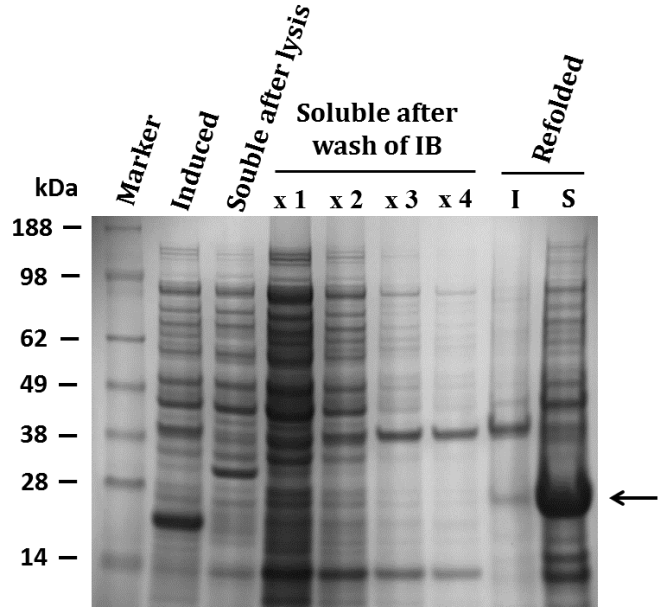

Figure 5-8: Purification of rfhSP-D from inclusion bodies. *Samples taken during purification for rfhSP-D from E. coli with refolding using 8 M urea were analysed by SDS-PAGE. Analysed samples included: induced whole bacterial cell lysate (Induced), soluble fraction after bacterial cell lysis (S after lysis), soluble fraction after washing of insoluble inclusion bodies up to four times (S after wash of IB: x1, x2, x3 or x4), Soluble and diluted insoluble fractions after refolding with 8 M urea (8 M Urea: I and S). Indicated is the band corresponding to rfhSP-D (arrow). SDS-PAGE was undertaken by Alastair Watson and Henry Hole at University of Southampton.*

5.3.2.2 *Purification of NT-rfhSP-D as a Soluble Protein*

After expression of NT-rfhSP-D, bacterial pellets were resuspended, lysed and subject to 6 rounds of sonication. Prior to sonication, NT-rfhSP-D protein was mainly in the insoluble fraction. Sonication did increase the proportion of NT-rfhSP-D in the soluble fraction. However, the majority of protein remained insoluble (Figure 5-9A).

It was hypothesised that NT-rfhSP-D was expressed as a soluble protein which associated with insoluble cell lysate and pelleted with the inclusion bodies rather than being expressed and stored in inclusion bodies themselves. To dissociate the NT-rfhSP-D from the outside of the inclusion bodies, the insoluble material was sonicated in the presence of 2 M. This was effective in increasing the proportion of soluble NT-rfhSP-D. After 1 round of sonication, the majority of NT-rfhSP-D became soluble (Figure 5-9B). The ability of lower urea concentrations of urea to allow isolation of soluble NT-rfhSP-D was subsequently investigated but was not effective (Figure 5-9C).

NT-rfhSP-D was successfully purified using nickel affinity chromatography. A large proportion of NT-rfhSP-D bound to the column, however, a large proportion flowed through the column without binding, perhaps due to overloading of the column (Figure 5-10). However, the result was that 22 mg of protein was purified from 500 ml of bacteria which equates to approximately 22 mg of pure rfhSP-D per litre of bacteria, which is higher than the 16.5 mg of non-pure rfhSP-D obtained using the traditional refold method. Washing of the column resulted in removal of non-specifically bound proteins. Moreover, elution of NT-rfhSP-D from the column resulted in a protein preparation with much fewer contaminating proteins than before addition to the nickel column. Due to the absence of an enzyme cleavage site in the NT-rfhSP-D construct, however, rfhSP-D could not be further purified form the NT-rfhSP-D fusion protein.

A

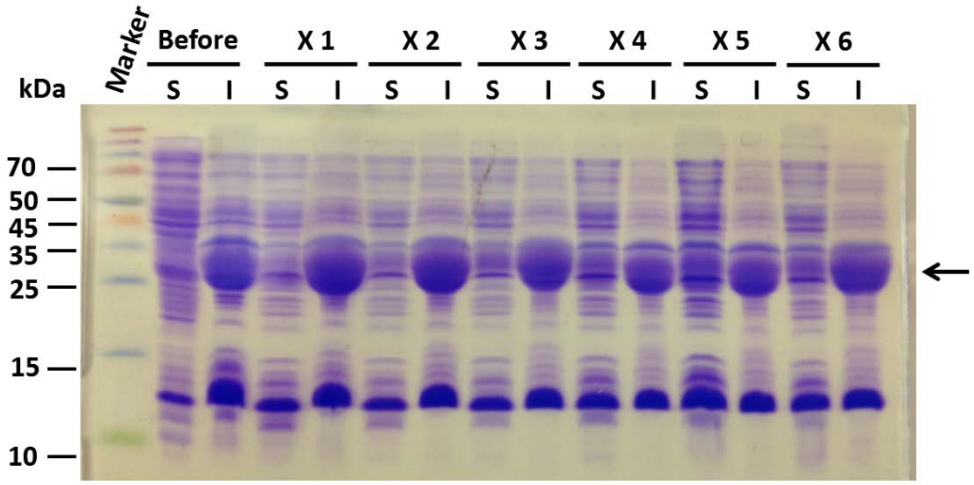
Marker
Before
X 1
X 2
X 3
X 4
X 5
X 6
kDa
S I S I S I S I S I S I S I
70
50
45
35
25
15
10

B

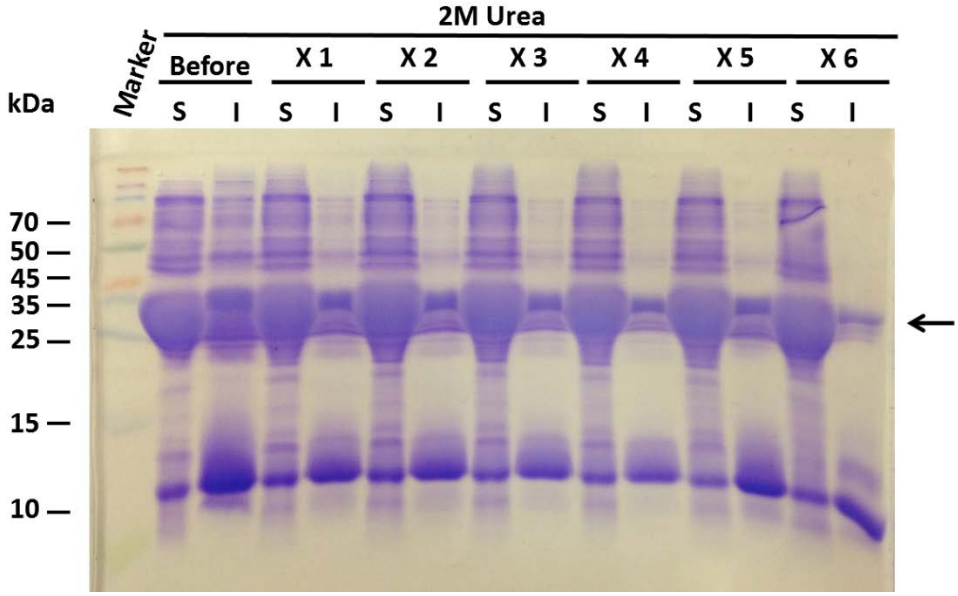
2M Urea
Marker
Before
X 1
X 2
X 3
X 4
X 5
X 6
kDa
S I S I S I S I S I S I S I
70
50
45
35
25
15
10

C

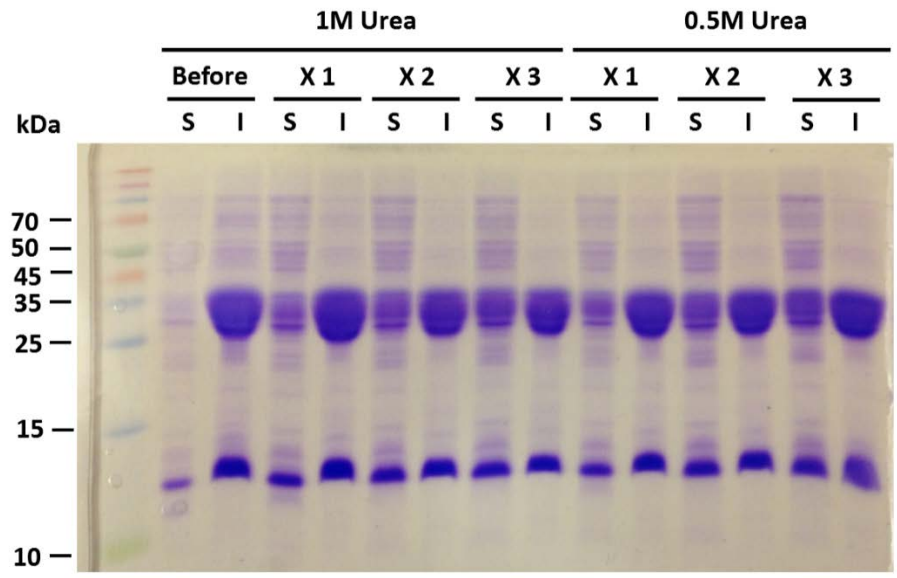

Figure 5-9: Isolation of soluble NT-rfhSP-D and analysis by SDS-PAGE. *After expression, the capacity to purify soluble protein was investigated and analysed using SDS-PAGE. Bacterial lysate was resuspended in 20 mM Tris, pH 8 (**A**) 20 mM Tris, containing 2 M urea, pH 8 (**B**) and 20 mM Tris, containing either 1 M or 0.5 M urea, pH 8 (**C**). The proportion of soluble (S) and insoluble (I) protein was compared with increasing cycles of sonication (x1 to x6). Indicated arrows are bands corresponding to the correct molecular weight for NT-rfhSP-D (34.5 kDa).*

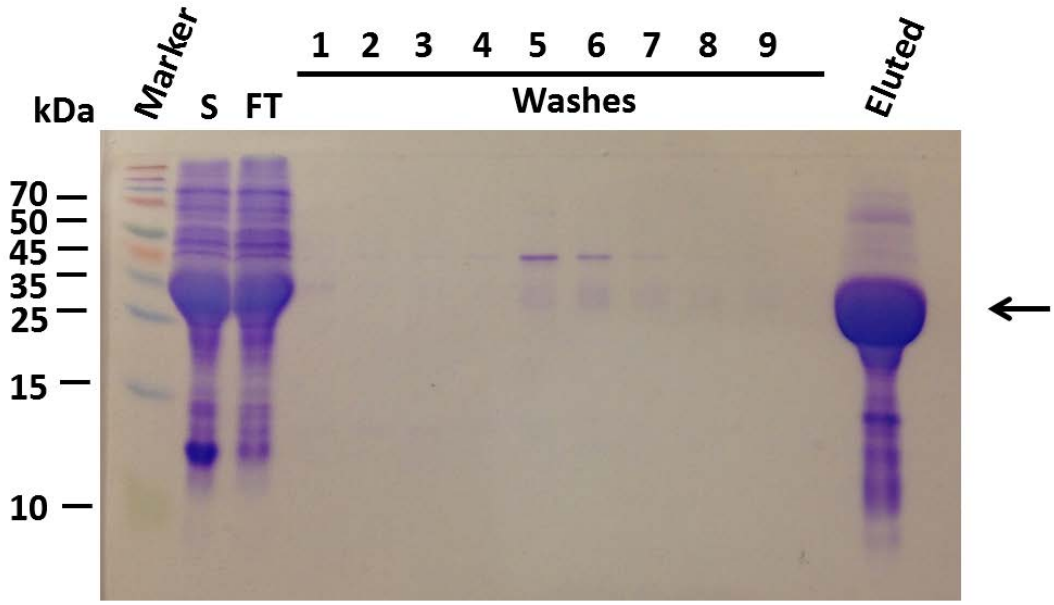

Figure 5-10: Analysis of the nickel affinity purification of NT-rfhSP-D by SDS-PAGE. *Each step during the nickel affinity purification of NT-rfhSP-D was analysed by SDS-PAGE. Analysed samples included soluble protein prior to application to the column (S) flow through from the column (FT) and different wash steps (washes 1-9). Washes 1, 2, 3 and 4 were with 2.0 M, 1.5 M, 1.0 M and 0.5 M of urea, respectively. Washes 5-9 corresponded to samples taken after additional sequential washing with 5 ml of 15 mM imidazole. Protein which was specifically eluted from the nickel column upon addition of 300 mM imidazole was also analysed. Note, the gel is highly overloaded.*

5.3.2.3 *Purification of NT^{dm}-rfhSP-D as a Soluble Protein with Subsequent Purification of rfhSP-D*

NT^{dm}-rfhSP-D was expressed at Karolinska Institutet (Sweden) by Nina Kronqvist and the product cleaved to release the expressed rfhSP-D. Purification of functional trimeric rfhSP-D, analysis of oligomeric state and identification by Western blotting was undertaken at University of Southampton by Alastair Watson.

Use of NT^{dm} as a fusion partner for rfhSP-D gave similar expression levels to use of the wild type NT tag. However, NT^{dm}-rfhSP-D was expressed as a highly soluble protein which was isolated without the need for resuspension of lysate in 2 M urea and with only one round of sonication. This allowed for efficient purification by nickel affinity chromatography with subsequent removal of NT^{dm} and purification of rfhSP-D (Figure 5-11). Initial expression of NT^{dm}-rfhSP-D yielded 276 mg of soluble protein/Litre of bacteria, equating to approximately 138 mg of rfhSP-D. However, due to the problem

with miscleavage by thrombin, this construct was recloned to contain a HRV 3C protease cleavage instead. Production of rfhSP-D using this construct after removal of NT^{dm} yielded mean (± SD) of 46 (± 9.9) mg per litre of bacteria (n = 4). Purified NT^{dm}-rfhSP-D and rfhSP-D protein was confirmed to be immunoreactive using a polyclonal α-rfhSP-D antibody by Western blot analysis (Figure 5-11B). rfhSP-D was stored until further purification of functional protein by affinity chromatography and gel filtration in Section 6.3.4.2.

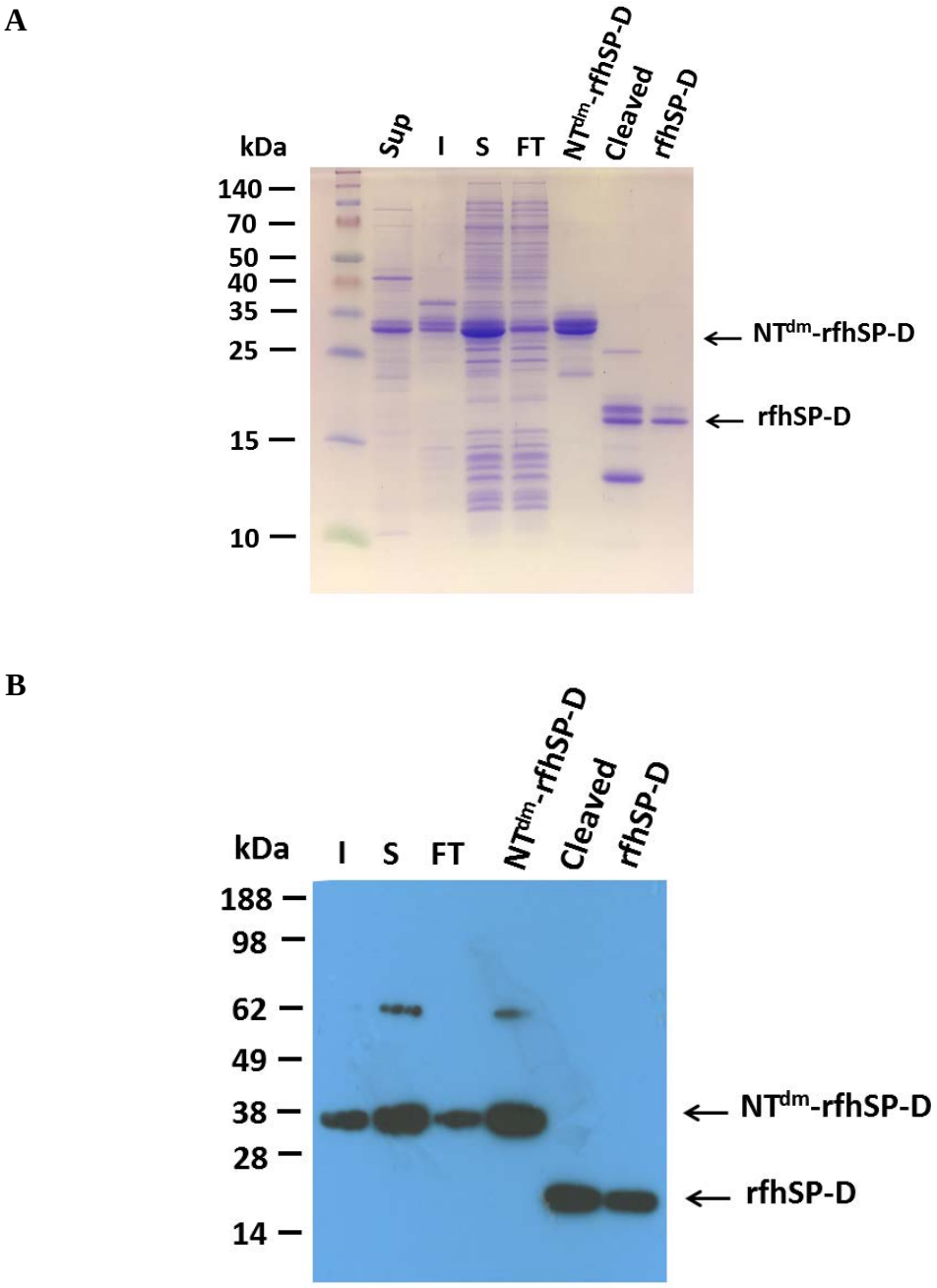

Figure 5-11: Purification of rfhSP-D as a soluble protein using NT^{dm}-rfhSP-D. *Samples at each step of purification of rfhSP-D as a soluble protein from NT^{dm}-rfhSP-D were analysed by SDS-PAGE and analysed by Coomassie staining (A) or Western blotting using an α-rfhSP-D antibody (B). Samples analysed included: supernatant after bacterial harvest (Sup), Insoluble fraction after cell lysis and sonication (I), Soluble fraction after cell lysis and sonication (S), flow through of nickel column (FT), purified NT^{dm}-rfhSP-D (NT^{dm}-rfhSP-D), cleaved NT^{dm}-rfhSP-D, (Cleaved), purified rfhSP-D (rfhSP-D). Purification of NT^{dm}-rfhSP-D and cleavage to release rfhSP-D and SDS-PAGE with Coomassie staining were undertaken at Karolinska Institutet (Sweden) by Nina Kronqvist. Western blot analysis was undertaken at University of Southampton by Alastair Watson. Spectra BR and SeeBlue Plus2 pre-stained markers were used for analysis of Coomassie stained gel (A) and Western blotting (B), respectively.*

5.4 Summary of Results

Within this chapter, rfhSP-A and rfhSP-D were purified as fusion proteins with NT and NT^{dm}, after which, tags were removed and rfhSP-A and rfhSP-D were subsequently purified. During purification, the ability of these tags to allow expression of rfhSP-A and rfhSP-D as soluble proteins was assessed. Therefore, alongside results in Chapter 4, this chapter addresses Aims 2 and 3 (Section 1.14):

- To clone SP-A1 and SP-A2 and express and purify a rfhSP-A molecule, equivalent to rfhSP-D.
- To investigate the utility of NT and NT^{dm} as novel solubility tags for allowing heterologous expression of soluble rfhSP-A and rfhSP-D and subsequent purification without the need for protein refolding.

The main findings reported in this chapter are:

- NT allowed purification of a mean (SD) of 12.7 (± 4.4) mg of rfhSP-A per litre of bacteria, although it was expressed as an insoluble protein and required solubilisation and refolding.
- NT^{dm} allowed the expression and purification of 23.3 (± 5.4) mg of rfhSP-A per litre of bacteria as a soluble protein which was purified without the need for refolding.
- After expression, rfhSP-D was successfully solubilised and refolded using the traditional method to be later purified by carbohydrate affinity chromatography.
- NT allowed the expression of rfhSP-D as a soluble protein, which was efficiently purified upon sonication in 2 M urea without the need for refolding. However, rfhSP-D was not subsequently purified from NT-rfhSP-D due to the absence of a cleavage site.
- NT^{dm} allowed the purification of 46 (± 9.9) mg of rfhSP-D per litre of bacteria of highly pure rfhSP-D without the requirement for refolding due to expression as a soluble protein. This is substantially higher than the 16.5 mg of non-pure rfhSP-D protein purified using the traditional refolding protocol.

5.5 Discussion

The formation of insoluble aggregates is a common problem faced upon expression of proteins in heterologous systems. Indeed, the current purification of rfhSP-D from inclusion bodies requires solubilisation and refolding which results in substantial protein loss due to precipitation. In this chapter, rfhSP-A and rfhSP-D were successfully purified through using NT and NT^{dm} and utility of these tags for the soluble expression of protein in a heterologous expression system was investigated, Aims 2 and 3 (Section 1.14).

5.5.1 Purification of rfhSP-A

As discussed in Chapter 4, NT was successful in allowing the expression of rfhSP-A. However, NT-rfhSP-A was expressed as an insoluble protein which required solubilisation using 8 M urea and subsequent refolding. It was hypothesised that, because nhSP-A interacts with various lipids, the protein may have been expressed as a soluble protein which associated with the insoluble lipid pellet rather than residing within the inclusion bodies themselves. To try and dissociate NT-rfhSP-A from the insoluble material, various strategies were trialled. Low concentrations of urea have previously been used to prevent the interaction of contaminants with inclusion bodies (283). Sonication of insoluble *E. coli* lysate in 2 M urea was thus hypothesised to disrupt potential interactions of NT-rfhSP-A with insoluble material whilst not denaturing the protein. However, this did not increase the proportion of NT-rfhSP-A in the soluble fraction. Neither did sonication in the presence of a high concentration of detergent (1% triton X-100) at various pH values. Thus, NT-rfhSP-A was refolded using the traditional method used for purifying rfhSP-D. This method allowed the purification of NT-rfhSP-A. However, the majority (mean (SD) of 77 (± 7.4) %) of the protein precipitated (Table 5-1). NT-rfhSP-A was, however, successfully purified using nickel affinity chromatography; subsequent removal of NT allowed purification of rfhSP-A with a mean (SD) yield of 12.7 (± 4.4) mg per litre of *E. coli*. This was extremely pure protein which was achieved through optimisation of the nickel affinity method.

In an unpublished study, NT has previously been shown to allow the soluble expression of the SP-C33Leu peptide, an extremely hydrophobic peptide which normally aggregates when in hydrophilic solutions. NT was purified upon washing of inclusion bodies with 0.7 % Tween-20 (250). However, the widely used solubility tag thioredoxin resulted in

the formation of insoluble aggregates. The ability of NT to allow the soluble expression of SP-C33Leu but not rfhSP-A in this present study needs to be investigated. Difference in size of the proteins may be an important factor with rfhSP-A being 19 kDa; it is considerably larger than the 3.4 kDa size of SP-C33Leu. However, as discussed below, rfhSP-D was also successfully expressed as a soluble protein through the use of NT. The ability to express rfhSP-D as a soluble protein but not rfhSP-A could be due to the widely reported propensity of SP-A to associate with lipids (17). Further optimisation of expression conditions, or use of different *E. coli* for example shuffle cells, thought to aid protein folded during heterologous expression, could potentially overcome this issue. Alternatively, butanol extraction of inclusion bodies may be something that could be explored to purify rfhSP-A. However, problems may be encountered with the protein remaining highly aggregated despite the lipids being removed by the extraction process.

Comparatively, the NT^{dm} tag allowed the soluble expression of rfhSP-A which was successfully purified without the need for refolding. In addition to this being purified as a soluble protein a mean (SD) yield of 23.3 (± 5.4) mg per litre of bacteria was obtained which is nearly a 2 fold higher yield than obtained with wild type NT.

The ability of NT^{dm} to allow soluble expression of rfhSP-A which was not possible with the wild type NT is likely because of the Asp40Lys and Lys65Asp mutations. As previously shown (249) and discussed in Section 1.13.3.2, Asp40 and Lys65 have been shown to be important charged amino acids which are essential in the formation of stable dimers upon lowering of the pH through formation of inter-subunit salt-bridges, an essential mechanism allowing the formation of spider silk fibres. However, a single Asp40Asn mutation was shown to reduce the propensity for dimer formation. Moreover, a Asp40Lys mutation was shown to prevent the formation of dimers throughout the tested pH range (7.5-5.0). Through reversing these charges and preventing these charged interactions, the propensity for NT monomers to interact, form dimers and larger aggregates is likely decreased allowing an increased solubility upon expression in *E. coli*.

5.5.2 Purification of rfhSP-D

Using the traditional refolding method for purifying rfhSP-D, 85 % of the solubilised protein precipitated leading to only 16.5 mg of protein after refolding, a considerable proportion of which was contaminating *E. coli* proteins. Comparatively, use of NT as a solubility tag negated the need for refolding due to NT-rfhSP-D being isolated as a soluble protein after sonication in 2 M urea. A preliminary non-optimised purification led to a yield of 44 mg of fusion protein per litre of bacteria, equating to approximately 22 mg of rfhSP-D. During this purification, however, there was a substantial amount of NT-rfhSP-D in the flow through of the nickel column, due likely to the column being overloaded. Upon optimisation and potential use of a larger nickel column or loading of less protein, yields may be considerably higher and used for comparison with yields obtained with NT^{dm}.

Use of NT^{dm} further increased the solubility of rfhSP-D, and purification of NT^{dm}-rfhSP-D as a soluble protein required no urea and substantially less sonication than the NT-rfhSP-D fusion protein. This is likely due to the importance of the two mutated amino acids in formation of salt bridges and dimer formation as discussed above. Initial yields of purified NT^{dm}-rfhSP-D were extremely high with 276 mg of soluble protein/litre of bacteria, corresponding to approximately 138 mg of rfhSP-D. However, due to problems with non-specific cleavage by thrombin, NT^{dm}-rfhSP-D was recloned to replace the thrombin cleavage site with a HRV 3C protease site. Upon purification of this new construct, substantially lower yields were obtained with approximately 138 mg of NT-rfhSP-D being purified, with a subsequent purification of 46 (± 9.9) mg of rfhSP-D per litre of bacteria. Notably, contrasting to the refolded rfhSP-D, this was highly pure protein (compare Figure 5-11 with Figure 5-8). The decrease in yield upon recloning of NT^{dm}-rfhSP-D could potentially be due to the codon usage of the sequence coding for the HRV 3C cleavage site or difficulty in translating the amino acids affecting levels of protein expression. Further optimisation of expression may be required, the selection of specific bacterial colonies transformed with the same plasmid has been reported to significantly impact on expression levels. (284). Screening of colonies and selection of a high expressing colony could overcome the discrepancy in protein yield purified upon replacement of this cleavage site.

The ability to express rfhSP-D as a soluble protein negates the process of solubilisation with subsequent refolding with the associated protein loss due to precipitation. Importantly, the yields of rfhSP-D purified using the NT^{dm} solubility tag are considerably higher than those obtained through refolding and will enable the straightforward production of large quantities of rfhSP-D to further characterise the structure-function relationship of SP-D. This is a big step forward and obviates the need for protein refolding so that rfhSP-D now has improved potential for development into a scalable industrial production system. This may enhance its therapeutic potential for treatment of various lung disease. However, rfhSP-D produced through this new method remains to be fully characterised structurally and functionally and compared with the well characterised rfhSP-D protein produced through the traditional refolding protocol.

5.5.3 Summary

NT^{dm} is a useful solubility tags for the heterologous soluble expression of rfhSP-A and rfhSP-D. NT is also a useful tag for allowing expression of rfhSP-A and the soluble expression of rfhSP-D. Through using these tags, a rfhSP-A molecule containing the Gly Xaa Yaa of the collagen-like stalk, thought to be important for stabilising the trimeric molecule, has for the first time been generated. In addition, rfhSP-D has been produced and purified in a straightforward manner without the need for solubilisation and refolding. The utility of NT and NT^{dm} could now be further investigating with a wider panel of proteins to investigate their use as general solubility tags for different types of proteins as compared with other solubility tags, some of which have the capacity for self-cleavage without the need of an enzyme (reviewed in (285)). After purification of rfhSP-A and rfhSP-D produced using NT or NT^{dm}, these proteins were characterised structurally and functionally, as described in Chapters 6 and 7.

Chapter 6: Characterising Oligomeric Structures and Isolating Functional rfhSP-A and rfhSP-D

6.1 Introduction

The trimeric structure of rfhSP-D is widely thought to be essential for its function. In Chapters 5 and 6, an equivalent rfhSP-A molecule was cloned, expressed and purified using both NT and NT^{dm} as either insoluble or soluble proteins, respectively. This chapter set out to investigate the oligomeric structure of these rfhSP-A and rfhSP-D proteins. In addition, this chapter aimed to investigate the impact of different refolding techniques on the oligomeric structure of rfhSP-A. This chapter also set out to gain an insight into the secondary structure of trimeric rfhSP-A using circular dichroism as compared with rfhSP-D, a previously well characterised molecule both structurally and functionally. Indication of similar secondary structures by circular dichroism may suggest that the rfhSP-A molecule is likely to be folded correctly and may exhibit functional lectin activity. For initial testing of whether rfhSP-A had functional lectin activity and to allow isolation of functional rfhSP-A, this chapter set out to apply purified rfhSP-A to various carbohydrate affinity columns.

6.1.1 Aims

This chapter aimed to characterise the oligomeric structures of rfhSP-A and rfhSP-D produced and purified using NT and NT^{dm} in Chapter 5. An additional aim was to characterise their ability to bind different carbohydrate columns and to use this as means for isolating functional carbohydrate binding rfhSP-A and rfhSP-D (Aims 4 and 5 - Section 1.14). This would allow the subsequent characterisation of the capacity of rfhSP-A to bind various natural ligands and the importance of the SP-A and SP-D N-terminal domain in interacting with RSV (Chapter 7).

6.2 Methods

6.2.1 Native-PAGE

To determine molecular weights, proteins were analysed by native-PAGE using 4-16 % NativePAGE gels (Invitrogen) using the NativePAGE Running Buffer Kit (Invitrogen). NativePAGE was undertaken with 5 µg of each protein, according to manufacturer's instructions. Electrophoresis was undertaken at 150 volts until good separation was obtained (approximately 90 min). 7 µl of NativeMark Unstained Protein Standard (Invitrogen) was also analysed for determination of approximate molecular weights.

6.2.2 Gel Filtration

Gel filtration was performed as described in Section 2.2.

6.2.3 Optimisation of NT-rfhSP-A Refolding

The optimised refold protocol given in Section 5.2.4 was used after iteratively altering individual refold conditions for purification of NT-rfhSP-A. These included: refolding in either a measuring cylinder or bucket; at a protein concentration of 2 mg/ml, 3 mg/ml or 4 mg/ml; at 4 °C or room temperature or with dilution of the urea concentration at the standard rate as above or more slowly. The slower removal of urea involved dialysis in solubilisation buffer containing 4 M urea with subsequent dialysis in solubilisation buffer containing 3 M urea, 2 M urea, 1.5 M urea, 1 M urea and 0.5 M urea. The use of a "redox system" was also trialled where solubilisation buffer was used during dialysis which contained 5 mM reduced glutathione, 0.5 mM oxidised glutathione, and 400 mM Arginine with the corresponding concentration of urea. Upon completion of refolding, rfhSP-A was dialysed into TBS.

6.2.4 Circular Dichroism

Trimeric rfhSP-A and rfhSP-D produced by refolding were dialysed into 50 mM potassium phosphate (pH 7.4) (without calcium). 200 µl of diluted protein was aliquoted into a quartz cuvette with a 1 mm path length. Circular dichroism spectra were measured for rfhSP-A and rfhSP-D both at room temperature and at 37 °C using a Jasco720

spectrophotometer machine (Jasco, US). 10 scans were taken between 190-260 nm with a 1 nm step resolution at a rate of 100 nm/min. Spectra for the blank of 50 mM potassium phosphate buffer, pH 7.4 were subtracted from the spectra of samples using Jasco Spectra Manager software. No software for smoothing of spectra was used.

6.2.5 Affinity Chromatography

6.2.5.1 *Preparation of Affinity Resin*

Mannose-sepharose and ManNAc-sepharose resins were prepared by crosslinking of mannose or ManNAc to Sepharose CL-4B (GE Healthcare). Sepharose CL-4B was first activated by incubation with mixing with 0.5 M Na_2CO_3, pH 11 and divinylsulfone in a 5:5:1 volume ratio at room temperature for 90 mins. Activated beads were washed 3 times in ddH_2O with 3 subsequent washes in 0.5 M Na_2CO_3, pH 11 and incubated with either 10 % (w/v) ManNAc or mannose in 0.5 M Na_2CO_3, pH 11 overnight with mixing. Carbohydrate coupled resins were washed two times in ddH_2O and once in 100 mM ethanolamine pH 9. Excess vinyl reactive groups were blocked by incubation in 100 mM ethanolamine pH 9 for two hours at room temperature.

6.2.5.2 *Affinity Chromatography*

Mannose-sepharose or ManNAc-sepharose resins prepared by divinylsulfone crosslinking or purchased mannan-sepharose or maltose-sepharose resins were packed into empty XK16 columns (GE healthcare) and equilibrated into TBS with 5 mM $CaCl_2$ pH 7.4. During affinity chromatography 10-20 ml columns were used. Protein in TBS with 5 mM $CaCl_2$, pH 7.4 was applied to the column, after which, the column was washed with > 1.5 column volumes of TBS with 5 mM $CaCl_2$, pH 7.4. The column was then washed with a "high salt wash" with > 1.5 column volume of 20 mM Tris 1 M NaCl with 5 mM $CaCl_2$ pH 7.4, the column was subsequently re-equilibrated in TBS with 5 mM $CaCl_2$, pH 7.4. The bound protein was eluted in TBS with 5 mM EDTA pH7.4. Elution from the column was at a flow rate of 0.5 ml/min. Upon elution, fractions were taken and stored at -20 °C until use. The elution was controlled using an ÄKTA purifier (UV900 monitor) with Unicorn (version 4.10) software and absorbance at λ = 280 nm was recorded. Columns were stored in 20 % ethanol (v/v) or according to manufacturer's instructions.

6.3 Results

6.3.1 Characterising the Oligomeric Structure of Recombinant Collectins

6.3.1.1 *Oligomeric Structure of NT-rfhSP-A and NT-rfhSP-D*

To characterise the oligomeric structure prior to removal of the NT tag, NT-rfhSP-A and NT-rfhSP-D were analysed by gel filtration (Figure 6-1A). NT-rfhSP-A was eluted with a predominant peak at 15.3 ml, an approximate elution volume that would be expected of a 34.5 kDa monomer. Secondary peaks corresponded to multimeric NT-rfhSP-A, potentially dimeric and tetrameric (69 kDa and 138 kDa, respectively). Similarly, upon analysis by native polyacrylamide gel electrophoresis (native-PAGE), a smear of bands appeared which corresponded to protein predominantly approximately 30 kDa to approximately 100 kDa, with a prominent band at approximately 30 kDa which is likely monomeric protein (Figure 6-1B), concurring with the gel filtration analysis.

Comparatively, NT-rfhSP-D eluted from the gel filtration column with peaks at 14.1 ml and 12.2 ml. The 14.1 ml peak could correspond to either monomeric or dimeric NT-rfhSP-D (expected molecular weights of 34.5 kDa or 69 kDa, respectively) (Figure 6-1A). However, the larger of the two peaks at 12.2 ml likely represents elution of multimeric NT-rfhSP-D (possibly a 138 kDa tetramer or larger). Analysis of NT-rfhSP-D by native-PAGE indicated that a majority of the protein was of a larger molecular weight than the 66 kDa marker with bands at approximately 100 kDa and approximately 200 kDa (Figure 6-1B). There was, however, a band at approximately 30 kDa which is likely monomeric NT-rfhSP-D, perhaps indicating that the secondary peak seen by gel filtration (14.1 ml - Figure 6-1B) is monomeric NT-rfhSP-D.

A

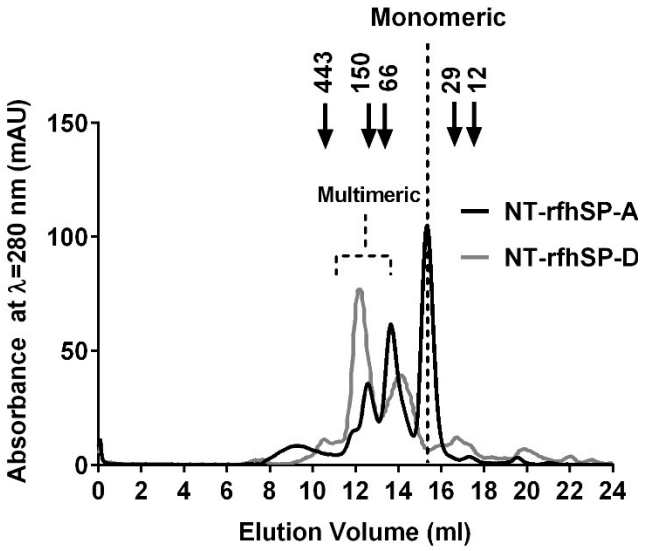

B

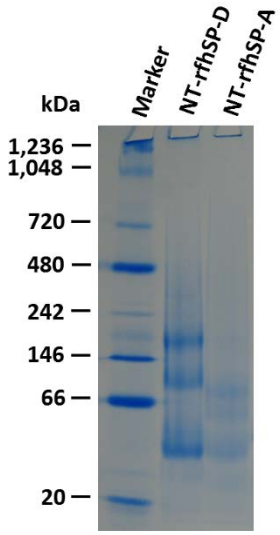

Figure 6-1: Oligomeric structure of NT-rfhSP-A and NT-rfhSP-D. *The oligomeric structure of NT-rfhSP-A and NT-rfhSP-D prior to removal of NT was characterised by gel filtration (**A**) and native-PAGE analysis (**B**). Gel filtration was undertaken using a 24 ml superdex 200 column. Indicated are the milli absorbance units at λ = 280 nm upon elution of proteins from the column. Elution volumes of NT-rfhSP-A and NT-rfhSP-D were compared with various protein standards including 12.4 kDa cytochrome c, 29 kDa carbonic anhydrase, 66 kDa BSA 150 kDa alcohol dehydrogenase and 443 kDa apoferritin. Indicated are the peaks corresponding to monomeric and multimeric protein.*

6.3.1.2 *Impact of Refold Protocol on Oligomeric Structure and Yields of rfhSP-A Produced using NT*

It was assumed that in order to form a functional rfhSP-A molecule, the trimeric structure found in native SP-A was required. To determine as to whether, upon removal of the NT domain, the CRD, neck and 8 x Gly Xaa Yaa of SP-A was sufficient to allow trimerisation of SP-A, rfhSP-A was analysed by native-PAGE and gel filtration. Upon initial analysis of the molecular weight of rfhSP-A by native-Page, due to the smear obtained on the gel, it was inconclusive as to whether rfhSP-A was trimeric or was not (Figure 6-2H). However, the most prominent band was closer to the 66 kDa marker than the 20 kDa marker; with the expected molecular weight of a trimeric rfhSP-A molecule being 56.4

kDa. In addition, the majority of the rfhSP-A protein appeared to be of a larger molecular weight than the rfhSP-D analysed: rfhSP-D is a structurally well characterised trimeric molecule with a similar molecular weight.

Gel filtration, however, confirmed the CRD, neck and 8 x Gly Xaa Yaa of rfhSP-A to be sufficient to allow the formation of stable trimeric rfhSP-A molecules; rfhSP-A remained trimeric upon freeze/thawing (Figure 6-2A). The proportion of trimeric rfhSP-A molecules, however, was dependent on specific parameters during the refolding protocol. The proportion of trimers ranged from 18-81 % of the total rfhSP-A protein, depending on the protein batch. The refold protocol was, therefore, optimised by comparing two or more refold protocols side by side to determine which protocol allowed the production of the highest proportion of trimeric molecules. Chromatographs of gel filtration for each refolding variable are given in Figure 6-2. A summary of conditions and percentage of total rfhSP-A which is trimeric is given in Table 6-1.

One key variable which impacted on the proportion of rfhSP-A trimers was the vessel used for the dialysis during the refold. The use of a bucket allowed efficient mixing of glycerol. Contrastingly, use of a measuring cylinder did not allow efficient mixing of the glycerol with glycerol settling at the bottom. This was found to be an important factor impacting on the ability of rfhSP-A to trimerise with more than half of the rfhSP-A refolding in a bucket being trimeric after removal of NT (57 %), while only a proportion of the rfhSP-A refolded in a measuring cylinder was trimeric (18 %). The majority of the protein refolded in a measuring cylinder was dimeric (45 %) (Figure 6-2B). Another variable impacting on the oligomeric structure of rfhSP-A was the protein concentration of NT-rfhSP-A during the refold. Too low a concentration (refolded at 2 mg/ml) resulted in only 19 % of rfhSP-A being trimeric (with 46 % being dimeric) (Figure 6-2C). Comparatively, higher protein concentrations during the refold resulted in a larger proportion of rfhSP-A being trimeric with 60 % and 56 % of rfhSP-A being trimeric through refolding at 3 mg/ml and 4 mg/ml, respectively (Figure 6-2D). Alteration of the temperature during the refold also impacted on the proportion of trimeric molecules to some degree. Refolding at 4 °C gave a slightly higher percentage of trimeric molecules (81 %) compared with refolding at room temperature (72 %) (Figure 6-2E). Other variables were compared but did not appear to impact on rfhSP-A oligomeric structure including a slower reduction of urea concentration and use of a glutathione redox system (Figure 6-2F and G, respectively).

Alteration of some parameters during the NT-rfhSP-A refold did impact on levels of protein precipitation and consequentially the yield of rfhSP-A, but only marginally. The major parameter which increased levels of protein precipitation during refolding was the use of a measuring cylinder where 91 % of the protein precipitated upon refolding in a measuring cylinder, as opposed to a bucket where only 79 % of protein precipitated. Interestingly, use of the glutathione redox protocol impacted minimally on the level of protein lost due to precipitation. However, upon use of this redox system, white precipitate appeared at a considerably later stage of the refold protocol and precipitate had a different consistency (Figure 6-3). Protein yields and levels of loss at each purification stage for each refold protocol are summarised in (Table 6-1).

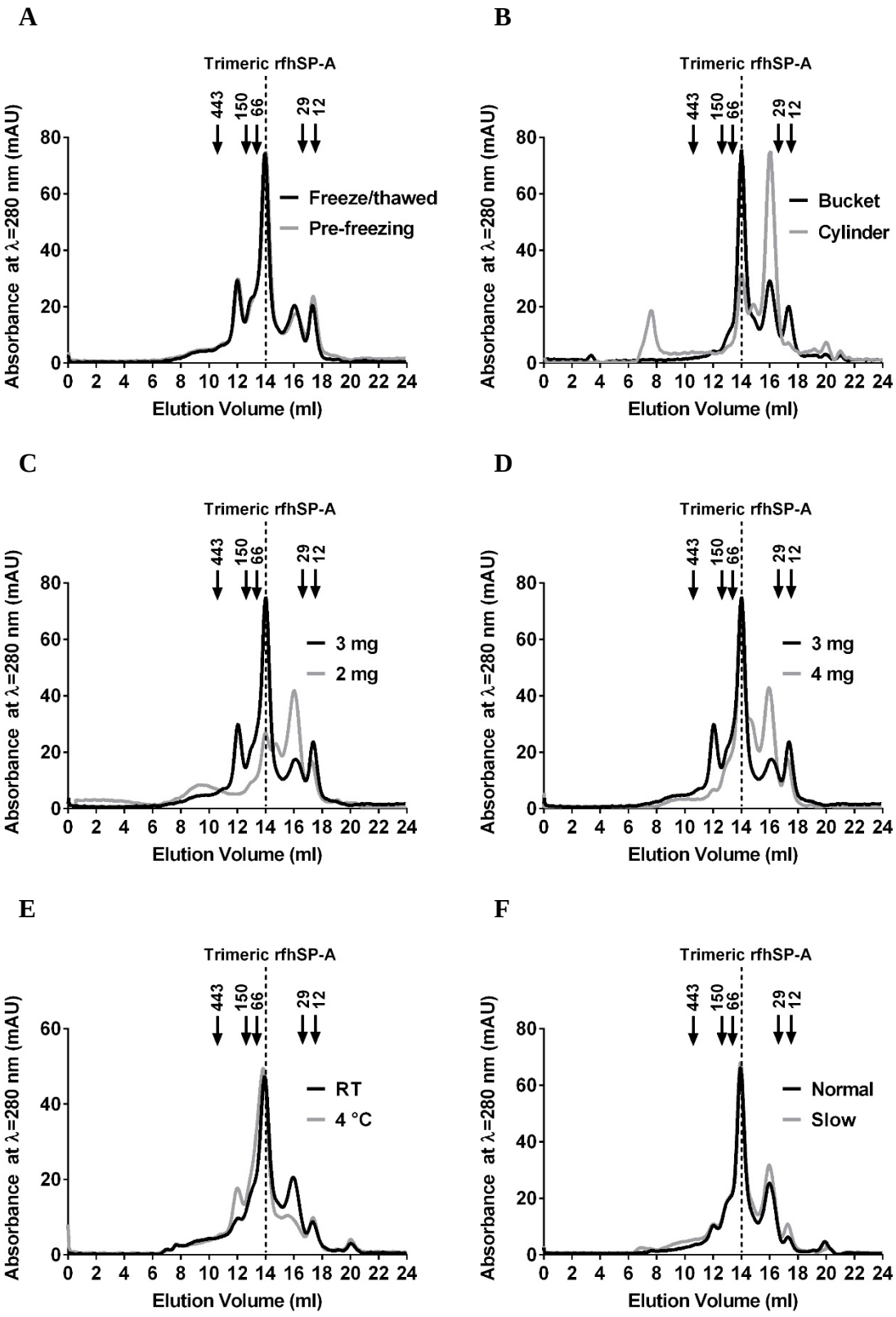
A
Trimeric rfhSP-A
443
150
66
29
12
Absorbance at λ=280 nm (mAU)
Elution Volume (ml)
Freeze/thawed
Pre-freezing
B
Bucket
Cylinder
C
3 mg
2 mg
D
3 mg
4 mg
E
RT
4 °C
F
Normal
Slow

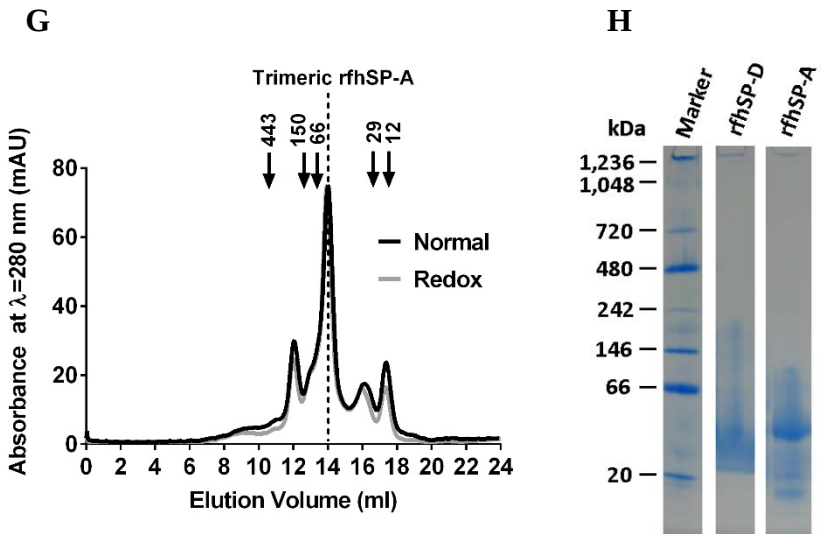

Figure 6-2: Oligomeric structure of rfhSP-A and effect of refolding. *The oligomeric structure of rfhSP-A after different refold protocols were analysed by gel filtration using a 24 ml superdex 200 column (**A**-**G**). Shown are the milli absorbance units at λ = 280 nm upon elution of proteins from the column. Elution volumes of rfhSP-A was compared with various protein standards including 12.4 kDa cytochrome c, 29 kDa carbonic anhydrase, 66 kDa BSA, 150 kDa alcohol dehydrogenase and 443 kDa apoferritin. Indicated are the peaks corresponding to trimeric rfhSP-A. Purified rfhSP-A produced using the initial refolding protocol was compared before and after freeze/thawing to determine stability (**A**). Two different refold protocols were undertaken concurrently to compare the impact of each refolding variable. The impact of the following refold parameters were compared: impact of refolding in a measuring cylinder or bucket (**B**); impact of refolding at a protein concentration of 2 mg/ml, 3 mg/ml or 4 mg/ml (**C** and **D**); impact of refolding at 4 °C or room temperature (RT) (**E**); impact of diluting urea concentration at standard rate (Normal) or more slowly (Slow) (**F**) or impact of using a refold protocol with oxidized and reduced glutathione (Redox) or standard protocol (Normal) (**G**). Protein purified at room temperature (seen in **E**) was also analysed by native-PAGE (**H**).*

Refold Variable	Percentage Trimers out of Total Protein (%)
Bucket	57
Cylinder	18
2 mg	19
4 mg	56
3 mg	60
Normal	51
Slow	55
Normal	60
Redox	61
4 °C	81
RT	72

Table 6-1: Summary of impact of refolding method on proportion of trimeric rfhSP-A. *Summarised above is the percentage of trimeric rfhSP-A produced after each refolding protocol. Percentage trimers were calculated using the peak integration within the Unicorn (v4.10) software upon analysis of the chromatographs seen in Figure 6-2. Refolding protocols included: refolding in a measuring cylinder or bucket; refolding at a protein concentration of 2 mg/ml, 3 mg/ml or 4 mg/ml; refolding at 4 °C or room temperature (RT); refolding through dilution of urea concentration at standard rate (Normal) or more slowly (Slow); refolding using the normal refold protocol (Normal) or using oxidized and reduced glutathione (Redox).*

Refold Variable	Total Amount (mg)				Percentage Yield at Each Step		
	Before refold	Post refold	Post nickel	rfhSP-A	Refold	Nickel	Cleavage
Bucket	300	62	35	16	79	44	44.8
Cylinder	300	29	16	5	91	44	32.6
2 mg	186	35	27	13	81	22	46.0
4 mg	292	44	29	15	85	35	50.5
3 mg	165	34	22	16	79	36	72.0
Normal	165	34	22	16	79	36	72.0
Redox	165	41	26	19	75	38	75.6
Normal	300	90	22	7	70	76	33.5
Slow	300	99	26	9	67	74	35.3
4 °C	200	56	15	8	72	73	50.0
RT	200	66	25	13	67	61	50.0

Table 6-2: Comparison of yields during refolding of NT-rfhSP-A under different conditions. *The total amount of rfhSP-A obtained after each stage of purification with each refold protocol was quantified by measuring OD at λ = 280 nm and compared. The amount of protein obtained from 1 l of bacterial culture after each purification step is given including after the following steps: solubilisation of inclusion bodies with 8 M (before refold); refolding by dilution of urea (Post refold); purification of NT-rfhSP-A using nickel affinity chromatography (Post nickel) and cleavage of NT and purification of rfhSP-A (rfhSP-A). The percentage of protein lost after each purification stages was then calculated including the following purification steps: solubilisation and refolding with 8 M urea (Refold), the nickel affinity step (Nickel) and the cleavage and purification of rfhSP-A step (Cleavage). The impact of the following refold parameters on protein yields was compared including: refolding in a measuring cylinder or bucket; refolding at protein concentrations of 2 mg/ml, 3 mg/ml or 4 mg/ml; refolding at 4 °C or room temperature; refolding with dilution of urea at the standard rate (Normal) or more slowly (Slow) or using oxidized and reduced glutathione refold system (Redox) or standard protocol (Normal).*

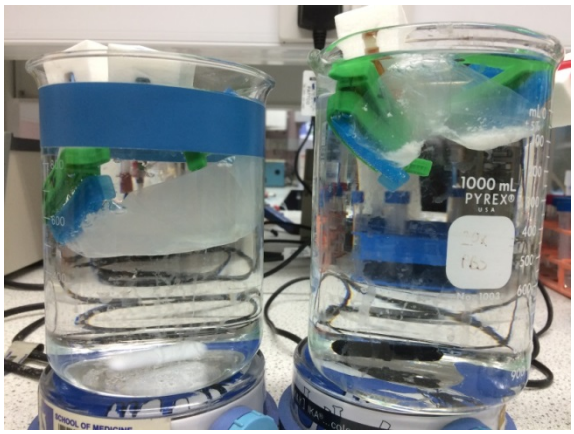

Figure 6-3: Impact of redox glutathione on precipitation. *Shown is an image of the protein precipitation after completion of refolding and dialysis into TBS without urea. The precipitation was compared between the normal refold protocol (left) and that using the oxidized and reduced glutathione refold system (right).*

6.3.1.3 *Oligomeric Structure of rfhSP-A Produced using NT^{dm}*

The oligomeric structure of rfhSP-A produced as a soluble protein using NT^{dm}, was also analysed. A considerably smaller proportion of rfhSP-A produced using NT^{dm}, only a mean (SD) of 24 (± 4.3) %, n = 4, was trimeric as compared with the 81 % of rfhSP-A which was trimeric upon production using NT with the optimised refold protocol (Figure 6-4). To try and increase the proportion of rfhSP-A which was trimeric after removal of NT^{dm}, expression was trialled in shuffle *E. coli* cells which are optimised for disulphide bond formation. However, this did not improve the proportion of protein which was trimeric upon removal of NT^{dm} (data not shown). A large proportion of rfhSP-A produced as a soluble protein using NT^{dm} appeared to be of higher molecular weight than trimeric rfhSP-A and eluted earlier than the 443 kDa standard. In addition, a proportion of rfhSP-A produced using NT^{dm} was also dimeric.

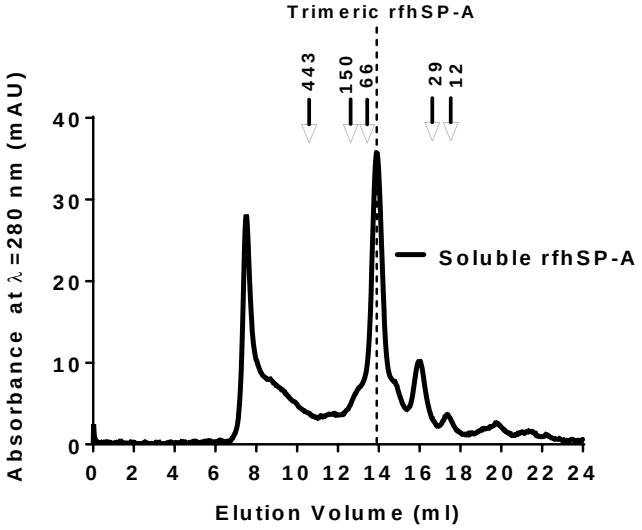

Figure 6-4: Oligomeric structure of rfhSP-A expressed as a soluble protein. *The oligomeric structure of rfhSP-A expressed as a soluble protein using NT^{dm}-rfhSP-A was analysed by gel filtration using a 24 ml superdex 200 column. Shown are the milli absorbance units at λ = 280 nm upon elution of protein from the column. Elution volumes of rfhSP-A was compared with various protein standards including 12.4 kDa cytochrome c, 29 kDa carbonic anhydrase, 66 kDa BSA, 150 kDa alcohol dehydrogenase and 443 kDa apoferritin. Indicated is the peak corresponding to trimeric rfhSP-A.*

6.3.1.4 *Oligomeric Structure of rfhSP-D Produced through Refolding*

Unlike rfhSP-A and rfhSP-D produced using NT and NT^{dm}, rfhSP-D produced through the traditional refolding protocol did not contain a His$_6$-tag and could not be further purified by nickel affinity chromatography prior to selecting for the functional carbohydrate binding protein. Due to the rfhSP-D containing numerous bacterial contaminants prior to this stage, the oligomeric structure of rfhSP-D could not be assessed until further purification was undertaken. The oligomeric structure of carbohydrate binding rfhSP-D was assessed in Section 6.3.4.1.

6.3.1.5 *Oligomeric Structure of rfhSP-D Produced using NT^{dm}*

The ability of rfhSP-D purified as a highly soluble protein using NT^{dm} to form trimeric molecules was also investigated. A mean (± SD) of 88.5 (± 4.0, n = 4) % of the rfhSP-D produced as a soluble protein using NT^{dm} was trimeric. This was compared with rfhSP-D previously purified using the traditional refolding method and affinity chromatography where 97 % of the rfhSP-D was trimeric (Figure 6-4).

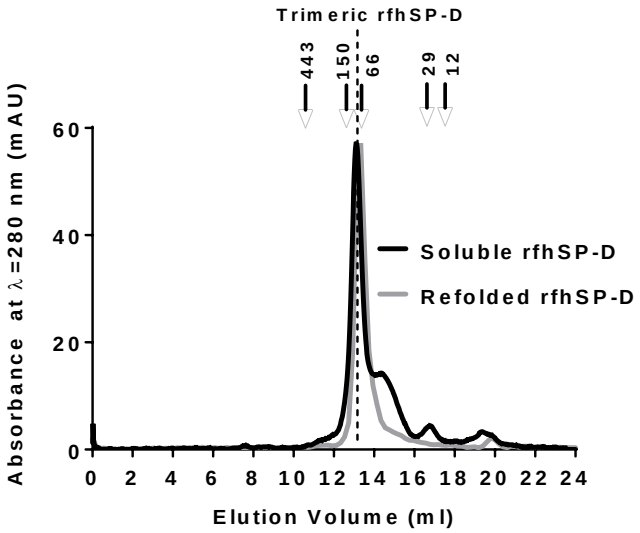

Figure 6-5: Trimeric structure of rfhSP-D produced using NT^{dm}. *Representative chromatographs showing the oligomeric structure of rfhSP-D expressed as a soluble protein using NT^{dm}-rfhSP-D compared with refolded rfhSP-D as analysed by gel filtration using a 24 ml superdex 200 column. Shown are the milli absorbance units at λ = 280 nm upon elution of protein from the column. Elution volumes of rfhSP-D were compared with various protein standards including 12.4 kDa cytochrome c, 29 kDa carbonic anhydrase, 66 kDa BSA, 150 kDa alcohol dehydrogenase and 443 kDa apoferritin. Indicated is the peak corresponding to trimeric rfhSP-D.*

6.3.2 Characterising the Secondary Structure of rfhSP-A by Circular Dichroism

To gain an insight into the secondary structure of trimeric rfhSP-A produced using NT and its similarity to rfhSP-D, trimeric rfhSP-A was purified by gel filtration and assessed by circular dichroism. rfhSP-A and rfhSP-D had similar circular dichroism spectra, both appearing to be dominated by α-helical structures (Figure 6-6A). This was seen by a high maximum:minimum molar ellipicity ratio of 1:1.4 and 1:1.2 for rfhSP-A and rfhSP-D, respectively, with α-helical structures having an approximately 1:2 ratio. Positive peaks for rfhSP-A and rfhSP-D occurred at 191 nm and 192 nm as expected for a predominantly α-helical structure. A series of troughs were also seen for the circular dichroism spectra of rfhSP-A at 207 and 226 nm which are expected for α-helical structures. An additional trough at 217 nm was seen in the circular dichroism spectra of rfhSP-A which likely corresponds to the presence of β-sheets or β-turns. The circular dichroism spectra for rfhSP-A was similar as that obtained upon analysis of rfhSP-D. Interestingly, there was a slight general shift of the rfhSP-A spectra curve towards the higher wavelength compared with the spectra obtained for rfhSP-D. This can be seen by the shift in the peaks and the points in which the curve crosses the axis (200 nm for rfhSP-A compared with 198 nm for rfhSP-D). This could potentially be due to an increased β-sheet or β-turn content or random coil.

Upon heating of rfhSP-A and rfhSP-D in phosphate buffer (no calcium) to 37 °C, the secondary structures changed considerably, potentially due to refolding of the secondary structures and movement towards a more disorded folding of the protein (Figure 6-6B and C). However, rfhSP-A and rfhSP-D secondary structures at room temperature appeared comparatively similar, thus the CRD of rfhSP-A may be folded correctly and could elicit functional collectin activity.

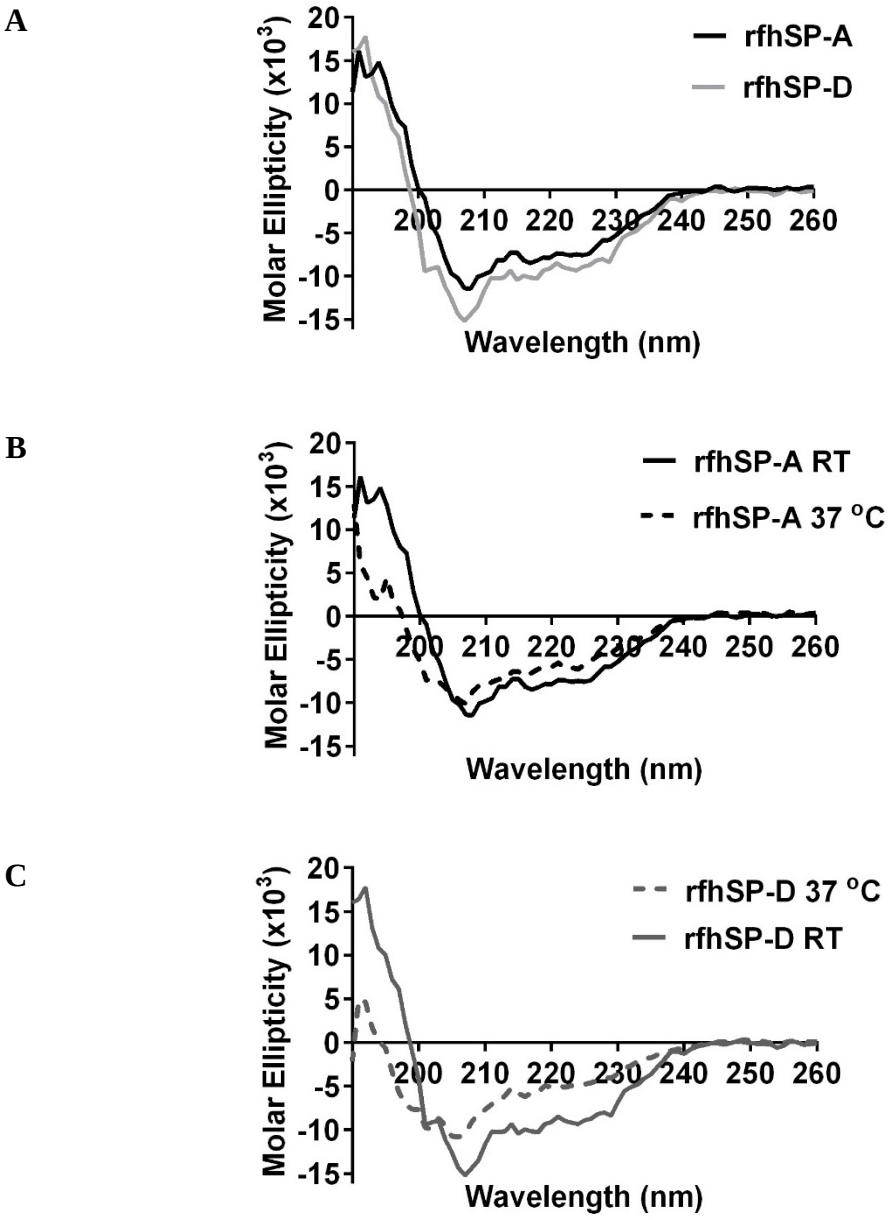

Figure 6-6: Analysis of rfhSP-A and rfhSP-D protein structure by circular dichroism at room temperature and 37 °C. *Trimeric rfhSP-A and rfhSP-D produced by refolding in 50 mM potassium phosphate (pH 7.4) were analysed by circular dichroism using a Jasco 720 spectrophotometer. Indicated is the molar Ellipticity (x10^3) calculated from the accumulated data from 10 scans undertaken with a 1 nm step resolution at 100 nm/min from 190-260 nm with the circular dichroism spectrum for 50 mM potassium phosphate buffer (pH 7.4) subtracted. Circular dichroism spectra were compared between rfhSP-A and rfhSP-D at room temperature (**A**). In addition, the impact of heating to 37 °C on the circular dichroism spectra was compared for rfhSP-A (**B**) and rfhSP-D (**C**).*

6.3.3 Purification of Functional Carbohydrate Binding rfhSP-A

The capacity of rfhSP-A composed of the CRD, neck and 8 x Gly Xaa Yaa to bind to known ligands of nhSP-A was investigated. To do this, carbohydrate affinity chromatography was used. This was also used as an additional step to purify only the functional carbohydrate binding rfhSP-A.

6.3.3.1 *Purification of rfhSP-A Produced using NT and Refolding*

A proportion of rfhSP-A purified through refolding was functional and bound to carbohydrate affinity chromatography columns in a calcium-dependent manner (Figure 6-7). However, the amount of functional carbohydrate binding rfhSP-A varied between different protein purification batches. Mannan affinity chromatography was the technique predominantly used due to the finding that rfhSP-A binds to mannan in solid-phase binding assays (Section 7.3.1). The proportion of rfhSP-A which bound to a mannan column and was purified by affinity chromatography ranged from 12 % (Figure 6-7A) to none of the total purified protein (Figure 6-7B). Importantly, a trimeric structure was not sufficient to allow purification by carbohydrate affinity chromatography. Indeed, the batch of protein purified at 4 °C yielded 81 % of trimeric protein. However, none of this protein bound to the mannan affinity column (Figure 6-7B).

Although a mannan affinity column was initially used to purify functional rfhSP-A, maltose affinity chromatography was also used but did not improve protein yields (Figure 6-7C). Mannose and ManNAc affinity columns were also trialled. However, no rfhSP-A was purified using these columns (Figure 6-7D and E, respectively). Protein purified by carbohydrate affinity chromatography was pooled, concentrated and analysed by gel filtration. 94 % of the rfhSP-A purified by affinity chromatography was trimeric (Figure 6-8A), highlighting the requirement of a trimeric structure to bind to a carbohydrate affinity column. The pooled functional protein was confirmed to be pure from contaminating proteins by SDS-PAGE and confirmed to be immunoreactive to a monoclonal α-nhSP-A antibody by Western blot analysis (Figure 6-8B and C, respectively).

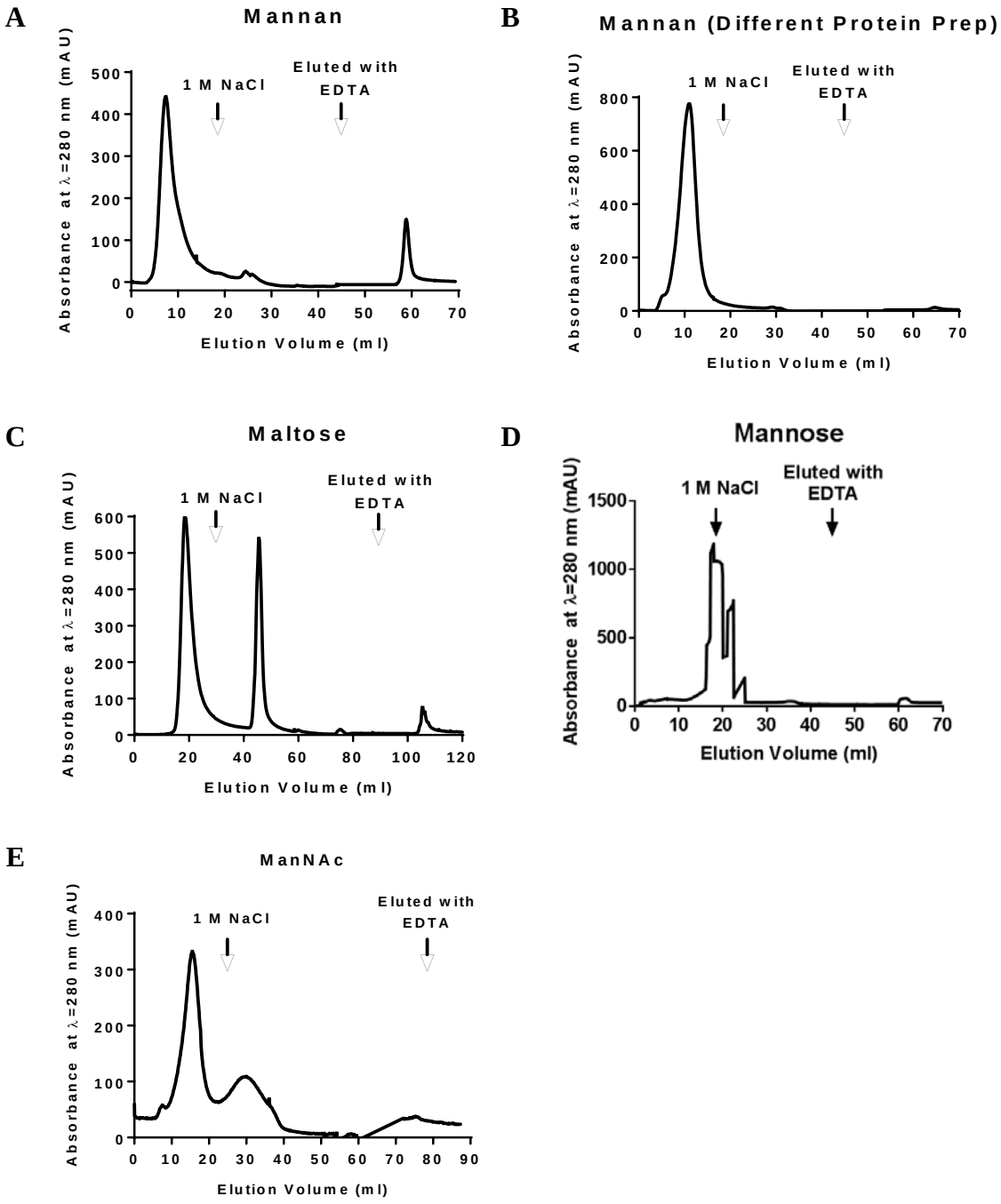

Figure 6-7: Purification of functional carbohydrate binding rfhSP-A using different carbohydrate affinity columns. *The capacity of rfhSP-A to bind to different approximately 15 ml carbohydrate affinity columns was tested. rfhSP-A was injected onto mannan (**A** and **B**, different protein preparations), maltose (**C**), mannose (**D**) and ManNAc (**E**) columns equilibrated in TBS in 5 mM $CaCl_2$. Columns were washed in 20 mM Tris, 1 M NaCl with 5 mM $CaCl_2$ and subsequently equilibrated in TBS with 5 mM $CaCl_2$. Functional carbohydrate bound rfhSP-A was eluted in TBS with 5 mM EDTA. Shown are the milli absorbance units at λ = 280 nm upon elution of protein from the column.*

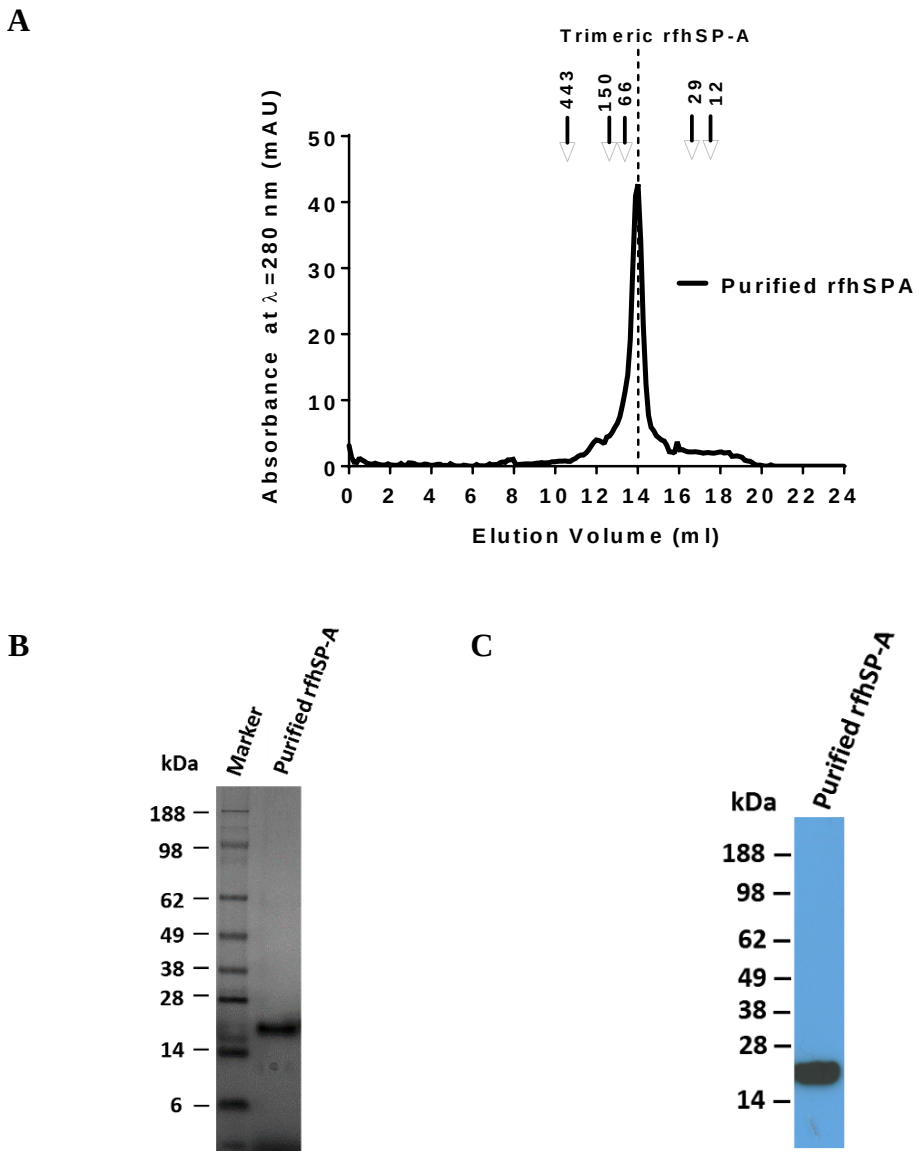

Figure 6-8: Characterising the purity of rfhSP-A. *Pooled carbohydrate affinity purified rfhSP-A was concentrated and its oligomeric structure analysed by gel filtration using a 24 ml superdex column (**A**). Shown are the milli absorbance units at λ = 280 nm upon elution of protein from the column. The elution volume of rfhSP-A was compared with various protein standards including 12.4 kDa cytochrome c, 29 kDa carbonic anhydrase, 66 kDa BSA, 150 kDa alcohol dehydrogenase and 443 kDa apoferritin. Indicated is the peak corresponding to trimeric rfhSP-A. The purity of carbohydrate affinity purified rfhSP-A was assessed by SDS-PAGE (**B**) and its identity confirmed by Western blot analysis using an α-nhSP-A antibody (**C**).*

6.3.3.2 *Purification of rfhSP-A produced as a Soluble Protein using NT^{dm}*

rfhSP-A, produced using NT^{dm} without the need for refolding, did not bind to either Mannan or ManNAc carbohydrate affinity columns (Figure 6-9). No functional protein produced by this method could therefore be purified.

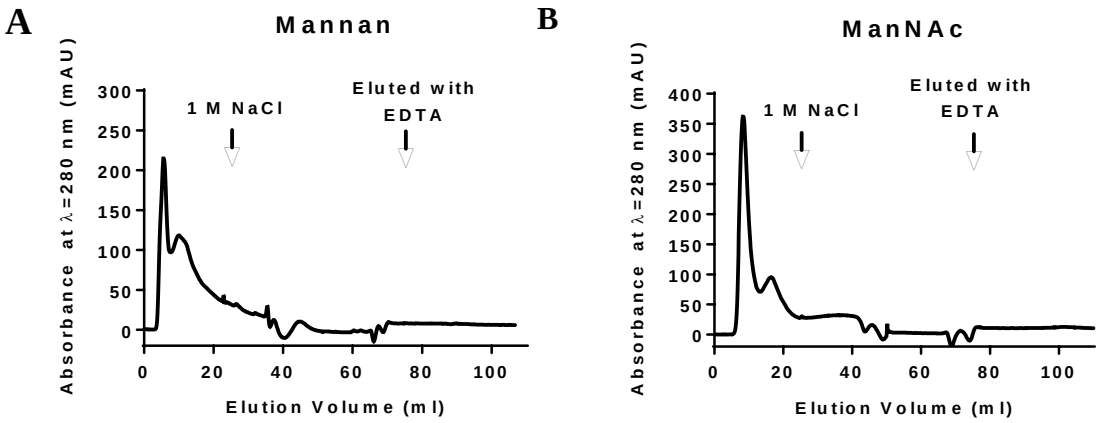

Figure 6-9: Purification of rfhSP-A produced as a soluble protein using NT^{dm} using carbohydrate affinity chromatography *The capacity of rfhSP-A to bind to different approximately 15 ml carbohydrate affinity columns was tested. rfhSP-A was injected onto mannan (**A**) and ManNAc (**B**) columns equilibrated in TBS in 5 mM $CaCl_2$, the columns were washed in 20 mM Tris, 1 M NaCl with 5 mM $CaCl_2$ and subsequently equilibrated in TBS with 5 mM $CaCl_2$. Functional rfhSP-A bound to the carbohydrate column was eluted in TBS with 5 mM EDTA. Shown are the milli absorbance units at λ = 280 nm upon elution of protein from the column.*

6.3.4 Purification of Functional Carbohydrate Binding rfhSP-D

The capacity of rfhSP-D to bind to carbohydrate affinity columns was also tested and used as a means to isolate functional protein. This was undertaken for rfhSP-D purified by both the traditional refolding method and as a soluble protein through the use of NT^{dm}

6.3.4.1 *Purification of rfhSP-D by Refolding*

rfhSP-D produced through the traditional refolding protocol was not first purified by nickel affinity chromatography after refolding due to the absence of a His_6-tag. Therefore, ManNAc-affinity chromatography was used as the subsequent purification step after refolding from inclusion bodies. Purification and analysis of rfhSP-D produced as an insoluble protein was undertaken at University of Southampton by Alastair Watson and Henry Hole. 31 % of the refolded rfhSP-D protein bound upon application to the ManNAc column and was eluted specifically in the presence of EDTA (Figure 6-10A). Importantly, a large proportion of the protein which did not bind was likely contamination of other *E. coli* proteins. To further purify just the trimeric rfhSP-D, the ManNAc binding rfhSP-D was applied to a preparative gel filtration column; fractions containing trimeric rfhSP-D were collected, pooled and concentrated (Figure 6-10B). To confirm the oligomeric structure and purity of the purified rfhSP-D, a sample of trimeric rfhSP-D was analysed using an analytical gel filtration column where 97 % of the analysed protein was found to be trimeric (Figure 6-10C). The purity of the functional trimeric rfhSP-D was analysed by SDS-PAGE. rfhSP-D was found to be pure after affinity purification with very low levels of detectable contaminating proteins and no detectable levels of contaminants after gel filtration (Figure 6-10D). Purified rfhSP-D was confirmed to be immunoreactive to a polyclonal α-rfhSP-D antibody by Western blot analysis (Figure 6-10E). Purification of functional trimeric rfhSP-D through refolding yielded 3.3 mg from 16.5 mg of soluble protein per litre of bacteria.

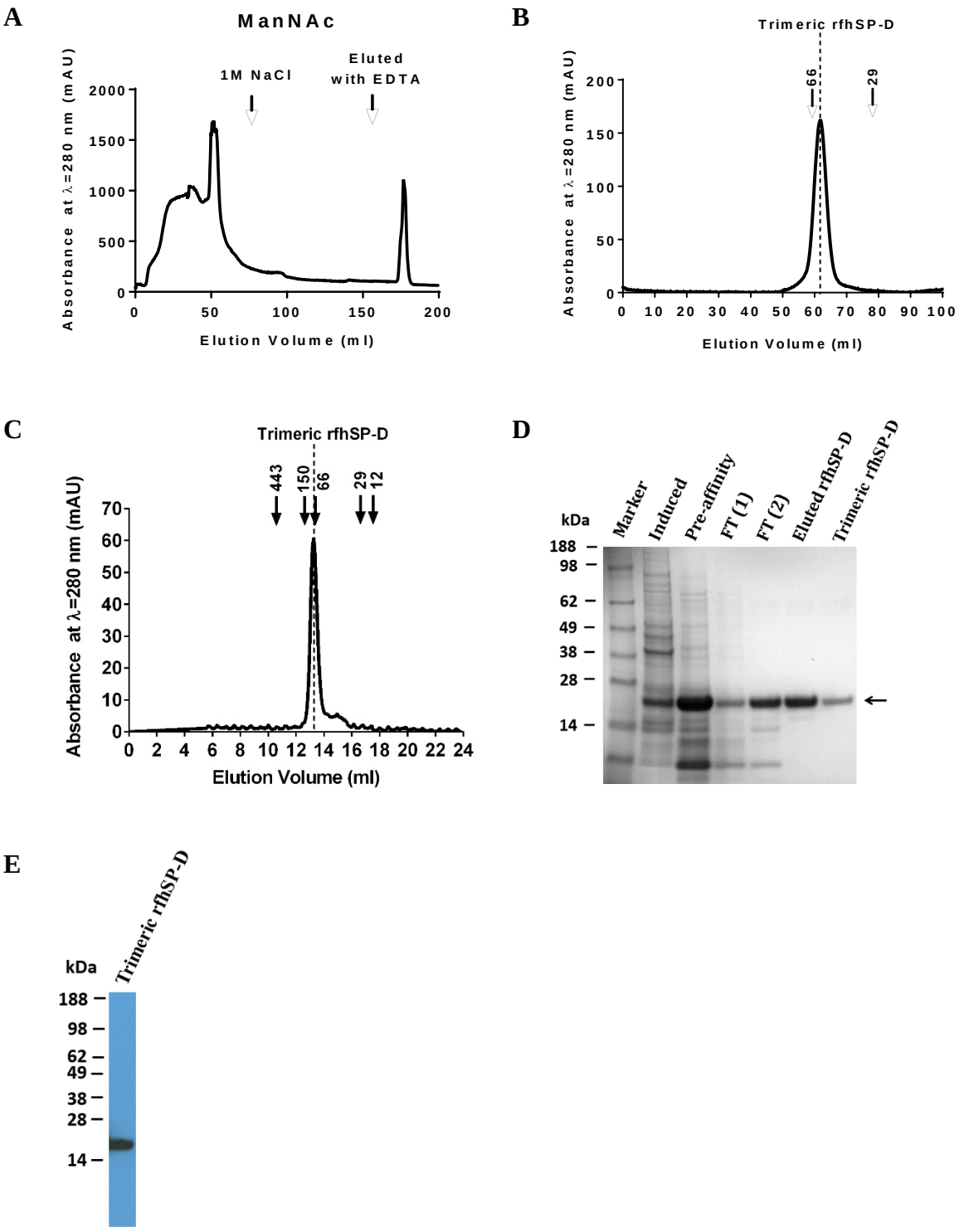

Figure 6-10: Purification of functional trimeric rfhSP-D expressed as an insoluble protein. *rfhSP-D purified from inclusion bodies was applied to an approximately 15 ml ManNAc affinity column equilibrated in TBS in 5 mM $CaCl_2$ using a 50 ml super loop (**A**). The columns was washed in 20 mM Tris, 1 M NaCl with 5 mM $CaCl_2$ and subsequently equilibrated in TBS with 5 mM $CaCl_2$. Functional carbohydrate bound rfhSP-D was eluted in TBS with 5 mM EDTA. To further purify only trimeric rfhSP-D, functional rfhSP-D was applied to an approximately 80 ml preparative superdex 200 column (**B**). Fractions containing trimeric rfhSP-D were pooled and*

*concentrated and applied to an analytical 24 ml superdex 200 gel filtration column (**C**). For gel filtration (**B** and **C**), The elution volume of rfhSP-D was compared with various protein standards including 12.4 kDa cytochrome c, 29 kDa carbonic anhydrase, 66 kDa BSA, 150 kDa alcohol dehydrogenase and 443 kDa apoferritin. Indicated are the peaks corresponding to trimeric rfhSP-D. For affinity chromatography and gel filtration (**A, B** and **C**), shown are the milli absorbance units at λ = 280 nm upon elution of protein from the column. Protein was analysed at each step of purification by SDS-PAGE with Coomassie staining (**D**). Samples analysed include: whole bacterial lysate after induction of expression (Induced), solubilised protein before affinity chromatography (Pre Affinity), peak fractions of flow through of affinity column corresponding to 40 (FT(1)) and 55 (FT(2)) ml (in A), functional rfhSP-D eluted with EDTA (Eluted rfhSP-D) and trimeric rfhSP-D further purified by gel filtration (Trimeric rfhSP-D). The identity of final purified functional trimeric rfhSP-D was confirmed by SDS-PAGE with Western blot analysis using an α-rfhSP-D antibody (**E**). Purification and analysis of rfhSP-D produced as an insoluble protein was undertaken at University of Southampton by Alastair Watson and Henry Hole.*

6.3.4.2 *Purification of rfhSP-D expressed as a Soluble Protein with NT^{dm}*

68 % of the rfhSP-D purified using NT^{dm} bound to a ManNAc column in a calcium-dependent manner and was eluted in the presence of EDTA (Figure 6-11A). With 46 (± 9.9) mg of rfhSP-D being purified by nickel affinity chromatography per litre of bacteria, this would correspond to a yield of approximately 31.3 mg of ManNAc affinity chromatography purified rfhSP-D upon scale up; this is substantially higher than the 3.3 mg obtained by the traditional refolding method. Comparatively, 29.5 % and 4.4 % bound to mannan and maltose columns in a calcium-dependent manner, respectively (Figure 6-11B and C, respectively). rfhSP-D purified through affinity chromatography was pooled and analysed by SDS-PAGE and Western blot analysis (Figure 6-12A and B, respectively).

Importantly, after digestion of NT^{dm}-rfhSP-D during purification, three bands were identified ((Figure 5-11 and Figure 6-12). In addition, after subsequent removal of NT by nickel affinity chromatography, there were still two different bands present in the purified rfhSP-D preparation (Figure 5-11). After ManNAc affinity purification of rfhSP-D, only one band remained and upon comparison side by side with digested NT^{dm}-rfhSP-D, the most intense band seen after cleavage was confirmed to be the functional carbohydrate binding protein which was identified to be immunoreactive to a polyclonal α-rfhSP-D antibody (Figure 6-12).

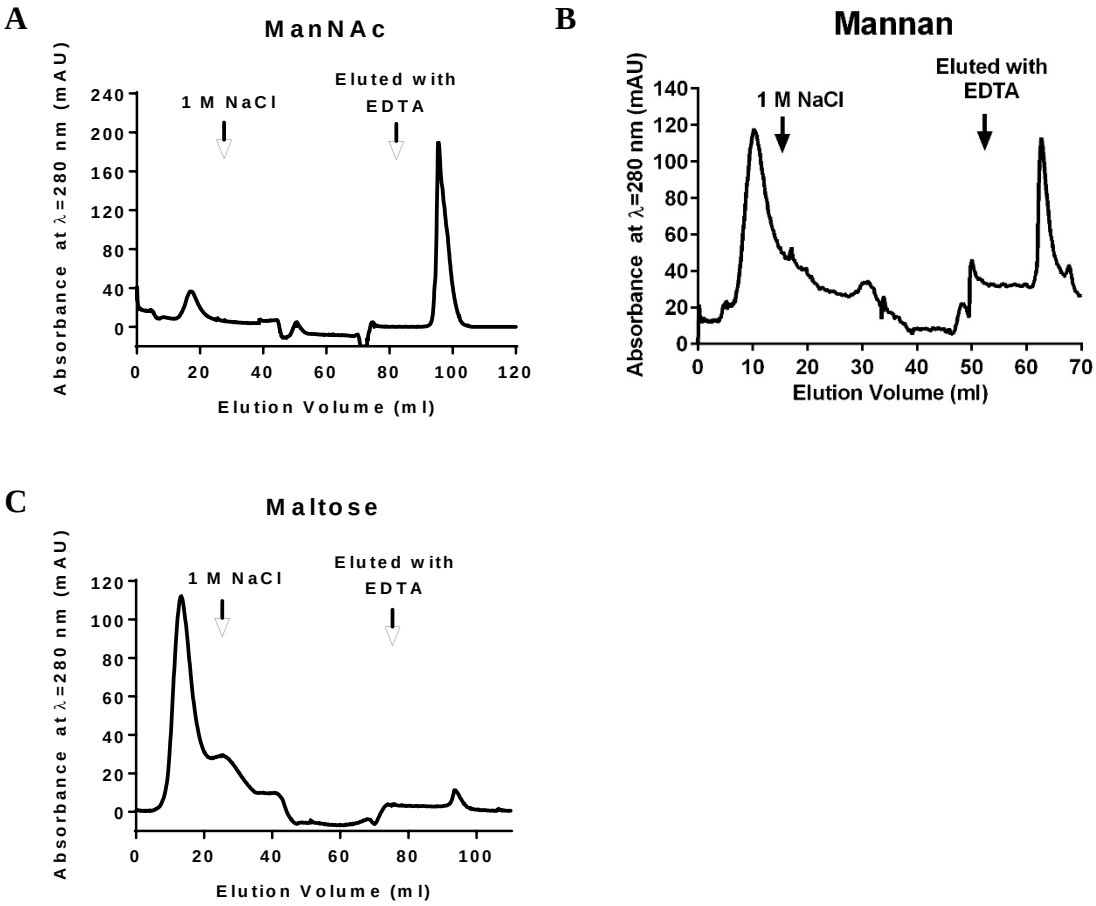

Figure 6-11: Purification of functional carbohydrate binding rfhSP-D and assessment of different columns. *The capacity of rfhSP-D produced as a soluble protein using NT^{dm} to bind to different approximately 15 ml carbohydrate affinity columns was tested. rfhSP-D was injected onto a ManNAc (**A**), mannan (**B**) or maltose (**C**) column equilibrated in TBS in 5 mM $CaCl_2$. The columns were washed in 20 mM Tris, 1 M NaCl with 5 mM $CaCl_2$ and subsequently equilibrated in TBS with 5 mM $CaCl_2$. Functional carbohydrate bound rfhSP-A was eluted in TBS with 5 mM EDTA. Shown are the milli absorbance units at λ = 280 nm upon elution of protein from the column.*

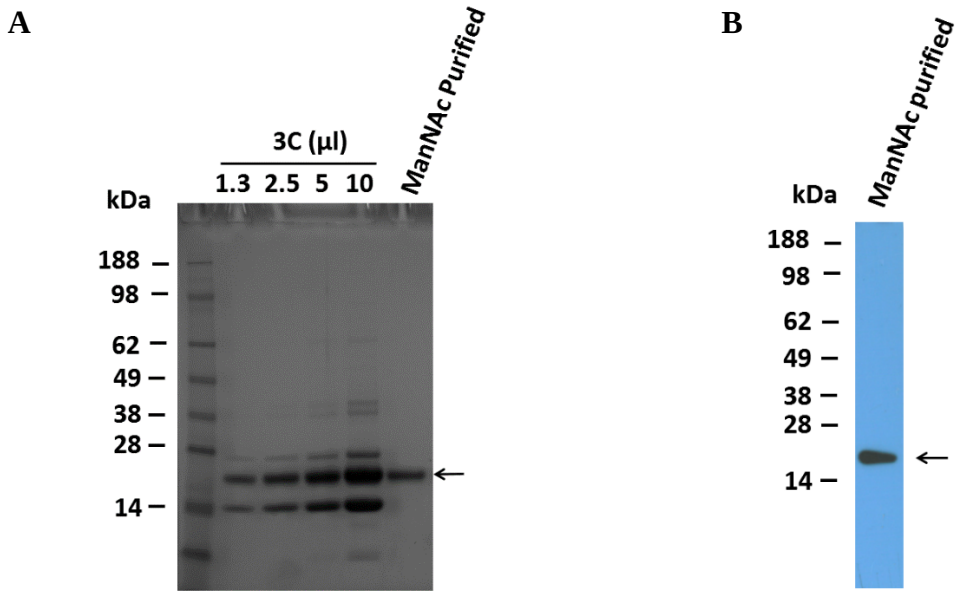

Figure 6-12: Analysis of rfhSP-D by SDS-PAGE and Western blot.*. Trimeric rfhSP-D purified by ManNAc affinity chromatography was assessed by SDS-PAGE with subsequent Coomassie staining (**A**) and Western blot analysis using an α-rfhSP-D antibody (**B**). To identify which of the bands produced after removal of NT^{dm} was the functional immunogenic rfhSP-D, different volumes of digested NT^{dm}-rfhSP-D (1.3 µl, 2.5 µl, 5 µl and 10 µl) were used as a comparison for the Coomassie stained SDS-PAGE (**A**).*

6.3.5 Purification of Dimeric rfhSP-A

For RSV neutralisation assays (Chapter 7) it was necessary to have an appropriate negative control. For this purpose dimeric rfhSP-A purified after expression and refolding from the NT-rfhSP-A protein was selected as an ideal candidate. This is due to it having been purified from *E. coli* in a similar manner to the trimeric rfhSP-A, but not being correctly folded as a trimeric protein. rfhSP-A which did not bind to a mannan affinity column (Figure 6-7B) was purified by application to a preparative gel filtration column (Figure 6-13A); fractions containing dimeric rfhSP-A were pooled and concentrated. The purified dimeric rfhSP-A was confirmed to be predominantly dimeric by analytical gel filtration where 92 % of the protein was found to be dimeric with only small levels of contamination by trimeric protein (1.1 %) (Figure 6-13B). The dimeric rfhSP-A did not function in binding to a mannan affinity column (Figure 6-13C).

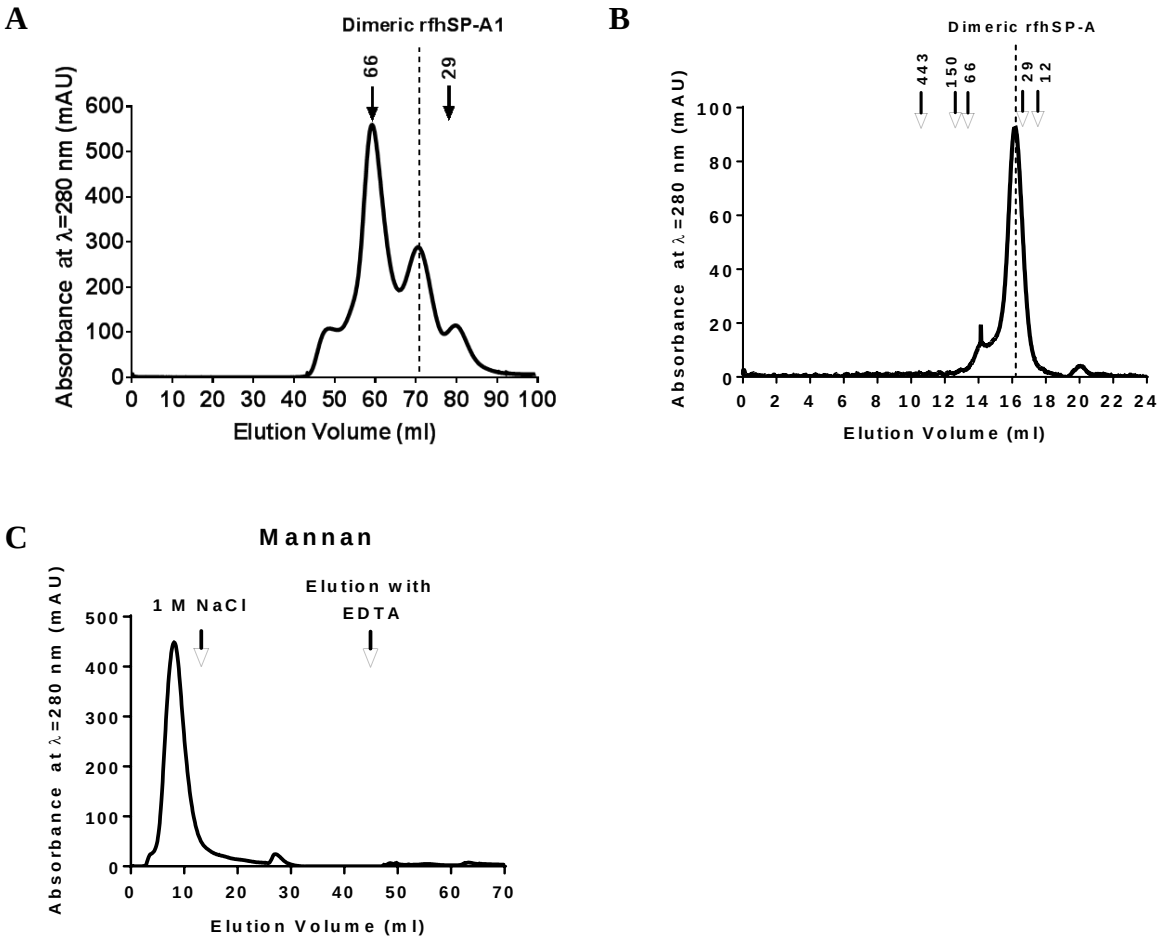

Figure 6-13: Purification of dimeric rfhSP-A. *rfhSP-A purified from NT-rfhSP-A (using the normal refold protocol with a bucket at a concentration of 3mg/ml) was applied to an approximately 80 ml preparative superdex 200 column (**A**). Fractions containing dimeric rfhSP-A were pooled and concentrated and applied to an analytical 24 ml superdex 200 gel filtration column (**B**). During gel filtration (**A** and **B**), the elution volume of rfhSP-A was compared with various protein standards including 12.4 kDa cytochrome c, 29 kDa carbonic anhydrase, 66 kDa BSA, 150 kDa alcohol dehydrogenase and 443 kDa apoferritin. Indicated are the peaks corresponding to dimeric rfhSP-A. Dimeric rfhSP-A was applied to an approximately 15 ml mannan affinity column equilibrated in TBS in 5 mM $CaCl_2$ using 50 ml a super loop (**C**). The column was washed in 20 mM Tris, 1 M NaCl with 5 mM $CaCl_2$ and subsequently equilibrated back into TBS with 5 mM $CaCl_2$. Functional carbohydrate bound rfhSP-D was eluted in TBS with 5 mM EDTA.*

6.4 Summary of Results

Within this chapter, the oligomeric structures of recombinant collectins were characterised. In additional, functional trimeric rfhSP-A and rfhSP-D which were expressed using NT or NT^{dm}, respectively, were purified. Thus, this chapter addressed Aims 4 and 5 (Section 1.14):

- To purify functional trimeric rfhSP-A.
- To purify functional trimeric rfhSP-D after expression as a soluble protein using NT or NT^{dm}.

Results are summarised below:

- Purified NT-rfhSP-A appeared to be monomeric. Comparatively, purified NT-rfhSP-D was multimeric (tetrameric or larger).
- After optimisation of the refold and subsequent removal of NT, rfhSP-A was successfully isolated as a trimeric molecule.
- The structure of trimeric rfhSP-A was mainly α-helical and similar to the structure of rfhSP-D produced using the traditional refolding method.
- Small amounts of functional rfhSP-A bound to maltose and mannan affinity columns and were purified. However, rfhSP-A did not bind to mannose or ManNAc columns; functional rfhSP-A purified by carbohydrate affinity chromatography was confirmed to be trimeric.
- Purified rfhSP-A expressed as a soluble protein using NT^{dm} was predominantly aggregated with only 24 (± 4.3) % being trimeric. No rfhSP-A produced using NT^{dm} was successfully purified using either mannan or ManNAc affinity chromatography.
- Functional trimeric rfhSP-D was successfully purified through refolding using ManNAc affinity chromatography and yielded 3.3 mg of protein/litre of bacteria.
- Comparatively, use of NT^{dm} allowed the purification of functional trimeric rfhSP-D which was successfully purified by both mannan and ManNAc affinity chromatography; this was not possible through using maltose affinity chromatography.
- Use of NT^{dm} increased yields of production from 3.3 mg/litre obtained using the traditional refolding protocol to a yield which would correspond to approximately 31.3 mg/litre upon scale of affinity chromatography.

6.5 Discussion

The formation of a trimeric unit is widely thought to be essential for the function of SP-D, this may also be the case for SP-A. In this chapter, the oligomeric structures of the recombinant collectins purified in Chapter 5 were characterised. In addition, the functional trimeric rfhSP-A and rfhSP-D expressed using NT and NT^{dm}, respectively, were purified using carbohydrate affinity chromatography (Aims 4 and 5 - Section 1.14).

6.5.1 The Structure of Purified Recombinant Collectins

Upon purification and analysis by gel filtration, the oligomeric structure of NT-rfhSP-D and NT-rfhSP-A were found to be substantially different. NT-rfhSP-A appeared to be predominantly monomeric contrasting with NT-rfhSP-D which was multimeric, potentially tetrameric or higher order (Figure 6-1). This was a surprising result as NT-rfhSP-D was expressed as a soluble protein and NT-rfhSP-A required refolding. It might be expected that the NT-rfhSP-D fusion protein with a higher propensity to form higher order oligomers and aggregates would have a lower solubility than a protein which remained as a monomer. However, as described in Chapter 5, this was not the case. One potential explanation for this oligomerisation of NT-rfhSP-D could be, as discussed below, the neck region of rfhSP-D having a higher propensity to trimerise than that of rfhSP-A, potentially leading to trimerisation of the fusion protein or further association of monomeric units. As seen in Figure 4-1 (approximately to scale), the long distance between the CRD and NT domain means that spatially it could be feasible for this to occur. It would be interesting to also characterise the oligomeric structure of NT^{dm}-rfhSP-A and NT^{dm}-rfhSP-D for comparison with NT-rfhSP-A and NT-rfhSP-D. This would aid with delineation of whether the difference in ability to form higher order oligomers between the fusion proteins correlates with the level of protein solubility during heterologous expression in *E. coli*.

Upon removal of NT and NT^{dm}, the oligomeric structures of rfhSP-A and rfhSP-D were characterised. rfhSP-A produced through refolding using NT was a mixture of trimers, dimers, monomers and higher-order oligomers, dependent on the refolding protocol. The refolding protocol was thus optimised by iterative alteration of a single refold condition to discern which of the conditions were important in influencing rfhSP-A trimerisation. The use of a bucket during dialysis as opposed to a measuring cylinder was found to be a

key variable which allowed the production of a larger proportion of trimers. This was hypothesised to be due to the ability of the glycerol to mix efficiently and act as a scaffold for effective refolding of NT-rfhSP-A. Indeed, glycerol is known to act as an osmolyte to increase protein stability, prevent aggregation, stabilise folding intermediates and decrease the folding rate (286). Notably, use of a bucket rather than a measuring cylinder during the refold decreased the level of protein loss due to precipitation during refolding (Table 6-2). Further increasing the glycerol concentration may thus be beneficial in further increasing the proportion of rfhSP-A trimers after refolding whilst decreasing protein loss due to precipitation. Other conditions which did not substantially impact on the proportion of rfhSP-A trimers included, the temperature of the refold, the speed of urea dilution and the use of a redox system which has previously been used (287). Although use of a redox system did not substantially alter the level of protein precipitation, the aggregated protein was of a different appearance with smaller clumps of precipitated protein. This is likely a consequence of preventing the disulphide bonds forming early during the refold or the inclusion of arginine in the refold buffer which is thought to suppress protein aggregation. Through optimising the refold process, the proportion of rfhSP-A trimers was successfully increased from only 18 % to up to 81 %. The refold of the NT-rfhSP-A fusion protein, which was predominantly monomeric, was thus crucial in subsequent formation of trimeric rfhSP-A units upon removal of the NT tag. Other refold techniques should also be tried, particularly using a rapid dilution technique as opposed to refolding by dialysis which was undertaken in this present study.

Comparative to refolded rfhSP-A, a much smaller proportion of rfhSP-A molecules produced and purified as a soluble fusion protein using NT^{dm} were trimeric (24 (± 4.3) % compared with up to 81 %). As compared with the refolded protein, the rfhSP-A expressed as a soluble protein was folded within the *E. coli* cytoplasm. An inability to fold correctly could be due to the increased translation rate found in prokaryotic expression systems leading to an inability for native folding (288). In addition, it could be due to the microenvironment within the *E. coli* which may differ from that required for correct folding in terms of pH, osmolarity, redox potential, presence of cofactors, and folding mechanisms. Within the overexpressing *E. coli* cell with high cytoplasmic protein concentrations, hydrophobic polypeptide stretches are present at high concentrations, this could lead to their interaction, resulting in misfolding of the protein (289). Use of shuffle *E. coli* cells engineered to form proteins containing disulphide bonds in the cytoplasm

(290) did not increase the proportion of rfhSP-A trimers formed. Other expression systems could be tried in addition to alternative methods for inducing expression, namely using an auto-induction method rather than IPTG. To note, the 7th Xaa of the 8 x Gly Xaa Yaa collagen stalk is missing in the rfhSP-A molecule produced using NT^{dm} but present in rfhSP-A produced through refolding using NT (appendix (Figure 8-2)). This may also have some impact on the oligomeric structure of rfhSP-A.

rfhSP-D expressed and purified as a soluble protein using NT^{dm}, resulted in a larger proportion (mean (± SD) of 88.5 (± 4.0) %) of trimers upon removal of the solubility tag than rfhSP-A produced through this same approach (24 (± 4.3) %). This may be due to the rfhSP-D being more suited to the folding microenvironment within the *E. coli* or the neck domain having a higher propensity to trimerise. The neck domain of rfhSP-D is known to be an efficient trimerising agent and previously allowed trimerisation of thioredoxin, a non-collagenous heterologous protein (36). A rfhSP-A CRD/rfhSP-D neck chimera could, therefore, overcome the issue of producing trimeric rfhSP-A after expression as a soluble protein whilst maintaining SP-A-specific CRD lectin functionality.

The rfhSP-D and rfrSP-A CRDs have previously been described to have different structural conformations. rfrSP-A has more extensive stabilising interactions across the neck-CRD interface, and thus a more widely spaced T-shaped CRD comparative to the Y-shaped CRD of rfhSP-D (Figure 1-2) (4). It might therefore be expected that upon analysis of rfhSP-A by gel filtration, due to the expected less compact structure of the CRD, it would appear as a larger apparent molecular weight protein and migrate through the gel filtration column more quickly than rfhSP-D. However, in fact, the reverse was found. The neck and CRD of SP-A has previously been reported to undergo conformational changes (292) and be more resistant to proteases in the presence of calcium (291). Moreover, full-length nhSP-A has been shown to assume a more compact structure in the presence of calcium (48). The surprising finding of a rfhSP-A trimer eluting from the gel filtration after the rfhSP-D may therefore be a consequence of conformational changes induced by the absence of calcium. Alternatively, it could be due to structural differences other than that of the CRD, potentially within the 24 amino acid collagen-like stalk which is not present in the resolved crystal structure of rfrSP-A or rfhSP-D. Other potential reasons could include structural differences between rat and human SP-A, having a composition of only SP-A1 contrasting to the native SP-A1/SP-

A2 mix or being an artefact of being expressed in *E. coli*. However, looking forward, trimeric rfhSP-A is now a useful tool with potential to allow a more detailed understanding of the structure of human SP-A. This could particularly be the case with future resolution of the rfhSP-A crystal and solution structures which could also give an insight into the mechanisms of human SP-A CRD-dependent ligand binding.

6.5.1.1 *Importance of the Collagen-like Stalk*

The SP-A collagen-like domain was not present in previous attempts to produce a functional, trimeric rfhSP-A molecule but has previously been suggested to be important for protein stabilisation (293). In this present study, the collagen-like stalk was hypothesised to allow the formation and stabilisation of a trimeric unit, thus was included in the cloned rfhSP-A constructs. Previous expression of a MBP-rfhSP-A protein lacking this collagen-like stalk resulted in chemical crosslinking with (bis(sulfosuccinimidyl)suberate) (BS3) being required in order to form a trimeric unit (232). This was also the case upon expression of this same rfhSP-A fragment without an expression partner (233). Importantly, this crosslinking had limited efficiency for production of a trimeric rfhSP-A molecule and there has been no evidence of the purification of a functional trimeric rfhSP-A protein. Further evidence of the importance of the collagen-like stalk has been provided by studies generating a rfhSP-A molecule lacking the collagen-like domain by the digestion of nhSP-A using collagenase. This has been reported to result in monomeric subunits (294) and a mixture of trimers and monomers, dependent on the buffer salt concentration (295). However, caution must be undertaken when interpreting this data due to an undetermined collagenase enzyme efficacy in digesting nhSP-D.

Upon review of rat SP-A, there have been reports of a requirement for a crosslinking reagent to form a trimeric rfrSP-A molecule with the absence of the collagen-like stalk (296), others however, have produced such a trimer at room temperature without crosslinking (32). Human and rat SP-A sequences are known to be different and likely have a differential propensity to form stable trimers upon deletion of the collagen-like-stalk. Importantly, this collagen-like stalk has been shown to be essential for the function of SP-D *in vivo* for preventing emphysema-like morphological changes in the SP-D$^{-/-}$ mice, where this protective effect was only seen upon treatment with a rfhSP-D molecule containing the collagen-like stalk (44).

Taken together, these previous studies and this present study suggests that the collagen-like stalk may be required to stabilise and potentially form trimeric fragments of human lung collectins. Similarly to rfhSP-D, this is likely to be crucial for functionality particularly in an *in vivo* setting where there is a considerably different environment both with an increased temperature (37 °C) and potential presence of proteases. In this present study through inclusion of this collagen-like stalk, a functional trimeric rfhSP-A molecule was successfully produced and purified without the requirement for chemical cross-linking. This was not possible without inclusion of such a collagen-like stalk.

6.5.1.2 *The Secondary Structure of rfhSP-A*

To gain an insight into the secondary structure of trimeric rfhSP-A produced using NT and its similarity to rfhSP-D, trimeric rfhSP-A and rfhSP-D were assessed by circular dichroism. Similar circular dichroism spectra were obtained with both proteins, which appeared to be predominantly influenced by α-helical structures (Figure 6-6). This is consistent with the previously reported crystal structures for rfrSP-A and rfhSP-D where each monomer has a long α-helix constituting the neck domain with the CRD being comprised of two α-helixes and 11 short (3-7 residue) beta strands (32, 297). There may be structural differences between rat and human SP-A. In addition, the rfrSP-A and rfhSP-D crystal structures lacked the 24 amino acid collagen-like stalk thought to be involved in trimer stabilisation. These are important things to consider when interpreting the circular dichroism spectra in this present study and comparing with previously resolved crystal structures.

Upon comparison with circular dichroism spectra previously obtained for SP-A, full-length recombinant SP-A1 and SP-A2 expressed in mammalian cells and nhSP-A also had a pronounced α-helical content, however, with a more pronounced dip at approximately 204 nm. This dip is likely a result of the long polyproline collagen-like chain which is largely absent for rfhSP-A and rfhSP-D analysed in this present study (42, 234). Upon heating of rfhSP-A and rfhSP-D to 37 °C, the secondary structure changed considerably, potentially due to refolding of the secondary structures and movement towards a more disorded protein structure. Circular dichroism was undertaken in phosphate buffer without the presence of calcium chloride due to possible interference by chloride ions at low wavelengths. Calcium, however, has been shown to induce conformational changes and stabilise the collectin structure as, discussed above. Indeed,

upon previous investigation by circular dichroism, a shift in spectra of SP-A and SP-D was shown, dependent on the presence of calcium or EDTA, respectively (294, 298). Looking forward, it would be intriguing to investigate the importance of temperature and presence of calcium ions on the structures of rfhSP-A and rfhSP-D. Further constructs lacking the collagen-like domain could give further insight into the importance of the collagen-like domain in stabilising the rfhSP-A and rfhSP-D trimeric structure at 37 °C, as discussed above.

Importantly, the secondary structure of the newly created rfhSP-A protein appeared similar to that of rfhSP-D which seemed promising upon moving to the next stage of testing protein functionality and attempting to purify functional rfhSP-A through its lectin activity.

6.5.2 Purification of Functional Carbohydrate Binding rfhSP-A

To further purify just the functional rfhSP-A and rfhSP-D whilst testing their capacity to bind known carbohydrate ligands, carbohydrate affinity chromatography was implemented. Due to preliminary solid phase binding assays where rfhSP-A was shown to bind to mannan (discussed in Chapter 7), mannan affinity chromatography was selected as the predominant method for purification. A proportion of rfhSP-A produced through refolding using NT was functional and bound to mannan-affinity columns in a calcium-dependent manner. This allowed for isolation of highly pure functional rfhSP-A. However, issues were, met with only low yields of functional rfhSP-A being purified. Purification of rfhSP-A using NT was undertaken 24 times with up to 12 % of the rfhSP-A being functional and purified by carbohydrate affinity chromatography. However, many of the purifications yielded negligible or no rfhSP-A upon purification by carbohydrate affinity chromatography.

A trimeric structure is thought to be important for the function of SP-D and potentially SP-A. Gel filtration was therefore implemented as a screening strategy to delineate the proportion of trimeric rfhSP-A in each batch of protein and thus whether the protein is likely to be functional. After optimisation of the refold strategy a high proportion of rfhSP-A was trimeric. However, some batches still yielded negligible or no functional rfhSP-A. It was hypothesised that the quality of the affinity column or the carbohydrate attached to the column may have influenced the ability of rfhSP-A to bind. However, use

of a new mannan column as well as other carbohydrate columns including mannose, ManNAc and maltose did not allow for improved purification. Furthermore, mannose and ManNAc did not allow successful purification of any rfhSP-A. This was surprising as SP-A has been reported to have a higher affinity for ManNAc than both maltose and mannan (56). However, this may be a reflection of batch to batch variation or quality of affinity columns as opposed to relative binding avidities to the carbohydrates. Further optimisation of refolding conditions could be undertaken for example using a rapid dilution method as opposed to refolding by dialysis. In addition, other affinity columns could be implemented including a fucose column as previously used (57). It is possible, however, that the trimeric rfhSP-A is folded incorrectly. In particularly, the disulphide bonds may have formed incorrectly; this needs to be further investigated.

The inability to purify large quantities of rfhSP-A by carbohydrate affinity chromatography could, however, be due to a functional SP-A trimer having too low a binding avidity for efficient purification. Indeed problems have previously been reported with the purification of full length trimeric SP-A by maltose affinity chromatography (270). The trimeric fragment of rat SP-A was previously purified by mannose affinity chromatography (32). However, there are functional differences between rat and human SP-A (4, 119). Mannose affinity chromatography has previously been shown to be inefficient in purification of recombinant human SP-A trimers which lacked the N-terminal domain (52). In this study, trimeric SP-A was purified using anion-exchange chromatography. Anion-exchange chromatography with subsequent gel filtration may be a viable way to purify trimeric rfhSP-A in the future, particularly for comparison with nhSP-A where there is currently no carbohydrate binding selective step being used. However, the trimeric rfhSP-A needs to be confirmed to be correctly folded and functional, perhaps using the RSV infection assay discusses in Chapter 7.

rfhSP-A produced using NT and purified using carbohydrate affinity chromatography was pooled and concentrated. Functional rfhSP-A was further analysed by gel filtration and found to be composed of only trimeric molecules. Thus, highlighting the importance of the formation of a trimeric unit in allowing an SP-A molecule to be functional, or at least to have a high enough binding avidity to be purified by carbohydrate affinity chromatography. The purified carbohydrate binding trimeric rfhSP-A was confirmed to be of high purity as assessed by SDS-PAGE, Western blotting and mass spectrometry; this protein was taken forward into functional assays described in Chapter 7. Dimeric

rfhSP-A produced through refolding with NT was also successfully purified by gel filtration for use as a negative control in these assays. Importantly, purified dimeric rfhSP-A had only a small contamination of higher order protein with 92 % corresponding to dimeric protein. Moreover, no dimeric rfhSP-A was found to be functional in binding to a mannan column.

rfhSP-A expressed as a soluble protein using NT^{dm} was not successfully purified by carbohydrate affinity chromatography. However, relatively fewer rounds of purification were undertaken for this protein. The inability of a proportion of rfhSP-A produced as a soluble protein to bind to a carbohydrate affinity column could partially be due to the protein containing a low proportion of trimeric molecules. In addition, it could be due to incorrect folding of the CRD and an inability to bind to carbohydrate ligands due to the folding environment within the *E. coli*. Thus optimisation of expression conditions or use of a different expression system could be trialled in the future.

Another factor which could impact on the ability of rfhSP-A to bind to an affinity column could include the absence of the Asn187 glycosylation which is absent in the CRD of rfhSP-A expressed in *E. coli*. This glycosylation has previously been shown to be important for neutralisation of IAV (29) and its absence could potentially impact on the correct folding of the CRD or the binding to carbohydrate ligands. SP-A is also a lipid binding molecule, the presence of lipids during the folding of rfhSP-A or binding of rfhSP-A to a column could be important. Batch to batch variation in binding to carbohydrate affinity columns could, therefore, be attributed to the different stringencies of washing the inclusion bodies and thus differential levels of contaminating lipids during the refold. Refolding of rfhSP-A could be undertaken with addition of DPPC or other surfactant lipids to investigate the importance of lipids during recombinant SP-A folding and binding. Further carbohydrate columns should be tested for their capacity to allow purification of rfhSP-A produced using NT^{dm}, including maltose and mannose affinity columns. Alternatively, trimeric rfhSP-A produced as a soluble protein could be purified using anion exchange chromatography and gel filtration and its functionality compared with that of rfhSP-A produced through refolding.

6.5.3 Purification of Functional Carbohydrate Binding rfhSP-D

As previously shown, rfhSP-D produced through refolding was effectively purified by ManNAc affinity chromatography. Upon analysis by gel filtration, ManNAc purified rfhSP-D contained only trimeric molecules. Thus highlighting either the presence of only trimeric rfhSP-D in the protein preparation or the requirement of a trimeric structure to function and bind to the affinity column. rfhSP-D produced as a soluble protein using NT^{dm} was successfully purified by both ManNAc and mannan affinity chromatography. Maltose affinity chromatography was not successfully implemented to purify rfhSP-D produced using NT^{dm}. However, there are mixed reports about the ability to purify trimeric SP-D using maltose (58, 260). Interestingly, trimeric SP-D has been reported to bind to maltose with a higher affinity than mannose (58). The ability of rfhSP-D produced using NT^{dm} to bind mannan but not maltose in this present study could either be a difference in binging properties of rfhSP-D, dependent on the method of production, or alternatively a difference due to the quality of the columns. Thus it would be interesting to also attempt to purify rfhSP-D produced through refolding by maltose affinity chromatography to compare with rfhSP-D produced as a soluble protein using NT^{dm}. Functional rfhSP-D produced as a soluble protein using NT^{dm} was successfully purified to allow subsequent characterisation in RSV infection assays as compared with rfhSP-D produced through the traditional refolding technique and nhSP-D

Use of the NT^{dm} expression system allowed a more straightforward production process and a significant increase in yields of functional protein produced with a yield which would equate to 31.3 mg of functional ManNAc-binding protein per litre of bacteria culture upon scale up compared with the 3.3 mg obtained by the traditional refolding method. Crucially, this soluble expression system allowed production of functional protein without the need for refolding. This expression/purification process has potential to be improved to further increase production yields, particularly through the use of an industrial fermenter, upstream processing or use of an alternative cleavage site: changing the cleavage site from thrombin to HRV 3C halved the yield of soluble protein isolated. This production process overcomes the previous problems associated with protein refolding and could increase the therapeutic potential of rfhSP-D. rfhSP-D produced as a soluble protein using this novel NT^{dm} tag now needs to be fully characterised as compared with rfhSP-D produced through the traditional refolding method.

6.5.4 Summary

No one has as yet successfully produced a functional rfhSP-A molecule equivalent to rfhSP-D and shown it to be trimeric. In this chapter a functional trimeric rfhSP-A molecule was successfully purified after expression using NT with subsequent refolding. NT^{dm} allowed the expression of rfhSP-A as a soluble protein. However, further optimisation is required to obtain a higher proportion of functional trimers using NT^{dm}. Trimeric rfhSP-A was shown to have a similar secondary structure to rfhSP-D, with the circular dichroism spectra being influenced predominately by α-helical structures. rfhSP-A was successfully purified by carbohydrate affinity chromatography. However, this was for only a small proportion (up to 12 %). This is hypothesised to be due to a large proportion of the trimeric rfhSP-A not being folded the correct way for functional lectin activity, or alternatively rfhSP-A having too low a binding avidity to allow efficient purification by carbohydrate affinity chromatography. Future alternative purification techniques could be trialled including gel filtration and anion-exchange chromatography, particularly as there is currently no selective carbohydrate affinity purification step standardly used for purification of nhSP-A which will be used for functional comparison. The successful production of a functional trimeric rfhSP-A molecule in this chapter allowed the investigation of the importance of the N-terminus and oligomeric structure of SP-A in its interaction with RSV, as described in Chapter 7.

Use of the NT^{dm} expression system allowed improved yields of rfhSP-D production. Moreover, through overcoming the previous problem of refolding to obtain functional rfhSP-D, this novel strategy may increase the therapeutic potential of rfhSP-D. It is now important to compare the function of rfhSP-D produced as a soluble protein with that produced through the traditional refolding technique.

Chapter 7 Collectin Ligand Binding and Neutralisation of RSV

7.1 Introduction

SP-A and SP-D are known to bind to an array of different bacteria, viruses and allergens through binding to carbohydrates in a calcium-dependent manner. In this chapter, the ability of rfhSP-A as compared with nhSP-A and nhSP-D to bind to various carbohydrates was tested. These included mannan, mannose, maltose, ManNAc and glucose in a similar to that undertaken previously (56). Moreover, the ability of rfhSP-A to bind to LPS from bacterial cell walls, whole HIV and RSV particles, recombinant glycosylated proteins from HIV and RSV and extracts from grass pollen and house dust mite was also tested as compared with nhSP-A and nhSP-D. Binding was assessed using both solid phase binding assays and surface plasmon resonance (SPR). In addition to rfhSP-A being functional and binding to known nhSP-A ligands, it was hypothesised that a trimeric rfhSP-A protein would be sufficient to neutralise RSV in an *in vitro* infection assay. Moreover, that it would lack the capacity to promote entrance of the virus to the host cell due to the absence of the N-terminal domain which may interact with host cell receptors or agglutinate RSV to potentially increase viral uptake.

7.1.1 Binding to Viral Ligands

SP-A and SP-D have been shown to bind to various enveloped RNA viruses through binding to their glycosylated attachment proteins, these include RSV and HIV.

7.1.1.1 *RSV Ligands*

As discussed in Section 1.11.2, the interaction of lung collectins with RSV is unclear, particularly with SP-A. SP-A has been shown to prevent RSV infection *in vivo* (118). However, it has also been shown to provide a route of entry for the virus *in vitro*. This was shown to be through binding to the G protein, important for attachment of the virus to the cell (148). Other contrasting reports, however, have suggested SP-A to bind to the F protein of RSV which mediates fusion of the virus to the host cell but not to the G protein (147).

The work in this chapter attempted to clarify the interaction of SP-A and SP-D with RSV by testing the capacity of rfhSP-A, nhSP-A and nhSP-D to bind to F and G proteins of RSV. Through a collaboration with Barney Graham (NIH, US) and Jason McLellan

(Dartmouth College, Hanover, US), recombinant F protein from RSV in the pre and post-fusion conformation (A2 strain) were available for use in collectin binding assays and were produced as previously described (141). The post-fusion state differs from the pre-fusion by the absence of only 10 amino acids in the F1 subunit. However, pre and post-fusion proteins are structurally different due to the requirement for refolding to form a stable post-fusion protein (299). Thus, delineation of differences in the capacity of SP-A and SP-D to interact with pre and post-fusion proteins could further delineate the mechanisms through which they interact with RSV.

A collaboration was, however, not successfully set up to allow the testing of the capacity of rfhSP-A, nhSP-A and nhSP-D to bind recombinant full-length RSV G protein. However, through collaboration with Ultan Power (Queen's University Belfast, Belfast, Northern Ireland), Sendai viruses expressing RSV F protein (A2 strain) and the central conserved region of RSV attachment glycoprotein G (aa130–230) fused to BB (a 28-kDa protein corresponding to the albumin-binding region of streptococcal G protein) (BBG2Na) were available for testing (300). BBG2Na, is a heavily studied vaccine candidate, thus the ability of rfhSP-A, nhSP-A and nhSP-D to interact with this protein is of additional interest. Sendai viruses are negative stranded *Paramyxoviridae* family RNA virus which have been extensively studied for use as vectors for vaccines, gene therapies and cancer immunotherapies and are used in the lab of Ultan Power to express large amounts of RSV F and BBG2Na proteins in a mammalian system. Previous use of Sendai virus in their lab expressing GFP has allowed characterisation of the pathology of paediatric bronchial epithelial cells caused by Sendai virus (301). There is no evidence that the expressed recombinant F and BBG2Na proteins integrate into the virion; through discussion with Ultan Power, in his work and the present study, it was assumed that the proteins are and not integrated into the virion of the Sendai virus (personal communication: email to Alastair Watson, 5th May 2014). Sendai viruses expressing F protein and BBG2Na were produced in embryonated chicken eggs, as previously described (302). Thus in binding assays a control of allotonic fluid was also used.

In this chapter the ability of rfhSP-A as compared to nhSP-A and nhSP-D to bind to recombinant pre and post-fusion F proteins expressed in mammalian cells is reported. In addition, the ability to bind F protein and the BBG2Na vaccine candidate containing the conserved region of RSV G protein expressed by Sendai virus was also tested.

7.1.1.2 *HIV Ligands*

SP-A and SP-D are expressed on most other mucosal surfaces including the vaginal mucosa and may be important for interacting with HIV at the site of infection alongside reservoir sites of viral replication, specifically the lung (154-156). SP-A and SP-D have been shown to bind various strains of B-clade HIV-1 including those propagated in cultured T cells which express the CCR5 chemokine receptor such as HIV IIIB and those propagated in clinical PBMCs which express the CXCR4 chemokine receptor including HIV BaL (154, 303). This was illustrated using particles inactivated with 2,2'-dithiodipyridine (aldrithiol-2; AT-2) which covalently modifies the essential zinc fingers within the nucleocapsid of HIV, an essential accessory factor to act as a nucleic acid chaperone to achieve efficient viral DNA synthesis, thus preventing virus infectivity (304). Infective HIV BaL and IIIB strains, were, however, also used to demonstrate the ability of SP-A and SP-D to prevent HIV infection. SP-A and SP-D were shown to reduce the HIV infection of CD4+ T cells. However, they also increased the infection of dendritic cells. Importantly, the B-clade HIV-1 HIV MN strain propagated predominantly in clinical PBMCs has not as yet been tested.

The interactions of SP-A and SP-D with HIV was shown to be mediated through binding to the HIV envelope glycoprotein gp120 by undertaking binding assays using recombinant proteins. gp120 is essential for fusion of HIV to the host cell and entrance of the HIV virus. gp120 forms the HIV envelope spike through non-covalent interactions of three copies of gp120 with three copies of gp 41 after cleavage from the gp160 precursor. Recombinant gp120 proteins are monomeric due to the absence of gp41. Importantly, there may be differences in the capacity of SP-A and SP-D to bind monomeric HIV envelope proteins as compared with trimeric proteins. Trimeric lab variants have, however, been generated which are composed of the ectodomain of HIV envelope protein including the entire gp120 component and approximately 20 kDa of gp41. These have been used in various neutralisation assays for eliciting effective humoral responses (305). A widely available recombinant trimeric envelope protein which is clinically relevant is from a clade-C isolate, HIV-1 CN54 (gp140 CN54). As far as the author is aware. The capacity for SP-A and SP-D to bind this trimeric glycoprotein from HIV-1 CN54 has not been previously tested.

In this chapter we test the ability of rfhSP-A to bind to AT-2 inactivated HIV BaL virions as well as HIV MN virions, which have not as yet been shown to be bound by SP-A and SP-D. Binding was compared with a negative control of non-viral cell lysate (NVCL) from the host cells used to propagate the HIV virus. The ability of rfhSP-A to bind to monomeric gp120 proteins from HIV-1 BaL and HIV-1 IIIB, as well as trimeric gp140 CN54, was also tested as compared with nhSP-A and nhSP-D.

7.1.2 Binding to Bacterial LPS

SP-A and SP-D bind LPS from an array of different bacterial pathogens (Table 1-3 and Table 1-4) and are thought to bind rough LPS but not smooth LPS due to SP-A preferentially binding to the lipid A moiety of LPS and SP-D interacting with the core oligosaccharides (101, 102). Interestingly, rfhSP-D has been shown to bind to LPS from *Haemophilus influenza* type B (Strain RM153) Eagan 4A mutant which has a truncated LPS structure and exposed core oligosaccharides but not to the Eagan wild type strain which has extensive O antigen glycan polymers attached (306). In this chapter rfhSP-A was tested for its ability to bind to rough and smooth LPS from *E. coli* (strains EH100 Ra and 0111.B4, respectively), LPS from *klebsiella pneumoniae* (ATCC 15380) and LPS from *H. influenzae* (Eagan wild type and Eagan 4A) as compared with nhSP-A and nhSP-D.

7.1.3 Interaction with Allergens

SP-A and SP-D have been shown to bind various different allergens particularly extracts of grass pollen and house dust mite in addition to fungal allergens from *A. fumigatus.* SP-A and SP-D are thought to be important in resisting allergenic challenge and subsequent hypersensitivity lung reactions (202). SP-A has been shown to bind *P. nigra*, *P. pratensis*, *S. cerale* and *A. elatior* (197). Comparatively, the ability of SP-D to bind grass pollen has predominantly been studied using *Dactylis glomerata*. In one study, both SP-A and SP-D were shown to bind to *D. glomerata.* However, only SP-D decreased pollen-induced IgE-dependent mast cell degranulation (198). SP-D has also been shown to enhance uptake of *D. glomerata* by macrophages (307). Moreover, SP-D has been shown to bind to and promote attachment of *Phleum pratense* to epithelial cells. This has been shown to promote the secretion of IL-8 (308). The interaction between SP-A and SP-D with both

D. pteronyssinus 1 and *D. farinae 1* house dust mite extracts has also been demonstrated (195). Importantly, this has been shown to prevent binding of IgE from sera of mite-sensitive asthmatic children to immobilised house dust mite (196).

In this chapter the capacity of rfhSP-A in comparison with nhSP-A and nhSP-D to bind extracts of grass pollen including *D. glomerata*, *P. nigra* and *P. praensis* and house dust mite including *D. farina* and *D. pteronyssinus* was assessed.

7.1.4 Infection Assays

As described above, the importance of SP-A in RSV infection is unclear. nhSP-A has been shown to both neutralise RSV or provide a route of entry to enhance infection of host cells. The main aim of this study, after production and purification of a functional rfhSP-A molecule, was to use a functional rfhSP-A molecule as a tool alongside rfhSP-D to investigate the importance of the N-terminal domain of SP-A and SP-D and their oligomeric structures in their interaction with RSV (Aim 7, Section 1.14). In this study a clinically relevant strain of RSV A originally isolated in Memphis by DeVincenzo et al. (Memphis 37 strain) was used in infection assays (309). The interaction of SP-A and SP-D with RSV has not been studied in an appropriate *in vitro* bronchial epithelial model, with much work being undertaken in mouse models or cell lines, particularly HEp-2 cells, a model often used for alveolar epithelial cells, or U937 cells, which are macrophage-like cells (128, 146). In this present study infection assays were undertaken in a relevant *in vitro* model of the bronchial epithelium. Human bronchial epithelial cells (AALEB) were used, which had been immortalised through specific transfection with the simian virus 40 early region and the telomerase catalytic subunit hTERT and which had a low passage number, as previously described (310). In this study the ability of rfhSP-A, nhSP-A and nhSP-D to neutralise RSV was investigated. In addition, the functionality of rfhSP-D produced using NT^{dm} in neutralising RSV was compared with that produced through the traditional refolding method. This work was undertaken through a collaboration with Tom Wilkinson, Karl Staples and C Mirella Spalluto (University of Southampton) who provided the RSV M37, a clinically relevant A2 strain (309) and bronchial epithelial AALEB cells (310) along with their expertise.

7.1.5 Aims

The aims of this chapter were to characterise the capacity of carbohydrate-affinity purified rfhSP-A to bind to the known natural ligands described above. An additional aim was to use rfhSP-A and rfhSP-D produced using NT and NT^{dm}, respectively, as tools to characterise the importance of the SP-A and SP-D N-terminal domain and oligomeric structure in their capacity to neutralise a clinically relevant strain of RSV and prevent the infection of human bronchial epithelial cells (Aims 6 and 7 - Section 1.14).

7.2 Methods

7.2.1 Reagents

Purified *H. influenzae* Eagan wild type and *H. influenzae* Eagan (E) 4A mutant LPS were kindly provided by Trevor Greenhough (Keele University, UK). Recombinant RSV pre and post-fusion F proteins were kindly provided by Jason S. McLellan (Dartmouth College, Hanover, US). Sendai viruses expressing either RSV F protein (Sendai F) or the BBG2Na (containing the core region of RSV G protein) (Sendai G) were grown in embryonated chicken eggs, as previously described (302), and kindly provided by Ultan Power (Queen's University Belfast). Allotonic fluid used as a negative control was previously purified by Jacqui Pugh (University of Southampton). In this study, it was assumed that the F protein and BBG2NA (containing RSV G protein core region) expressed by the virus were not incorporated into the virion, based on advice through communication with Ultan Power (Personal communication: email to Alastair Watson, 5th May 2014). Through collaboration with Tom Wilkinson, Karl Staples and C Mirella Spalluto (University of Southampton) the M37 clinically relevant A2 strain of RSV (Ambsio, UK) (309) and bronchial epithelial AALEB cells (310) were provided.

HIV reagents were provided by NIH AIDS Research and Reference Reagent Program, UK. These included recombinant HIV gp120 (BaL), HIV gp120 (IIIB) and gp140 (CN54) proteins. In addition, whole HIV BaL and HIV MN viral particles were also provided which had been inactivated using AT-2, as previously described (304). Negative controls for inactivated HIV virus were also provided by NIH AIDS Research and Reference Reagent Program which were NVCL controls prepared from the cells used to amplify the HIV virus strains including H9 T cell line lysate for the HIV BaL negative control (311) and SupT1-R5 T cell line MN negative control (312).

7.2.2 Solid Phase Binding

7.2.2.1 *Mannan Binding Assay*

Maxisorp plates were coated with 100 µl of mannan (50 µg/ml) in 0.1 M $NaHCO_3$, pH 9.6 at 4 °C overnight. Plates were washed 4 times with 200 µl of TBS with 0.05 % Tween-20 (v/v) and blocked with 150 µl of TBS with 2 % low endotoxin, fatty-acid free BSA (w/v) (block buffer) for 6 hours at room temperature. 100 µl of nhSP-A or rfhSP-A were incubated at varying concentrations in either TBS with 10 mM $CaCl_2$ (TBSC) or TBS with 50 mM EDTA (TBSE) at 4 °C overnight with subsequent washing four times with 200 µl of either TBSC or TBSE. Detection was undertaken with a polyclonal rabbit α-nhSP-A primary antibody diluted 1:1,000 (produced in house). After subsequent washing four times with 200 µl of TBSC, binding was detected by incubation with a secondary antibody of goat α-rabbit-HRP conjugated antibody diluted 1:10,000 (Table 2-1). After incubation with the secondary antibody, four final washes were undertaken with 200 µl of TBSC with 0.05 % Tween-20. Incubations with antibodies were undertaken for 1 hour at room temperature with 100 µl of antibody diluted in block buffer with 10 mM $CaCl_2$. Binding was detected by addition of 100 µl of TMB reagent mix with subsequent inhibition of reaction after 15 mins with 0.5 M H_2SO_4. Absorbance was measured at OD = 450 nm using a SpectraMax 340PC Microplate Reader spectrophotomer (Molecular Devices, USA).

7.2.2.2 *Inhibition Assay with Soluble Ligands*

Inhibition assays were undertaken similarly to the mannan binding assay described above but with incubations of 5 µg/ml of either rfhSP-A or nhSP-A with increasing concentrations of soluble ligands in the presence of calcium, as previously described (58). Soluble ligands included mannan, mannose, maltose, ManNAc, glucose, LPS from *E. coli* 0111:B4 (smooth LPS) and LPS from *E. coli* E4100 Ra (rough LPS).

7.2.3 SPR

SPR was undertaken using a Biacore T100 biomolecular interaction analysis system which allows real-time biomolecular interaction analysis (BIA) using SPR technology.

7.2.3.1 *Immobilisation of Ligands*

Proteins were immobilised onto a CM5 Biacore chip (GE Healthcare) by amine coupling using an amine coupling kit (GE Healthcare). During this process, the chip surface was activated using a mixture of 1-ethyl-3-(3-dimethylaminopropyl) carbodiimide hydrochloride (EDC) and N-hydroxysuccinimide (NHS). Proteins were diluted to 50 μg/ml in 10 mM NaOAc buffer (pH 5.0) (Bio-Rad); 10 mM NaOAc buffer (pH 5.0) was selected as the best buffer for immobilisation of rfhSP-A after comparison of the same buffer at pH values of 4.0, 4.5 and 5.5 using a test immobilisation which was undertaken without activation of the surface with EDC/NHS. During test immobilisations, a target of 2000 response units was set. However, due to an inability to immobilise rfhSP-A, the maximum number of response units achievable was targeted. For rfhSP-A this was 690 response units, for nhSP-A 909 response units and for nhSP-D 4500 response units. 2000 response units of HIV gp120 (BaL), HIV gp120 (IIIB) and gp140 (CN54) recombinant proteins were also immobilised onto an additional CM5 Biacore chip as above to allow use of rfhSP-A, nhSP-A and nhSP-D as analytes for any impact of immobilisation on binding to be discerned. The first of the four flow cells on the CM5 chips was left blank to allow any non-specific binding to the chip to be subtracted from the binding to the surface with immobilised ligand.

7.2.3.2 *Analytes*

The capacity for various analytes to be bound by the immobilised collectins was tested. These included carbohydrate and bacterial LPS analytes in addition to various RSV and HIV analytes. Carbohydrate analytes used for SPR included mannan as well as maltosyl-BSA. Bacterial LPS analytes used for SPR included *H. influenzae* strain RM153 Eagan wild type and *H. influenzae* strain RM153 Eagan 4A mutant LPS, LPS from *K. pneumoniae* as well as Smooth LPS from *E. coli* 0111:B4. RSV analytes used for SPR included recombinant RSV pre and post-fusion F proteins. In addition, Sendai virus expressing either RSV F protein (Sendai F) or BBG2Na (Sendai G) in addition to the

negative control of allotonic fluid were used as analytes. Whole inactivated RSV A (Memphis 37 strain) virus amplified in HEp-2 cells (as described in Section 7.2.6) was also used as an analyte in addition to NVCL control. Prior to use, Sendai and RSV virus analytes were inactivated by treatment with ultraviolet light for 40 mins. HIV analytes used for SPR included recombinant HIV gp120 (BaL), HIV gp120 (IIIB) and gp140 (CN54) proteins. In addition, whole AT-2 inactivated HIV BaL and HIV MN viral particles as well as their corresponding NVCL negative controls were used.

Analytes were diluted in either HBS-P with 5 mM $CaCl_2$ or HBS-EP (containing 3 mM EDTA) (GE Healthcare) as following: Sendai F, Sendai G, allontoic fluid, inactivated RSV, NVCL, inactivated HIV MN particle and inactivated HIV BaL particle analytes were diluted to 100 µg/ml; all other analytes were diluted to 10 µg/ml. rfhSP-A and nhSP-D in addition to nhSP-A purified from two separate patients were also used as analytes to investigate their capacity to bind immobilised HIV gp120 (BaL), HIV gp120 (IIIB) and gp140 (CN54) and to investigate the impact of immobilising the collectins on their ability to bind ligands. Collectins were diluted as above to 10 µg/ml.

7.2.3.3 *Binding*

After 60 secs of equilibration of the CM5 chip with immobilised ligands in either HBS-P 5 mM $CaCl_2$ or HBS-EP buffer, analytes were flown over the chip for 120 sec, after which, analytes were allowed to dissociate in HBS-P 5 mM $CaCl_2$ or HBS-EP buffer for 90 secs. Samples and buffers were flown at 10 µl/min. Between each sample the flow cells were regenerated in HBS-EP buffer to remove any bound analytes. Changes in response units were recorded and the changes in response units for the empty flow cell subtracted from the results for each ligand to account for any non-specific binding. Data were analysed using BIAevaluation software (version 4.1) and BIAsimulation software (version 3.1).

7.2.3.4 *Analysing Ratios for Comparative Binding Levels*

For analytes of a known molecular weight, the ratio of number of bound analyte molecules: number of immobilised collectin trimers was calculated to give an indication of the amount that the ligand binds to the analyte. To do this the below equation was used:

$$Ratio = 1: \frac{\frac{MW\ of\ analyte}{MW\ of\ trimer} \times Immobilised\ RU}{Bound\ RU}$$

The used predicted Molecular weight (MW) of trimers was 57 kDa, 105 kDa and 130 kDa for rfhSP-A, nhSP-A and nhSP-D, respectively. For rfhSP-A, nhSP-A and nhSP-D, 690, 909 and 4500 Response units (RU) were immobilised onto the chip, respectively. The amounts of analyte bound (RU) were read at the maximum level at the time point of 175 sec with any non-specific binding to the empty flow cell subtracted. Mannan was prepared by alkaline degradation and as previously described yields polymers of approximately 40 kDa (313). Maltosyl-BSA and BSA have a known molecular weight of 66 kDa. For LPS, the molecular mass is 10-20 kDa (according to product information, Sigma-Aldrich). However, it is important to note that LPS is heterogeneous and forms aggregates of varying sizes. For calculation of ratios, a value of 15 kDa was used. Recombinant RSV pre and post-fusion F proteins have a known molecular weight of 70 kDa and 68 kDa, respectively. Likewise the F protein and BBG2Na (G protein) expressed by the Sendai virus have known molecular weights of 70 kDa and 39 kDa respectively. During calculation of ratios it was assumed that the F and BBG2Na proteins were individual soluble proteins and were not incorporated into the Sendai virus virion. This was due to advice from Ultan Power (Personal communication: email to Alastair Watson, 5th May 2014). However, should this not be the case, the number of RSV F or BBG2Na proteins binding would be considerably lower due to the majority of the RU being due to the virion which the protein is incorporated within. Recombinant gp120 and gp140 proteins have a known molecular weight of 120 and 140 kDa respectively. However, the molecular weight of whole inactivated HIV particles, house dust mite or pollen extracts or whole RSV virions was unknown and ratios could not be calculated. Due to the multimeric nature of the collectins it was not possible to determine kinetic binding constants. Moreover, some analytes, have multiple residues available to be bound by the collectins or a multimeric nature adding further complexity. This ratio was only calculated for rough interpretation of relative binding and caution must be used when interpreting the relative levels of binding, no concrete conclusions were drawn through comparing relative binding in this present study.

7.2.4 Western Blot Analysis for Detection of RSV F protein

Western blot analysis was undertaken as described in Section 2.5 however using a monoclonal mouse α-RSV A strain F primary antibody (Ambsio, Oxford, UK, Cat~

C01626M, Lot# 5H24412, Clone # B1358M) diluted 1:1,000 with subsequent use of a HRP-conjugated Goat α-Mouse IgG (H+L) antibody (Life Technologies, UK) (62-6520) diluted 1:10,000.

7.2.5 Culturing AALEB cells

Cryo-preserved AALEB cell stocks were thawed rapidly in a water bath at 37 °C, transferred to 10 ml of pre-warmed BEGM media (Lonza) with fetal bovine serum and recommended supplements (BEGM SingleQuot Kit Suppl. & Growth Factors, Lonza) (Culture media) according to manufacturer's instructions (Lonza). After centrifugation at 400 x g for 5 mins, the supernatant was removed and AALEB cells were resuspended in 12 ml of pre-warmed culture media and transferred to T75 flasks. Surfaces used for AALEB culture were pre-coated with collagen (ThermoFisher Scientific) according to manufacturer's instructions; this included T75 flasks and 24 well plates. Cells were cultured at 37 °C with 5 % CO_2. AALEB cells were grown to 80 % confluency and split through washing with 10 ml of phosphate-buffered saline (PBS) and subsequent incubation with 2 ml of trypsin-EDTA (0.25 %) (ThermoFisher Scientific). Trypsin was inactivated by addition of 8 ml of culture media, which was subsequently removed after centrifugation at 400 x g for 5 mins. AALEB cells were resuspended in 12 ml of culture media and transferred back to the T75 flask or seeded into 24 well plates at a concentration of 1 x 10^6 AALEB cells in log phase growth per plate.

7.2.6 Generation of RSV stocks

2 x 10^6 HEp-2 cells in log phase growth were seeded per T75 flask and grown to approximately 80 % confluency over 24 hours in DMEM with 4 mM L-glutamine 10 % FCS (v/v). Cells were washed three times in DMEM, 4 mM L-glutamine, after which, they were infected with 12.5 µl of RSV M37 diluted in 4 ml DMEM with 4 mM L-glutamine per T75 flask whilst incubating at 37 °C with agitation. After 2 hours, RSV containing media was removed and 13 ml of new DMEM with 4 mM L-glutamine was applied to the cells. Cells were then left to incubate for 72 hours at 37 °C. Cells were detached from the plates through shaking with glass beads. Cells were lysed by mixing the following: detached cells, media and beads. This was undertaken with 6 cycles of 10 secs of mixing using a vortex and 10 secs of resting on ice. Glass beads and cell debris

were removed by centrifugation at 400 x g for 5 mins. This was repeated for the resultant supernatant, after which, sucrose was added to a final concentration of 10 % (v/v). The viral stock was then aliquoted into 500 µl aliquots, snap frozen and stored at -80 °C. For use as a negative control in binding and infection assays, HEp-2 NVCL was also processed and stored at -80 °C.

7.2.7 Focus Forming Assay

AALEB cells were cultured in 24 well plates to 80 % confluency, serum starved in BEGM media without supplements and without serum but with 1 x ITS and 0.02 % BSA (w/v) (starvation media) for 24 hours. Cells were then infected as above, with varying doses of RSV and left for either 24, 48 or 72 hours. After washing with PBS, cells were fixed in 80 % methanol and left at -20 °C overnight. Plates were blocked in PBS with 5 % (w/v) skimmed milk (blocking solution) for 30 mins at room temperature and stained for 1 hour at room temperature with monoclonal mouse α-RSV A strain F primary antibody (same antibody as above) diluted 1:2,000 in blocking solution. Wells were washed twice in blocking solution and stained for 1 hour at room temperature with goat α-mouse HRP-conjugated secondary antibody (Table 2-1) diluted 1:1,000 in blocking solution. Wells were washed twice with PBS and stained with 3,3′-Diaminobenzidine (DAB) (Abcam, UK) according to manufacturer's instructions. The RSV titres were determined by counting numbers of infected cell foci by light microscopy after 48 hours. Focus forming units (FFU)/ml were calculated using the following formulae:

$$FFU/ml = \frac{Number\ of\ Foci}{(Volume\ of\ Media\ (ml)\ x\ Dilution\ Factor)}$$

Representative images of cells infected with different dilutions of virus were taken using an Olympus IX microscope (Olympus, UK) with a x 4 and x 10 objective lens, images were produced using Cell^{p} software (Olympus).

7.2.8 Infection of AALEB cells

AALEB cells were seeded into each 24 well plate and grown to 80 % confluency in culture media. 24 well plates were pre-coated with collagen according to manufacturer's instructions. Cells were then serum starved for 24 hours with starvation media (serum

free). Cells were infected with RSV-A M37 diluted in DMEM with 4 mM L-glutamine (infection media) at a multiplicity of infection (MOI) of either 0.08 or 0.4 for 2 hours at 37 °C. To investigate the capacity of collectins to neutralise RSV, prior to infection of the cells, RSV was preincubated either with gel filtration buffer and no collectin or with varying concentrations of rfhSP-A, rfhSP-D (produced through refolding or using NT^{dm}), nhSP-A, nhSP-D or dimeric rfhSP-A in gel filtration buffer for 1 hour at 37 °C; BSA was also used as a negative control. Cells were infected for 2 hours with 200 µl of the neutralised RSV, after which soluble RSV was removed and cells were washed twice with 500 µl of infection media. Infected cells were left for 24 hours in starvation media for infected RSV to amplify.

7.2.9 Quantifying RSV Neutralisation by RT-qPCR

7.2.9.1 *Harvesting RNA*

RNA was harvested from cells infected at an MOI of 0.08 using peqGOLD TriFast (Peqlab, Germany), according to manufacturer's instructions and stored at -80 °C until use. The RNA concentration and quality were determined using a NanoDrop 1000 (Thermo Scientific, USA). RNA with a 260/280 ratio of greater than 1.8 were used for synthesis of cDNA.

7.2.9.2 *Synthesis of cDNA*

cDNA was generated by reverse transcription carried out in 20 µl reactions with 500 ng of RNA, 2 µl of 10 x RT buffer, 2 µl of 10 x RT random primers, 0.8 µl of dNTP mix, 1 µl of MultiScribe Reverse Transcriptase and 1 µl of RNase Inhibitor (all AB Biosciences, Allston, USA). Water was added accordingly to reach a final volume of 20 µl dependent on the concentration of RNA.

7.2.9.3 *qPCR*

RSV infection and amplification was quantified by analysis of RSV N gene expression, using previously designed primers (314). RT PCR was undertaken in 5 µl reactions with 2.5 µl of High-Capacity cDNA Reverse Transcription Kit, 1.25 µl water and 0.25 µl of both forward and reverse primers. PCR was undertaken with an Applied Biosystems 7900HT Fast Real-Time PCR System machine with, after initiation with a 95 °C hot lid start for 10 mins, 40 cycles of: 15 secs at 90 °C, 60 secs at 60 °C. Thresholds were set

where DNA amplification was in the log-linear phase of DNA amplification. Expression of RSV N gene was normalised against expression of Hypoxanthine Phosphoribosyltransferase 1 (HPRT1) housekeeping gene using the $2^{-\Delta Ct}$ method. To ensure a single specific amplification product, melt curve analysis was undertaken between 50-95 °C using SDS v2.4 software (2012); melting temperatures were calculated using the BioMath - Tm Calculator for Oligos (Promega, 2002) (315). Average % relative infection was then calculated by normalisation against the RSV infected control which was pre-incubated without collectin.

7.2.10 Quantifying RSV Neutralisation by Flow Cytometry

Cells infected with an MOI of 0.4 were analysed by flow cytometry. Infected cells were detached from wells using 2 drops per well (using a Pasteur pipette) of trypsin-EDTA (0.25 %). Cells were left to detach for 5 mins at 37 °C after which the trypsin was inactivated by addition of 500 µl of infection media with 10 % fetal bovine serum. Cells were further detached from the wells by pipetting up and down twice with a Pasteur pipette with subsequent aliquoting into 5 ml polypropylene (round-bottom) tubes (BD Biosciences, UK). 100 µl of each cell suspension was pooled, mixed and split into three for use as controls which were either unstained, stained with primary antibody only or stained with secondary antibody only. Cell suspensions were washed by addition of 2 ml of PBS and vortexing with subsequent centrifugation at 400 x g for 5 mins (4 °C) and removal of supernatants.

Cells were fixed in 200 µl of Cytofix/Cytoperm (BD Biosciences) at 4 °C for 20 mins. Cells were then washed in 1 ml of 1 x Perm/Wash (final concentration) (BD Biosciences) diluted in PBS, 2 mM EDTA, 0.5 % (w/v) BSA (FACS buffer). Cells were stained by incubation with 100 µl of mouse α-RSV-F protein primary antibody (antibody described in Section 7.2.4) diluted 1 in 200 in 1 x Perm/Wash (diluted as above) with 10 µl of Fcγ blocker (Invitrogen). Cells were subsequently washed with 0.5 ml of Perm/Wash (diluted as above) and stained with 100 µl of goat α-mouse antibody (H+L) conjugated with Alexa-Fluor 488 2° antibody (Invitrogen, A11001, Lot 56881A) at 4 °C for 30 mins. Cells were then washed twice with 0.5 ml of 1 x Perm/Wash (diluted as above), suspended in 350 µl of FACS buffer and analysed using a FACSAria cell sorter (BD Biosciences). 10,000 events were recorded. AALEB cells were gated for according to forward and side

scatter. Cells were regarded as infected if above the fluorescence threshold which was set to approximately 1 % of the uninfected control. The proportion of cells which were infected were approximately 30-40 % of AALEB cells in the no collectin control. Average relative percentage infection was calculated by normalisation to this control.

7.2.11 Statistical Analysis

To calculate statistical significance of reductions in RSV infection compared to the control of RSV incubated without collectin, an unpaired two tailed student's t-test with equal variance was used. To calculate significant differences between treatments with different collectins, a two-way ANOVA with multiple comparisons was used corrected using the Bonferroni method.

7.3 Results

7.3.1 Solid Phase Binding of Collectins

To confirm the capacity of purified rfhSP-A and rfhSP-D proteins to bind to mannan, their ability to bind to immobilised mannan was compared with that of nhSP-A and nhSP-D. rfhSP-A, rfhSP-D and nhSP-D bound to mannan in a calcium-dependent manner (Figure 7-1). Upon increasing the concentration of the collectins, increasing levels of bound collectin were detected by the corresponding antibody. This binding was inhibited in the presence of EDTA. nhSP-A also bound to immobilised mannan in the presence of calcium. However, this was only partially inhibited by EDTA at concentrations lower than 1.25 μg/ml.

To test the capacity of rfhSP-A and nhSP-A to bind additional ligands, they were applied to mannan coated plates in the presence of increasing concentrations of various soluble ligands (Figure 7-2 and Figure 7-3, respectively). Addition of soluble mannan prevented the binding of both rfhSP-A and nhSP-A (Figure 7-2A and Figure 7-3A, respectively), confirming their capacity to bind to mannan and not non-specifically to the plate. Smooth soluble *E. coli* LPS also inhibited the binding of both rfhSP-A and nhSP-A to mannan coated plates (Figure 7-2F and Figure 7-3F, respectively). Maltose, glucose and rough LPS from *E. coli* inhibited the binding of nhSP-A but not rfhSP-A to mannan coated plates (Figure 7-2C, E and G and Figure 7-3 C, E and G, respectively). However, soluble mannose and ManNAc did not inhibit the binding of rfhSP-A or nhSP-A to mannan coated plates (Figure 7-2B and D and Figure 7-3B and D, respectively).

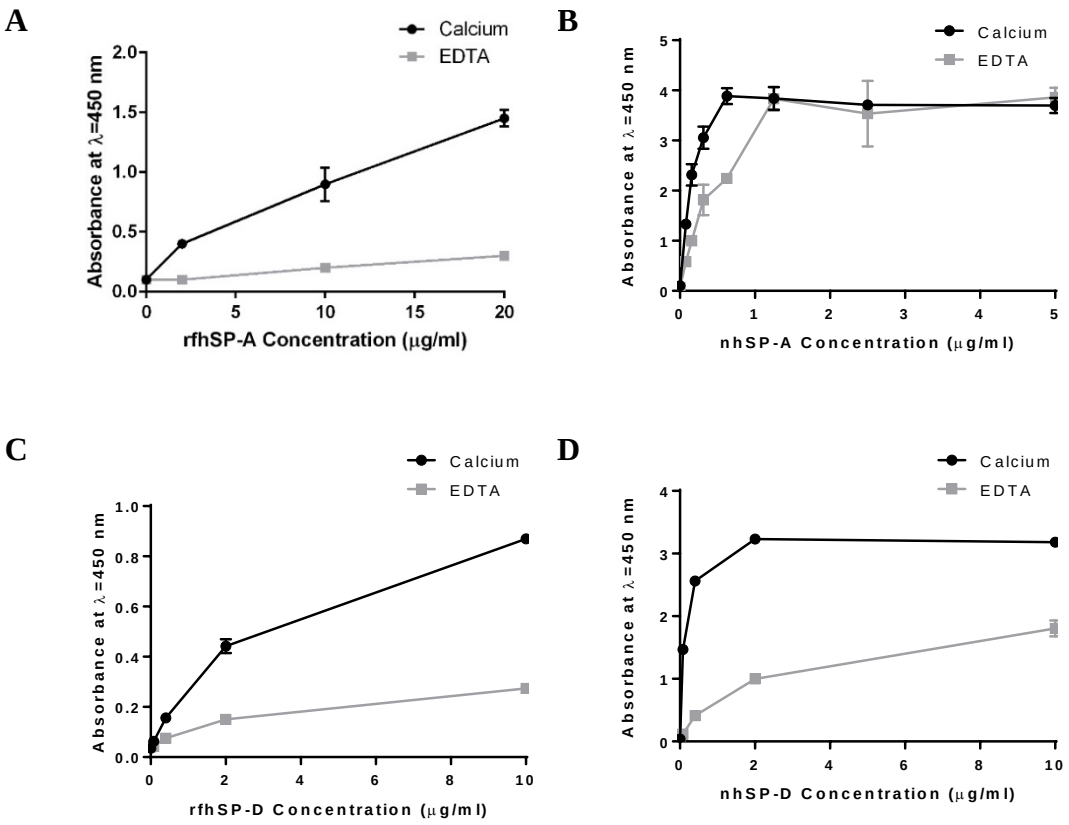

Figure 7-1: Binding of collectins to immobilised mannan. *Increasing concentrations of rfhSP-A produced using NT (**A**) nhSP-A (**B**), rfhSP-D (produced by refolding) (**C**) or nhSP-D (**D**) were applied to maxisorp plates in the presence of calcium or EDTA. Plates had been coated with 100 µl of 50 µg/ml of mannan and subsequently blocked. After washing, binding was detected with either an α-nhSP-A antibody or an α-rfhSP-D antibody with subsequent detection using a HRP conjugated antibody; absorbance at λ = 450 nm was detected after application of TMB reagent. Shown is the mean of one experiment ± SD, experiments were undertaken in triplicates.*

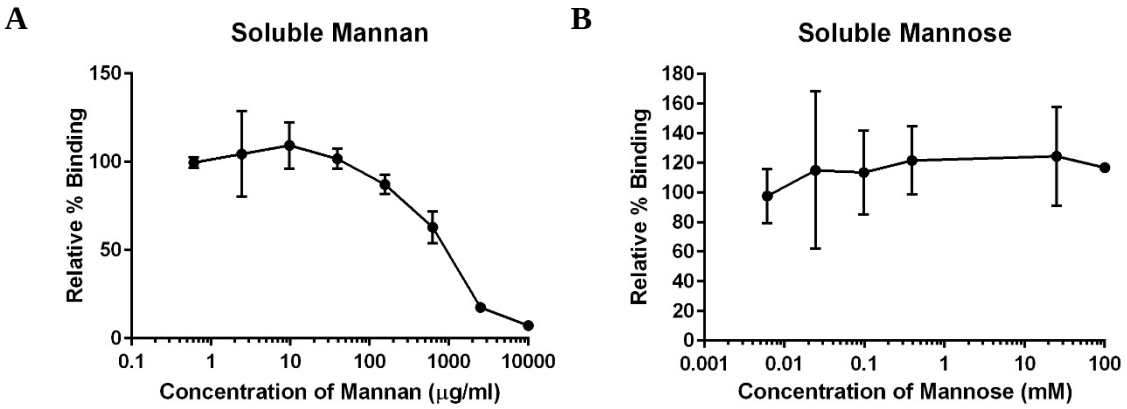

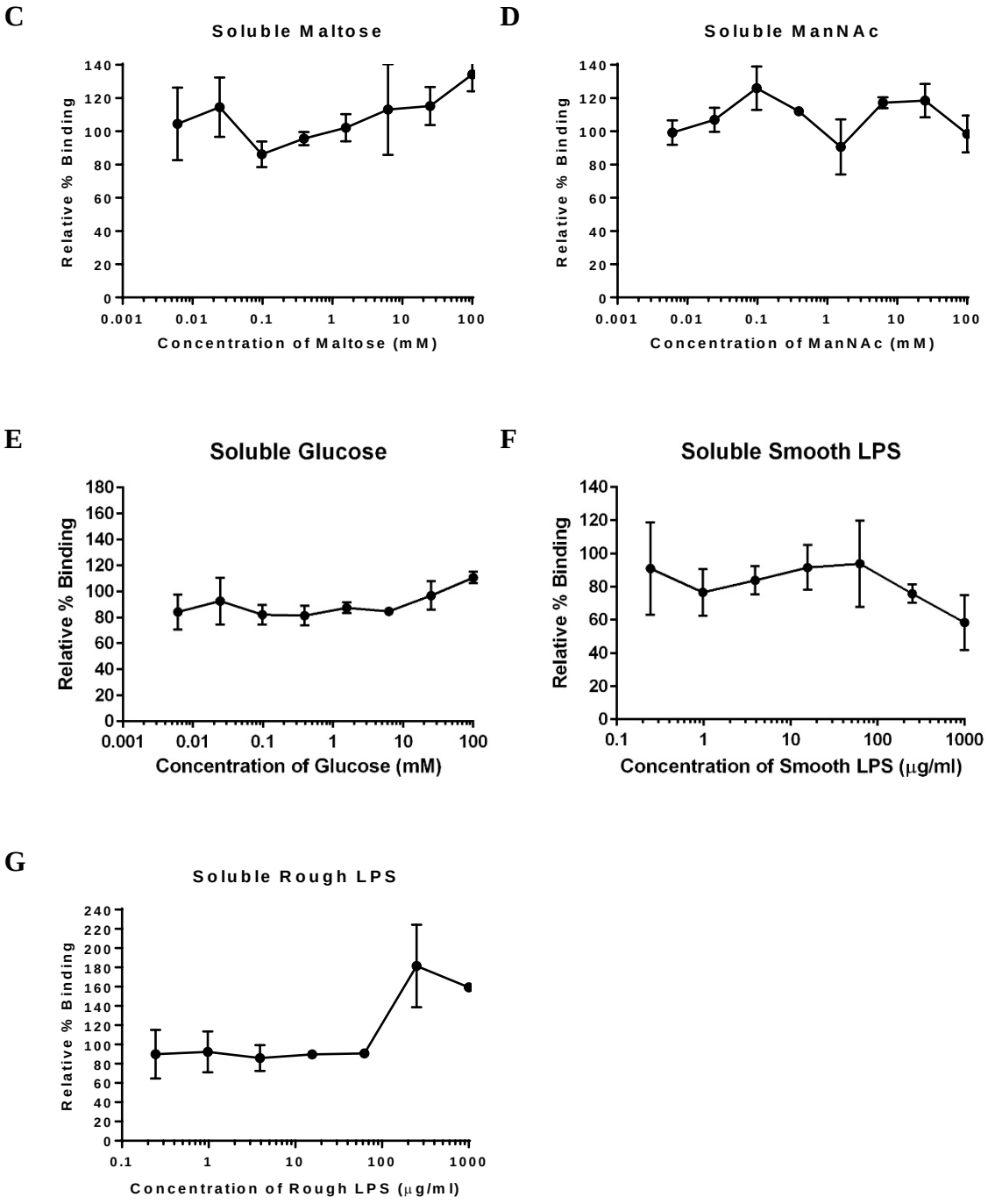

Figure 7-2: Binding of rfhSP-A to different ligands. *5 μg/ml of rfhSP-A produced using NT was applied to mannan-coated maxisorp plates in the presence of both calcium and increasing concentrations of soluble ligands. Plates had been coated with 100 μl of 50 μg/ml of mannan and subsequently blocked. Soluble ligands tested included mannan (A), mannose (B), maltose (C), ManNAc (D), glucose (E), smooth LPS from E. coli (H) and rough LPS from E. coli (G). After washing, binding was detected using an α-nhSP-A antibody with subsequent detection using a HRP conjugated antibody; absorbance at λ = 450 nm was detected after application of TMB reagent. Shown is the mean of one experiment ± SD, experiments were undertaken in triplicates.*

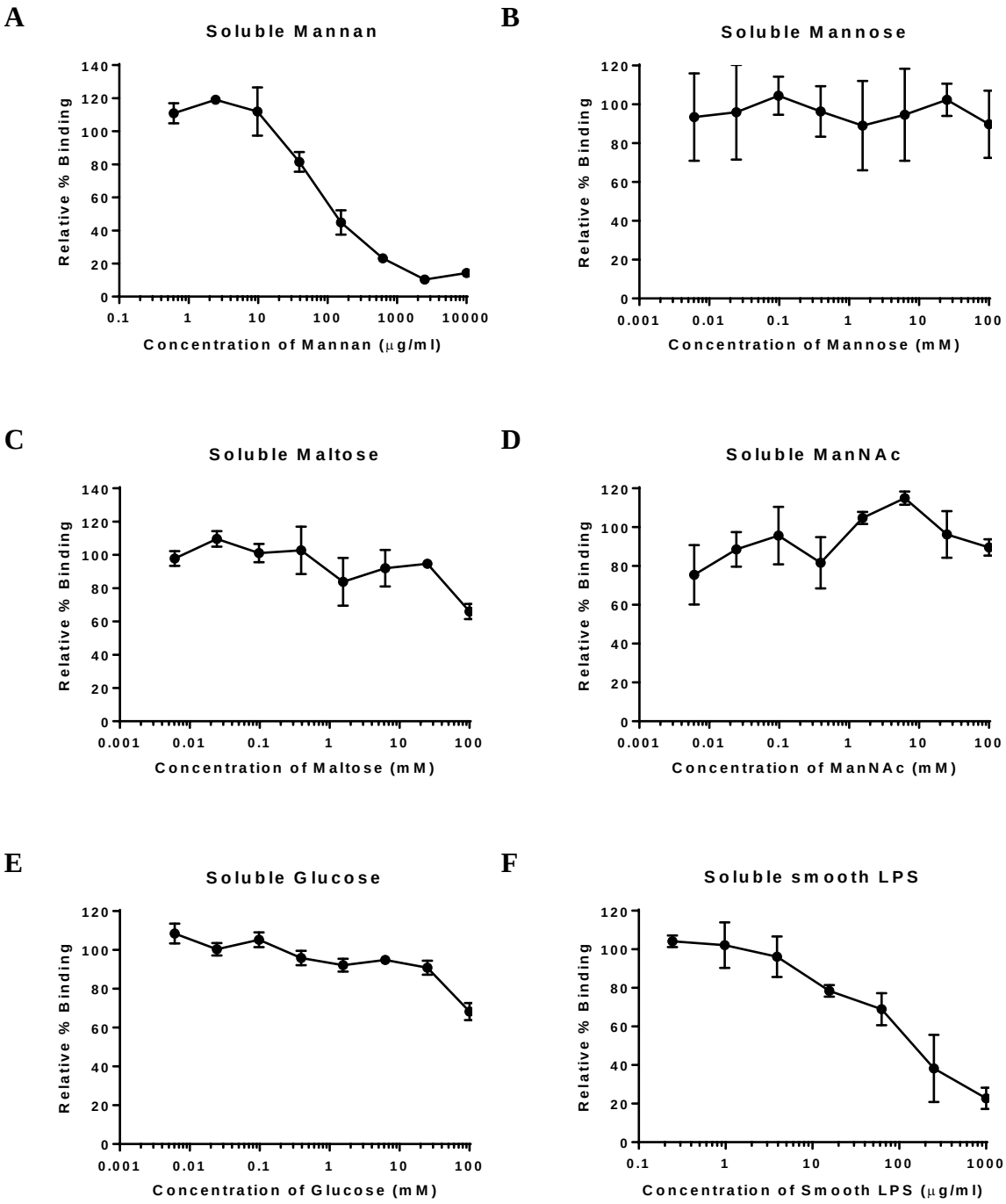
A
Soluble Mannan
Relative % Binding
Concentration of Mannan (μg/ml)
B
Soluble Mannose
Relative % Binding
Concentration of Mannose (mM)
C
Soluble Maltose
Relative % Binding
Concentration of Maltose (mM)
D
Soluble ManNAc
Relative % Binding
Concentration of ManNAc (mM)
E
Soluble Glucose
Relative % Binding
Concentration of Glucose (mM)
F
Soluble smooth LPS
Relative % Binding
Concentration of Smooth LPS (μg/ml)

G

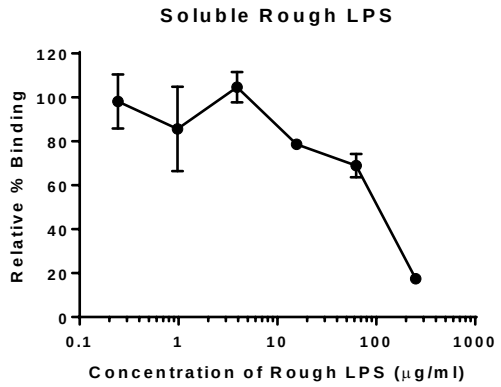

Figure 7-3: Binding of nhSP-A to different ligands. *5 μg/ml of nhSP-A was applied to mannan-coated maxisorp plates in the presence of both calcium and increasing concentrations of soluble ligands. Plates had been coated with 100 μl of 50 μg/ml of mannan and subsequently blocked. Soluble ligands tested included mannan (A), mannose (B), maltose (C), ManNAc (D), glucose (E), smooth E. coli LPS (H) and rough LPS from E. coli (G). After washing, binding was detected using an α-nhSP-A antibody with subsequent detection using a HRP conjugated antibody; absorbance at λ = 450 nm was detected after application of TMB reagent. Shown is the mean of one experiment ± SD, experiments were undertaken in triplicates.*

7.3.2 SPR

To further characterise the capacity of rfhSP-A to bind to various ligands SPR was implemented where rfhSP-A was immobilised onto a Biacore sensor chip and various carbohydrate, LPS, RSV and HIV analytes were flown over to detect binding.

7.3.2.1 *Immobilisation of rfhSP-A*

It was first essential to immobilise the recombinant proteins onto a Biacore chip. Initial tests indicated that only low levels of rfhSP-A were effectively immobilised onto the biosensor chip. The amine coupling immobilisation conditions were therefore optimised using 10 mM sodium acetate at various pH values (Figure 7-4). rfhSP-A immobilised to the chip most effectively in 10 mM sodium acetate at pH 5.0 with 580 response units being immobilised after 100 secs compared with 99, 700, 95 and 0 response units at pH values of 5.5, 5.0, 4.5 and 4.0 respectively. Immobilisation using 10 mM sodium acetate at pH 5.0 was therefore chosen for immobilisation of rfhSP-A to the chip.

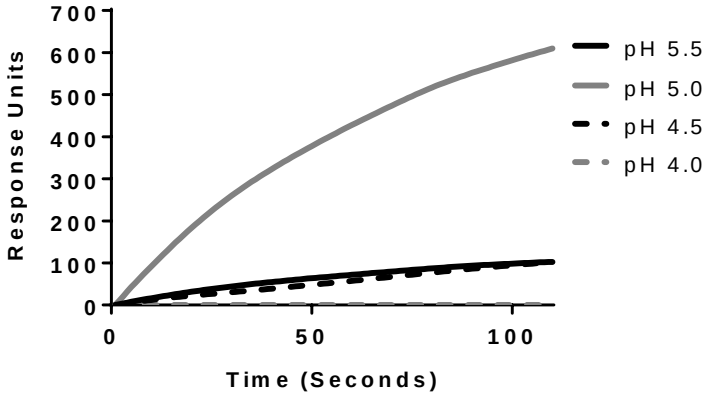

Figure 7-4: Optimisation of conditions for optimal immobilisation of rfhSP-A to a Biacore chip.*The capacity of rfhSP-A to bind to a Biacore sensor chip was tested in 10 mM sodium acetate buffer over 120 seconds at different pH values: pH 5.5, 5.0, 4.5 and 4.0. The level of immobilisation is shown as measured by level of response units.*

7.3.2.2 *Assessment of RSV Analytes by SDS-PAGE*

The purity of RSV analytes was then investigated to give an indication of the level of contamination for each of the analytes; this was undertaken by SDS-PAGE. The purified recombinant pre and post-fusion F proteins were pure with the F1 subunit being clearly seen at approximately 45 kDa expected size (Figure 7-5A). As expected, the post-fusion F1 subunit was slightly smaller than the pre-fusion due to it lacking 10 amino acids. The F2 subunit could also be seen, which was of the approximately 25 kDa expected size for both the pre and post-fusion F protein. No protein contaminants could be detected by SDS-PAGE with Coomassie staining.

Upon analysis of Sendai virus expressing recombinant F protein, no 45 kDa or 25 kDa bands could be discerned above the background protein from the lysed virus and contaminating allotonic fluid (Figure 7-5B). This was also found for Sendai virus expressing the recombinant central domain of G protein (BBG2Na) where no 39 kDa protein could be seen above the background protein contamination.

Similarly, no 45 kDa or 25 kDa bands for RSV F protein or approximately 90 kDa bands for full-length RSV G protein could be seen in the RSV virus stock. The protein bands seen looked similar between the RSV stock and the control cell lysate from the HEp-2 cells in which the RSV was amplified, no additional bands could be discerned. Analytes

were also analysed by Western blot analysis for detection of F protein, with only RSV viral stocks containing immunoreactive proteins; results are presented in Section 7.3.3.4. Thus whole RSV and Sendai virus analytes were highly contaminated with only a small proportion of the total protein concentration (non-detectable by SDS-PAGE) being of the wanted analyte.

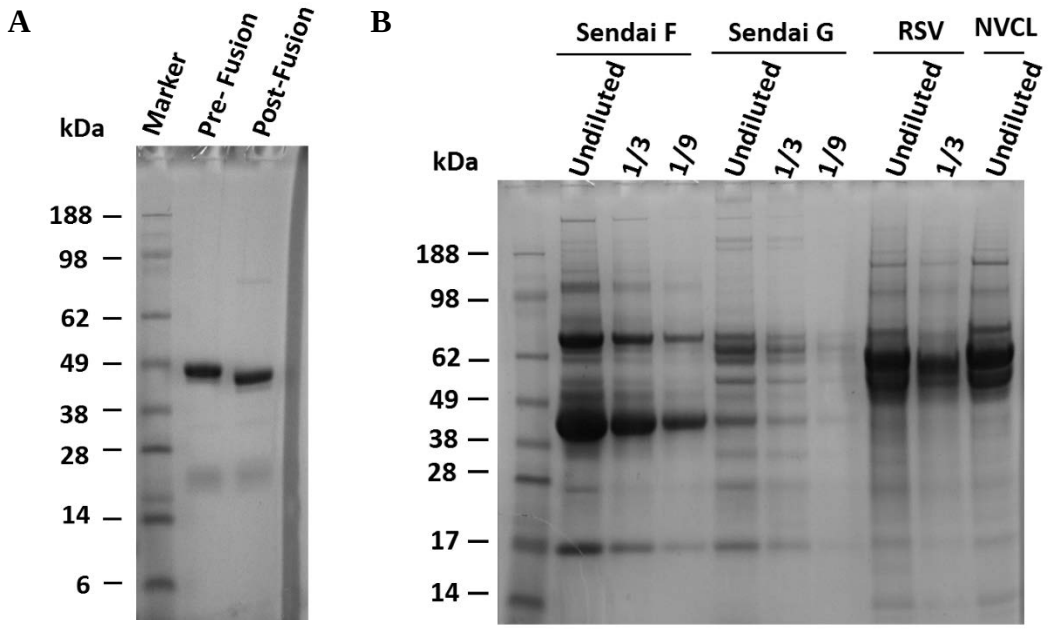

Figure 7-5: Analysis of analytes by SDS-PAGE. *Analytes to be used for SPR binding assays were assessed for purity using SDS-PAGE. Analysed were recombinant purified RSV F pre and post-fusion proteins (**A**). (**B**) Also analysed were Sendai virus expressing RSV F protein (Sendai F) and Sendai virus expressing the central domain for RSV G protein attached to albumin binding domain of Streptococcal protein G (BBG2Na) (Sendai G), both were grown in allotonic fluid. In addition, RSV viral stock used for infection assays (RSV) and negative control HEp-2 NVCL were analysed. Different dilutions of analytes were loaded onto the gel (Undiluted, 1/3 and 1/9).*

7.3.2.3 *Binding of rfhSP-A to Ligands*

To evaluate the capacity of various analytes to bind to rfhSP-A immobilised on a biacore sensor chip, analytes were flown over the chip for 120 seconds, after which running buffer was flown over the chip to allow the analyte to dissociate. Mannan was bound by immobilised rfhSP-A in a calcium-dependent manner, this was not seen in the presence

of EDTA (Figure 7-6A). Comparatively maltosyl BSA did not bind to immobilised rfhSP-A (data not shown).

rfhSP-A bound Sendai virus expressing recombinant BBG2Na (contaning core region of RSV G protein) at low levels in a calcium-dependent manner (Figure 7-6B). However, Sendai virus expressing F protein was not bound (Figure 7-6C) nor was allotonic fluid (Figure 7-6D). Whole inactivated RSV, NVCL, soluble pre-fusion F protein or soluble post-fusion F protein did not bind to immobilised rfhSP-A (Figure 7-6E, F, data not shown and data not shown, respectively).

rfhSP-A bound at low levels to the HIV protein gp120 IIIB in a calcium-dependent manner (Figure 7-6G). However, rfhSP-A did not bind to gp120 BaL, gp140CN54 or whole inactived HIV particles HIV MN or HIV BaL or their corresponding negative controls (data not shown).

Immobilised rfhSP-A did not bind to soluble house dust mite extracts from *D. farina* or *D. pteronyssinus* or to grass pollen extracts from *D. glomerata*, *P. nigra* or *Pao praensis* (data not shown). rfhSP-A bound at low levels to *K. pneumoniae* LPS (Figure 7-6H). However, it did not bind to *H. Influenza* LPS Eagan wild type, LPS Eagan 4A or smooth *E. coli* LPS (data not shown). Importantly, rfhSP-A also did not bind to BSA or buffer alone (Figure 7-6I and data not shown). The capacity of souble rfhSP-A to bind to immobilised gp120 IIIB, gp120 BaL or gp140 CN54 was also investigated to assess whether the inability of rfhSP-A to bind some analytes was an artefact of immobilisation. However, no binding was seen (data not shown).

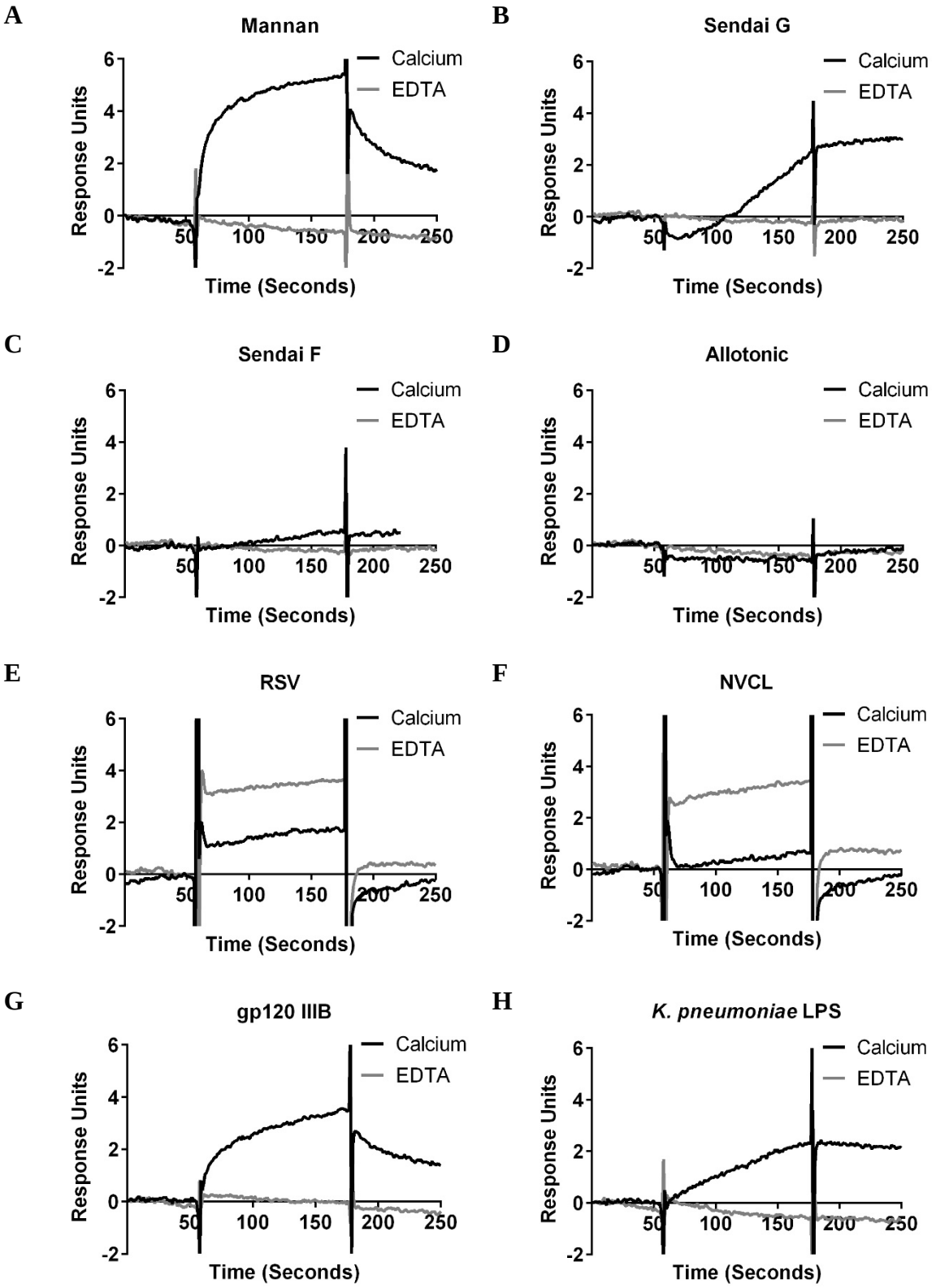
A
Mannan
B
Sendai G
C
Sendai F
D
Allotonic
E
RSV
F
NVCL
G
gp120 IIIB
H
K. pneumoniae LPS
Calcium
EDTA
Response Units
Time (Seconds)

I

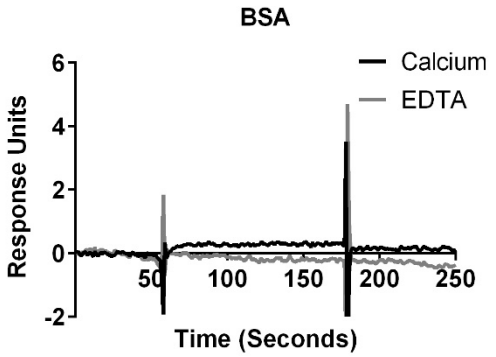

Figure 7-6: Binding of analytes to immobilised rfhSP-A analysed by SPR. *690 response units of rfhSP-A were immobilised by amine coupling to a Biacore sensor chip. After 60 secs of equilibration in buffer, analytes were flown over the chip for 120 secs either in HBS-P with 5 mM $CaCl_2$ (Calcium) or HBS-EP (containing 3 mM EDTA) (EDTA) and changes in response units recorded with any background binding to the empty flow cell subtracted. Buffer was subsequently flown over the chip to allow the analytes to dissociate. Analysed analytes included mannan (**A**), maltosyl BSA, purified RSV F protein pre-fusion, purified RSV F protein post-fusion, Sendai virus expressing BBG2Na (Sendai G) (**B**), Sendai virus expressing RSV F protein (Sendai F) (**C**), allotonic fluid (**D**), RSV viral stock (RSV) (**E**), RSV NVLC (**F**), purified HIV gp120 IIIB (**G**), purified gp120 BaL, purified gp140 CN54, inactivated HIV MN particles, NVCL from cells used to produce HIV MN (HIV MN –C), inactivated HIV BaL particles, NVCL from cells used to produce HIV BaL (HIV BaL –C), house dust mite extracts from D. farina and D. pteronyssinus, grass pollen extracts from D. glomerata, P. nigra and P. praensis, LPS from H. influenzae Eagan wild type and mutant Eagan 4A, LPS from K. pneumoniae (**H**), smooth LPS from E. coli and BSA as a negative control (**I**). Importantly, only positive results and selected negative results are included in figure. Shown are representative results of n = 2. Note y axes are different according to the scale of response units.*

7.3.2.4 *Binding of nhSP-A to Ligands*

nhSP-A also bound at low levels to mannan in a calcium-dependent manner (Figure 7-7A) and like rfhSP-A bound to Sendai virus expressing BBG2Na (contaning core region of RSV G protein) (Figure 7-7B). Contrasting to rfhSP-A, nhSP-A also bound at low levels to Sendai virus expressing F protein (Figure 7-7C). However, this binding was not inhibited in the presence of EDTA. Similarly to rfhSP-A, nhSP-A did not bind to allotonic fluid, whole inactivated RSV, AALEB NVCL, soluble pre-fusion F protein or soluble post-fusion F protein (Figure 7-7D, E, F, data not shown and data not shown, respectively).

However, similarly to rfhSP-A, nhSP-A bound at low levels to the HIV protein gp120 IIIB in a calcium-dependent manner (Figure 7-7 G). nhSP-A did not bind to gp120 BaL,

gp140 CN54 or whole inactived HIV particles HIV MN or HIV BaL or their corresponding negative controls (NVCL) (data not shown).

Immobilised nhSP-A did not bind to soluble house dust mite extracts from *D. farina* or *D. pteronyssinus* or to grass pollen extracts from *D. glomerata*, *P. nigra* or *P. praensis* (data not shown). nhSP-A also bound at low levels to *K. pneumoniae* LPS (Figure 7-7J). However, unlike rfhSP-A, nhSP-A also bound to *H. influenza* Eagan wild type, Eagan 4A and smooth E. coli LPS Figure 7-7H, I and K, respectively). Notably, more *H. influenza* Eagan 4A LPS was bound by nhSP-A than Eagan wild type LPS with response units of 6.4 compared with 1.56 after 175 secs. Importantly, nhSP-A did not bind to buffer alone (data not shown). However, it did bind to BSA at low levels (Figure 7-7L). The capacity of souble nhSP-A to bind to immobilised gp120 IIIB, gp120 BaL or gp140 CN54 was also investigated to assess whether the inability of rfhSP-A was an artefact of immobilisation. However, no binding was detected (data not shown).

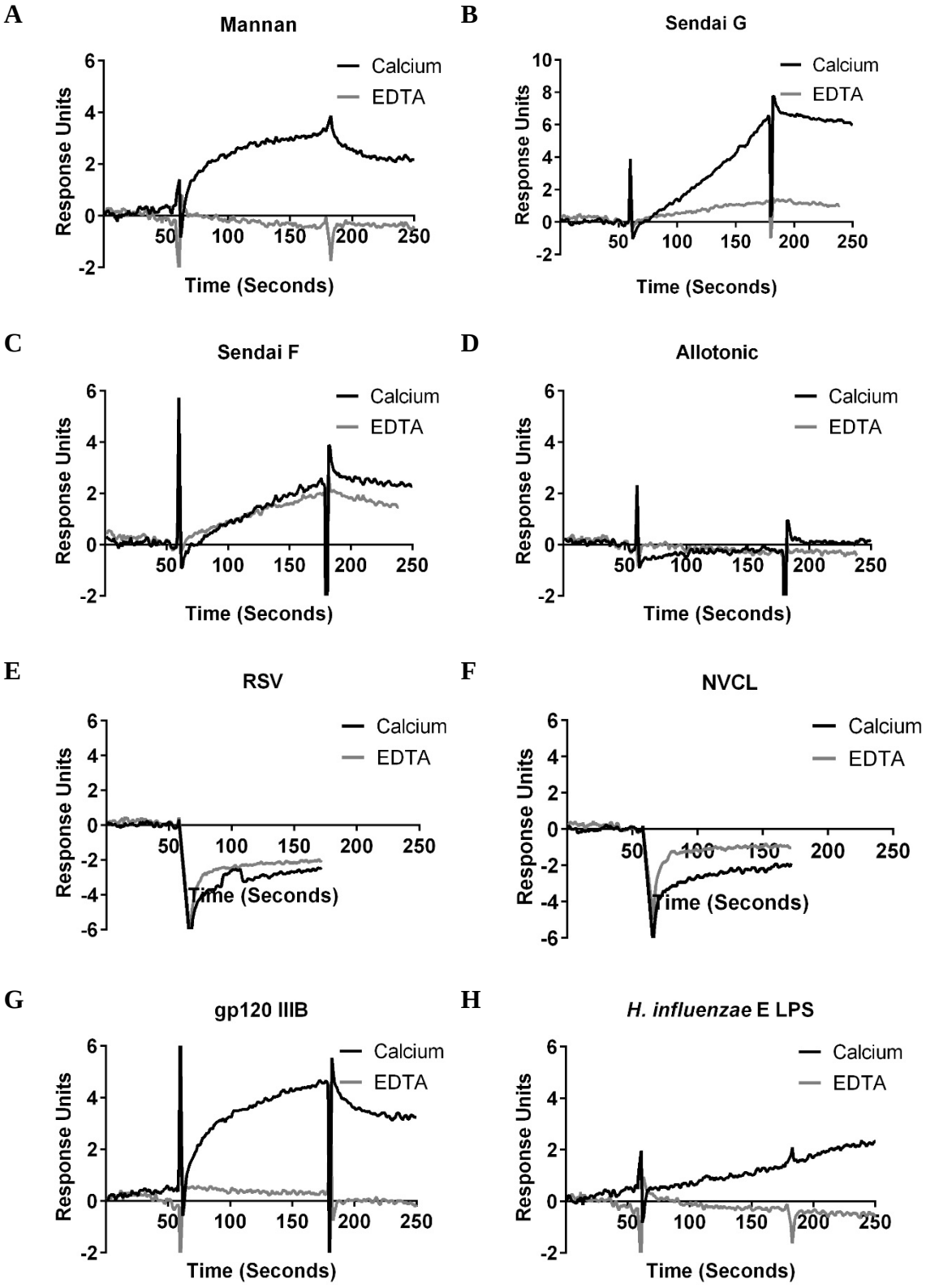
A
Mannan
Calcium
EDTA
Response Units
Time (Seconds)
B
Sendai G
C
Sendai F
D
Allotonic
E
RSV
F
NVCL
G
gp120 IIIB
H
H. influenzae E LPS

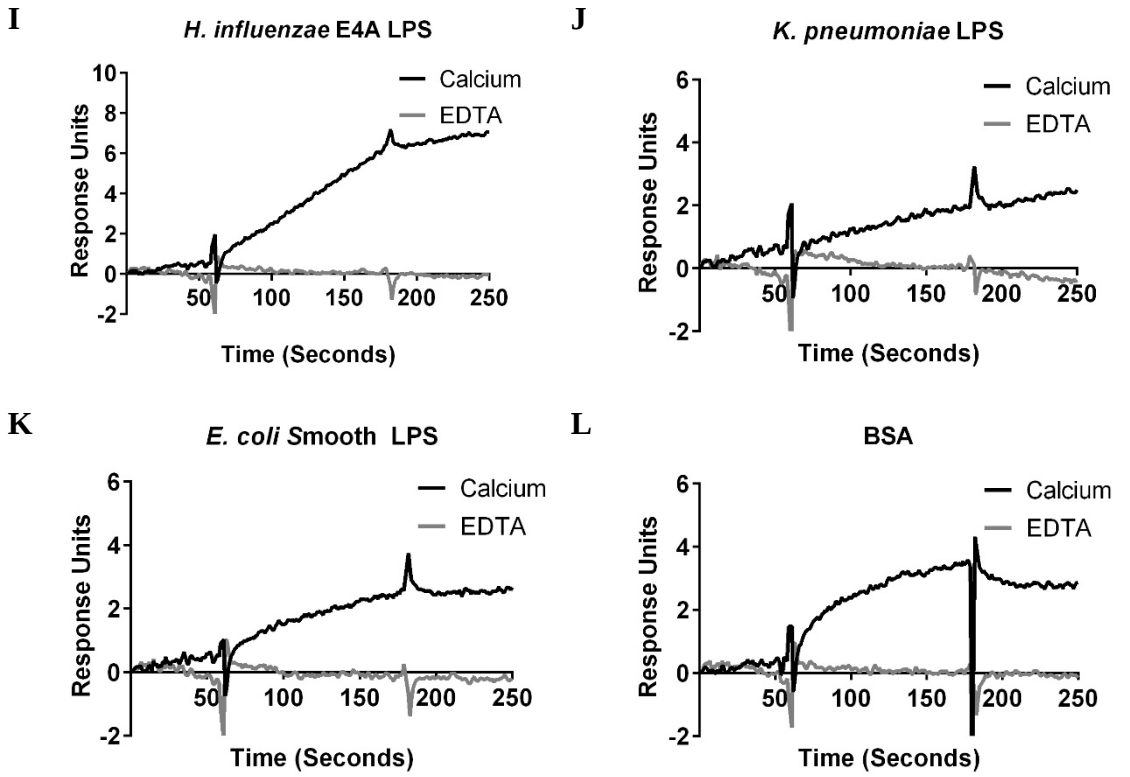

Figure 7-7: Binding of analytes to immobilised nhSP-A analysed by SPR. *909 response units of nhSP-A were immobilised by amine coupling to a Biacore sensor chip. After 60 secs of equilibration in buffer, analytes were flown over the chip for 120 secs either in HBS-P with 5 mM $CaCl_2$ (Calcium) or HBS-EP (containing 3 mM EDTA) (EDTA) and changes in response units recorded with any background binding to the empty flow cell subtracted. Buffer was subsequently flown over the chip to allow the analytes to dissociate. Analysed analytes included mannan (**A**), maltosyl BSA, purified RSV F protein pre-fusion, purified RSV F protein post-fusion, Sendai virus expressing BBG2Na (Sendai G) (**B**), Sendai virus expressing RSV F protein (Sendai F) (**C**), allotonic fluid (**D**), RSV viral stock (RSV) (**E**), NVLC (**F**), purified HIV gp120 IIIB (**G**), purified gp120 BaL, purified gp140 CN54, inactivated HIV MN particles, NVCL from cells used to produce HIV MN (HIV MN –C), inactivated HIV BaL particles, NVCL from cells used to produce HIV BaL (HIV BaL –C), house dust mite extracts from D. farina and D. pteronyssinus, grass pollen extracts from D. glomerata, P. nigra and P. praensis, LPS from H. influenzae Eagan wild type (**H**) and mutant Eagan 4A (**I**), LPS from K. pneumoniae (**J**), smooth LPS from E. coli (**K**) and BSA as a negative control (**L**). Importantly, only positive results and selected negative results are included in figure. Shown are representative results of n = 2. Note y axes are different according to the scale of response units.*

7.3.2.5 *Binding of nhSP-D to Ligands*

nhSP-D bound to both Mannan and maltosyl BSA in a calcium-dependent manner (Figure 7-8A and B, respectively). In addition, immobilised nhSP-D bound to both soluble RSV F protein pre and post-fusion (Figure 7-8C and D). nhSP-D bound to both Sendai virus expressing BBG2Na (contaning core region of RSV G protein) and F proteins at very low levels but slightly more to Sendai virus expressing F proteins (6 response units compared with 3.4 response units at 175 seconds) (Figure 7-8 E and F, respectively). nhSP-D did not bind to the allotonic fluid negative control (Figure 7-8G) nor to the whole inactivated RSV or cell lysate without RSV (RSV negative control) (Figure 7-8H and I, respectively).

nhSP-D also bound to HIV proteins in a calcium-dependent manner. Similar levels of soluble gp120 IIIB, gp120 BaL and gp140 CN54 were bound by the immobilised nhSP-D (Figure 7-8J, K and L, respectively). Moreover, nhSP-D bound to whole inactivated HIV particles HIV MN but to a higher degree to HIV BaL (542 and 1318 response units at 175 seconds, respectively) (Figure 7-8M O). There was some background binding of the NVCL negative controls for HIV MN and HIV BaL virus particles (Figure 7-8N and P, respectively). However, binding was much lower than for the inactivated HIV particles (246 and 29 response units at 175 seconds, respectively).

Immobilised nhSP-D bound to soluble house dust mite extracts from *D. farinae*, and *D. pteronyssinus* in a calcium-dependent manner to similar levels (Figure 7-8Q and R, respectively). In addition immobilised nhSP-D bound to grass pollen extract from *D.* glomerata (Figure 7-8S). nhSP-D did not, however, bind to either and *P. nigra* or *P.* praensis (Figure 7-8T and U, respectively).

In terms of the capacity of nhSP-D to bind to LPS, immobilised nhSP-D bound to *H. influenza* Eagan wild type, Eagan 4 A, *K. pneumoniae* and smooth *E. coli* LPS in a calcium-dependent manner (Figure 7-8V, W, X and Y, respectively). More soluble *H. influenza* Eagan wild type was bound by immobilised nhSP-D than Eagan 4A with 51 response units compared with 38.6 being bound at 175 secs respectively. Soluble smooth *E. coli* LPS was bound least by immobilised nhSP-D out of the four types of LPS with only 35.7 response units being bound after 175 seconds.

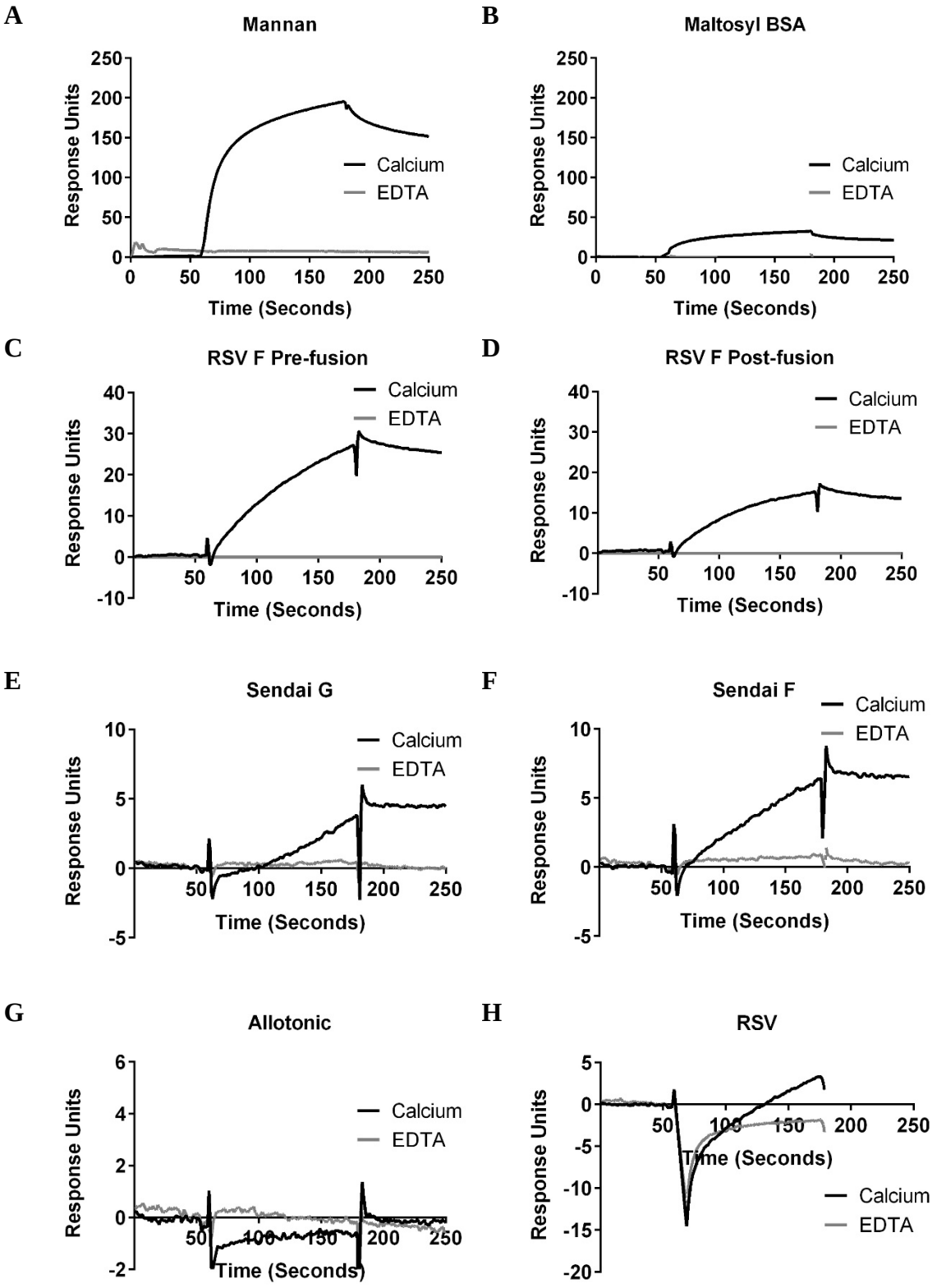
A
Mannan
Response Units
Time (Seconds)
Calcium
EDTA
B
Maltosyl BSA
C
RSV F Pre-fusion
D
RSV F Post-fusion
E
Sendai G
F
Sendai F
G
Allotonic
H
RSV

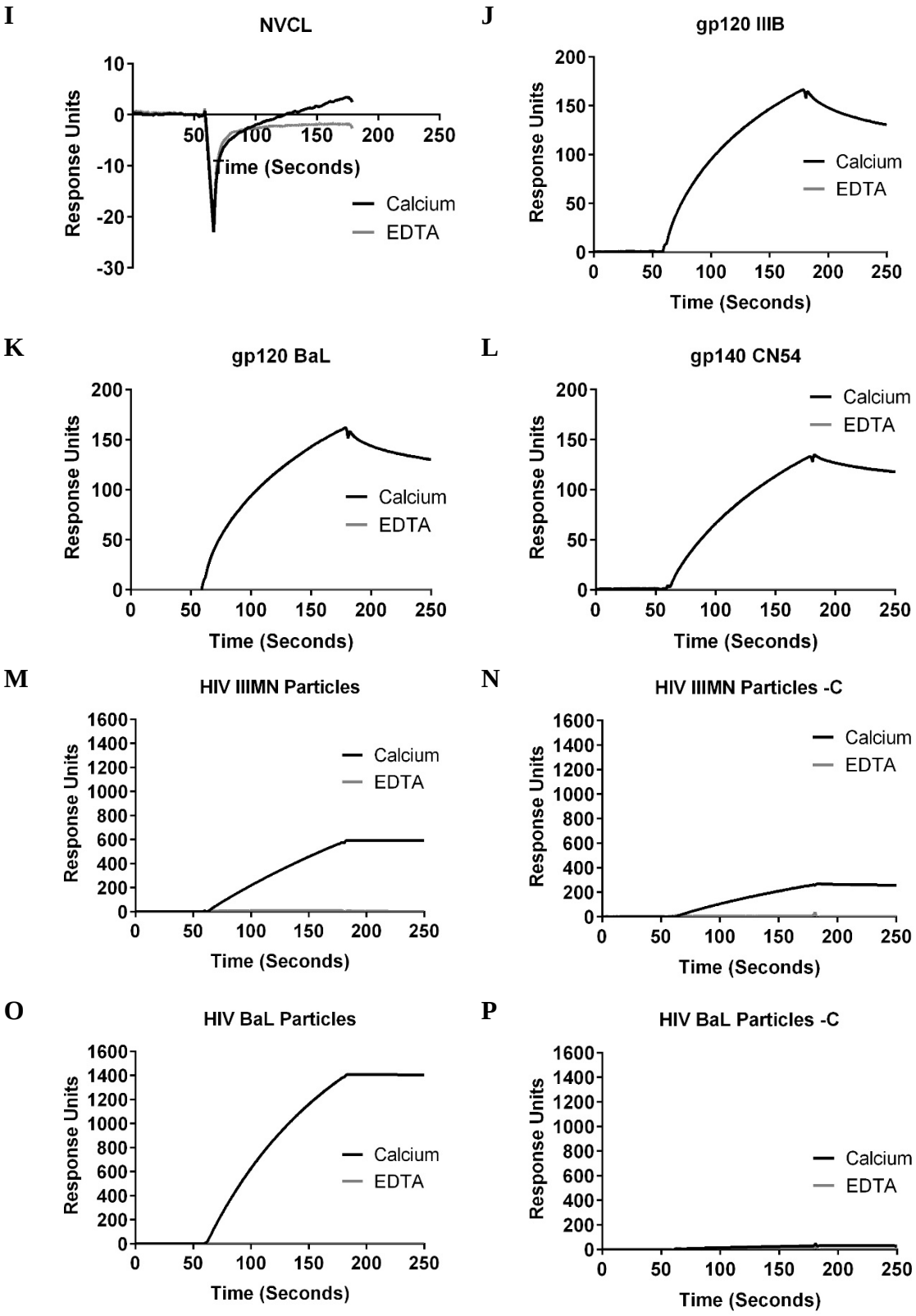
I
NVCL
Response Units
Time (Seconds)
Calcium
EDTA
J
gp120 IIIB
K
gp120 BaL
L
gp140 CN54
M
HIV IIIMN Particles
N
HIV IIIMN Particles -C
O
HIV BaL Particles
P
HIV BaL Particles -C

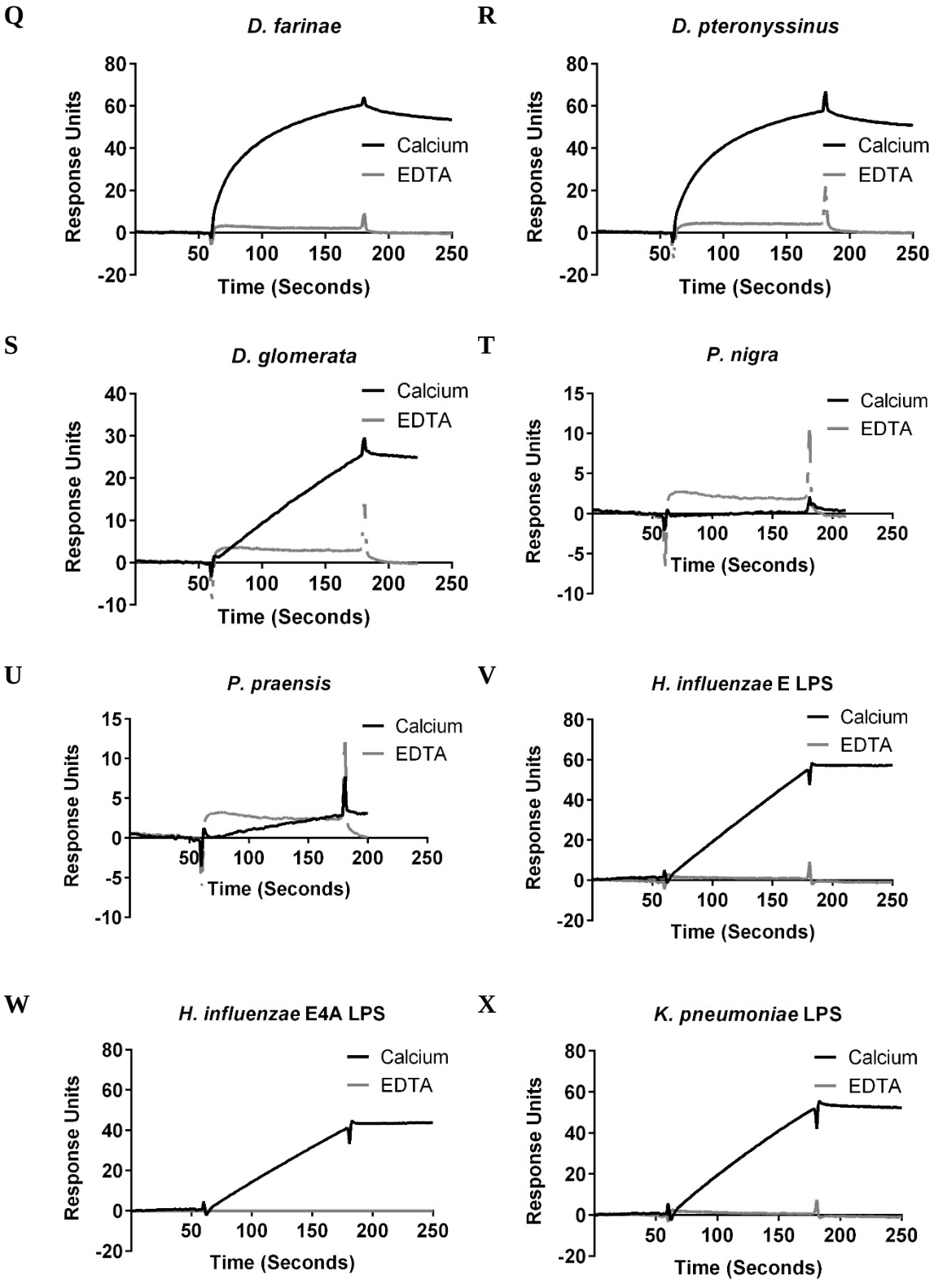
Q
D. farinae
R
D. pteronyssinus
S
D. glomerata
T
P. nigra
U
P. praensis
V
H. influenzae E LPS
W
H. influenzae E4A LPS
X
K. pneumoniae LPS
Response Units
Time (Seconds)
Calcium
EDTA

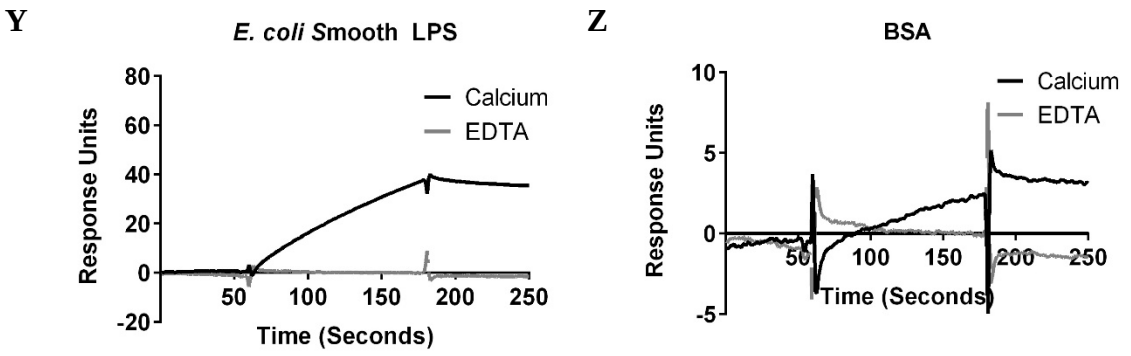

Figure 7-8: Binding of analytes to immobilised nhSP-D analysed using SPR. *4500 response units of nhSP-D were immobilised by amine coupling to a Biacore sensor chip. After 60 secs of equilibration in buffer, analytes were flown over the chip for 120 secs either in HBS-P with 5 mM $CaCl_2$ (Calcium) or HBS-EP (containing 3 mM EDTA) (EDTA) and changes in response units recorded with any background binding to the empty flow cell subtracted. Buffer was subsequently flown over the chip to allow the analytes to dissociate. Analysed analytes included mannan (**A**), maltosyl BSA (**B**), purified RSV F protein pre-fusion (**C**), purified RSV F protein post-fusion (**D**), Sendai virus expressing BBG2Na (Sendai G) (**E**), Sendai virus expressing RSV F protein (Sendai F) (**F**), allotonic fluid (**G**), RSV viral stock (RSV) (**H**), RSV NVLC (**I**), purified HIV gp120 IIIB (**J**), purified gp120 BaL (**K**), purified gp140 CN54 (**L**), inactivated HIV MN particles (**M**), NVCL from cells used to produce HIV MN (HIV MN –C) (**N**), inactivated HIV BaL particles (**O**), NVCL from cells used to produce HIV BaL (HIV BaL –C) (**P**), house dust mite extracts from D. farina (**Q**)and D. pteronyssinus (**R**), grass pollen extracts from D. glomerata (**S**), P. nigra (**T**) and P. praensis (**U**), LPS from H. influenzae Eagan wild type (**V**) and mutant Eagan 4A (**W**), LPS from K. pneumoniae (**X**), smooth LPS from E. coli (**Y**) and BSA as a negative control (**Z**). Shown are representative results of n = 2. Note y axes are different according to the scale of response units.*

7.3.2.6 *Comparative Binding of Analytes to rfhSP-A, nhSP-D and nhSP-A*

For analytes of a known molecular weight, the ratio of the number of bound analytes to number of immobilised collectin trimers was calculated: ratios are summarised in Table 7-1. This gives an insight into the relative levels of binding although caution must be taken when interpreting these results due to the multimeric nature of the ligands and some analytes; for this reason binding kinetics could not be calculated. Molecular weights of grass pollen and house dust mite extracts and whole inactivated RSV or HIV particles were unknown and thus were not compared. However, the capacity for rfhSP-A, nhSP-A and nhSP-D to bind to these or not is also summarised in Table 7-1.

Immobilised rfhSP-A and nhSP-A bound similar levels of mannan with an analyte:ligand ratio of 1:89 for both. Comparatively, nhSP-D bound more mannan (1:7). As compared

with mannan, nhSP-D bound less maltosyl-BSA (1:70 compared with 1:7). Moreover, maltosyl-BSA did not bind to rfhSP-A or nhSP-A at all.

SP-D but not SP-A or rfhSP-A bound to soluble RSV pre and post-fusion protein but bound slightly more to RSV pre-fusion protein (1:79 and 1:136, respectively). Both rfhSP-A and nhSP-A bound to BBG2Na (containing RSV G protein) with a similar analyte:ligand ratio (1:105 and 1:112, respectively); nhSP-D bound to BBG2Na to a lesser extent (1:224). rfhSP-A bound negligible levels of F protein expressed by Sendai virus. Comparatively, nhSP-A and nhSP-D both bound to F protein expressed by Sendai virus at low levels (1:156 and 1:276, respectively); importantly, SP-A binding to F protein expressed by Sendai virus was not inhibited by EDTA. nhSP-D bound to monomeric gp120 IIIB, gp120 BaL and trimeric gp140 CN54 to similarly high levels (1:25, 1:26, 1:36, respectively). However, rfhSP-A and nhSP-A only bound to gp120 IIIB and at lower levels (1:411 and 1:187, respectively).

nhSP-A but not rfhSP-A bound to LPS from *H. influenzae*, but bound LPS from strain E4A more than from Eagan wild type (1:18 and 1:55, respectively). Comparatively, nhSP-D bound to LPS from *H. influenzae* LPS from Eagan wild type more than mutant E4A (1:9 and 1:12, respectively). rfhSP-A, nhSP-A and nhSP-D all bound *K. pneumoniae* LPS with nhSP-D binding the most and rfhSP-A binding the least (1:77, 1:40 and 1:9, respectively). Both nhSP-A and nhSP-D but not rfhSP-A bound smooth LPS from *E. coli* to similar levels (1:35 and 1:13, no binding, respectively).

	rfhSP-A	**nhSP-A**	**nhSP-D**
Mannan *	89	89	7
Maltosyl-BSA	-	-	70
RSV F Pre-fusion	-	-	79
RSV F Post-fusion	-	-	136
Sendai G	105	112	224
Sendai F	1551	156	276
RSV	-	-	-
gp120 IIIB	411	187	25
gp120 BaL	-	-	26
gp140 CN54	-	-	36
HIV MN Particles	-	-	Bound
HIV BaL Particles	-	-	Bound
D. farinae	-	-	Bound
D. pteronyssinus	-	-	Bound
D. glomerata	-	-	Bound
D. nigra	-	-	Bound
P. Praensis	-	-	Bound
H. influenzae LPS E wild type *	-	55	9
H. influenzae LPS E4A *	-	18	12
K. pneumoniae LPS *	77	40	9
E. coli LPS Smooth *	-	35	13
BSA	2336	132	952

Table 7-1: Summary of binding and ratio of collectin trimers required to bind one molecule of analyte. *To allow comparison of relative binding levels, the maximum level of binding (RU) at 175 secs was used along with the amount of collectin immobilised, molecular weight of the collectin trimer and the molecular weight of the analyte to allow a ratio of bound analytes:number of immobilised collectin trimers. Importantly, some analytes used in SPR analysis had an unknown molecular weight so a ratio could not be calculated. Binding for an analyte of unknown molecular weight is indicated (Bound). Some analytes have a range of molecular weights or the used molecular weights is based on an estimate based on product data available (*). It is assumed that the F protein and BBG2NA (containing RSV G protein core region) are expressed by the*

virus and not incorporated into the virion, based on advice through communication with Ultan Power (Personal communication: email to Alastair Watson, 5th May 2014). Should this not be the case, the actual molecular weight of the analyte would be magnitudes higher.

7.3.3 RSV Neutralisation Assays

7.3.3.1 *Testing of α-RSV F Protein Antibody*

In order to quantify titres of the M37 RSV stock and detect infection by flow cytometry, it was necessary to identify an antibody capable of specifically detecting this RSV strain. Whole M37 RSV stock was therefore analysed by SDS-PAGE with subsequent Western blot analysis using the available α-RSV F protein antibody. Other RSV reagents used in SPR analysis were analysed alongside including HEp-2 cell lysate as a negative control, purified RSV F pre and post-fusion protein, Sendai virus expressing RSV F protein, Sendai virus expressing RSV G core antigen and allotonic fluid.

The α-RSV F protein antibody specifically recognised F proteins in the RSV M37 stock but did not recognise any of the other RSV reagents (Figure 7-9). This antibody was thus taken forward for use in quantifying the RSV stock titre and detection of infected epithelial cells using flow cytometry.

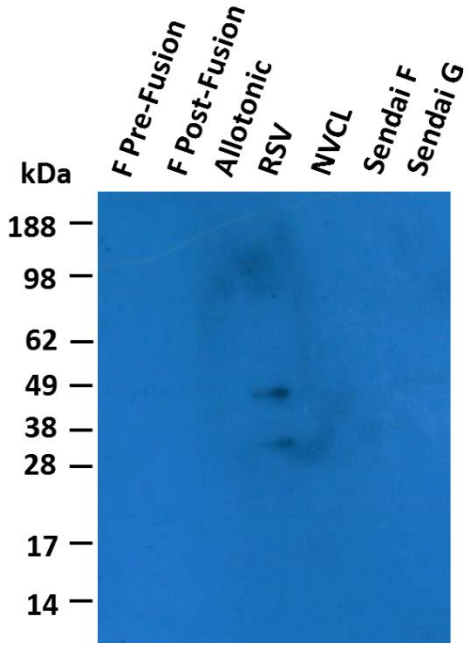

Figure 7-9: Determining the use of α-RSV F protein antibody for detecting M37 RSV. *M37 RSV stock, HEp-2 NVCL, purified RSV F pre-fusion protein, purified RSV F post-fusion protein, Sendai virus expressing RSV F protein, Sendai virus expressing BBG2Na and allotonic fluid were subject to SDS-PAGE with subsequent Western blotting using an α-RSV F protein antibody.*

7.3.3.2 *Titration of RSV Viral Stocks*

RSV viral stocks were generated by amplification in AALEB cells. It was then necessary to both calculate the titre of the viral stock and determine an appropriate dilution and time point to infect a sufficient proportion of cells for detection in neutralisation assays.

A serial dilution of the generated RSV viral stock was used to infect AALEB cells which were left for 24, 48 or 72 hours, after which, they were fixed and stained using the α-RSV F protein antibody. At dilutions of up to 1 in 225, infected AALEB cells could be seen after 24 hours (Figure 7-10). After 24 hours, individually infected cells could still be seen without the spread of virus to neighbouring cells to form infected foci. After 48 hours, infected cells could be detected using a dilution of up to 1 in 5625 (Figure 7-11). However, contrasting to the 24 hour time point, foci of infected cells could be identified where virus from a single infected cell had spread to infect neighbouring cells. Infected foci were easy to identify by eye and allowed implementation of the focus-forming assay which allowed the determination of the viral titre to be 3×10^6 FFU/ml. At higher magnification, after 48 or 72 hours, syncytia could be seen between AALEB cells which had allowed the formation of multinucleated cells (Figure 7-12).

From these results it was determined that for neutralisation assays the 24 hour time point would be appropriate for use. At 24 hours the ability of collectins to prevent the infection of individual cells could be assessed, rather than the use of later time points where the capacity of collectins to prevent infection and the subsequent spread of virus to neighbouring cells would be measured.

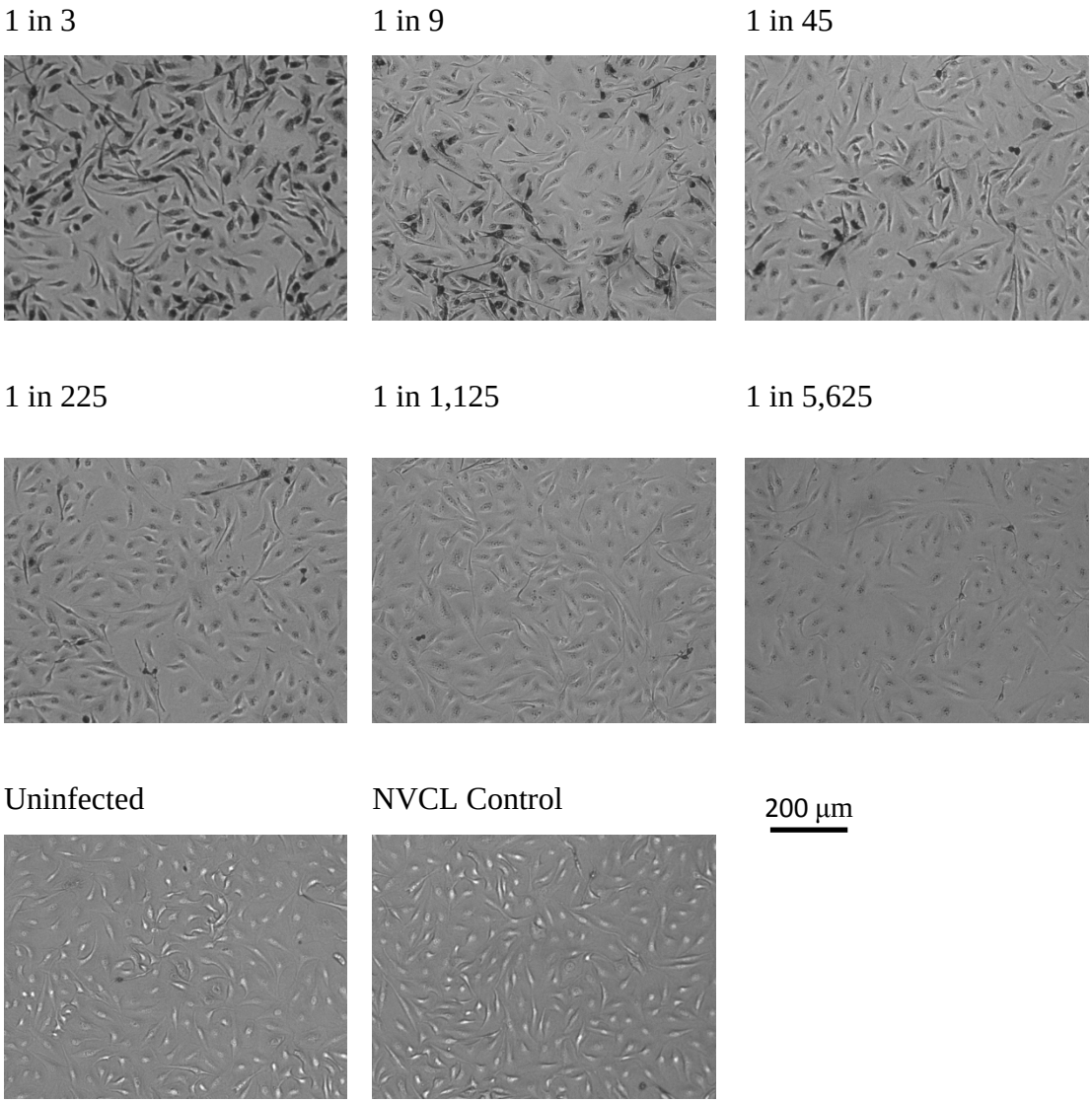

Figure 7-10: Images of AALEB cells after 24 hours of infection with a serial dilution of RSV. *AALEB cells were infected with increasing dilutions of RSV stock ranging from 1 in 3 to a 1 in 28,125 dilution, washed and left for 24 hours. Infected cells were identified using an α-RSV antibody and subsequently a secondary antibody conjugated with HRP. Infected cells were visualised using DAB substrate and images were taken using a x 4 objective lens, antibody staining is in black. Also included were cells mock infected with AALEB NVCL Control or with media alone (uninfected).*

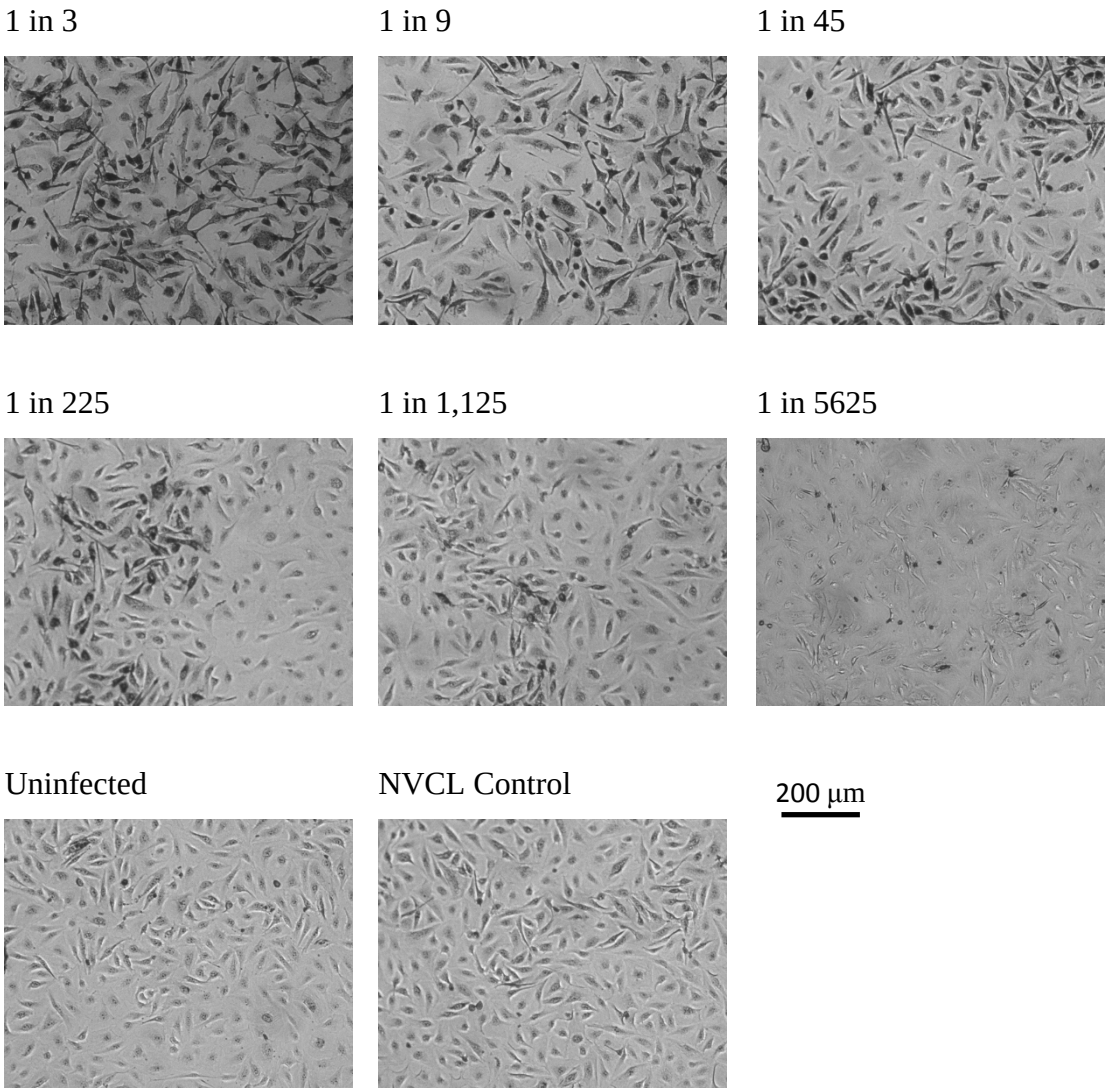

Figure 7-11: Images of AALEB cells after 48 hours of infection with a serial dilution of RSV.*AALEB cells were infected with increasing dilution of RSV stock ranging from 1 in 3 to a 1 in 28,125 dilution, washed and left for 48 hours. Infected cells were identified using an α-RSV antibody and subsequently a secondary antibody conjugated with HRP. Infected cells were visualised using DAB substrate and images were taken using a x 4 objective lens, antibody staining is in black. Also included were cells mock infected with AALEB NVCL Control or with media alone (uninfected).*

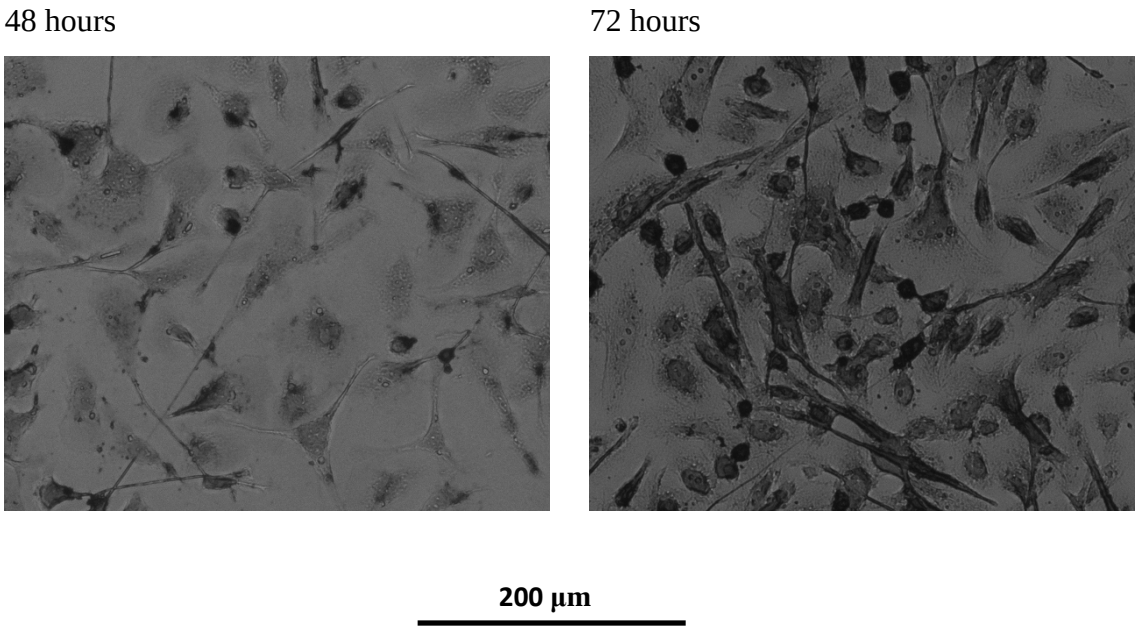

Figure 7-12: Images of AALEB cells after infection with RSV. *AALEB cells were infected with a 1 in 225 dilution of RSV stock, washed and left for either 48 hours (**A**) or 72 hours (**B**). Infected cells were identified using an α-RSV antibody and subsequently a secondary antibody conjugated with HRP. Infected cells were visualised using DAB substrate and images were taken using a x 10 objective lens, antibody staining is in black.*

7.3.3.3 *Collectin Neutralisation of a Low Dose of RSV as Determined by RT-qPCR*

To determine the capacity of collectins to neutralise a low dose of RSV (MOI of 0.08), RSV RNA was quantified by RT-qPCR at 24 hours after infection. Pre-incubation of RSV with nhSP-A significantly reduced RSV infection at 5 μg/ml by a mean (± SD) of 30 (± 22.8) % ($p < 0.05$). Pre-treatment with nhSP-D also significantly reduced RSV infection at 5 μg/ml by 55.4 (± 14) % ($p < 0.05$). Comparatively, pre-treatment with trimeric rfhSP-A significantly reduced infection in a dose-dependent manner by 54.9 (9.0) % ($p < 0.01$) and 63.7 (22.2) % ($p < 0.001$) at 1 μg/ml and 5 μg/ml, respectively. Importantly, pre-treatment of RSV with 5 μg/ml of BSA did not reduce infection levels.

Upon comparison of the neutralisation capacity of rfhSP-A compared with nhSP-A, rfhSP-A significantly reduced RSV infection more effectively at both 1 μg/ml (54.9 (9.0) % compared with 14.5 (21.7) % ($p < 0.05$)) and 5 μg/ml (63.7.6 (22.2) % compared with 30 (22.8) % ($p < 0.05$)).

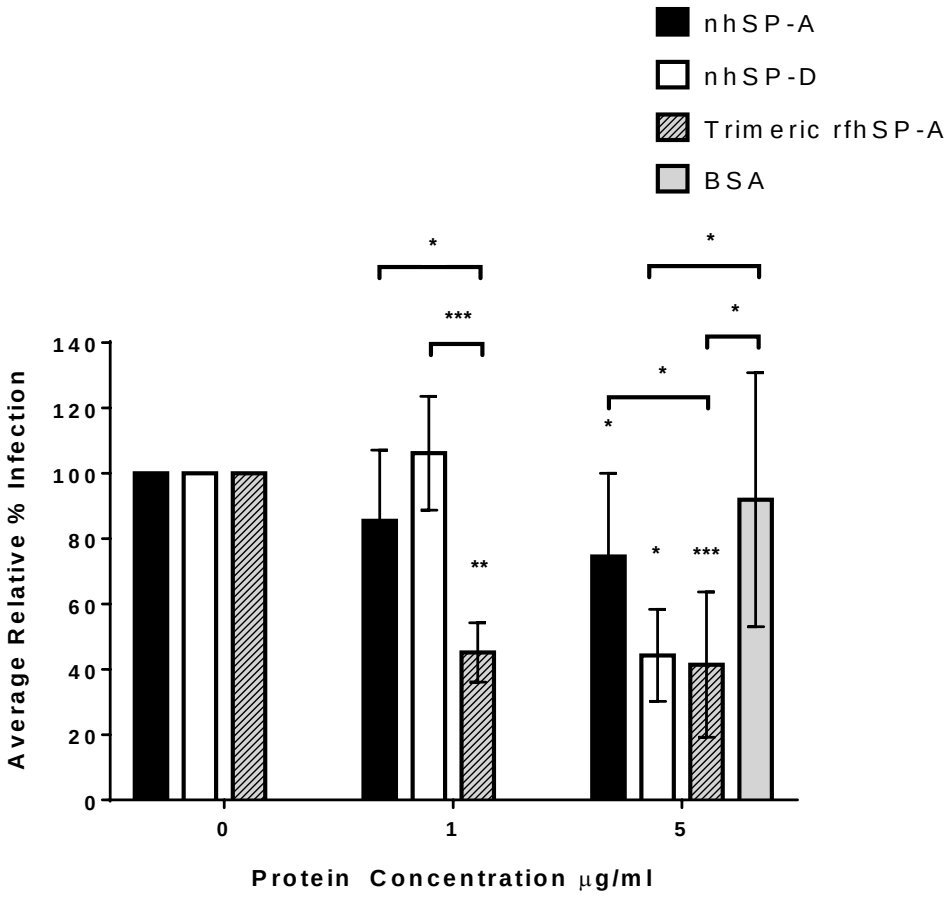

Figure 7-13: Neutralisation of RSV by collectins detected by RT-qPCR. *AALEB cells infected with a low dose of RSV (MOI of 0.08) were left to allow the RSV to replicate for 24 hours, after which, RSV RNA was quantified using RT-qPCR. Prior to infection, RSV was incubated for 1 hour at 37 °C either with gel filtration buffer or with 1 µg/ml or 5 µg/ml of nhSP-A, nhSP-D or trimeric rfhSP-A. RSV was also pre-incubated with 5 µg/ml of BSA as a control. Shown is the mean (± SD) of at least 3 experiments undertaken in duplicate. Indicated are significant differences between untreated and treated virus (calculated using unpaired two tailed student's t-test with equal variance) and significant differences between different treatments (calculated using two-way ANOVA with multiple comparisons corrected using the Bonferroni method) (* $p < 0.05$, ** $p < 0.01$, *** $p < 0.001$).*

7.3.3.4 *Optimisation of Neutralisation Assay for Flow Cytometry*

To investigate the capacity of collectins to neutralise a higher dose of RSV and to validate the results obtained above by RT-qPCR, an additional technique was implemented: flow cytometry. Prior to undertaking the neutralisation assay, the flow cytometry assay and dilution of virus were first optimised (Figure 7-14). A gate was first set selecting for single viable AALEB cells through setting defined forward scatter and side scatter limits (Figure 7-14A). Infected cells were characterised by fluorescence of the cells detected using the FITC-A filter (Figure 7-14B). A gate was set to define AALEB cells as infected should fluorescence be higher than the point in which approximately 1 % of the uninfected negative control was defined as infected. This allowed sufficient sensitivity to detect a shift in percentage cells infected when using a 1 in 45 dilution of RSV, whilst minimising the background noise (Figure 7-14C). Infection of AALEB cells with a serial dilution of RSV confirmed that a 1 in 45 dilution (MOI of 0.4) was appropriate to achieve 30-40 % of cells infected, as detected by flow cytometry (Figure 7-14D).

For the neutralisation assay, different collectins in gel filtration buffer were incubated with RSV virus. It was therefore important to investigate the effect of adding gel filtration buffer to the virus prior to infection. However, adding gel filtration buffer did not impact on the percentage of cells infected (Figure 7-14E). Moreover, reducing the infection volume from 300 µl to 200 µl did not impact on infection levels, allowing less collectin to be used in the neutralisation assay. To confirm that it was replicative RSV virus being detected in the assay a UV treated RSV virus control was tested (Figure 7-14F). Treatment of RSV reduced the mean (± SD) levels of infection from 32.9 % (± 1.1) to 1.6 % (± 0.3) which was close to the uninfected control of 0.89 % (± 0.1) of cells being infected.

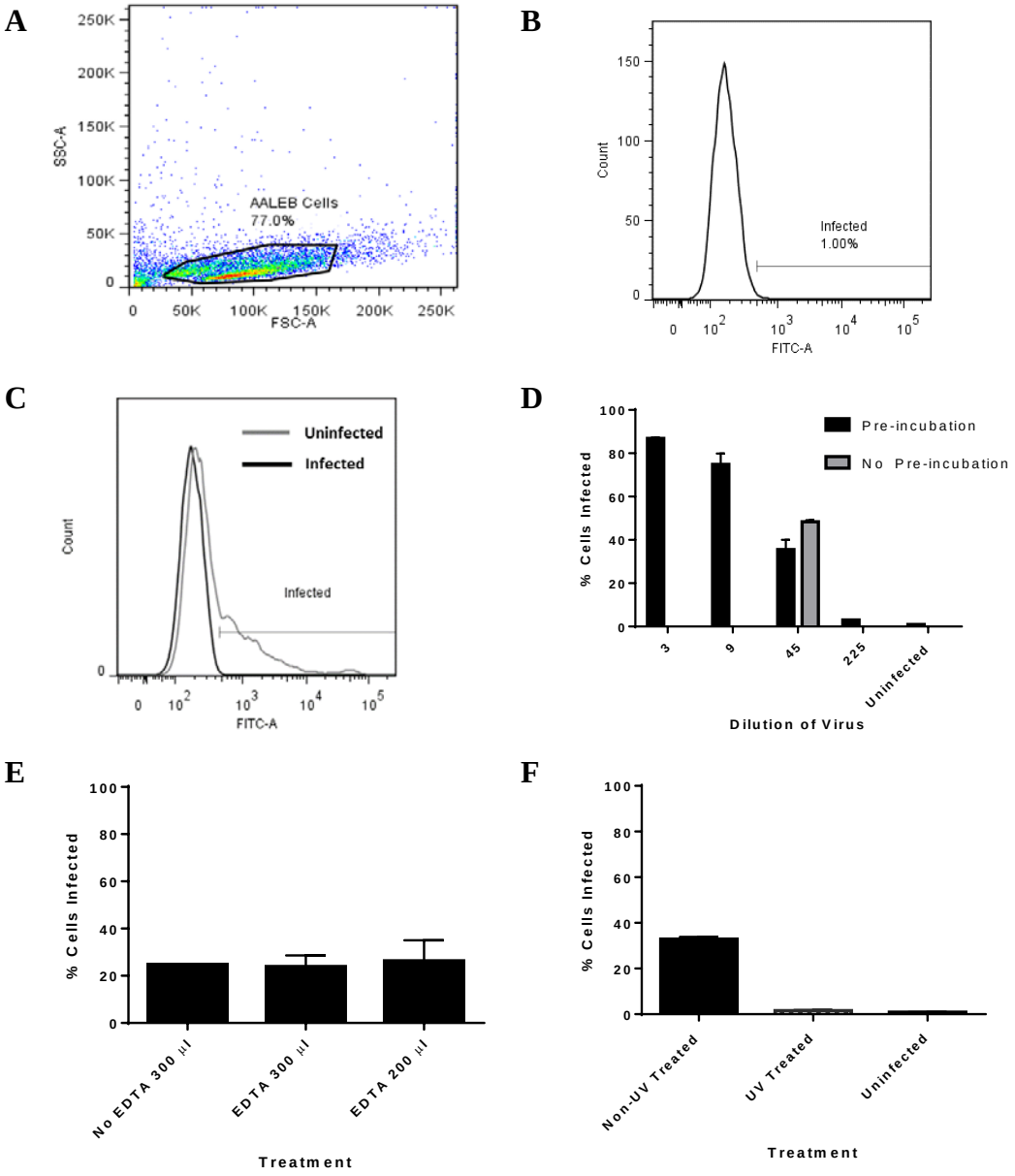

Figure 7-14: Optimisation of RSV neutralisation assay using flow cytometry. *Shown is the gating strategy used to characterise AALEB cells by forward scatter and side scatter (**A**). Also shown is the gating strategy used to define infected cells by their level of fluorescence as detected using the FITC-A filter where the cut off was set to the point at which the uninfected control had approximately 1 % of the cells infected (**B**). The difference between fluorescence between an uninfected sample and a sample infected with RSV diluted 1 in 45 is shown (**C**). AALEB cells were infected with a serial dilution of RSV as well as an uninfected control. In addition, the impact of preincubating the RSV virus alone for 1 hour at 37 °C was compared to that of directly infecting the cells (**D**). Different infection strategies were tested to see the effect of adding 20 µl of gel filtration buffer to the RSV or reducing the volume (**E**).The effect of UV treating virus on the percentage of cells detected as being infected is also shown compared to the uninfected control (**F**). Shown are representative gating strategies (**A, B** and **C**). Given is the mean (± SD) of one experiment undertaken in duplicates (**D**, **E** and **F**).*

7.3.3.5 *Investigating the Capacity for Neutralisation of RSV by Collectins using Flow Cytometry*

The capacity of trimeric rfhSP-A to neutralise RSV and prevent infection of AALEB cells was confirmed using flow cytometry and compared with the neutralisation capacity of nhSP-A. Dimeric rfhSP-A was also used for comparison as a misfolded negative control produced in a similar manner to carbohydrate binding trimeric rfhSP-A (Figure 7-15A).

nhSP-A reduced RSV infection in a biphasic manner by a mean (± SD) of 24.7 (± 27.2) % at 0.02 μg/ml ($p > 0.05$) and significantly by 38.5 (± 28.4) % and 24.7 (± 29.6) % at 1 μg/ml and 5 μg/ml, respectively ($p < 0.05$). rfhSP-A significantly reduced RSV infection in a dose-dependent manner by 39.8 (± 6.8), 85.9 (± 4.2) and 96.4 (± 1.9) % at 0.2 μg/ml 1 μg/ml and 5 μg/ml, respectively ($p < 0.001$, $p < 0.001$ and $p < 0.0001$, respectively). Importantly, At 5 μg/ml rfhSP-A reduced relative infection levels to only 3.7 ± (2.2) % ($p < 0.0001$) which was close to and not significantly different from the uninfected control 2.5 (± 0.2) % ($p = 0.2$).

Similarly to the results obtained by RT-qPCR, rfhSP-A neutralised RSV significantly more effectively than nhSP-A at both 1 μg/ml and 5 μg/ml ($p < 0.01$ and $p < 0.0001$, respectively). Interestingly, dimeric rfhSP-A also reduced RSV infection significantly by 34.3 (± 20.5) %, 43.2 (± 24.5) % and 34 (± 16.1) % at 0.2 μg/ml, 1 μg/ml and 5 μg/ml, respectively ($p < 0.05$, $p < 0.05$ and $p < 0.01$, respectively). However rfhSP-A was significantly more effective at reducing RSV infection at 1 μg/ml and 5 μg/ml than dimeric rfhSP-A ($p < 0.001$ and $p < 0.0001$, respectively). There was, however, no significant difference between the capacity of nhSP-A and dimeric rfhSP-A to reduce RSV infection. Interestingly, unlike rfhSP-A, the capacity of nhSP-A and dimeric rfhSP-A to neutralise RSV was most effective at 1 μg/ml with a slight decrease in efficacy at the higher concentration of 5 μg/ml.

Upon investigation of pre-treatment of RSV with SP-D, both nhSP-D and rfhSP-D significantly reduced levels of infection by up to 47.2 (± 25.6) and 37.8 (± 21.7) % at 5 μg/ml and 0.2 μg/ml, respectively ($p < 0.05$). However, preincubation of RSV with BSA did not reduce infection levels. rfhSP-D produced as a soluble protein through using NT^{dm} was also effective at preventing infection of RSV and neutralised RSV by up to 32.2 (± 25.6) at 5 μg/ml, with a similar level of efficacy as rfhSP-D produced through the traditional refolding method (37.8 (± 21.7) %). The neutralisation of RSV by nhSP-D,

rfhSP-D produced by refolding and rfhSP-D produced using NT^{dm} was not dose-dependent. There was no significant improvement of RSV neutralisation upon increasing doses from 0.2 μg/ml to 1 μg/ml or even to 5 μg/ml.

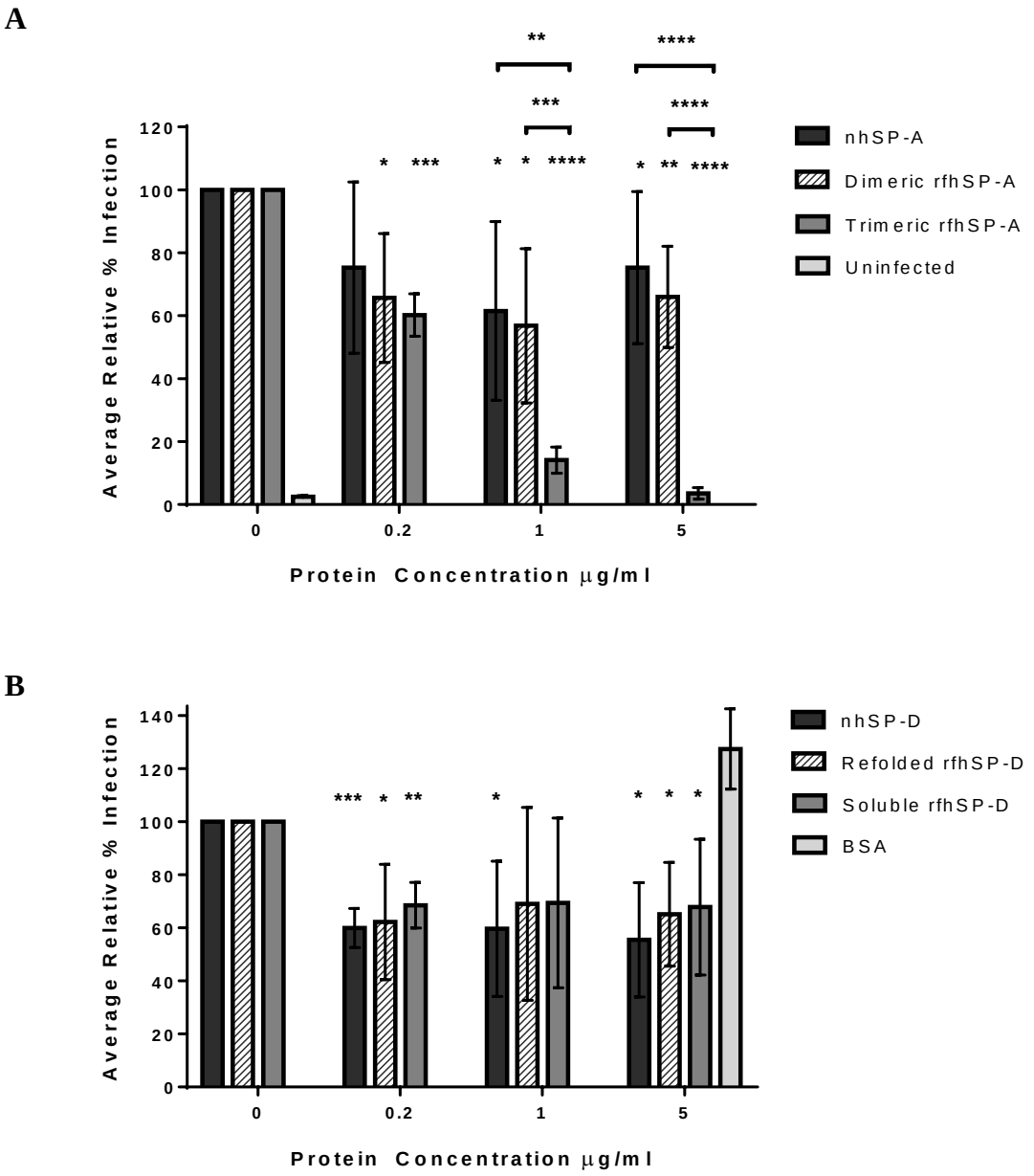

Figure 7-15: Neutralisation of RSV by collectins detected by flow cytometry.*Human bronchial epithelial (AALEB) cells infected with a high dose of RSV (MOI of 0.4) were left to allow the RSV to replicate for 24 hours, after which, levels of infected cells were analysed using flow cytometry using an α-RSV F protein antibody. Prior to infection, RSV was incubated for 1 hour at 37 °C either in gel filtration buffer or with 0.02 µg/ml, 1 µg/ml or 5 µg/ml of nhSP-A, dimeric rfhSP-A or trimeric rfhSP-A (**A**). RSV was also pre-incubated with 0.02 µg/ml, 1 µg/ml or 5 µg/ml of nhSP-D, rfhSP-D produced by refolding or rfhSP-D produced as a soluble protein using NT^{dm} (**B**). Shown is the mean (± SD) of at least 3 experiments undertaken in duplicate. Indicated are significant differences between untreated and treated virus (calculated using unpaired two tailed student's t-test with equal variance) and significant differences between different treatments (calculated using two-way ANOVA with multiple comparisons corrected using the Bonferroni method) (* p < 0.05, ** p < 0.01, *** p < 0.001, **** p < 0.0001).*

7.4 Summary of Results

Within this chapter, the capacity of rfhSP-A to bind to known ligands of SP-A was investigated as compared with nhSP-A and nhSP-D. In addition, the importance of the oligomeric structure of SP-A and SP-D in neutralising RSV was addressed using rfhSP-A and rfhSP-D, thus addressing Aims 6 and 7 (Section 1.14):

- To characterise the capacity of rfhSP-A to bind to known natural SP-A ligands compared with nhSP-A and nhSP-D.
- To use rfhSP-A and rfhSP-D to characterise the importance of the SP-A and SP-D N-terminal domain (and oligomeric structures) in neutralisation of a clinically relevant strain of RSV using human bronchial epithelial cells.

The main results reported in this chapter are:

- Both rfhSP-A and nhSP-A bound to mannan in a calcium-dependent manner. However, their capacity to bind to mannose, maltose, ManNAc and glucose was inconclusive.
- rfhSP-A also bound to LPS from *k. pneumonia*, gp120 IIIB and BBG2Na (containing core region of RSV G protein) expressed by Sendai virus in a calcium-dependent manner, as detected by SPR (albeit at low levels). However, rfhSP-A did not bind to maltosyl-BSA, LPS from *H. influenza*, LPS from *E. coli,* RSV pre-fusion or post-fusion F protein, RSV F protein expressed by Sendai virus, whole inactivated RSV particles, gp120 BaL, gp140 CN54, whole inactivated HIV virions, house dust mite extracts or grass pollen extracts.
- nhSP-A bound to LPS from *K. pneumoniae*, *H. influenzae strains* Eagan wild type and E4A and smooth and rough LPS from *E. coli*. nhSP-A also bound gp120 IIIB, BBG2Na (containing core region of RSV G protein) expressed by Sendai virus and BSA in a calcium-dependent manner. nhSP-A bound to *H. influenzae* strain E4A more than strain Eagan wild type. nhSP-A also bound to RSV F protein (expressed by Sendai virus), however, this was not calcium-dependent. nhSP-A did not bind to maltosyl-BSA, RSV pre-fusion or post-fusion F protein, whole RSV stock, gp120 BaL, gp120 CN54, whole inactivated HIV virions or house dust mite or grass pollen extracts.

- nhSP-D bound to LPS from *K. pneumonia*, smooth LPS from *E. coli* and LPS from *H. influenzae* strains Eagan wild type and E4A in a calcium-dependent manner. nhSP-D bound to *H. influenzae* Eagan wild type slightly more than E4A. nhSP-D also bound to gp120 IIIB, gp120 BaL and gp140 CN54 in a calcium-dependent manner to similar degrees. nhSP-D bound to inactivated HIV MN and BaL particles but to BaL particles to a higher degree. nhSP-D bound to house dust mite extracts from *D. farina* and *D. pteronyssinus* in a calcium-dependent manner to similar degrees. nhSP-D also bound to grass pollen extracts from *D. glomerata* in a calcium-dependent manner but not to extracts from *P. nigra* or *P. Praensis*.
- rfhSP-A neutralised RSV and prevented infection of immortalised bronchial epithelial cells in a dose-dependent manner ($p < 0.0001$); this was to near levels of the uninfected control at 5 µg/ml, as detected by flow cytometry. Importantly, rfhSP-A neutralised RSV significantly more effectively than nhSP-A and the dimeric rfhSP-A negative control ($p < 0.0001$). The capacity of rfhSP-A to neutralise RSV was confirmed using both RT-qPCR and flow cytometry.
- nhSP-D neutralised RSV and reduced infection of immortalised bronchial epithelial cells in a dose-dependent manner, as determined by RT-qPCR. Both nhSP-D and rfhSP-D reduced infection of immortalised bronchial epithelial cells to similar levels as determined by flow cytometry. However, this was not dose-dependent.
- rfhSP-D expressed and purified using NT^{dm} as a soluble protein was functional and significantly reduced RSV infection ($p < 0.05$) with an efficacy similar to rfhSP-D produced using the traditional refolding protocol.

7.5 Discussion

Prior to this study, a functional rfhSP-A molecule had not been produced and demonstrated to be trimeric. In this present study, through inclusion of a collagen-like stalk which is thought to stabilise the trimeric structure, in addition to use of a novel expression system, this has successfully been achieved. nhSP-A has been reported to provide a route of entry for RSV to allow infection of host cells but also to neutralise RSV. In this chapter the ability of rfhSP-A to bind known natural ligands of SP-A compared with nhSP-A and nhSP-D was assessed. Moreover, the importance of the collectin N-terminal domain was assessed in its ability to neutralise a clinically relevant strain of RSV (Aims 6 and 7 - Section 1.14).

7.5.1 Solid Phase Binding Assay

rfhSP-A was successfully purified by carbohydrate affinity chromatography in Chapter 6. In this present chapter, rfhSP-A was confirmed to bind to mannan in a calcium-dependent manner using solid phase binding assays. As expected, nhSP-A was also found to bind to immobilised mannan in a concentration-dependent manner. However, for nhSP-A, this only appeared to be partially calcium-dependent at concentrations below 1 µg/ml. This may be an artefact of the assay due to non-specific binding or overloading of the assay with too much protein. Alternatively it could be due to functional differences between nhSP-A purified from healthy volunteers and the highly oligomeric nhSP-A purified from PAP in this present study. Both nhSP-D and rfhSP-D also bound to mannan in a calcium-dependent manner. However, as anticipated, less rfhSP-A and rfhSP-D appeared to bind to mannan coated plates than nhSP-A and nhSP-D, likely a result of the decreased binding avidity due to being composed as trimers as opposed to a higher order oligomer.

Based on previous methodology used to investigate the capacity of SP-D to bind various carbohydrate ligands (58), the ability of rfhSP-A and nhSP-A to bind these ligands in addition to rough and smooth LPS from *E. coli* was tested. This was done through incubation of collectins on mannan coated plates in the presence of different soluble ligands. Binding of rfhSP-A to mannan coated plates was shown to be inhibited upon incubation with soluble mannan. This confirmed the rfhSP-A binding to be mannan

specific and not non-specific binding to the plates. However the ability of mannose, maltose, ManNAc and rough *E. coli* LPS to inhibit rfhSP-A binding to mannan coated plates was not demonstrated and results were inconclusive. Incubation with soluble smooth *E. coli* LPS, however, did appear to inhibit binding of rfhSP-A to mannan to some degree. This was surprising due to the previously reported mechanism of SP-A binding to LPS through the lipid-A moiety which is not accessible in smooth LPS (102). Perhaps differences in the LPS or techniques used for purification could explain this.

Soluble mannan also inhibited the binding of nhSP-A to mannan coated plates and soluble maltose and glucose appeared to inhibit binding to mannan coated plates to some degree at concentrations above 10 mM. However, the ability of nhSP-A to bind mannose and ManNAc was not detected. This is a surprising results due to it being well established that SP-A has the capacity to bind all of the monosaccharides tested in this present study (56). Binding of nhSP-A to mannan coated plates was, however, inhibited by incubation with soluble rough and smooth LPS from *E. coli* with rough LPS having a slightly higher capacity for inhibition. nhSP-A is expected to bind rough LPS considerably better than smooth LPS due to the more exposed lipid A moiety, characteristic of rough LPS.

The ability of nhSP-A to bind mannan but not to mannose and ManNAc could be an artefact of the assay used in this study, potentially due to use of too high a concentration of protein. Alternatively it could be a consequence of using protein purified by butanol extraction from PAP as opposed to purification by washing with EGTA from healthy individuals. Lower concentrations of SP-A have been previously used in a similar assay (56). Use of lower amounts of SP-A or further optimisation of this assay could allow for conclusive results about which sugars both rfhSP-A and nhSP-A purified in this present study have the capacity to bind to.

7.5.2 SPR

rfhSP-A, nhSP-A and nhSP-D were successfully immobilised to the Biacore chip through amine coupling using sodium acetate at pH 5. Although large quantities of nhSP-D were successfully immobilised to the Biacore chip, less rfhSP-A (690 RU) and nhSP-A (909) were successfully immobilised. However, sufficient levels of collectin were immobilised to the chip to allow detectable binding responses. To allow comparison of relative binding levels, the maximum level of binding (RU) at 175 secs was used along with the amount

of collectin immobilised, molecular weight of the collectin trimer and the molecular weight of the analyte to calculate a bound analyte:immobilised collectin trimer ratio. This allowed the relative levels of binding to be compared between collectins and between analytes. Some molecular weights for example AT-2 inactivated virus or allergen extracts were not known so such a ratio could not be calculated. In addition, although the molecular weight of mannan is thought to be approximately 40 kDa, mannan is a polymer of mannose and the collectins have the opportunity to bind to multiple residues (313). Other ligands also have multiple carbohydrate residues available for binding, meaning that caution must be used when comparing relative binding. Complexity is also added due to the potential of each monomeric CRD having the capacity to bind the ligand, whilst also having the potential to not be available for binding due to spatial restrictions attributed to the orientation of the oligomeric structure or due to binding of a neighbouring CRD. Importantly, certain CRDs may also not be available for binding as a result of immobilisation onto the sensor chip. Due to the multimeric nature of the collectins and issues discussed above it was not possible to determine kinetic binding constants.

SPR confirmed the capacity of rfhSP-A, nhSP-A and nhSP-D to bind mannan in a calcium dependent manner. nhSP-A and rfhSP-A bound to mannan to the same level with a bound analyte:immobilised collectin trimer ligand ratio of 1:89. This may be surprising due to the expected higher avidity of nhSP-A for ligands than rfhSP-A. nhSP-D has been widely reported to have a higher avidity of binding compared with rfhSP-D (316). Comparative to nhSP-A and rfhSP-A, nhSP-D bound to mannan to a much higher degree (1:7). nhSP-D also bound to maltosyl-BSA but to a lower degree than mannan (1:70). SP-D has previously been reported to bind to mannose with a higher affinity than maltose (58). This result, therefore, may be expected. Surprisingly however, rfhSP-A and nhSP-A did not bind to maltosyl-BSA. Future work could investigate the ability of collectins to bind other carbohydrates using SPR including ManNAc and glucose.

7.5.2.1 *Binding to RSV*

Neither rfhSP-A nor nhSP-A bound to recombinant RSV F protein either in the pre or post-fusion conformation. However, nhSP-D did bind to both RSV pre and post-fusion F protein but had a higher capacity to bind the pre-fusion conformation (1:79 compared with 1:136). This may be expected due to the likely importance of SP-D in neutralisation

of RSV through binding to the pre-fusion F protein prior to infection of the host cell. SP-D binding to RSV or viral components upon entry to the host cell could have biological importance. Negligible levels of F protein expressed by Sendai virus was bound by rfhSP-A. Although nhSP-A did bind at low levels (1:156) to F protein expressed by Sendai virus, this was a calcium-independent interaction. nhSP-D also bound to RSV F protein expressed by Sendai virus at low levels however this was a calcium-dependent interaction (1:276). rfhSP-A, nhSP-A and nhSP-D all bound BG2Na (containing the core region of RSV G protein) expressed by Sendai virus in a calcium-dependent manner (1:105, 1:112 and 1:224 trimers, respectively). Allotonic fluid was not bound by rfhSP-A, nhSP-A or nhSP-D showing these interactions to not be as a results of protein contamination present from the allotonic fluid in the viral stocks.

The work in this chapter is in agreement with previous reports of SP-A interacting with RSV through the G protein (148). The finding that immobilised SP-A bound F protein expressed by Sendai virus also agrees with previous findings that SP-A interacts with the F protein (147). However, this previous study demonstrated the interaction of SP-A with RSV F protein to be calcium-dependent; this was calcium-independent in this present study. Importantly, amino acid or glycosylation differences attributed to the strain of RSV may explain differences in binding found in the literature. In addition, the potential for the interaction to be to the Sendai virus itself as opposed to the expressed F protein must be considered in addition to the binding to the albumin-binding domain of streptococcal G protein. An appropriate control of Sendai virus expressing neither RSV F nor BBG2Na should be included with future analysis, in addition to Sendai virus expressing full-length RSV G protein or purified full-length G protein from various strains of RSV.

The illustration that nhSP-D binds to BBG2Na (containing core region of RSV G protein) agrees with a previous report showing that rfhSP-D binds to the RSV G protein (128). However, this report did not test the ability of nhSP-D to bind RSV F protein. In this present study, nhSP-D was found to bind both RSV pre and post-fusion F protein and F protein expressed by Sendai virus, which as far as the author is aware, has not been previously shown. In another study, nhSP-D was found to bind neither RSV F nor G protein (147). However, nhSP-D has been previously been shown to bind to Vero cells infected with vaccinia virus expressing F or G proteins of RSV (145). Differences, however, may be explained through differences in the RSV strains used or differences in

glycosylation as a consequence of being produced in different cell types or coming from different sources.

Binding of neither rfhSP-A, nhSP-A nor nhSP-D to the M37 RSV viral stock (used later in neutralisation assays) was detected. However, as seen upon assessment by SDS-PAGE, the viral stock and Sendai viruses expressing either NBBG2Na or F protein were highly contaminated by NVCL or proteins from allotonic fluid. Such contamination may cause problems through interrupting the binding of collectins to the virus or alternatively causing non-specific binding, although appropriate controls of NVCL and allotonic fluid were used. High levels of contamination also resulted in a lower concentration of the analyte being used in the binding studies than would be present in pure viral stocks or stocks without allotonic fluid contamination. Higher concentrations of analytes than those used in the present study could be used in the future. Moreover, future purification of viral stocks or purification of RSV F and G proteins may allow more conclusive elucidation about the nature of the interaction of SP-A and SP-D with RSV. It would also be interesting to assess the capacity of different collectins to bind F and G proteins from different strains of RSV. Investigating the ability of rfhSP-D to bind RSV and other related ligands was beyond the scope of this study. However, this would be extremely interesting to compare with the binding capacity of nhSP-D.

The functional importance of potential interactions of collectins with RSV was subsequently studied using neutralisation assays and is discussed in Section 7.5.3.

7.5.2.2 *Binding to HIV*

The ability of rfhSP-A, nhSP-A and nhSP-D to interact with HIV was also tested. nhSP-A was found to bind to purified gp120 IIIB in a calcium-dependent manner (1:187) but not to gp120 BaL, trimeric gp140 CN54 nor inactivated BaL or IIIMN HIV particles. The inability of nhSP-A to bind HIV BaL particles contradicts previously published results (303). Although this is the same strain of HIV, batch to batch variation or different sources of the virus could explain the discrepancy in results. Alternatively, this may be explained by functional differences attributed to patient variability of the nhSP-A purified in this study. Importantly, previous results showing the interaction of SP-A with HIV used nhSP-A purified through washing the BAL pellet with EGTA. In this present study use of this technique yielded purified protein of a different oligomeric state to that purified through

butanol extraction. However, nhSP-A purified by butanol extraction was used in the functional assays in this present study. The purification technique may impact on the function of the SP-A and potentially explain the differences in results. Butanol extraction purified nhSP-A, however, has previously been shown to be functional in enhancing uptake of liposomes by ATII cells, stimulating directed actin-based responses in alveolar macrophages and enhancing phagocytosis of pathogens amongst other functions (94, 107, 254). However, as far as the author is aware, a direct comparison of the function of SP-A purified through the different techniques has not been undertaken.

Further work using SPR analysis to compare the capacity of nhSP-A purified from healthy or PAP individuals using either EGTA washing or butanol extraction to bind a range of ligands would allow these potential differences to be delineated. This would be important, particularly for gp140 CN54 and gp120 BaL proteins which prior to this present study, nhSP-A has not previously been shown to bind to. The inability of nhSP-A to bind gp120 BaL or gp140 CN54 was not an artefact of nhSP-A immobilisation as these HIV ligands were also immobilised onto a Biacore chip and binding was not detected upon use of nhSP-A purified from two different patients as analytes.

Extremely low levels of calcium-dependent binding of rfhSP-A to gp120 IIIB were also found with a bound analyte:immobilised rfhSP-A trimer ratio of 1:411. However, no binding was detected for recombinant gp120 BaL or whole inactivated particles. Comparatively, nhSP-D bound to gp120 IIIB (1:25), gp120 BaL (1:26) and trimeric gp140 CN54 (1:36). nhSP-D also bound to inactivated HIV BaL particles and HIV MN. It appeared that nhSP-D bound to more HIV BaL than HIV MN. However, the inactivated particles have unknown molecular weights and weight differences are likely between different strains. Caution must, therefore be used when comparing relative levels of binding. Low levels of SP-D binding to NVCL controls were also found especially for the H9 T cell line lysate used to amplify HIV MN. However, binding levels were significantly lower than found upon analysis of the inactivated particles. This background binding to control NVCL may be attributed to cell surface receptors found on the cells used to amplify the HIV. SP-D has been shown to interact with numerous different cell receptors, reviewed in (74). It would be interesting to test relative binding levels of SP-D and SP-A to recombinant putative cell receptors by SPR to comprehensively identify which cell surface receptors SP-A and SP-D interact with. The ability of SP-D to bind inactivated HIV BaL particles and recombinant gp120 IIIB agrees with previously

reported results (129). However, the finding that SP-D binds inactivated HIV MN particles, as far as the author is aware, has not previously been demonstrated.

The capacity of rfhSP-D to bind HIV ligands was beyond the scope of this present study. rfhSP-D has previously been shown to inhibit infection of Jurkat T cells, U937 monocytic cells and activated PBMCs and prevent the production of pro inflammatory cytokine (317). However, this study failed to investigate the interactions of HIV with dendritic cells and the impact of rfhSP-D binding. nhSP-D has previously been shown to prevent the infection of T cells but enhance infection of dendritic cells (129). This could be due to agglutination of the HIV virus due to the oligomeric structure of nhSP-D and enhanced uptake of HIV by the dendritic cells. Alternatively, it could be due to the binding of the N-terminal domain of SP-D binding to a receptor on the dendritic cell, providing a route of entry for HIV. However, rfhSP-D, lacks this N-terminal domain integral to both of these potential mechanisms for enhanced dendritic cell uptake. It would, therefore, be intriguing to see whether, alongside the capacity of rfhSP-D to prevent T cell infection, it lacks the capacity to be hijacked by HIV to allow enhanced infection of dendritic cells and transfer to T cells. Dendritic cells are key reservoirs of HIV and are thought to be important disseminators of HIV virus by trans-infection of CD4+ T cells (318). rfhSP-D may, therefore, have therapeutic potential in contrast to the full-length SP-D molecule. Moreover, the finding in this present study of the capacity of rfhSP-A to bind to HIV gp120 IIIB protein needs further delineation. It would be extremely interesting to test the impact of rfhSP-A on infection of T cells, dendritic cells and PBMCs with this strain of HIV and others.

7.5.2.3 ***Binding to Allergens***

Binding of rfhSP-A and nhSP-A to house dust mite and grass pollen extracts was not detected in this present study. This contrasts with previous studies where nhSP-A has been shown to bind to house dust mite extracts from both *D. pteronyssinus 1* and *D. farina* (195). In addition, this contrasts with previous studies demonstrating the capacity of nhSP-A to bind *D. glomerata*, *P. nigari* and *P. praensis* grass pollen extracts (197, 198).

nhSP-D bound to house dust mite extracts from both *D. pteronyssinus 1* and *D. farina* in a calcium-dependent manner, as previously demonstrated (195). In this present study, nhSP-D was also found to bind to *D. glomerata* grass pollen in a calcium-dependent

manner, as previously demonstrated (198, 307). nhSP-D binding to *P. praensis* has also previously been demonstrated but only negligible levels of binding were detected in this present study (308). Negligible levels of binding to *P. nigari* were also found. However, as far as the author is aware, nhSP-D binding to *P. nigari* has not been previously demonstrated. Importantly the molecular weights of the house dust mite and pollen extracts is unknown, relative levels of binding are, therefore, hard to interpret. It would be interesting to further investigate the capacity of rfhSP-A, nhSP-A and nhSP-D to bind fungal allergens as has previously been demonstrated, reviewed in (319).

The binding of SP-D to grass and house dust mite allergens is known to have functional importance in terms of enhancing phagocytosis and clearance of the allergens by macrophages but also prevention of allergen induced IgE release and cytokine release from lymphocytes (188, 320). SP-D has previously been shown to augment allergic airway disease and has been prevented by administration of rfhSP-D in mice (199). The binding of SP-D to these allergen ligands is in accordance with these studies.

7.5.2.4 *Binding to Bacterial LPS*

In this present study, nhSP-A was found to bind LPS from *H. influenzae* Eagan wild type with a bound analyte:immobilised collectin trimer ratio of 1:55. nhSP-A also bound to LPS from *H. influenzae* E4A (1:18), smooth LPS from *E. coli* (1:35) and *K. pneumoniae* (1:40). However, rfhSP-A was only found to bind LPS from *K. pneumoniae* (1:77) and not to other types of LPS. nhSP-A has previously been shown to bind LPS from *K. pneumoniae* (110). The increased capacity of nhSP-A to bind LPS from *K. pneumoniae* as compared with rfhSP-A is expected due to the lower binding avidity as a result of the fewer CRDs. This may also explain rfhSP-A not binding to LPS from *H. influenzae* Eagan wild type, *H. influenzae* E4A and smooth LPS from *E. coli* LPS. Alternatively, the absence of the glycosylation within the CRD of rfhSP-A or of the N-terminal domain may have some impact on the ability of rfhSP-A to bind LPS ligands. The finding that nhSP-A bound to the E4A mutant *H. influenzae* LPS (1:18) more than the wild type (1:55) was expected due to the more exposed lipid-A moiety available for SP-A binding. The ability of nhSP-A to bind to smooth *E. coli* LPS was surprising due to the previous studies where nhSP-A has been shown to bind rough but not smooth LPS (84, 102). Other studies have, however, found SP-A to preferentially bind rough LPS but also to bind smooth *E. coli*

LPS at low levels using the same strain as used in this present study (O111:B4) (102, 306).

In this present study, nhSP-D bound smooth LPS from *E. coli* to a high level (1:13). The capacity of nhSP-D to bind smooth LPS was anticipated to be low due to the previous finding of SP-D binding to the core oligosaccharides of LPS which is less exposed in smooth LPS (101). Moreover, nhSP-D was found to bind to similar degrees but slightly higher to Eagan wild type (1:9) as compared with the E4A mutant *H. influenzae* LPS with exposed core oligosaccharides (1:12), this contrasts with results of a previous study (306). nhSP-D also bound to LPS from *K. pneumoniae* to a high level (1:9), as has previously been reported (321). The differing capacity of nhSP-A and nhSP-D to bind different types of LPS to varying degrees highlights the overlapping but distinct functions of these proteins. It would be particularly interesting to investigate the comparative ability of rfhSP-D to bind these types of LPS as well.

The finding that nhSP-A bound to BSA at low levels in a calcium-dependent manner (1:132) was surprising. The binding of nhSP-A to BSA was also found in preliminary solid phase binding assays (data not shown). This interaction could potentially due to contamination of BSA for instance with endotoxin. If this interaction is a true interaction, this should be considered in the future upon deciding on blocking reagents used in assays such as Western blotting and ELISAs.

7.5.2.5 *Future Binding Studies*

As discussed above, analysis of the ability of rfhSP-D to bind known ligands as compared with nhSP-D would be of significant interest, particularly ligands of RSV and HIV. Moreover, SP-A1 and SP-A2 have previously been shown to have different binding preferences (57, 234, 235). Use of this SPR experimental approach could allow differences between SP-A1 and SP-A2 to be rapidly assessed; this could be undertaken through production of an equivalent rfhSP-A2 molecule. In the future for use as an additional control, a rfhSP-A misfolded negative control could also be included in these binding assays, as used for the infection assays discussed later. This could be comprised of dimeric or monomeric rfhSP-A purified by gel filtration which lacks the capacity to bind carbohydrate affinity columns. Further investigation of the capacity of rfhSP-A, nhSP-A and nhSP-D to bind RSV F and G proteins is also an important future step. It

would be particularly useful to use proteins from the same strain of RSV as used in the RSV neutralisation assays discussed below.

7.5.3 Neutralisation of RSV

As discussed in Section 1.11.2, the interaction of lung collectins with RSV is unclear, particularly for SP-A. SP-A has been shown to prevent RSV infection *in vivo* (118). However, it has also been shown to provide a route of entry for the virus *in vitro.* The overarching aim of this study was to produce a rfhSP-A molecule and delineate the importance of the N-terminal domain on the interaction of SP-A with RSV and the resulting impact on infection of bronchial epithelial cells. The ability of rfhSP-D produced as a soluble protein using NT^{dm} to neutralise RSV was also assessed as compared with nhSP-D and rfhSP-D produced through the traditional refolding method.

In this chapter, rfhSP-A and nhSP-A were shown to bind BBG2Na containing the core region of RSV G protein expressed by Sendai virus, albeit at low levels. The ability of rfhSP-A to neutralise RSV and prevent infection of bronchial epithelial cells was thus subsequently analysed alongside rfhSP-D, nhSP-A and nhSP-D. Bronchial epithelial cells were initially infected with a low dose of RSV (MOI of 0.08) after pre-incubation with or without different collectins. nhSP-A, nhSP-D and trimeric rfhSP-A reduced RSV infection in a dose-dependent manner. However, rfhSP-A reduced RSV infection significantly more effectively than both nhSP-A and nhSP-D ($p < 0.05$). To confirm these results, bronchial epithelial cells were infected with a higher dose of RSV (MOI of 0.4) and the ability of different collectins to reduce RSV infection was assessed using a different technique, namely flow cytometry. With the high dose of RSV, nhSP-A reduced RSV infection in a biphasic manner with a mean (SD) reduction of 24.7 (± 27.2) % at 0.02 μg/ml (not significant) and 38.5 (± 28.4) % and 24.7 (± 29.6) % at 1 μg/ml and 5 μg/ml, respectively. Comparatively, rfhSP-A significantly reduced RSV infection in a dose-dependent manner significantly more effectively than nhSP-A ($p < 0.0001$ at 5 μg/ml) by up to 96.4 (± 1.9) %, resulting in infection levels of only 3.6 (± 1.9) % which was similar to the background level of the uninfected control (2.5 (± 0.2) %). Due to its efficacy in neutralisation of RSV, rfhSP-A may have therapeutic potential for prevention of RSV infection, particularly in premature neonates at high risk of infection. This now needs to be further investigated using *in vivo* pre-clinical models or ex vivo human tissue models of infection.

nhSP-A has previously been reported to provide a route of entry for RSV into HEp-2C cells (148). However, nhSP-A has also been shown to neutralise RSV *in vitro* and *in vivo* (118, 205). There were experimental differences between these studies. Firstly, nhSP-A was shown to provide a route of entry using a low dose of RSV (estimated MOI of 0.08) compared with the MOI of 1 used to demonstrate the ability of nhSP-A to reduce RSV infection (93, 147). Indeed, in the present study, differences in the ability of nhSP-A to neutralise RSV were seen upon use of different doses of RSV and analytical techniques. This, therefore, may be an important factor influencing the capacity of SP-A to neutralise RSV. Both of these studies used HEp-2 cells and a strain of RSV A2. However, this discrepancy between reports may be as a result of the use of slightly different RSV strains or being from different sources. In addition, there may be some impact on the use of different culture medias with different L-glutamine concentrations. These experimental differences in addition to potential patient variability and different techniques used to purify the nhSP-A could explain the differences in experimental results.

The importance of nhSP-A during RSV infection in an *in vivo* setting is likely very different due to the presence of lipid surfactant as well as various immune cells and cytokines. nhSP-A likely has an important role in agglutination of RSV and, as previously demonstrated, enhances phagocytosis of RSV by macrophages (146). nhSP-A was previously shown to neutralise RSV reducing infection levels by 13.3 % and 53.3 % at a concentration of 10 μg/ml and 20 μg/ml, respectively (147). In this present study, lower concentrations of nhSP-A were used but the capacity for neutralisation was not dissimilar with infection levels being reduced by up to 38.5 (± 28.4) % at 1 μg/ml. Further work investigating the importance of rfhSP-A in enhancing the uptake of RSV by macrophages in addition to clearance *in vivo* is now essential.

rfhSP-A was significantly more effective at reducing RSV infection than nhSP-A and notably reduced infection levels to near the level of the uninfected control. It is tempting to hypothesise that this is due to the ability of rfhSP-A to bind to and neutralise RSV whilst lacking the N-terminal domain which may provide a route of entry into the host cell through binding putative receptors. However, other factors may be important for this increased neutralisation capacity. Firstly, infection assays were undertaken by adding a concentration of protein by weight, as assessed by OD λ = 280 nm. This was done to allow comparison with the previous literature. In addition, nhSP-A and rfhSP-A are

different proteins and it is possible that all domains of the molecule are important for interacting with RSV. The SP-A1 gene of nhSP-A has a molecular weight of 26.2 kDa (excluding glycosylations and other post translational modifications) comparative to the 18.8 kDa molecular weight of rfhSP-A. This resulted in 39 % fewer functional CRDs being added into the assay for nhSP-A as compared with rfhSP-A for the same protein concentration. However, this difference does not account for the striking improvement of the neutralisation capacities of rfhSP-A as compared with nhSP-A. As discussed above, the nhSP-A was purified by butanol extraction from PAP without selection for functional carbohydrate binding protein. This may also have some effect on the ability of nhSP-A to neutralise RSV.

As discussed above, in this present study, rfhSP-A bound to BBG2Na (containing RSV G protein core region) at low levels. It may be tempting to hypothesise that the striking efficacy of rfhSP-A in neutralising RSV is through binding to the RSV G protein. However, the RSV G protein has previously been demonstrated to not be essential for infection of host cells (322). The mechanism through which rfhSP-A neutralises RSV, thus needs to be further elucidated. It is possible that rfhSP-A neutralises through binding to the trimeric F protein. However, such an interaction was not found in this present study; this may however be a consequence of strain specific differences or low concentrations of analytes or levels of contamination as discussed above.

nhSP-A did not increase levels of RSV infection as has previously been found (148). This could be explained by the use of different host cells and different doses and strains of RSV. Alternatively, the nhSP-A purified in this present study was of an extremely higher order oligomeric structure. This could potentially affect the accessibility of the N-terminal domain to interact with the host cells.

Importantly, in this study, dimeric rfhSP-A, which was originally included as a negative control, also reduced RSV infection, however substantially less so than trimeric rfhSP-A. This could either be an artefact attributed to the presence of a contaminant in the rfhSP-A protein preparations produced in *E. coli*. Alternatively, it could be a true reduction in RSV infection, suggesting that one or two of the CRDs are correctly folded in the dimeric molecule which retains the capacity to bind to RSV with subsequent neutralisation. Interestingly, a monomeric SP-A CRD/neck has previously been shown to function in binding to ATII cells and inhibiting phospholipid secretion, suggesting that the trimeric

structure with three correctly folded CRDs may not be essential for SP-A function (294). This may explain the results obtained in this present study. It would, thus, also be interesting to investigate the capacity of monomeric rfhSP-A to neutralise RSV.

The ability of rfhSP-D produced as a soluble protein using NT^{dm} to reduce RSV infection was compared with both rfhSP-D produced through the traditional refolding method and nhSP-D. rfhSP-D produced using NT^{dm}, reduced RSV infection levels by a similar level as rfhSP-D produced using the traditional refolding technique (up to 32.2 (± 25.6) % compared with up to 37.8 (± 21.7) %). Furthermore, the capacity of nhSP-D to reduce RSV infection levels was slightly higher but similar (up to 47.2 (± 25.6) %), suggesting that, comparative to nhSP-A, the oligomeric structure may not impact on the ability of SP-D to neutralise RSV as was seen for SP-A. Addition of BSA as a negative control of a protein of a similar size as rfhSP-D did not neutralise RSV, in fact it appeared to enhance infection slightly. This indicates that the reduction in RSV infection is unlikely to be an artefact of adding a non-specific protein into the assay.

Following from the work in this chapter, the impact of rfhSP-A on RSV induced cytokine production, which is key to the pathogenesis caused by RSV, is an important next step. This is particularly the case if rfhSP-A is able to bind RSV G protein which is known to cause pathogenesis through mimicking of cellular cytokines (323). The ability of rfhSP-A to modulate RSV clearance by macrophages both *in vitro* and *in vivo* is now of crucial importance, as is identification of the mechanism or putative receptor on the host cell by which nhSP-A has been shown to enhance RSV entrance. The comparative capacity of an equivalent rfhSP-A2 molecule or a rfhSP-A molecule with a physiological ratio of SP-A1:SP-A2 to neutralise RSV would allow functional differences between the two genes attributed to the CRD to be discerned. It would also be intriguing to investigate the interaction of rfhSP-A and nhSP-A using an imaging technique such as cryo-electron microscopy to visualise the interaction of these collectins with purified RSV.

The importance of the N-terminal domain and oligomeric structure on the interaction of SP-A with an array of other pathogens can now be studied. Of particular interest is the interactions of SP-A with *M. tuberculosis* and HIV which have been reported to enhance attachment of *M. tuberculosis* to alveolar macrophages and enhance infection of dendritic cells by HIV (303, 324).

7.5.4 Summary

In summary, rfhSP-A was shown to bind to BBG2Na containing RSV G protein expressed by Sendai virus, mannan, LPS from *K. pneumoniae* and recombinant gp120 IIIB of HIV in a calcium-dependent manner, albeit at low levels.

rfhSP-A was significantly more effective than nhSP-A at neutralising different doses of RSV and preventing infection of human bronchial epithelial cells. Notably, upon investigation of the capacity of rfhSP-A to neutralise a high dose of RSV, rfhSP-A reduced levels of infected cells to near the uninfected control. This striking increase in efficacy of rfhSP-A to neutralise RSV as compared with nhSP-A may be due to the capacity of rfhSP-A to neutralise RSV whilst lacking the N-terminal domain. This N-terminal domain may allow agglutination of RSV through the oligomeric structure of SP-A or mediate binding to host cell receptors. These mechanisms may enhance uptake of RSV to the host. However, this needs to be further elucidated.

Importantly, rfhSP-D purified using the novel improved expression strategy through use of NT^{dm}, had similar efficacy in neutralising RSV as rfhSP-D produced using the traditional refolding method. However, contrasting to SP-A, the oligomeric structure did not impact greatly on the capacity of SP-D to reduce RSV infection.

Further work now needs to be undertaken, particularly through using further optimised binding studies to delineate this interaction of SP-A and rfhSP-A with RSV virions and purified F and G proteins from different strains. In addition, the impact of rfhSP-A as compared with nhSP-A on the clearance of RSV and RSV-mediated pathology in pre-clinical *in vivo* or *ex vivo* models now needs to be tested. rfhSP-A is now a useful tool for investigating the importance of the human SP-A structure for various natural functions. Importantly, rfhSP-A and rfhSP-D may have therapeutic potential particularly due to the demonstration of the use of this novel NT^{dm} expression strategy in allowing straightforward production of soluble functional rfhSP-D with improved yields.

Chapter 8: Summary and Future Directions

SP-A and SP-D are important anti-pathogenic and immunomodulatory innate immune molecules (reviewed in (4)). A functional rfhSP-D molecule has been produced and given insights into the structure/function relationship of SP-D and its mode of ligand binding (224, 297). This protein has potential for treatment of various respiratory diseases, particularly for preventing neonatal chronic lung diseases as an adjunct treatment to current lipid surfactants, which lack SP-A and SP-D. The current methodology for production of rfhSP-D involves expression as an insoluble protein which requires refolding and substantial loss in protein yields.

No one has as yet generated an equivalent trimeric rfhSP-A molecule. A trimeric rfrSP-A molecule has been generated previously and the crystal structure characterised. However, as discussed in Section 1.7.1, there are structural and functional differences between rat and human SP-A. In particular, unlike rat SP-A, human SP-A is composed of two different genes (4, 119). It was hypothesised in this present study that through inclusion of the Gly Xaa Yaa collagen-like stalk, a functional trimeric rfhSP-A would be successfully generated. A functional rfhSP-A molecule could be used as an investigative tool to help elucidate the importance of the N-terminus and oligomeric structure for various functions of SP-A. This is particularly relevant for its interaction with RSV where conflicting *in vitro* studies have shown SP-A to either neutralise RSV or provide a route of entry for RSV into host cells (147, 148).

The overarching aim of this study was to clone, express and purify a rfhSP-A molecule equivalent to the functional fragment of rfhSP-D and test this SP-A fragment in its capacity to bind various ligands and neutralise RSV. For comparison in functional assays, nhSP-A and nhSP-D were purified and attempts to quantify the SP-A1:SP-A2 ratio of nhSP-A using mass spectrometry are reported. An additional aim was to assess the utility of NT and NT^{dm} from spider silk protein as novel solubility tags to allow heterologous expression of soluble rfhSP-A and rfhSP-D and subsequent purification, without the need for protein refolding (full list of aims given in - Section 1.14).

In this study nhSP-A and nhSP-D were successfully purified using different techniques. Differences between the purification techniques and their impact on the nhSP-A oligomeric structure were found and should be considered in future studies. Moreover, the lack of an affinity purification step for selecting for functional nhSP-A should also be considered when comparing SP-A functionality with other collectins. Peptides, which

distinguished between SP-A1 and SP-A2, were successfully detected by mass spectrometry. However, further optimisation of protein preparation prior to mass spectrometry needs to be undertaken to allow detection of peptides suitable for quantifying an SP-A1:SP-A2 ratio.

SP-A1 and SP-A2 genes were successfully cloned and rfhSP-A1 and rfhSP-A2 were subcloned into expression vectors. It was only upon subcloning of NT-rfhSP-A and NT^{dm}-rfhSP-A using the rfhSP-A1 sequence and subsequent expression of these fusion proteins that rfhSP-A was successfully expressed. The inability of rfhSP-A1 or rfhSP-A2 to be expressed alone was hypothesised to be due to either toxicity of the proteins to the *E. coli* or an inability of the *E. coli* to express the N-terminal amino acid sequence of the fragments. Use of NT allowed the expression of rfhSP-A as an insoluble protein which, upon refolding, allowed efficient purification of an average yield of 12.7 (± 4.4) mg/litre. After optimisation of the refold protocol, up to 81 % of rfhSP-A produced through this method was trimeric and a fraction (up to 12 %) was successfully purified by carbohydrate affinity chromatography. Comparatively, NT^{dm} allowed for an increased yield of 23.3 (± 5.4) mg of rfhSP-A as compared with the 12.7 (± 4.4) mg/litre yield using NT. Moreover, this was expressed as a soluble protein without the need for refolding. However, only 24 (± 4.3) % of this protein was trimeric and no functional protein was purified by carbohydrate affinity chromatography. The inability to purify large quantities of rfhSP-A by carbohydrate affinity purification was hypothesised to be a result of the binding avidity for a trimeric molecule being too low or the CRDs of rfhSP-A being misfolded. Other purification techniques could be explored in the future to allow higher yields of protein to be purified.

NT and NT^{dm} were successful in allowing the expression of rfhSP-D as a soluble molecule. rfhSP-D expressed using NT^{dm} was purified with a yield after carbohydrate affinity chromatography which would correspond to approximately 31.3 mg/litre upon scale up. This was substantially higher than the 3.3 mg/litre obtained using the traditional refolding protocol. Importantly, this was using a non-optimised production process, which through further optimisation could increase yields substantially.

rfhSP-A was shown to be functional and bound various ligands including BBG2Na (containing RSV G protein) expressed by Sendai virus, mannan, LPS from *K. pneumoniae* and recombinant gp120 IIIB of HIV in a calcium-dependent manner, albeit

at low levels. rfhSP-A as well as nhSP-A and nhSP-D were not shown to interact with whole RSV particles using the viral stock included in the RSV neutralisation assay. This was hypothesised to be due to contamination by cell lysate preventing this interaction or too low a concentration being used for binding to be discerned. Production of an equivalent rfhSP-A2 molecule and comparison of binding capacities would allow functional differences between the two genes to be discerned in the future, in addition to generating a rfhSP-A molecule with a physiological ratio of rfhSP-A1/rfhSP-A2. Future crystallisation of rfhSP-A or resolution of its solution structure could give important insights into the structure of the human SP-A neck and CRD and its mechanism of calcium-dependent ligand binding.

rfhSP-A was significantly more effective than nhSP-A at neutralising different doses of RSV and prevented infection of human bronchial epithelial cells by up to 96.4 (± 1.9) % as compared with 38.5 (± 28.4) %. Notably, upon infection with a high dose of RSV, rfhSP-A reduced levels of infected cells to near uninfected control levels. This may be due to the capacity of rfhSP-A to neutralise RSV whilst lacking the N-terminal domain, which may be important for being used as a route of entry by RSV to the host cell.

nhSP-D was shown to bind to various known ligands including RSV pre and post-fusion F proteins, F and BBG2Na proteins expressed by Sendai virus, recombinant HIV gp120 proteins, inactivated HIV particles, house dust mite extracts, pollen extracts and LPS from *H. influenzae*, *K. pneumoniae* and *E. coli*. Importantly, as far as the author is aware, nhSP-D has not previously been shown to bind to HIV gp140 (CN54) and the capacity to bind RSV F pre or post-fusion protein has not been distinguished. Future studies including rfhSP-D produced through both refolding and the new soluble production method using NT^{dm} is now essential to allow the importance of the SP-D oligomeric structure to be discerned in addition to any potential difference in the functionality of rfhSP-D produced using these two different techniques.

nhSP-D reduced levels of RSV infection of human bronchial epithelial cells by up to 47.2 (± 25.6) %. rfhSP-D neutralised RSV to a similar level of efficacy as nhSP-D (37.8 (± 21.7) %) suggesting that, unlike SP-A, the oligomeric structure of SP-D does not appear to impact greatly on its capacity to neutralise RSV. Moreover, rfhSP-D expressed using NT^{dm} neutralised RSV with similar efficacy as rfhSP-D produced through the traditional refolding method (up to 32.2 (± 25.6) % compared with 37.8 (± 21.7) %).

Further work now needs to be undertaken to fully elucidate the mechanism through which rfhSP-A neutralises different strains of RSV. Moreover, the impact of rfhSP-A in pre-clinical *in vivo* models now needs to be undertaken to investigate its impact on RSV-induced pathology. rfhSP-A is now a useful tool through which the importance of the N-terminus and human SP-A oligomeric structure in various functions can be investigated. This may be particularly useful in delineating the mechanism through which SP-A enhances the attachment of *M. tuberculosis* to macrophages and infection of dendritic cells and transfer to T cells by HIV (303, 324).

To summarise, in this study, introduction of a novel expression strategy has allowed the successful production and purification of a functional rfhSP-D molecule without the need for refolding. Moreover, an equivalent functional trimeric rfhSP-A molecule has been successfully made for the first time. rfhSP-A has been successfully shown to neutralise RSV more effectively than the native oligomeric protein, preventing infection of human bronchial epithelial cells. Contrastingly, the capacity of rfhSP-D and nhSP-D to neutralise RSV was not substantially different. rfhSP-A is now a useful tool for investigating the structure/function relationship of SP-A with an array of different pathogens. rfhSP-A and rfhSP-D may have therapeutic potential, particularly as adjunct treatments to current lipid surfactant treatments. This could protect the premature neonatal lung from infection and inflammation and prevent the development of neonatal chronic lung disease.

Appendices

Below are cloned cDNA and amino acid sequences for recombinant proteins (Figure 8-1 and Figure 8-2)

rfhSP-A1

A

```
ATGGCTAGCGGAGCCCCTGGTATCCCTGGAGAGTGTGGAGAGAAGGGGGAGCCTGGCGAGAGGGGCCCTC
CAGGGCTTCCAGCTCATCTAGATGAGGAGCTCCAAGCCACACTCCACGACTTTAGACATCAAATCCTGCA
GACAAGGGGAGCCCTCAGTCTGCAGGGCTCCATAATGACAGTAGGAGAGAAGGTCTTCTCCAGCAATGGG
CAGTCCATCACTTTTGATGCCATTCAGGAGGCATGTGCCAGAGCAGGCGGCCGCATTGCTGTCCCAAGGA
ATCCAGAGGAAAATGAGGCCATTGCAAGCTTCGTGAAGAAGTACAACACATATGCCTATGTAGGCCTGAC
TGAGGGTCCCAGCCCTGGAGACTTCCGCTACTCAGACGGGACCCCTGTAAACTACACCAACTGGTACCGA
GGGGAGCCCGCAGGTCGGGGAAAAGAGCAGTGTGTGGAGATGTACACAGATGGGCAGTGGAATGACAGGA
ACTGCCTGTACTCCCGACTGACCATCTGTGAGTTCTGAGAGGCATTTAGGCCATGGGGGATCC
```

B

```
M A S G A P G I P G E C G E K G E P G E R G P P G L P A H L D E E L
Q A T L H D F R H Q I L Q T R G A L S L Q G S I M T V G E K V F S S
N G Q S I T F D A I Q E A C A R A G G R I A V P R N P E E N E A I A
S F V K K Y N T Y A Y V G L T E G P S P G D F R Y S D G T P V N Y T
N W Y R G E P A G R G K E Q C V E M Y T D G Q W N D R N C L Y S R L
T I C E F Stop E A F R P W G I
```

rfhSP-A2

C

```
ATGGCTAGCGGAGCCCCTGGTGTCCCTGGAGAGCGTGGAGAGAAGGGGGAGGCTGGCGAGAGAGGCCCTC
CAGGGCTTCCAGCTCATCTAGATGAGGAGCTCCAAGCCACACTCCACGACTTCAGACATCAAATCCTGCA
GACAAGGGGAGCCCTCAGTCTGCAGGGCTCCATAATGACAGTAGGAGAGAAGGTCTTCTCCAGCAATGGG
CAGTCCATCACTTTTGATGCCATTCAGGAGGCATGTGCCAGAGCAGGCGGCCGCATTGCTGTCCCAAGGA
ATCCAGAGGAAAATGAGGCCATTGCAAGCTTCGTGAAGAAGTACAACACATATGCCTATGTAGGCCTGAC
TGAGGGTCCCAGCCCTGGAGACTTCCGCTACTCAGATGGGACCCCTGTAAACTACACCAACTGGTACCGA
GGGGAGCCTGCAGGTCGGGGAAAAGAGCAGTGTGTGGAGATGTACACAGATGGGCAGTGGAATGACAGGA
ACTGCCTGTACTCCCGACTGACCATCTGTGAGTTCTGAGAGGCATTTAGGCCATGGGGGATCC
```

D

```
M A S G A P G V P G E R G E K G E A G E R G P P G L P A H L D E E L
Q A T L H D F R H Q I L Q T R G A L S L Q G S I M T V G E K V F S S
N G Q S I T F D A I Q E A C A R A G G R I A V P R N P E E N E A I A
S F V K K Y N T Y A Y V G L T E G P S P G D F R Y S D G T P V N Y T
N W Y R G E P A G R G K E Q C V E M Y T D G Q W N D R N C L Y S R L
T I C E F Stop E A F R P W G
```

Figure 8-1: Cloned rfhSP-A1 and rfhSP-A2 DNA sequences and corresponding amino acid sequences. *Shown are the cloned DNA sequences for rfhSP-A1 (**A**) and rfhSP-A2 (**B**) and corresponding amino acid sequences (**C** and **D**, respectively). Indicated are amino acids which are different between rfhSP-A1 and rfhSP-A2 (bold) in addition to the stop codon (grey).*

A **NT-rfhSP-A**

M G H H H H H H M S H T T P W T N P G L A E N F M N S F M Q G L S
S M P G F T A S Q L D D M S T I A Q S M V Q S I Q S L A A Q G R T
S P N K L Q A L N M A F A S S M A E I A A S E E G G G S L S T K T
S S I A S A M S N A F L Q T T G V V N Q P F I N E I T Q L V S M F
A Q A G M N D V S A G N S A L V P R **G S P** **G I P G E C G E K G E P**
G E R G P P G L P A H L D E E L Q A T L H D F R H Q I L Q T R G A
L S L Q G S I M T V G E K V F S S N G Q S I T F D A I Q E A C A R
A G G R I A V P R N P E E N E A I A S F V K K Y N T Y A Y V G L T
E G P S P G D F R Y S D G T P V N Y T N W Y R G E P A G R G K E Q
C V E M Y T D G Q W N D R N C L Y S R L T I C E F

B **rfhSP-A (after cleavage from NT-rfhSP-A)**

G S P G I P G E C G E K G E P G E R G P P G L P A H L D E E L Q A
T L H D F R H Q I L Q T R G A L S L Q G S I M T V G E K V F S S N
G Q S I T F D A I Q E A C A R A G G R I A V P R N P E E N E A I A
S F V K K Y N T Y A Y V G L T E G P S P G D F R Y S D G T P V N Y
T N W Y R G E P A G R G K E Q C V E M Y T D G Q W N D R N C L Y S
R L T I C E F

C **NT^{dm}-rfhSP-A**

M G H H H H H H M S H T T P W T N P G L A E N F M N S F M Q G L S
S M P G F T A S Q L D K M S T I A Q S M V Q S I Q S L A A Q G R T
S P N D L Q A L N M A F A S S M A E I A A S E E G G G S L S T K T
S S I A S A M S N A F L Q T T G V V N Q P F I N E I T Q L V S M F
A Q A G M N D V S A G N S A L E V L F Q **G P** **G I P G E C G E K G E**
P G E R G P P G L P A H L D E E L Q A T L H D F R H Q I L Q T R G
A L S L Q G S I M T V G E K V F S S N G Q S I T F D A I Q E A C A
R A G G R I A V P R N P E E N E A I A S F V K K Y N T Y A Y V G L
T E G P S P G D F R Y S D G T P V N Y T N W Y R G E P A G R G K E
Q C V E M Y T D G Q W N D R N C L Y S R L T I C E F

D **rfhSP-A (after cleavage from NT^{dm}-rfhSP-A)**

GPGIPGECGEKGEPGERGPPGLP AHLDEELQAT
LHDFRHQILQTRGALSLQGSIMTVGEKVFSSNG
QSITFDAIQEACARAGGRIAVPRNPEENEAIAS
FVKKYNTYAYVGLTEGPSPGDFRYSDGTPVNYT
NWYRGEPAGRGKEQCVEMYTDGQWNDRNCLYSR
LTICEF

E **NT^{dm}-rfhSP-D**

MGHHHHHHM SHTTPWTNPGLAENFMNSFMQGLS
SMPGFTASQLDK MSTIAQSMVQSIQSLAAQGRT
SPND LQALNMAFASSMAEIAASEEGGGSLSTKT
SSIASAMSNAFLQTTGVVNQPFINEITQLVSMF
AQAGMNDVSAGNSA LEVLFQ GPGPGLKGDKGIP
GDKGAKGESGLP DVASLRQQVEALQGQVQHLQA
AFSQYKKVELFPNGQSVGEKIFKTAGFVKPFTE
AQLLCTQAGGQLASPRSAAENAALQQLVVAKNE
AAFLSMTDSKTEGKFTYPTGESLVYSNWAPGKP
NDDGGSEDCVEIFTNGKWNDRACGEKRLVVCEF

F **rfhSP-D (after cleavage from NT^{dm}-rfhSP-D)**

GPGLKGDKGIPGDKGAKGESGLP DVASLRQQVE
ALQGQVQHLQAAFSQYKKVELFPNGQSVGEKIF
KTAGFVKPFTEAQLLCTQAGGQLASPRSAAENA
ALQQLVVAKNEAAFLSMTDSKTEGKFTYPTGES
LVYSNWAPGKPNDDGGSEDCVEIFTNGKWNDRA
CGEKRLVVCEF

G **rfhSP-D produced through refolding**

M G S P G L K G D K G I P G D K G A K G E S G L P D V A S L R Q Q
V E A L Q G Q V Q H L Q A A F S Q Y K K V E L F P N G Q S V G E K
I F K T A G F V K P F T E A Q L L C T Q A G G Q L A S P R S A A E
N A A L Q Q L V V A K N E A A F L S M T D S K T E G K F T Y P T G
E S L V Y S N W A P G K P N D D G G S E D C V E I F T N G K W N D
R A C G E K R L V V C E F

Figure 8-2: Amino acid sequences of recombinant proteins. *Given are amino acid sequences for different protein constructs including: NT-rfhSP-A (**A**); rfhSP-A after cleavage from NT-rfhSP-A (**B**); NT^{dm}-rfhSP-A (**C**); rfhSP-A after cleavage from NT^{dm}-rfhSP-A (**D**); NT^{dm}-rfhSP-D (**E**); rfhSP-D after cleavage from NT^{dm}-rfhSP-D (**F**) and rfhSP-D produced through the traditional refolding method. Highlighted in grey is the sequence corresponding to the His_6-tag, highlighted in yellow is the sequence for the thrombin cleavage site, highlighted in green is the sequence corresponding to the HRV 3C protease cleavage site, highlighted in light blue are the Asp40Lys and Lys65Asp mutations in NT^{dm}, bold and underlined is the Gly Xaa Yaa collagen-like stalk of rfhSP-A and rfhSP-D. To note rfhSP-A and rfhSP-D produced using NT^{dm} have the 7^{th} Xaa of the 8 x Gly Xaa Yaa collagen-like stalk missing due to the method of cloning and the HRV 3C protease cleavage site included. rfhSP-D is also missing the start codon methionine present in the rfhSP-D produced using the traditional refolding method. Importantly, rfhSP-D produced through the traditional refolding method contains the sequence "GSP" for the 8^{th} Gly Xaa Yaa of the collagen stalk, this is "GPP" in native SP-D. As far as the author is aware, this change occurred after initial cloning (72, 325) and during recloning of rfhSP-D (31).*

List of References

1. Wright JR. Immunoregulatory functions of surfactant proteins. Nature Reviews Immunology. 2005;5(1):58-68.

2. Pattle RE. Properties, function and origin of the alveolar lining layer. Nature. 1955;175(4469):1125-6.

3. Halliday HL. Surfactants: past, present and future. Journal of Perinatology. 2008;28:S47-S56.

4. Kishore U, Greenhough TJ, Waters P, Shrive AK, Ghai R, Kamran MF, Bernal AL, Reid KBM, Madan T, Chakraborty T. Surfactant proteins SP-A and SP-D: Structure, function and receptors. Mol Immunol. 2006;43(9):1293-315.

5. Wright JR. Immunomodulatory functions of surfactant. Physiological Reviews. 1997;77(4):931-62.

6. Crouch E, Wright JR. Surfactant proteins A and D and pulmonary host defense. Annual Review of Physiology. 2001;63:521-54.

7. Vanhaesebrouck P, Allegaert K, Bottu J, Debauche C, Devlieger H, Docx M, Francois A, Haumont D, Lombet J, Rigo J, Smets K, Vanherreweghe I, Van Overmeire B, Van Reempts P. The EPIBEL study: outcomes to discharge from hospital for extremely preterm infants in Belgium. Pediatrics. 2004;114(3):663-75.

8. Neergaard Kv. Neue Auffassungen über einen Grundbegriff der Atemmechanik. Zeitschrift für die gesamte experimentelle Medizin. 1929;66(1):373-94.

9. Pattle RE, Thomas LC. Lipoprotein composition of the film lining the lung. Nature. 1961;189((4767)):844-.

10. Weaver TE, Whitsett JA. Function and Regulation of Expression of Pulmonary Surfactant-Associated Proteins. Biochemical Journal. 1991;273:249-64.

11. Goerke J. Pulmonary surfactant: functions and molecular composition. Biochimica Et Biophysica Acta-Molecular Basis of Disease. 1998;1408(2-3):79-89.

12. Goss V, Hunt AN, Postle AD. Regulation of lung surfactant phospholipid synthesis and metabolism. Biochim Biophys Acta Mol Cell Biol Lipids. 2013;1831(2):448-58.

13. Perez-Gil J, Weaver TE. Pulmonary Surfactant Pathophysiology: Current Models and Open Questions. Physiology. 2010;25(3):132-41.

14. Bae YM, Bae CW, Oh MH, Lee SH, Woo KM, Jung KB. Effect of exogenous surfactant therapy on levels of pulmonary surfactant proteins A and D in preterm infants with respiratory distress syndrome. J Perinat Med. 2009;37(5):561-4.

15. Amato M, Petit K, Fiore HH, Doyle CA, Frantz ID, Nielsen HC. Effect of exogenous surfactant on the development of surfactant synthesis in premature rabbit lung. Pediatr Res. 2003;53(4):671-8.

16. Veldhuizen R, Nag K, Orgeig S, Possmayer F. The role of lipids in pulmonary surfactant. Biochimica Et Biophysica Acta-Molecular Basis of Disease. 1998;1408(2-3):90-108.

17. Perez-Gil J. Structure of pulmonary surfactant membranes and films: The role of proteins and lipid-protein interactions. Biochimica Et Biophysica Acta-Biomembranes. 2008;1778(7-8):1676-95.

18. de la Serna JB, Perez-Gil J, Simonsen AC, Bagatolli LA. Cholesterol rules - Direct observation of the coexistence of two fluid phases in native pulmonary surfactant membranes at physiological temperatures. J Biol Chem. 2004;279(39):40715-22.

19. Kishore U, Reid KB. Structures and functions of mammalian collectins. Results and problems in cell differentiation. 2001;33:225-48.

20. Friedrich W, Schmalisch G, Stevens PA, Wauer RR. Surfactant protein SP-B counteracts inhibition of pulmonary surfactant by serum proteins. European journal of medical research. 2000;5(7):277-82.

21. Lu KW, Perez-Gil J, Echaide M, Taeusch HW. Pulmonary surfactant proteins and polymer combinations reduce surfactant inhibition by serum. Biochimica Et Biophysica Acta-Biomembranes. 2011;1808(10):2366-73.

22. King RJ, Clements JA. Surface-active materials from dog lung.2. Composition and physiological correlations. American Journal of Physiology. 1972;223(3):715-&.

23. Persson A, Rust K, Chang D, Moxley M, Longmore W, Crouch E. CP4 - a pneumocyte-derived collagenous surfactant-associated protein - evidence for heterogeneity of collagenous surfactant proteins. Biochemistry. 1988;27(23):8576-84.

24. Drickamer K. CA2+ dependent carbohydrate-recognition domains in animal proteins. Current Opinion in Structural Biology. 1993;3(3):393-400.

25. Holmskov UL. Collectins and collectin receptors in innate immunity. APMIS Supplementum. 2000;100:1-59.

26. Hakansson K, Reid KBM. Collectin structure: A review. Protein Science. 2000;9(9):1607-17.

27. Holmskov U, Teisner B, Willis AC, Reid KBM, Jensenius JC. Purification and characterization of a bovine serum lectin (CL-43) with structural homology to conglutinin and SP-D and carbohydrate specificity similar to mannan-bindin protein. J Biol Chem. 1993;268(14):10120-5.

28. Lu JH, Wiedemann H, Holmskov U, Thiel S, Timpl R, Reid KBM. Structural similarity between lung surfactant protein-D and conglutinin - 2 distinct , C-type lectins containing collage-like sequences. European Journal of Biochemistry. 1993;215(3):793-9.

29. van Eijk M, White MR, Crouch EC, Batenburg JJ, Vaandrager AB, van Golde LMG, Haagsman HP, Hartshorn KL. Porcine pulmonary collectins show distinct interactions with influenza A viruses: Role of the N-linked oligosaccharides in the carbohydrate recognition domain. J Immunol. 2003;171(3):1431-40.

30. Benne CA, Kraaijeveld CA, van Strijp JA, Brouwer E, Harmsen M, Verhoef J, van Golde LM, van Iwaarden JF. Interactions of surfactant protein A with influenza A viruses: binding and neutralization. The Journal of infectious diseases. 1995;171(2):335-41.

31. Shrive AK, Tharia HA, Strong P, Kishore U, Burns I, Rizkallah PJ, Reid KBM, Greenhough TJ. High-resolution structural insights into ligand binding and immune cell recognition by human lung surfactant protein D. Journal of Molecular Biology. 2003;331(2):509-23.

32. Head JF, Mealy TR, McCormack FX, Seaton BA. Crystal structure of trimeric carbohydrate recognition and neck domains of surfactant protein A. J Biol Chem. 2003;278(44):43254-60.

33. Heinrich SM, Griese M. Assessment of Surfactant Protein A (SP-A) dependent agglutination. BMC Pulm Med. 2010;10.

34. Hoppe HJ, Reid KBM. Collectins - soluble proteins containing collagenous regions and lectin domains - and their roles in innate immunity. Protein Science. 1994;3(8):1143-58.

35. Zhang PN, McAlinden A, Li S, Schumacher T, Wang HL, Hu SS, Sandell L, Crouch E. The amino-terminal heptad repeats of the coiled-coil neck domain of pulmonary surfactant protein D are necessary for the assembly of trimeric subunits and dodecamers. J Biol Chem. 2001;276(23):19862-70.

36. Li P, Zhou JY, Zhou YY, Qian CD, Li O, Min H, Wu XC. The Coiled-Coil Neck Domain of Human Pulmonary Surfactant Protein D Drives Trimerization and Stabilization of Thioredoxin, a Heterologous Non-Collagenous Protein. Protein Pept Lett. 2009;16(3):306-11.

37. Kovacs H, O'Donoghue SI, Hoppe HJ, Comfort D, Reid KBM, Campbell ID, Nilges M. Solution structure of the coiled-coil trimerization domain from lung surfactant protein D. J Biomol NMR. 2002;24(2):89-102.

38. Ross GF, Notter RH, Meuth J, Whitsett JA. Phospholipid binding and biophysical activity of pulmonary surfactant-associated protein (SAP)-35 and its non-collagenous COOH-terminal domains. J Biol Chem. 1986;261(30):14283-91.

39. Crouch E, Persson A, Chang D, Heuser J. Molecular-structure of pulmonary surfactant protein-D (SP-D). J Biol Chem. 1994;269(25):17311-9.

40. Leth-Larsen R, Holmskov U, Hojrup P. Structural characterization of human and bovine lung surfactant protein D. Biochemical Journal. 1999;343:645-52.

41. Phelps DS, Floros J. Proline hydroxylation alters the electrophoretic mobility of pulmonary surfactant-associated protein-A. Electrophoresis. 1988;9(5):231-3.

42. Garcia-Verdugo I, Sanchez-Barbero F, Bosch FU, Steinhilber W, Casals C. Effect of hydroxylation and N-187-linked glycosylation on molecular and functional properties of recombinant human surfactant protein A. Biochemistry. 2003;42(32):9532-42.

43. Wallis R, Drickamer K. Asymmetry adjacent to the collagen-like domain in rat liver mannose-binding protein. Biochemical Journal. 1997;325:391-400.

44. Knudsen L, Wucherpfennig K, Mackay RM, Townsend P, Muhlfeld C, Richter J, Hawgood S, Reid K, Clark H, Ochs M. A recombinant fragment of human surfactant protein D lacking the short collagen-like stalk fails to correct morphological alterations in lungs of SP-D deficient mice. Anatomical record (Hoboken, NJ : 2007). 2009;292(2):183-9.

45. Voss T, Eistetter H, Schafer KP, Engel J. Macromolecular organization of natural and recombinant lung surfactant protein SP-28-36 - structural homology with the complement factor CLQ. Journal of Molecular Biology. 1988;201(1):219-27.

46. BrownAugsburger P, Hartshorn K, Chang D, Rust K, Fliszar C, Welgus HG, Crouch EC. Site-directed mutagenesis of Cys-15 and Cys-20 of pulmonary surfactant protein D - Expression of a trimeric protein with altered anti-viral properties. J Biol Chem. 1996;271(23):13724-30.

47. Uemura T, Sano H, Katoh T, Nishitani C, Mitsuzawa H, Shimizu T, Kuroki Y. Surfactant protein A without the interruption of Gly-X-Y repeats loses a kink of oligomeric structure and exhibits impaired phospholipid liposome aggregation ability. Biochemistry. 2006;45(48):14543-51.

48. Palaniyar N, Ridsdale RA, Holterman CE, Inchley K, Possmayer F, Harauz G. Structural changes of surfactant protein A induced by cations reorient the protein on lipid bilayers. Journal of Structural Biology. 1998;122(3):297-310.

49. Strang CJ, Slayter HS, Lachmann PJ, Davis AE. Ultrastructure and composition of bovine conglutinin. Biochemical Journal. 1986;234(2):381-9.

50. Griese M, Heinrich S, Ratjen F, Kabesch M, Paul K, Ballmann M, Rietschel E, Kappler M. Surfactant Protein A in Cystic Fibrosis: Supratrimeric Structure and Pulmonary Outcome. PLoS One. 2012;7(12).

51. Kotecha S, Davies PL, Clark HW, McGreal EP. Increased prevalence of low oligomeric state surfactant protein D with restricted lectin activity in bronchoalveolar lavage fluid from preterm infants. Thorax. 2013;68(5):460-7.

52. Sanchez-Barbero F, Strassner J, Garcia-Canero R, Steinhilber W, Casals C. Role of the degree of oligomerization in the structure and function of human surfactant protein A. J Biol Chem. 2005;280(9):7659-70.

53. Kotecha S, Doull I, Davies P, McKenzie Z, Madsen J, Clark HW, McGreal EP. Functional heterogeneity of pulmonary surfactant protein-D in cystic fibrosis. Biochimica et biophysica acta. 2013;1832(12):2391-400.

54. Leth-Larsen R, Garred P, Jensenius H, Meschi J, Hartshorn K, Madsen J, Tornoe I, Madsen HO, Sorensen G, Crouch E, Holmskov U. A common polymorphism in the SFTPD gene influences assembly, function, and concentration of surfactant protein D. J Immunol. 2005;174(3):1532-8.

55. Zhang LQ, Ikegami M, Crouch EC, Korfhagen TR, Whitsett JA. Activity of pulmonary surfactant protein-D (SP-D) in vivo is dependent on oligomeric structure. J Biol Chem. 2001;276(22):19214-9.

56. Haurum JS, Thiel S, Haagsman HP, Laursen SB, Larsen B, Jensenius JC. Studies on the carbohydrate-binding characteristics of human pulmonary surfactant-associated protein A and comparison with two other collectins:

mannan-binding protein and conglutinin. The Biochemical journal. 1993;293 (Pt 3):873-8.

57. Oberley RE, Snyder JM. Recombinant human SP-A1 and SP-A2 proteins have different carbohydrate-binding characteristics. Am J Physiol-Lung Cell Mol Physiol. 2003;284(5):L871-L81.

58. Crouch EC, Smith K, McDonald B, Briner D, Linders B, McDonald J, Holmskov U, Head J, Hartshorn K. Species differences in the carbohydrate binding preferences of surfactant protein D. Am J Respir Cell Mol Biol. 2006;35(1):84-94.

59. Suzuki Y, Fujita Y, Kogishi K. Reconstitution of tubular myelin from synthetic lipids and proteins associated with pig pulmonary surfactant American Review of Respiratory Disease. 1989;140(1):75-81.

60. Kuroki Y, Akino T. Pulmonary surfactant protein-A (SP-A) specificially binds dipalitoylphosphatidylcholine J Biol Chem. 1991;266(5):3068-73.

61. Ogasawara Y, McCormack FX, Mason RJ, Voelker DR. Chimeras of surfactant protein-A and protein -D identify the carbohydrate-recognition domains as essential for phospholipid interaction J Biol Chem. 1994;269(47):29785-92.

62. Childs RA, Wright JR, Ross GF, Yuen CT, Lawson AM, Chai WG, Drickamer K, Feizi T. Specificity of lung surfactant protein SP-A for both the carbohydrate and the lipid moieties of certain neutral glycolipids. J Biol Chem. 1992;267(14):9972-9.

63. Kuroki Y, Gasa S, Ogasawara Y, Makita A, Akino T. Binding of pulmonary surfactant protein-A to galactosylceranide and asialo-G(M2). Archives of Biochemistry and Biophysics. 1992;299(2):261-7.

64. Ogasawara Y, Kuroki Y, Akino T. Pulmonary surfactant protein-D specifically binds to phosphatidylinositol. J Biol Chem. 1992;267(29):21244-9.

65. Strong P, Kishore U, Morgan C, Bernal AL, Singh M, Reid KBM. A novel method of purifying lung surfactant proteins A and D from the lung lavage of alveolar proteinosis patients and from pooled amniotic fluid. Journal of Immunological Methods. 1998;220(1-2):139-49.

66. Kuroki Y, Akino T. Pulmonary surfactant protein-A (SP-A) specifically binds dipalmitoylphosphatidulcholine. J Biol Chem. 1991;266(5):3068-73.

67. Vaniwaarden JF, Shimizu H, Vangolde PHM, Voelker DR, Vangolde LMG. Rat surfactant protein-D enhances the production of oxygen radicals by rat alveolar macrophages. Biochemical Journal. 1992;286:5-8.

68. Kuroki Y, Gasa S, Ogasawara Y, Makita A, Akino T. Binding of pulmonary surfactant protein-A to galactosylceramide and asialo-G(M2. Archives of Biochemistry and Biophysics. 1992;299(2):261-7.

69. Haagsman HP, Sargeant T, Hauschka PV, Benson BJ, Hawgood S. Binding of calcium to SP-A, a surfactant -associated protein. Biochemistry. 1990;29(38):8894-900.

70. Jaekel A, Reid KBM, Clark H. Surfactant protein A (SP-A) binds to phosphatidylserine and competes with annexin V binding on late apoptotic cells. Protein & Cell. 2010;1(2):188-97.

71. Persson AV, Gibbons BJ, Shoemaker JD, Moxley MA, Longmore WJ. The major glycolopid recognized by SP-D in surfactant is phosphatidylinositol. Biochemistry. 1992;31(48):12183-9.

72. Kishore U, Wang JY, Hoppe HJ, Reid KBM. The alpha-helical neck region of human lung surfactant protein D is essential for the binding of the carbohydrate recognition domains to lipopolysaccharides and phospholipids. Biochemical Journal. 1996;318:505-11.

73. Ogasawara Y, Voelker DR. Altered carbohydrate-recognition specificity engineered into surfactant protein-D reveals different binding mechanisms for phosphatidyllinositol and glucosylceramide. J Biol Chem. 1995;270(24):14725-32.

74. Jakel A, Qaseem AS, Kishore U, Sim RB. Ligands and receptors of lung surfactant proteins SP-A and SP-D. Frontiers in Bioscience-Landmark. 2013;18:1129-40.

75. Chroneos ZC, Abdolrasulnia R, Whitsett JA, Rice WR, Shepherd VL. Purification of a cell-surface receptor for surfactant protein A. J Biol Chem. 1996;271(27):16375-83.

76. Yamada C, Sano H, Shimizu T, Mitsuzawa H, Nishitani C, Himi T, Kuroki Y. Surfactant protein a directly interacts with TLR4 and MD-2 and regulates inflammatory cellular response - Importance of supratrimeric oligomerization. J Biol Chem. 2006;281(31):21771-80.

77. Gil M, McCormack FX, Levine AM. Surfactant Protein A Modulates Cell Surface Expression of CR3 on Alveolar Macrophages and Enhances CR3-mediated Phagocytosis. J Biol Chem. 2009;284(12):7495-504.

78. Nepomuceno RR, HenschenEdman AH, Burgess WH, Tenner AJ. cDNA cloning and primary structure analysis of C1qR(p), the human C1q/MBL/SPA receptor that mediates enhanced phagocytosis in vitro. Immunity. 1997;6(2):119-29.

79. McGreal EP, Ikewaki N, Akatsu H, Morgan BP, Gasque P. Human C1qRp is identical with CD93 and the mNI-11 antigen but does not bind C1q. J Immunol. 2002;168(10):5222-32.

80. Gardai SJ, Xiao YQ, Dickinson M, Nick JA, Voelker DR, Greene KE, Henson PM. By binding SIRP alpha or calreticulin/CD91, lung collectins act as dual function surveillance molecules to suppress or enhance inflammation. Cell. 2003;115(1):13-23.

81. Strayer DS, Yang SJ, Jerng HH. Surfactant protein-A-binding proteins - characterization and structures. J Biol Chem. 1993;268(25):18679-84.

82. Wissel H, Looman AC, Fritzsche I, Rustow B, Stevens PA. SP-A-binding protein BP55 is involved in surfactant endocytosis by type II pneumocytes. Am J Physiol-Lung Cell Mol Physiol. 1996;271(3):L432-L40.

83. Kresch MJ, Christian C, Lu HW. Isolation and partial characterization of a receptor to surfactant protein A expressed by rat type II pneumocytes. American Journal of Respiratory Cell and Molecular Biology. 1998;19(2):216-25.

84. Sano H, Sohma H, Muta T, Nomura S, Voelker DR, Kuroki Y. Pulmonary surfactant protein A modulates the cellular response to smooth and rough lipopolysaccharides by interaction with CD14. J Immunol. 1999;163(1):387-95.

85. Malhotra R, Thiel S, Reid KBM, Sim RB. Human leukocyte--C1Q receptor binds other soluble-proteins with collagen domains. Journal of Experimental Medicine. 1990;172(3):955-9.

86. Sim RB, Moestrup SK, Stuart GR, Lynch NJ, Lu JH, Schwaeble WJ, Malhotra R. Interaction of clq and the collectins with the potential receptors calreticulin (cC1qR/collectin receptor) and megalin. Immunobiology. 1998;199(2):208-24.

87. Ogden CA, deCathehneau A, Hoffmann PR, Bratton D, Ghebrehiwet B, Fadok VA, Henson PM. C1q and mannose binding lectin engagement of cell surface calreticulin and CD91 initiates macropinocytosis and uptake of apoptotic cells. Journal of Experimental Medicine. 2001;194(6):781-95.

88. Vandivier RW, Ogden CA, Fadok VA, Hoffmann PR, Brown KK, Botto M, Walport MJ, Fisher JH, Henson PM, Greene KE. Role of surfactant proteins D, D, and C1q in the clearance of apoptotic cells in vivo and in vitro: Calreticulin and CD91 as a common collectin receptor complex. J Immunol. 2002;169(7):3978-86.

89. Nadesalingam J, Reid KBM, Palaniyar N. Collectin surfactant protein D binds antibodies and interlinks innate and adaptive immune systems. Febs Letters. 2005;579(20):4449-53.

90. Nadesalingam J, Bernal AL, Dodds AW, Willis AC, Mahoney DJ, Day AJ, Reid KBM, Palaniyar N. Identification and characterization of a novel interaction between pulmonary surfactant protein D and decorin. J Biol Chem. 2003;278(28):25678-87.

91. Hartshorn KL, White MR, Tecle T, Holmskov U, Crouch EC. Innate defense against influenza A virus: Activity of human neutrophil defensins and interactions of defensins with surfactant protein D. J Immunol. 2006;176(11):6962-72.

92. Doss M, White MR, Tecle T, Gantz D, Crouch EC, Jung G, Ruchala P, Waring AJ, Lehrer RI, Hartshorn KL. Interactions of alpha-, beta-, and theta-Defensins with Influenza A Virus and Surfactant Protein D. J Immunol. 2009;182(12):7878-87.

93. Holmskov U, Lawson P, Teisner B, Tornoe I, Willis AC, Morgan C, Koch C, Reid KBM. Isolation and characterization of a new member of the scavenger receptor superfamily, glycoprotein-340 (gp-340), as a lung surfactant protein-D binding molecule. J Biol Chem. 1997;272(21):13743-9.

94. Tino MJ, Wright JR. Surfactant proteins A and D specifically stimulate directed actin-based responses in alveolar macrophages. Am J Physiol-Lung Cell Mol Physiol. 1999;276(1):L164-L74.

95. Jaekel A, Clark H, Reid KBM, Sim RB. Surface-bound myeloperoxidase is a ligand for recognition of late apoptotic neutrophils by human lung surfactant proteins A and D. Protein & Cell. 2010;1(6):563-72.

96. Oosting RS, Wright JR. Characterization of the surfactant protein-A receptor - cell and ligand specificity American Journal of Physiology. 1994;267(2):L165-L72.

97. Watford WT, Smithers MB, Frank MM, Wright JR. Surfactant protein A enhances the phagocytosis of C1q-coated particles by alveolar macrophages. Am J Physiol-Lung Cell Mol Physiol. 2002;283(5):L1011-L22.

98. Lausen M, Lynch N, Schlosser A, Tornoe I, Saekmose SG, Teisner B, Willis AC, Crouch E, Schwaeble W, Holmskov U. Microfibril-associated protein 4 is present in lung washings and binds to the collagen region of lung surfactant protein D. J Biol Chem. 1999;274(45):32234-40.

99. Schlosser A, Thomsen T, Shipley JM, Hein PW, Brasch F, Tornoe I, Nielsen O, Skjodt K, Palaniyar N, Steinhilber W, McCormack FX, Holmskov U. Microfibril-associated protein 4 binds to surfactant protein A (SP-A) and colocalizes with SP-A in the extracellular matrix of the lung. Scand J Immunol. 2006;64(2):104-16.

100. Vaniwaarden F, Welmers B, Verhoef J, Haagsman HP, Vangolde LMG. Pulmonary surfactant protein-A enhances the hosst-defence mechanism of rat alveolar macrophages. American Journal of Respiratory Cell and Molecular Biology. 1990;2(1):91-8.

101. Kuan SF, Rust K, Crouch E. Interactions of surfactant protein-D with bacterial lipopolysaccharides - surfactant protein-D is an Escherichia-coli binding-protein in bronchoalveolar lavage. J Clin Invest. 1992;90(1):97-106.

102. Van Iwaarden JF, Pikaar JC, Storm J, Brouwer E, Verhoef J, Oosting RS, Van Golde LMG, Van Strijp JAG. Binding of surfactant protein A to the lipid A moiety of bacterial lipopolysaccharides. Biochemical Journal. 1994;303(2):407-11.

103. Hartshorn KL. Role of surfactant protein A and D (SP-A and SP-D) in human antiviral host defense. Frontiers in bioscience (Scholar edition). 2010;2:527-46.

104. Pikaar JC, Voorhout WF, Vangolde LMG, Verhoef J, Vanstrijp JAG, Vaniwaarden JF. Opsonic activities of surfactant protein-A and protein-D in phagocytosis of gram-negative bacteria by alveolar macrophages. J Infect Dis. 1995;172(2):481-9.

105. Geertsma MF, Nibbering PH, Haagsman HP, Daha MR, Vanfurth R. Binding of surfactant protein-A to C1Q receptors mediates phagoytosis of Staphylococcus-aureus by monocytes. Am J Physiol-Lung Cell Mol Physiol. 1994;267(5):L578-L84.

106. McNeely TB, Coonrod JD. Comparison of the opsonic activity of human surfactant protein A for Staphylococcus-aureus and Streptococcus-pneumoniae with rabbit and human macrophages. J Infect Dis. 1993;167(1):91-7.

107. Tino MJ, Wright JR. Surfactant protein A stimulates phagocytosis of specific pulmonary pathogens by alveolar macrophages. Am J Physiol-Lung Cell Mol Physiol. 1996;270(4):L677-L88.

108. LeVine AM, Bruno MD, Huelsman KM, Ross GF, Whitsett JA, Korfhagen TR. Surfactant protein A-deficient mice are susceptible to group streptococcal infection. J Immunol. 1997;158(9):4336-40.

109. LeVine AM, Kurak KE, Wright JR, Watford WT, Bruno MD, Ross GF, Whitsett JA, Korfhagen TR. Surfactant protein-A binds group B Streptococcus enhancing phagocytosis and clearance from lungs of surfactant protein-A-deficient mice. American Journal of Respiratory Cell and Molecular Biology. 1999;20(2):279-86.

110. Kabha K, Schmegner J, Keisari Y, Parolis H, SchlepperSchaefer J, Ofek I. SP-A enhances phagocytosis of Klebsiella by interaction with capsular polysaccharides and alveolar macrophages. Am J Physiol-Lung Cell Mol Physiol. 1997;272(2):L344-L52.

111. Jain-Vora S, LeVine AM, Chroneos Z, Ross GF, Hull WM, Whitsett JA. Interleukin-4 enhances pulmonary clearance of Pseudomonas aeruginosa. Infection and Immunity. 1998;66(9):4229-36.

112. LeVine AM, Kurak KE, Bruno MD, Stark JM, Whitsett JA, Korfhagen TR. Surfactant protein-A-deficient mice are susceptible to Pseudomonas aeruginosa infection. American Journal of Respiratory Cell and Molecular Biology. 1998;19(4):700-8.

113. Hickman-Davis J, Gibbs-Erwin J, Lindsey JR, Matalon S. Surfactant protein A mediates mycoplasmacidal activity of alveolar macrophages by production of peroxynitrite. Proceedings of the National Academy of Sciences of the United States of America. 1999;96(9):4953-8.

114. Hall-Stoodley L, Watts G, Crowther JE, Balagopal A, Torrelles JB, Robison-Cox J, Bargatze RF, Harmsen AG, Crouch EC, Schlesinger LS. Mycobacterium tuberculosis binding to human surfactant proteins A and D, fibronectin, and small airway epithelial cells under shear conditions. Infection and Immunity. 2006;74(6):3587-96.

115. Hartshorn KL, White MR, Shepherd V, Reid K, Jensenius JC, Crouch EC. Mechanisms of anti-influenza activity of surfactant proteins A and D: Comparison with serum collectins. Am J Physiol-Lung Cell Mol Physiol. 1997;273(6):L1156-L66.

116. Vaniwaarden JF, Vanstrijp JAG, Ebskamp MJM, Welmers AC, Verhoef J, Vangolde LMG. Surfactant protein-A is opsonin in phagocytosis of herpes-simplex virus type-1 by rat alveolar macrophages. American Journal of Physiology. 1991;261(2):L204-L9.

117. Gaiha GD, Dong T, Palaniyar N, Mitchell DA, Reid KBM, Clark HW. Surfactant protein a binds to HIV and inhibits direct infection of CD4(+) cells, but enhances dendritic cell-mediated viral transfer. J Immunol. 2008;181(1):601-9.

118. LeVine AM, Gwozdz J, Stark J, Bruno M, Whitsett J, Korfhagen T. Surfactant protein-A enhances respiratory syncytial virus clearance in vivo. J Clin Invest. 1999;103(7):1015-21.

119. Allen MJ, Harbeck R, Smith B, Voelker DR, Mason RJ. Binding of rat and human surfactant proteins A and D to Aspergillus fumigatus conidia. Infection and Immunity. 1999;67(9):4563-9.

120. Phelps DS, Rose RM. Increae recovery of surfactant protein-A in AIDS-related pneumonia. American Review of Respiratory Disease. 1991;143(5):1072-5.

121. Schelenz S, Malhotra R, Sim RB, Holmskov U, Bancroft GJ. Binding of host collectins to the pathogenic yeast cryptococcus-neoformans - human surfactant protein-D acts as an agglutinin for acapsular yeast-cells. Infection and Immunity. 1995;63(9):3360-6.

122. Clark H, Stehle T, Ezekowitz A, Reid K. Collectins and The Acute-Phase Response. Press A, editor. Washington, D.C.2004. 199-218 p.

123. Lim BL, Wang JY, Holmskov U, Hoppe HJ, Reid KBM. Expression of the carbohydrate-recognition domain of lung surfactant protein-D and demonstration of its binding to lipopolysaccharides of gram-negative bacteria. Biochemical and Biophysical Research Communications. 1994;202(3):1674-80.

124. Restrepo CI, Dong Q, Savov J, Mariencheck WI, Wright JR. Surfactant protein D stimulates phagocytosis of Pseudomonas aeruginosa by alveolar macrophages. American Journal of Respiratory Cell and Molecular Biology. 1999;21(5):576-85.

125. Walker MM, Karim QN, Worku M, Murray E, Eggleton P, Reid KBM, Thursz MR. Direct observation of kinetics and agglutination of Helicobacter pylori with the collectin, surfactant protein D. Gut. 1999;45:A41-A2.

126. Ferguson JS, Voelker DR, McCormack FX, Schlesinger LS. Surfactant protein D binds to Mycobacterium tuberculosis bacilli and lipoarabinomannan via carbohydrate-lectin interactions resulting in reduced phagocytosis of the bacteria by macrophages. J Immunol. 1999;163(1):312-21.

127. Hartshorn KL, Crouch EC, White MR, Eggleton P, Tauber AI, Chang D, Sastry K. Evidence for a protective role of pulmonary surfactant protein-D (SP-D) against influenza-A viruses. J Clin Invest. 1994;94(1):311-9.

128. Hickling TP, Bright H, Wing K, Gower D, Martin SL, Sim RB, Malhotra R. A recombinant trimeric surfactant protein D carbohydrate recognition domain inhibits respiratory syncytial virus infection in vitro and in vivo. European Journal of Immunology. 1999;29(11):3478-84.

129. Madsen J, Gaiha GD, Palaniyar N, Dong T, Mitchell DA, Clark HW. Surfactant Protein D Modulates HIV Infection of Both T-Cells and Dendritic Cells. PLoS One. 2013;8(3).

130. O'Riordan DM, Standing JE, Kwon K-Y, Chang D, Crouch EC, Limper AH. Surfactant protein D interacts with Pneumocystis carinii and mediates organism adherence to alveolar macrophages. J Clin Invest. 1995;95(6):2699-710.

131. Strong P, Reid KBM, Clark H. Intranasal delivery of a truncated recombinant human SP-D is effective at down-regulating allergic hypersensitivity in mice sensitized to allergens of Aspergillus fumigatus. Clin Exp Immunol. 2002;130(1):19-24.

132. Thompson WW, Shay DK, Weintraub E, Brammer L, Cox N, Anderson LJ, Fukuda K. Mortality associated with influenza and respiratory syncytial virus in the United States. JAMA-J Am Med Assoc. 2003;289(2):179-86.

133. Collins PL, Graham BS. Viral and host factors in human respiratory syncytial virus pathogenesis. J Virol. 2008;82(5):2040-55.

134. McNamara PS, Smyth RL. The pathogenesis of respiratory syncytial virus disease in childhood. Br Med Bull. 2002;61:13-28.

135. Behera AK, Matsuse H, Kumar M, Kong X, Lockey RF, Mohapatra SS. Blocking intercellular adhesion molecule-1 on human epithelial cells decreases respiratory syncytial virus infection. Biochem Biophys Res Commun. 2001;280(1):188-95.

136. Krusat T, Streckert HJ. Heparin-dependent attachment of respiratory syncytial virus (RSV) to host cells. Arch Virol. 1997;142(6):1247-54.

137. Malhotra R, Ward M, Bright H, Priest R, Foster MR, Hurle M, Blair E, Bird M. Isolation and characterisation of potential respiratory syncytial virus receptor(s) on epithelial cells. Microbes Infect. 2003;5(2):123-33.

138. Marr N, Turvey SE. Role of human TLR4 in respiratory syncytial virus-induced NF-kappaB activation, viral entry and replication. Innate Immun. 2012;18(6):856-65.

139. Harcourt J, Alvarez R, Jones LP, Henderson C, Anderson LJ, Tripp RA. Respiratory syncytial virus G protein and G protein CX3C motif adversely affect CX3CR1+ T cell responses. Journal of immunology (Baltimore, Md : 1950). 2006;176(3):1600-8.

140. Schlender J, Zimmer G, Herrler G, Conzelmann KK. Respiratory syncytial virus (RSV) fusion protein subunit F2, not attachment protein G, determines the specificity of RSV infection. J Virol. 2003;77(8):4609-16.

141. McLellan JS, Yang Y, Graham BS, Kwong PD. Structure of respiratory syncytial virus fusion glycoprotein in the postfusion conformation reveals preservation of neutralizing epitopes. J Virol. 2011;85(15):7788-96.

142. Updated guidance for palivizumab prophylaxis among infants and young children at increased risk of hospitalization for respiratory syncytial virus infection. Pediatrics. 2014;134(2):415-20.

143. Haynes LM, Caidi H, Radu GU, Miao C, Harcourt JL, Tripp RA, Anderson LJ. Therapeutic monoclonal antibody treatment targeting respiratory syncytial virus (RSV) G protein mediates viral clearance and reduces the pathogenesis of RSV infection in BALB/c mice. The Journal of infectious diseases. 2009;200(3):439-47.

144. Thomas NJ, Diangelo S, Hess JC, Fan R, Ball MW, Geskey JM, Willson DF, Floros J. Transmission of Surfactant Protein Variants and Haplotypes in Children Hospitalized With Respiratory Syncytial Virus. Pediatr Res. 2009;66(1):70-3.

145. LeVine AM, Elliott J, Whitsett JA, Srikiatkhachorn A, Crouch E, DeSilva N, Korfhagen T. Surfactant protein-D enhances phagocytosis and pulmonary clearance of respiratory syncytial virus. American Journal of Respiratory Cell and Molecular Biology. 2004;31(2):193-9.

146. Barr FE, Pedigo H, Johnson TR, Shepherd VL. Surfactant protein-A enhances uptake of respiratory syncytial virus by monocytes and U937 macrophages. Am J Respir Cell Mol Biol. 2000;23(5):586-92.

147. Ghildyal R, Hartley C, Varrasso A, Meanger J, Voelker DR, Anders EM, Mills J. Surfactant protein a binds to the fusion glycoprotein of respiratory syncytial virus and neutralizes virion infectivity. J Infect Dis. 1999;180(6):2009-13.

148. Hickling TP, Malhotra R, Bright H, McDowell W, Blair ED, Sim RB. Lung surfactant protein A provides a route of entry for respiratory syncytial virus into host cells. Viral Immunol. 2000;13(1):125-35.

149. Hartshorn KL, Webby R, White MR, Tecle T, Pan C, Boucher S, Moreland RJ, Crouch EC, Scheule RK. Role of viral hemagglutinin glycosylation in anti-influenza activities of recombinant surfactant protein D. Respiratory Research. 2008;9.

150. Reading PC, Morey LS, Crouch EC, Anders EM. Collectin-mediated antiviral host defense of the lung: Evidence from influenza virus infection of mice. Journal of Virology. 1997;71(11):8204-12.

151. Hartshorn KL, Reid KBM, White MR, Jensenius JC, Morris SM, Tauber AI, Crouch E. Neutrophil deactivation by influenza a viruses: Mechanisms of protection after viral opsonization with collectins and hemagglutination-inhibiting antibodies. Blood. 1996;87(8):3450-61.

152. Benne CA, Kraaijeveld CA, Vanstrijp JAG, Brouwer E, Harmsen M, Verhoef J, Vangolde LMG, Vaniwaarden JF. Interactions of surfactant protein-A with influenza-A viruses- binding and neutralization. J Infect Dis. 1995;171(2):335-41.

153. Leth-Larsen R, Zhong F, Chow VT, Holmskov U, Lu J. The SARS coronavirus spike glycoprotein is selectively recognized by lung surfactant protein D and activates macrophages. Immunobiology. 2007;212(3):201-11.

154. Madsen J, Kliem A, Tornoe I, Skjodt K, Koch C, Holmskov U. Localization of lung surfactant protein D on mucosal surfaces in human tissues. J Immunol. 2000;164(11):5866-70.

155. MacNeill C, Umstead TM, Phelps DS, Lin Z, Floros J, Shearer DA, Weisz J. Surfactant protein A, an innate immune factor, is expressed in the vaginal mucosa and is present in vaginal lavage fluid. Immunology. 2004;111(1):91-9.

156. Leth-Larsen R, Floridon C, Nielsen O, Holmskov U. Surfactant protein D in the female genital tract. Molecular Human Reproduction. 2004;10(3):149-54.

157. Clarke JR, Taylor IK, Fleming J, Nukuna A, Williamson JD, Mitchell DM. The epidemiology of HIV-1 infection of the lungs in AIDS patients. Aids. 1993;7(4):555-60.

158. Chun TW, Carruth L, Finzi D, Shen XF, DiGiuseppe JA, Taylor H, Hermankova M, Chadwick K, Margolick J, Quinn TC, Kuo YH, Brookmeyer R, Zeiger MA, BarditchCrovo P, Siliciano RF. Quantification of latent tissue reservoirs and total body viral load in HIV-1 Infection. Nature. 1997;387(6629):183-8.

159. Pastva AM, Wright JR, Williams KL. Immunomodulatory roles of surfactant proteins A and D: implications in lung disease. Proceedings of the American Thoracic Society. 2007;4(3):252-7.

160. Hartshorn KL, Crouch E, White MR, Colamussi ML, Kakkanatt A, Tauber B, Shepherd V, Sastry KN. Pulmonary surfactant proteins A and D enhance

neutrophil uptake of bacteria. Am J Physiol-Lung Cell Mol Physiol. 1998;274(6):L958-L69.

161. Hickman-Davis JM, Lindsey JR, Zhu S, Matalon S. Surfactant protein A mediates mycoplasmacidal activity of alveolar macrophages. Am J Physiol-Lung Cell Mol Physiol. 1998;274(2):L270-L7.

162. Hickman-Davis JM, Gibbs-Erwin J, Lindsey JR, Matalon S. Surfactant protein A mediates mycoplasmacidal activity of alveolar macrophages by production of peroxynitrite. Am J Respir Crit Care Med. 1999;159(3):A506-A.

163. Wright JR, Youmans DC. Pulmonary surfactant protein-A stimulates chemotaxis of alveolar macrophage. American Journal of Physiology. 1993;264(4):L338-L44.

164. Schagat T, Wright JR. Surfactant protein A regulates neutrophil chemotaxis. J Leukoc Biol. 2000:20-.

165. Crouch EC, Persson A, Griffin GL, Chang D, Senior RM. Interactions of pulmonary surfactant protein-D (SP-D) with human blood leukocytes. American Journal of Respiratory Cell and Molecular Biology. 1995;12(4):410-5.

166. Gaynor CD, McCormack FX, Voelker DR, McGowan SE, Schlesinger LS. Pulmonayr surfactant protein-A mediates enhanced phagocytosis of Mycobacterium-tuberculosis by a direct interaction with human macrophags J Immunol. 1995;155(11):5343-51.

167. Wu HX, Kuzmenko A, Wan SJ, Schaffer L, Weiss A, Fisher JH, Kim KS, McCormack FX. Surfactant proteins A and D inhibit the growth of Gram-negative bacteria by increasing membrane permeability. J Clin Invest. 2003;111(10):1589-602.

168. Schaeffer LM, McCormack FX, Wu HX, Weiss AA. Bordetella pertussis lipopolysaccharide resists the bactericidal effects of pulmonary surfactant protein A. J Immunol. 2004;173(3):1959-65.

169. McCormack FX, Gibbons R, Ward SR, Kuzmenko A, Wu HX, Deepe GS. Macrophage-independent fungicidal action of the pulmonary collectins. J Biol Chem. 2003;278(38):36250-6.

170. van Rozendaal B, van Spriel AB, van de Winkel JGJ, Haagsman HP. Role of pulmonary surfactant protein D in innate defense against Candida albicans. J Infect Dis. 2000;182(3):917-22.

171. Brummer E, Stevens DA. Collectins and fungal pathogens: roles of surfactant proteins and mannose binding lectin in host resistance. Medical Mycology. 2010;48(1):16-28.

172. Ansfield MJ, Kaltreider HB, Caldwell JL, Herskowitz FN. Hyporesponsiveness of canine bronchoalveolar lymphocytes to mitogens - inhibition of lymphocyte-proliferation by alveolar macrophages. J Immunol. 1979;122(2):542-8.

173. Rosseau S, Hammerl P, Maus U, Gunther A, Seeger W, Grimminger F, Lohmeyer J. Surfactant protein A down-regulates proinflammatory cytokine production evoked by Candida albicans in human alveolar macrophages and monocytes. J Immunol. 1999;163(8):4495-502.

174. Borron P, McIntosh JC, Korfhagen TR, Whitsett JA, Taylor J, Wright JR. Surfactant-associated protein A inhibits LPS-induced cytokine and nitric oxide production in vivo. Am J Physiol-Lung Cell Mol Physiol. 2000;278(4):L840-L7.

175. Kremlev SG, Umstead TM, Phelps DS. Surfactant protein A regulates cytokine production in the monocytic cell line THP-1. Am J Physiol-Lung Cell Mol Physiol. 1997;272(5):L996-L1004.

176. Fisher JH, Larson J, Cool C, Dow SW. Lymphocyte activation in the lungs of SP-D null mice. American Journal of Respiratory Cell and Molecular Biology. 2002;27(1):24-33.

177. Atochina EN, Gow AJ, Beck JM, Haczku A, Inch A, Kadire H, Tomer Y, Davis C, Preston AM, Poulain F, Hawgood S, Beers MF. Delayed clearance of Pneumocystis carinii infection, increased inflammation, and altered nitric oxide metabolism in lungs of surfactant protein-D knockout mice. J Infect Dis. 2004;189(8):1528-39.

178. Jakel A, Clark H, Reid KB, Sim RB. Surface-bound myeloperoxidase is a ligand for recognition of late apoptotic neutrophils by human lung surfactant proteins A and D. Protein Cell. 2010;1(6):563-72.

179. Jakel A, Clark H, Reid KB, Sim RB. The human lung surfactant proteins A (SP-A) and D (SP-D) interact with apoptotic target cells by different binding mechanisms. Immunobiology. 2010;215(7):551-8.

180. Clark H, Palaniyar N, Hawgood S, Reid KBM. A recombinant fragment of human surfactant protein D reduces alveolar macrophage apoptosis and pro-inflammatory cytokines in mice developing pulmonary emphysema. In: Diederich M, editor. Apoptosis: From Signaling Pathways to Therapeutic Tools. Annals of the New York Academy of Sciences. 1010. New York: New York Acad Sciences; 2003. p. 113-6.

181. Knudsen L, Ochs M, MacKay R, Townsend P, Deb R, Muehlfeld C, Richter J, Gilbert F, Hawgood S, Reid K, Clark H. Truncated recombinant human SP-D attenuates emphysema and type II cell changes in SP-D deficient mice. Respiratory Research. 2007;8.

182. Borron P, Veldhuizen RAW, Lewis JE, Possmayer F, Caveney A, Inchley K, McFadden RG, Fraher LJ. Surfactant associated protein-a inhibits human lymphocyte proliferation and IL-2 production. American Journal of Respiratory Cell and Molecular Biology. 1996;15(1):115-21.

183. Borron PJ, Mostaghel EA, Doyle C, Walsh ES, McHeyzer-Williams MG, Wright JR. Pulmonary surfactant proteins a and D directly suppress CD3(+)/CD4(+) cell function: Evidence for two shared mechanisms(1). J Immunol. 2002;169(10):5844-50.

184. Mukherjee S, Giamberardino C, Thomas J, Evans K, Goto H, Ledford JG, Hsia B, Pastva AM, Wright JR. Surfactant Protein A Integrates Activation Signal Strength To Differentially Modulate T Cell Proliferation. J Immunol. 2012;188(3):957-67.

185. Shepherd VL. Pulmonary surfactant protein D: a novel link between innate and adaptive immunity. Am J Physiol-Lung Cell Mol Physiol. 2002;282(3):L516-L7.

186. Brinker KG, Garner H, Wright JR. Surfactant protein A modulates the differentiation of murine bone marrow-derived dendritic cells. Am J Physiol-Lung Cell Mol Physiol. 2003;284(1):L232-L41.

187. Hansen S, Lo B, Evans K, Neophytou P, Holmskov U, Wright JR. Surfactant protein D augments bacterial association but attenuates major histocompatibility complex class II presentation of bacterial antigens. Am J Respir Cell Mol Biol. 2007;36(1):94-102.

188. Wang JY, Shieh CC, You PF, Lei HY, Reid KBM. Inhibitory effect of pulmonary surfactant proteins A and D on allergen-induced lymphocyte proliferation and histamine release in children with asthma. Am J Respir Crit Care Med. 1998;158(2):510-8.

189. Qaseem AS, Sonar S, Mahajan L, Madan T, Sorensen GL, Shamji MH, Kishore U. Linking surfactant protein SP-D and IL-13: Implications in asthma and allergy. Mol Immunol. 2013;54(1):98-107.

190. Haczku A. Protective role of the lung collectins surfactant protein A and surfactant protein D in airway inflammation. J Allergy Clin Immunol. 2008;122(5):861-79.

191. von Bredow C, Harti D, Schmid K, Schabaz F, Brack E, Reinhardt D, Griese M. Surfactant protein D regulates chemotaxis and degranulation of human eosinophils. Clin Exp Allergy. 2006;36(12):1566-74.

192. Ledford JG, Mukherjee S, Kislan MM, Nugent JL, Hollingsworth JW, Wright JR. Surfactant Protein-A Suppresses Eosinophil-Mediated Killing of Mycoplasma pneumoniae in Allergic Lungs. PLoS One. 2012;7(2).

193. Winkler C, Atochina-Vasserman EN, Holz O, Beers MF, Erpenbeck VJ, Krug N, Roepcke S, Lauer G, Elmlinger M, Hohlfeld JM. Comprehensive characterisation of pulmonary and serum surfactant protein D in COPD. Respir Res. 2011;12:29.

194. Mackay RA, Grainge CL, Lau LC, Barber C, Clark HW, Howarth PH. Airway surfactant protein D (SP-D) deficiency in adults with severe asthma. Chest. 2016.

195. Deb R, Shakib F, Reid K, Clark H. Major house dust mite allergens Dermatophagoides pteronyssinus 1 and Dermatophagoides farinae 1 degrade and inactivate lung surfactant proteins A and D. J Biol Chem. 2007;282(51):36808-19.

196. Wang JY, Kishore U, Lim BL, Strong P, Reid KB. Interaction of human lung surfactant proteins A and D with mite (Dermatophagoides pteronyssinus) allergens. Clin Exp Immunol. 1996;106(2):367-73.

197. Malhotra R, Haurum J, Thiel S, Jensenius JC, Sim RB. Pollen grains bind to lung alveolar type II cells (A549) via lung surfactant protein A (SP-A). Biosci Rep. 1993;13(2):79-90.

198. Malherbe DC, Erpenbeck VJ, Abraham SN, Crouch EC, Hohlfeld JM, Wright JR. Surfactant protein D decreases pollen-induced IgE-dependent mast cell degranulation. American journal of physiology Lung cellular and molecular physiology. 2005;289(5):L856-66.

199. Fakih D, Pilecki B, Schlosser A, Jepsen CS, Thomsen LK, Ormhoj M, Watson A, Madsen J, Clark HW, Barfod KK, Hansen S, Marcussen N, Jounblat R, Chamat

S, Holmskov U, Sorensen GL. Protective effects of surfactant protein D treatment in 1,3-beta-glucan-modulated allergic inflammation. American journal of physiology Lung cellular and molecular physiology. 2015;309(11):L1333-43.

200. Madan T, Kishore U, Shah A, Eggleton P, Strong P, Wang JY, Aggrawal SS, Sarma PU, Reid KBM. Lung surfactant proteins A and D can inhibit specific IgE binding to the allergens of Aspergillus fumigatus and block allergen-induced histamine release from human basophils. Clin Exp Immunol. 1997;110(2):241-9.

201. Madan T, Kishore U, Singh M, Strong P, Clark H, Hussain EM, Reid KB, Sarma PU. Surfactant proteins A and D protect mice against pulmonary hypersensitivity induced by Aspergillus fumigatus antigens and allergens. J Clin Invest. 2001;107(4):467-75.

202. Kishor U, Madan T, Sarma PU, Singh M, Urban BC, Reid KB. Protective roles of pulmonary surfactant proteins, SP-A and SP-D, against lung allergy and infection caused by Aspergillus fumigatus. Immunobiology. 2002;205(4-5):610-8.

203. Avery ME, Mead J. Surface properties in relation to atelectasis and hyaline membrane disease. AMA journal of diseases of children. 1959;97(5, Part 1):517-23.

204. Endo H, Oka T. An immunohistochemocal study of bronchial cells producing surfactant protein-A in the developing human fetal lung. Early Human Development. 1991;25(3):149-56.

205. Fujiwara T, Chida S, Watabe Y, Maeta H, Morita T, Abe T. Artificial surfactant therapy in hyaline-membrane disease. Lancet. 1980;1(8159):55-9.

206. Guyer B, Freedman MA, Strobino DM, Sondik EJ. Annual summary of vital statistics: Trends in the health of Americans during the 20th century. Pediatrics. 2000;106(6):1307-17.

207. Schoendorf KC, Kiely JL. Birth weight and age-specific analysis of the 1990 US infant mortality drop - Was it surfactant? Archives of Pediatrics & Adolescent Medicine. 1997;151(2):129-34.

208. Horbar JD, Wright EC, Onstad L, Philips JB, Cassady G, Fanaroff AA, Hack M, Edwards W, Little GA, Foley KA, Bauer CR, Bandstra ES, Yaffe SJ, Wright LL, Malloy MH, Korones SB, Cooke R, Tyson JE, Uauy RD, Lucey JF, Shankaran S, Ostrea E. Decreasing mortality associated with the introduction of surfactant therapy - and observational study of neonates weighing 601 to 1300 grams at birth. Pediatrics. 1993;92(2):191-6.

209. Malloy MH, Freeman DH. Respiratory distress syndrome mortality in the United States, 1987 to 1995. Journal of perinatology : official journal of the California Perinatal Association. 2000;20(7):414-20.

210. Long W, Corbet A, Cotton R, Courtney S, McGuiness G, Walter D, Watts J, Smyth J, Bard H, Chernick V. A controlled trial of synthetic surfactant in infants weighing 1250 g or more with respiratory-distress syndrome. New England Journal of Medicine. 1991;325(24):1696-703.

211. Shapiro DL, Notter RH, Morin FC, Deluga KS, Golub LM, Sinkin RA, Weiss KI, Cox C. Double-Blind, Randomized Trial of a Calf Lung Surfactant Extract

Administered at Birth to Very Premature-Infants for Prevention of Respiratory-Distress Syndrome. Pediatrics. 1985;76(4):593-9.

212. Soll RF, Hoekstra RE, Fangman JJ, Corbet AJ, Adams JM, James LS, Schulze K, Oh W, Roberts JD, Dorst JP, Kramer SS, Gold AJ, Zola EM, Horbar JD, McAuliffe TL, Lucey JF. Multicenter trial of single-dose modified bovine surfactant extract (SURVANTA) for prevention of respiratory-distress syndrome. Pediatrics. 1990;85(6):1092-102.

213. Kresch MJ, Clive JM. Meta-analyses of surfactant replacement therapy of infants with birth weights less than 2000 grams. Journal of perinatology : official journal of the California Perinatal Association. 1998;18(4):276-83.

214. Bernstein IM, Horbar JD, Badger GJ, Ohlsson A, Golan L, Vermont Oxford N. Morbidity and mortality among very-low-birth-weight neonates with intrauterine growth restriction. American Journal of Obstetrics and Gynecology. 2000;182(1):198-206.

215. Resch B, Kurath S, Manzoni P. Epidemiology of respiratory syncytial virus infection in preterm infants. Open Microbiol J. 2011;5:135-43.

216. Sato A, Ikegami M. SP-B and SP-C Containing New Synthetic Surfactant for Treatment of Extremely Immature Lamb Lung. PLoS One. 2012;7(7).

217. Baroutis G, Kaleyias J, Liarou T, Papathoma E, Hatzistamatiou Z, Costalos C. Comparison of three treatment regimens of natural surfactant preparations in neonatal respiratory distress syndrome. European Journal of Pediatrics. 2003;162(7-8):476-80.

218. Walti H, Monset-Couchard M. A risk-benefit assessment of natural and synthetic exogenous surfactants in the management of neonatal respiratory distress syndrome. Drug Safety. 1998;18(5):321-37.

219. Ygberg S, Nilsson A. The developing immune system - from foetus to toddler. Acta Paediatrica. 2012;101(2):120-7.

220. Robertson B. Surfactant inactivation and surfactant therapy in acute respiratory distress syndrome (ARDS). Monaldi archives for chest disease = Archivio Monaldi per le malattie del torace / Fondazione clinica del lavoro, IRCCS [and] Istituto di clinica tisiologica e malattie apparato respiratorio, Universita di Napoli, Secondo ateneo. 1998;53(1):64-9.

221. Kerr MH, Paton JY. Surfactant protein levels in severe respiratory syncytial virus infection. Am J Respir Crit Care Med. 1999;159(4):1115-8.

222. Shah PS. Current perspectives on the prevention and management of chronic lung disease in preterm infants. Paediatric drugs. 2003;5(7):463-80.

223. Coalson JJ, Winter VT, Siler-Khodr T, Yoder BA. Neonatal chronic lung disease in extremely immature baboons. Am J Respir Crit Care Med. 1999;160(4):1333-46.

224. Clark HW. Untapped Therapeutic Potential of Surfactant Proteins: Is There a Case for Recombinant SP-D Supplementation in Neonatal Lung Disease? Neonatology. 2010;97(4):380-7.

225. Mackay RM, Deadman M, Moxon ER, Clark H. A recombinant fragment of human SP-D promotes phagocytosis of Haemophilus influenzae strains whose in vivo pathogenicity is inversely related to SP-D binding. Early Human Development. 2006;82(9):617-.

226. Madan T, Reid KBM, Clark H, Singh M, Nayak A, Sarma PU, Hawgood S, Kishore U. Susceptibility of mice genetically deficient in SP-A or SP-D gene to Invasive Pulmonary Aspergillosis. Mol Immunol. 2010;47(10):1923-30.

227. Lin KW, Jen KY, Suarez CJ, Crouch EC, Perkins DL, Finn PW. Surfactant Protein D-Mediated Decrease of Allergen-Induced Inflammation Is Dependent upon CTLA4. J Immunol. 2010;184(11):6343-9.

228. Clark H, Knudsen L, Mackay R, Hawgood S, Reid K, Ochs M. Early treatment with a recombinant fragment of human surfactant protein D reduces the degree of emphysematous change developing in SP-D knock-out mice. Early Human Development. 2005;81(5):475-6.

229. Roona Deb R-MM, Paul Townsend, Kenneth Reid, Howard Clark. A Novel Role for Lung Surfactant Protein-D in Allergic Sensitization. Unpublished. 2012.

230. DiAngelo S, Lin ZW, Wang GR, Phillips S, Ramet M, Luo JM, Floros J. Novel, non-radioactive, simple and multiplex PCR-cRFLP methods for genotyping human SP-A and SP-D marker alleles. Disease Markers. 1999;15(4):269-81.

231. Voss T, Melchers K, Scheirle G, Schafer KP. Structural comparison of recombinant pulmonary surfact protein SP-D derived from 2 human coding sequences - implications for the chain composition of natural human SP-A. American Journal of Respiratory Cell and Molecular Biology. 1991;4(1):88-94.

232. Murray E. Doctor of Philosophy Thesis: Roles of lung surfactant protein SP-A and SP-D in innate immunity and allergy. Wolfson College, Department of Biochemistry, Oxford: University of Oxford; 2001.

233. Sotiriadis G, Dodagatta-Marri E, Kouser L, Alhamlan FS, Kishore U, Karteris E. Surfactant Proteins SP-A and SP-D Modulate Uterine Contractile Events in ULTR Myometrial Cell Line. PLoS One. 2015;10(12):e0143379.

234. Sanchez-Barbero F, Rivas G, Steinhilber W, Casals C. Structural and functional differences among human surfactant proteins SP-A1, SP-A2 and co-expressed SP-A1/SP-A2: role of supratrimeric oligomerization. Biochemical Journal. 2007;406:479-89.

235. Floros J, Wang GR, Mikerov AN. Genetic Complexity of the Human Innate Host Defense Molecules, Surfactant Protein A1 (SP-A1) and SP-A2-Impact on Function. Crit Rev Eukaryot Gene Expr. 2009;19(2):125-37.

236. Wang G, Phelps DS, Umstead TM, Floros J. Human SP-A protein variants derived from one or both genes stimulate TNF-alpha production in the THP-1 cell line. American journal of physiology Lung cellular and molecular physiology. 2000;278(5):L946-54.

237. Wang G, Umstead TM, Phelps DS, Al-Mondhiry H, Floros J. The effect of ozone exposure on the ability of human surfactant protein a variants to stimulate cytokine production. Environmental health perspectives. 2002;110(1):79-84.

238. Mikerov AN, Umstead TM, Huang W, Liu W, Phelps DS, Floros J. SP-A1 and SP-A2 variants differentially enhance association of Pseudomonas aeruginosa with rat alveolar macrophages. American journal of physiology Lung cellular and molecular physiology. 2005;288(1):L150-8.

239. McCormack FX. Structure, processing and properties of surfactant protein A. Biochimica Et Biophysica Acta-Molecular Basis of Disease. 1998;1408(2-3):109-31.

240. Spissinger T, Schafer KP, Voss T. Assembly of the surfactant protein SP-A - deletions in the globular deletions in the globular domain intefere with the correct folding of the molecule. European Journal of Biochemistry. 1991;199(1):65-71.

241. Tagaram HRS, Wang G, Umstead TM, Mikerov AN, Thomas NJ, Graff GR, Hess JC, Thomassen MJ, Kavuru MS, Phelps DS, Floros J. Characterization of a human surfactant protein A1 (SP-A1) gene-specific antibody; SP-A1 content variation among individuals of varying age and pulmonary health. Am J Physiol-Lung Cell Mol Physiol. 2007;292(5):L1052-L63.

242. Ayoub NA, Garb JE, Tinghitella RM, Collin MA, Hayashi CY. Blueprint for a high-performance biomaterial: full-length spider dragline silk genes. PLoS One. 2007;2(6):e514.

243. Rising A, Hjalm G, Engstrom W, Johansson J. N-terminal nonrepetitive domain common to dragline, flagelliform, and cylindriform spider silk proteins. Biomacromolecules. 2006;7(11):3120-4.

244. Hijirida DH, Do KG, Michal C, Wong S, Zax D, Jelinski LW. 13C NMR of Nephila clavipes major ampullate silk gland. Biophys J. 1996;71(6):3442-7.

245. Andersson M, Holm L, Ridderstrale Y, Johansson J, Rising A. Morphology and composition of the spider major ampullate gland and dragline silk. Biomacromolecules. 2013;14(8):2945-52.

246. Askarieh G, Hedhammar M, Nordling K, Saenz A, Casals C, Rising A, Johansson J, Knight SD. Self-assembly of spider silk proteins is controlled by a pH-sensitive relay. Nature. 2010;465(7295):236-U125.

247. Landreh M, Askarieh G, Nordling K, Hedhammar M, Rising A, Casals C, Astorga-Wells J, Alvelius G, Knight SD, Johansson J, Joernvall H, Bergman T. A pH-Dependent Dimer Lock in Spider Silk Protein. Journal of Molecular Biology. 2010;404(2):328-36.

248. Hedhammar M, Rising A, Grip S, Martinez AS, Nordling K, Casals C, Stark M, Johansson J. Structural properties of recombinant nonrepetitive and repetitive parts of major ampullate spidroin 1 from Euprosthenops australis: Implications for fiber formation. Biochemistry. 2008;47(11):3407-17.

249. Kronqvist N, Otikovs M, Chmyrov V, Chen G, Andersson M, Nordling K, Landreh M, Sarr M, Jornvall H, Wennmalm S, Widengren J, Meng Q, Rising A, Otzen D, Knight SD, Jaudzems K, Johansson J. Sequential pH-driven dimerization and stabilization of the N-terminal domain enables rapid spider silk formation. Nature communications. 2014;5:3254.

250. Rising AN, K; Landreh, M; Lindqvist, A; Johansson, J. The N-terminal domain of spider silk proteins as a solubility enhancing tag for recombinant production of a surfactant protein C analogue. Unpublished.

251. Smith PK, Krohn RI, Hermanson GT, Mallia AK, Gartner FH, Provenzano MD, Fujimoto EK, Goeke NM, Olson BJ, Klenk DC. Measurement of protein using bicinchoninic acid. Anal Biochem. 1985;150(1):76-85.

252. Madsen J, Tornoe I, Nielsen O, Koch C, Steinhilber W, Holmskov U. Expression and localization of lung surfactant protein A in human tissues. Am J Respir Cell Mol Biol. 2003;29(5):591-7.

253. Duvoix A, Mackay RM, Henderson N, McGreal E, Postle A, Reid K, Clark H. Physiological concentration of calcium inhibits elastase-induced cleavage of a functional recombinant fragment of surfactant protein D. Immunobiology. 2011;216(1-2):72-9.

254. Wright JR, Wager RE, Hawgood S, Dobbs L, Clements JA. Surfactant apoprotein MR = 26,000-36,000 enhances uptake of liposomes by type-II cells. J Biol Chem. 1987;262(6):2888-94.

255. Suwabe A, Mason RJ, Voelker DR. Calcium dependent association of surfactant protein A with pulmonary surfactant: application to simple surfactant protein A purification. Arch Biochem Biophys. 1996;327(2):285-91.

256. Silveyra P, Floros J. Genetic complexity of the human surfactant-associated proteins SP-A1 and SP-A2. Gene. 2013;531(2):126-32.

257. Berg T, Leth-Larsen R, Holmskov U, Hojrup P. Structural characterisation of human proteinosis surfactant protein A. Biochimica Et Biophysica Acta-Protein Structure and Molecular Enzymology. 2000;1543(1):159-73.

258. Simon DJ, Pitts J, Hertz NT, Yang J, Yamagishi Y, Olsen O, Tesic Mark M, Molina H, Tessier-Lavigne M. Axon Degeneration Gated by Retrograde Activation of Somatic Pro-apoptotic Signaling. Cell. 2016;164(5):1031-45.

259. Floros J. Human surfactant protein A (SP-A) variants: why so many, why such a complexity? Swiss medical weekly. 2001;131(7-8):87-90.

260. Sorensen GL, Hoegh SV, Leth-Larsen R, Thomsen TH, Floridon C, Smith K, Kejling K, Tornoe I, Crouch EC, Holmskov U. Multimeric and trimeric subunit SP-D are interconvertible structures with distinct ligand interaction. Mol Immunol. 2009;46(15):3060-9.

261. Carey B, Trapnell BC. The molecular basis of pulmonary alveolar proteinosis. Clin Immunol. 2010;135(2):223-35.

262. Mason RJ, Nielsen LD, Kuroki Y, Matsuura E, Freed JH, Shannon JM. A 50-kDa variant form of human surfactant protein D. Eur Respir J. 1998;12(5):1147-55.

263. Leth-Larsen R, Garred P, Jensenius H, Meschi J, Hartshorn K, Madsen J, Tornoe I, Madsen HO, Sorensen G, Crouch E, Holmskov U. A common polymorphism in the SFTPD gene influences assembly, function, and concentration of surfactant protein D. Journal of immunology (Baltimore, Md : 1950). 2005;174(3):1532-8.

264. Guo CJ, Atochina-Vasserman EN, Abramova E, Foley JP, Zaman A, Crouch E, Beers MF, Savani RC, Gow AJ. S-nitrosylation of surfactant protein-D controls inflammatory function. PLoS Biol. 2008;6(11):e266.

265. Crouch E, Persson A, Chang D. Accumulation of surfactant protein D in human pulmonary alveolar proteinosis. Am J Pathol. 1993;142(1):241-8.

266. Casals C. Role of surfactant protein A (SP-A)/lipid interactions for SP-A functions in the lung. Pediatr Pathol Mol Med. 2001;20(4):249-68.

267. Hattori A, Kuroki Y, Katoh T, Takahashi H, Shen HQ, Suzuki Y, Akino T. Surfactant protein A accumulating in the alveoli of patients with pulmonary alveolar proteinosis: oligomeric structure and interaction with lipids. Am J Respir Cell Mol Biol. 1996;14(6):608-19.

268. Voss T, Schafer KP, Nielsen PF, Schafer A, Maier C, Hannappel E, Maassen J, Landis B, Klemm K, Przybylski M. Primary structure differences of human surfactant-associated proteins isolated from normal and proteinosis lung. Biochim Biophys Acta. 1992;1138(4):261-7.

269. Doyle IR, Davidson KG, Barr HA, Nicholas TE, Payne K, Pfitzner J. Quantity and structure of surfactant proteins vary among patients with alveolar proteinosis. Am J Respir Crit Care Med. 1998;157(2):658-64.

270. Hickling TP, Malhotra R, Sim RB. Human lung surfactant protein A exists in several different oligomeric states: oligomer size distribution varies between patient groups. Mol Med. 1998;4(4):266-75.

271. Palaniyar N, Ridsdale RA, Possmayer F, Harauz G. Surfactant protein A (SP-A) forms a novel supraquaternary structure in the form of fibers. Biochem Biophys Res Commun. 1998;250(1):131-6.

272. Floros J, Hoover RR. Genetics of the hydrophilic surfactant proteins A and D. Biochim Biophys Acta. 1998;1408(2-3):312-22.

273. Berg T, Leth-Larsen R, Holmskov U, Hojrup P. Structural characterisation of human proteinosis surfactant protein A. Biochim Biophys Acta. 2000;1543(1):159-73.

274. Gronenborn AM, Filpula DR, Essig NZ, Achari A, Whitlow M, Wingfield PT, Clore GM. A novel, highly stable fold of the immunoglobulin binding domain of streptococcal protein G. Science. 1991;253(5020):657-61.

275. Lindman S, Hernandez-Garcia A, Szczepankiewicz O, Frohm B, Linse S. In vivo protein stabilization based on fragment complementation and a split GFP system. Proc Natl Acad Sci U S A. 2010;107(46):19826-31.

276. Sambrook J, Russell DW. Molecular Cloning: A laboratory manual (3rd ed). . New York: Cold Spring Harbor Laboratory Press.; 2001.

277. Rosano GL, Ceccarelli EA. Recombinant protein expression in Escherichia coli: advances and challenges. Front Microbiol. 2014;5:172.

278. Dumon-Seignovert L, Cariot G, Vuillard L. The toxicity of recombinant proteins in Escherichia coli: a comparison of overexpression in BL21(DE3), C41(DE3), and C43(DE3). Protein Expr Purif. 2004;37(1):203-6.

279. Hersch SJ, Elgamal S, Katz A, Ibba M, Navarre WW. Translation initiation rate determines the impact of ribosome stalling on bacterial protein synthesis. J Biol Chem. 2014;289(41):28160-71.

280. Murray E. Roles of lung surfactant proteins SP-A and SP-D in innate immunity and allergy. PhD thesis: published, University of Oxford, Wolfson College. 2001.

281. Rising A, Johansson J. Toward spinning artificial spider silk. Nat Chem Biol. 2015;11(5):309-15.

282. Candelas GC, Arroyo G, Carrasco C, Dompenciel R. Spider silkglands contain a tissue-specific alanine tRNA that accumulates in vitro in response to the stimulus for silk protein synthesis. Dev Biol. 1990;140(1):215-20.

283. Palmer I, Wingfield PT. Preparation and extraction of insoluble (inclusion-body) proteins from Escherichia coli. Curr Protoc Protein Sci. 2012;Chapter 6:Unit6 3.

284. Sivashanmugam A, Murray V, Cui C, Zhang Y, Wang J, Li Q. Practical protocols for production of very high yields of recombinant proteins using Escherichia coli. Protein Sci. 2009;18(5):936-48.

285. Li Y. Self-cleaving fusion tags for recombinant protein production. Biotechnol Lett. 2011;33(5):869-81.

286. Vagenende V, Yap MG, Trout BL. Mechanisms of protein stabilization and prevention of protein aggregation by glycerol. Biochemistry. 2009;48(46):11084-96.

287. Taylor GF, Wood SP, Mors K, Glaubitz C, Werner JM, Williamson PT. Morphological differences between beta(2) -microglobulin in fibrils and inclusion bodies. Chembiochem. 2011;12(4):556-8.

288. Widmann M, Christen P. Comparison of folding rates of homologous prokaryotic and eukaryotic proteins. J Biol Chem. 2000;275(25):18619-22.

289. Lebendiker M, Danieli T. Production of prone-to-aggregate proteins. FEBS Lett. 2014;588(2):236-46.

290. Derman AI, Prinz WA, Belin D, Beckwith J. Mutations that allow disulfide bond formation in the cytoplasm of Escherichia coli. Science. 1993;262(5140):1744-7.

291. Sohma H, Hattori A, Kuroki Y, Akino T. Calcium and dithiothreitol dependent conformational changes in beta-sheet structure of collagenase resistant fragment of human surfactant protein A. Biochem Mol Biol Int. 1993;30(2):329-36.

292. Haagsman HP, Sargeant T, Hauschka PV, Benson BJ, Hawgood S. Binding of calcium to SP-A, a surfactant-associated protein. Biochemistry. 1990;29(38):8894-900.

293. Orgeig S, Hiemstra PS, Veldhuizen EJ, Casals C, Clark HW, Haczku A, Knudsen L, Possmayer F. Recent advances in alveolar biology: evolution and function of alveolar proteins. Respir Physiol Neurobiol. 2010;173 Suppl:S43-54.

294. Murata Y, Kuroki Y, Akino T. Role of the C-terminal domain of pulmonary surfactant protein A in binding to alveolar type II cells and regulation of phospholipid secretion. The Biochemical journal. 1993;291 (Pt 1):71-6.

295. Haagsman HP, White RT, Schilling J, Lau K, Benson BJ, Golden J, Hawgood S, Clements JA. Studies of the structure of lung surfactant protein SP-A. The American journal of physiology. 1989;257(6 Pt 1):L421-9.

296. McCormack FX, Damodarasamy M, Elhalwagi BM. Deletion mapping of N-terminal domains of surfactant protein A. The N-terminal segment is required for phospholipid aggregation and specific inhibition of surfactant secretion. J Biol Chem. 1999;274(5):3173-81.

297. Hakansson K, Lim NK, Hoppe HJ, Reid KBM. Crystal structure of the trimeric alpha-helical coiled-coil and the three lectin domains of human lung surfactant protein D. Structure with Folding & Design. 1999;7(3):255-64.

298. Taneva S, Voelker DR, Keough KM. Adsorption of pulmonary surfactant protein D to phospholipid monolayers at the air-water interface. Biochemistry. 1997;36(26):8173-9.

299. Krarup A, Truan D, Furmanova-Hollenstein P, Bogaert L, Bouchier P, Bisschop IJ, Widjojoatmodjo MN, Zahn R, Schuitemaker H, McLellan JS, Langedijk JP. A highly stable prefusion RSV F vaccine derived from structural analysis of the fusion mechanism. Nature communications. 2015;6:8143.

300. Murby M, Samuelsson E, Nguyen TN, Mignard L, Power U, Binz H, Uhlen M, Stahl S. Hydrophobicity engineering to increase solubility and stability of a recombinant protein from respiratory syncytial virus. European journal of biochemistry / FEBS. 1995;230(1):38-44.

301. Villenave R, Touzelet O, Thavagnanam S, Sarlang S, Parker J, Skibinski G, Heaney LG, McKaigue JP, Coyle PV, Shields MD, Power UF. Cytopathogenesis of Sendai virus in well-differentiated primary pediatric bronchial epithelial cells. J Virol. 2010;84(22):11718-28.

302. Touzelet O, Loukili N, Pelet T, Fairley D, Curran J, Power UF. De novo generation of a non-segmented negative strand RNA virus with a bicistronic gene. Virus research. 2009;140(1-2):40-8.

303. Gaiha GD, Dong T, Palaniyar N, Mitchell DA, Reid KB, Clark HW. Surfactant protein A binds to HIV and inhibits direct infection of CD4+ cells, but enhances dendritic cell-mediated viral transfer. Journal of immunology (Baltimore, Md : 1950). 2008;181(1):601-9.

304. Rossio JL, Esser MT, Suryanarayana K, Schneider DK, Bess JW, Jr., Vasquez GM, Wiltrout TA, Chertova E, Grimes MK, Sattentau Q, Arthur LO, Henderson LE, Lifson JD. Inactivation of human immunodeficiency virus type 1 infectivity with preservation of conformational and functional integrity of virion surface proteins. J Virol. 1998;72(10):7992-8001.

305. Harris A, Borgnia MJ, Shi D, Bartesaghi A, He H, Pejchal R, Kang YK, Depetris R, Marozsan AJ, Sanders RW, Klasse PJ, Milne JL, Wilson IA, Olson WC, Moore JP, Subramaniam S. Trimeric HIV-1 glycoprotein gp140 immunogens and native HIV-1 envelope glycoproteins display the same closed and open quaternary molecular architectures. Proc Natl Acad Sci U S A. 2011;108(28):11440-5.

306. Abdul Salim A. Doctor of Philosophy Thesis: Structural studies of the interaction of bacterial lipopolysaccharides with C-reactive protein and lung surfactant protein D. Keele University: Keele University; 2012.

307. Erpenbeck VJ, Malherbe DC, Sommer S, Schmiedl A, Steinhilber W, Ghio AJ, Krug N, Wright JR, Hohlfeld JM. Surfactant protein D increases phagocytosis and aggregation of pollen-allergen starch granules. American journal of physiology Lung cellular and molecular physiology. 2005;288(4):L692-8.

308. Schleh C, Erpenbeck VJ, Winkler C, Lauenstein HD, Nassimi M, Braun A, Krug N, Hohlfeld JM. Allergen particle binding by human primary bronchial epithelial cells is modulated by surfactant protein D. Respir Res. 2010;11:83.

309. DeVincenzo JP, Wilkinson T, Vaishnaw A, Cehelsky J, Meyers R, Nochur S, Harrison L, Meeking P, Mann A, Moane E, Oxford J, Pareek R, Moore R, Walsh E, Studholme R, Dorsett P, Alvarez R, Lambkin-Williams R. Viral load drives disease in humans experimentally infected with respiratory syncytial virus. Am J Respir Crit Care Med. 2010;182(10):1305-14.

310. Lundberg AS, Randell SH, Stewart SA, Elenbaas B, Hartwell KA, Brooks MW, Fleming MD, Olsen JC, Miller SW, Weinberg RA, Hahn WC. Immortalization and transformation of primary human airway epithelial cells by gene transfer. Oncogene. 2002;21(29):4577-86.

311. Martin SJ, Matear PM, Vyakarnam A. HIV-1 infection of human CD4+ T cells in vitro. Differential induction of apoptosis in these cells. Journal of immunology (Baltimore, Md : 1950). 1994;152(1):330-42.

312. Herold N, Anders-Osswein M, Glass B, Eckhardt M, Muller B, Krausslich HG. HIV-1 entry in SupT1-R5, CEM-ss, and primary CD4+ T cells occurs at the plasma membrane and does not require endocytosis. J Virol. 2014;88(24):13956-70.

313. Nakajima T, Ballou CE. Characterization of the carbohydrate fragments obtained from Saccharomyces cerevisiae mannan by alkaline degradation. J Biol Chem. 1974;249(23):7679-84.

314. Perkins SM, Webb DL, Torrance SA, El Saleeby C, Harrison LM, Aitken JA, Patel A, DeVincenzo JP. Comparison of a real-time reverse transcriptase PCR assay and a culture technique for quantitative assessment of viral load in children naturally infected with respiratory syncytial virus. Journal of clinical microbiology. 2005;43(5):2356-62.

315. Promega. BioMath - Tm Calculator for Oligos 2002 [[7th June 2012]. Available from: http://www.promega.com/techserv/tools/biomath/calc11.htm.

316. Holmskov U, Thiel S, Jensenius JC. Collections and ficolins: humoral lectins of the innate immune defense. Annu Rev Immunol. 2003;21:547-78.

317. Pandit H, Gopal S, Sonawani A, Yadav AK, Qaseem AS, Warke H, Patil A, Gajbhiye R, Kulkarni V, Al-Mozaini MA, Idicula-Thomas S, Kishore U, Madan T. Surfactant protein D inhibits HIV-1 infection of target cells via interference with gp120-CD4 interaction and modulates pro-inflammatory cytokine production. PLoS One. 2014;9(7):e102395.

318. Rinaldo CR. HIV-1 Trans Infection of CD4(+) T Cells by Professional Antigen Presenting Cells. Scientifica (Cairo). 2013;2013:164203.

319. Nayak A, Dodagatta-Marri E, Tsolaki AG, Kishore U. An Insight into the Diverse Roles of Surfactant Proteins, SP-A and SP-D in Innate and Adaptive Immunity. Frontiers in immunology. 2012;3:131.

320. Singh M, Madan T, Waters P, Parida SK, Sarma PU, Kishore U. Protective effects of a recombinant fragment of human surfactant protein D in a murine model of pulmonary hypersensitivity induced by dust mite allergens. Immunol Lett. 2003;86(3):299-307.

321. Sahly H, Ofek I, Podschun R, Brade H, He Y, Ullmann U, Crouch E. Surfactant protein D binds selectively to Klebsiella pneumoniae lipopolysaccharides containing mannose-rich O-antigens. Journal of immunology (Baltimore, Md : 1950). 2002;169(6):3267-74.

322. Karron RA, Buonagurio DA, Georgiu AF, Whitehead SS, Adamus JE, Clements-Mann ML, Harris DO, Randolph VB, Udem SA, Murphy BR, Sidhu MS. Respiratory syncytial virus (RSV) SH and G proteins are not essential for viral replication in vitro: clinical evaluation and molecular characterization of a cold-passaged, attenuated RSV subgroup B mutant. Proc Natl Acad Sci U S A. 1997;94(25):13961-6.

323. Barreira ER, Precioso AR, Bousso A. Pulmonary surfactant in respiratory syncytial virus bronchiolitis: the role in pathogenesis and clinical implications. Pediatr Pulmonol. 2011;46(5):415-20.

324. Gaynor CD, McCormack FX, Voelker DR, McGowan SE, Schlesinger LS. Pulmonary surfactant protein A mediates enhanced phagocytosis of Mycobacterium tuberculosis by a direct interaction with human macrophages. Journal of immunology (Baltimore, Md : 1950). 1995;155(11):5343-51.

325. Lu J, Willis AC, Reid KB. Purification, characterization and cDNA cloning of human lung surfactant protein D. The Biochemical journal. 1992;284 (Pt 3):795-802.